Volume 14, No. 1

December, 1963

SOVIET ATOMIC ENERGY

АТОМНАЯ ЭНЕРГИЯ
(ATOMNAYA ÉNERGIYA)

TRANSLATED FROM RUSSIAN

CONSULTANTS BUREAU

SOVIET ATOMIC ENERGY

A translation of **ATOMNAYA ÉNERGIYA**
A publication of the Academy of Sciences of the USSR

Vol. 14, No. 1 December, 1963

CONTENTS

Annual Subscription: $95 **Single Issue: $30** **Single Article: $15**

EDITOR'S NOTE

Translated from Atomnaya Énergiya, Vol. 14, No. 1,
January, 1963

The present issue of Atomnaya Énergiya is devoted to Igor' Vasil'evich Kurchatov – a great Soviet physicist, head of atomic science and technology in the Soviet Union – in honor of the 60th anniversary of his birthday.

Some of the articles presented here are outside the usual range of topics reported in this journal. The authors of these articles, mostly colleagues or students of Igor' Vasil'evich, are engaged on the most widely differing scientific problems and in these papers they have tried to present material which is as interesting as possible, to form a worthy tribute to I. V. Kurchatov. The articles dealing directly with the activity of I. V. Kurchatov do not pretend to give a complete presentation of his very varied activity, but only present some of its aspects.

IGOR' VASIL'EVICH KURCHATOV

I. K. Kikoin

Translated from Atomnaya Énergiya, Vol. 14, No. 1,
pp. 5-9, January, 1963
Original article submitted November 19, 1962

In the biography of an outstanding scientist our interests are broader than a mere recital of his concrete scientific achievements and discoveries. No less instructive are the views of important scientists on social problems, organizational problems in science, problems of the relationship between science and technology. The relationships between important scientists and those about them are also of considerable interest.

The name of Igor' Vasil'evich Kurchatov is so popular in our country (and abroad) that his main scientific achievements are quite widely known, and it is hardly necessary to repeat them. The reader might like to have a certain understanding of the character, ideas, and views of this outstanding Soviet physicist, state and social worker, scientific head of atomic science and engineering in the Soviet Union.

The author first met Igor' Vasil'evich, then a young physicist, in 1927 during a lively scientific argument at a seminar in the Leningrad Physicotechnical Institute with Abram Fedorovich Ioffe. I. V. Kurchatov was the speaker and they were discussing one of the papers on the theory of current rectification by crystals. Some of those present disagreed with the views of the speaker, which is usual in seminars. However, the manner in which the disagreements were answered was unusual. Igor' Vasil'evich reached complete clarity in the argument and was not satisfied until each of his opponents expressed his wholehearted agreement. If the agreement was not sufficiently clear, the speaker again and again returned to his arguments, presenting new proof, until at last he achieved his aim. This aspect of the character of Igor' Vasil'evich, his impatience with any lack of agreement, with any outside tendency to smooth over roughnesses, has appeared in his varied activity throughout his life. He demanded clarity in the statement of a scientific problem, in the method of its solution, in the interpretation and formulation of the results. He was equally impatient with vagueness in the solution of organizational problems.

When he had clearly grasped some new scientific problem and decided that it had to be solved, he devoted more time and energy to its solution than would be possible for an ordinary person. This was the case, for example, when he was engaged in his investigations of ferroelectricity. When it became clear to him that ferroelectrics were the electrical analog of ferromagnets, he immediately embarked upon a series of very difficult and unusually convincing experiments to prove this. He soon brought in specialists on the growing of Rochelle salt single crystals; he organized the production of large single crystal specimens of very high quality, developed unusual new methods for the investigation of dielectrics, piezoelectrics, thermal, and other properties of Rochelle salt. To develop a rigid theory of ferroelectricity, Kurchatov often traveled from Leningrad to Kharkov to consult with L. D. Landau and other theoreticians to avoid being limited by the discussion and advice of the theoreticians of the Leningrad school. When he was sure that the phenomenon of ferroelectricity could have technical importance, he organized the combined work of physicists and leading engineers. In particular, V. P. Vologdin and a large group of engineers were brought into this work. Only when the basic scientific problems had been solved and the technical problems had been given a sufficient and reliable industrial base did Igor' Vasil'evich permit himself to go on to other problems.

Purposefulness in the solution of problems was a feature of the whole of his scientific and organizational activity. It enabled him to become a leader in scientific problems connected with the development of atomic science and technology in the Soviet Union.

I. V. Kurchatov demonstrated a tremendous capacity for work. When he worked in the Leningrad Physicotechnical Institute he could be seen in the laboratory from early morning to late at night. A typical episode comes to mind. A new imported high-voltage apparatus arrived in the Institute. For several evenings the Institute scientists could see Igor' Vasil'evich, with his sleeves rolled up, together with his co-workers, assembling the transformer and its safety devices, kenotrons, insulators, and other components. In those days physicists did not help laboratory technicians. Naturally, the assembly of specimens and the measurements themselves were performed directly by scientists.

Relaxation in the laboratory consisted of tidying it up, and the favorite occupation of Igor' Vasil'evich when he was tired was painting the tables and parts of the equipment.

A few years later, when I. V. Kurchatov was working on nuclear topics, the Institute workers were often witnesses to the following amusing scene. A man with some tiny object in his hand would dash along the corridor of the Institute at the speed of a 100-meter sprinter. This was I. V. Kurchatov hurrying to deliver a target which had just been irradiated by a neutron source to the laboratory for an investigation into the short-lived nucleus.

In spite of the fact that his experimental work kept him busy, he found time to write monographs and textbooks, although this was usually done at night or during his vacations. At this time he published such serious works as Ferroelectricity, The Neutron, etc.

His breadth of perception enabled him to switch to a new, hitherto unfamiliar topic with surprising speed and almost immediately to become a leader in this new field. For example, during the Great Fatherland War he was working on the problem of ship protection. Together with A. P. Aleksandrov he brilliantly solved this technical problem, although he had not hitherto dealt with problems of this kind.

Perhaps the clearest example is his changeover to nuclear physics at the start of the 1930's. At that time in the Leningrad Physicotechnical Institute there was practically no "nuclear" tradition, apart from the small laboratory of D. V. Skobel'tsyn, dealing with the physics of cosmic rays. The only place where radioactivity was studied to any extent, and where there was a small cyclotron, was the L. V. Mysovskii Laboratory in the Radium Institute. I. V. Kurchatov established a close connection with this Institute and he soon published a number of papers together with L. V. Mysovskii. The appearance of Igor' Vasil'evich within the physics section of the Institute abruptly changed the character of the work. A new group of scientists was brought in and interest was aroused in the new and rapidly developing branch of physics. The work of this laboratory, under the leadership of I. V. Kurchatov, was soon brought up to the level of foreign laboratories with considerable experience in this field.

As a real scientist, I. V. Kurchatov quite rightly assumed that a scientist should be constantly thinking about his work (except, perhaps, when he is asleep). In fact, his close friends felt that he did not stop thinking about scientific work for a minute. In the last years of his life, when his doctors ordered him to stay in bed, he had bedside telephones installed in order to keep in touch with the Institute laboratories and keep abreast of all fundamental work. When friends visited his house and tried to draw the conversation away from day-to-day scientific and organizational work, he invariably steered the discussion back to topics connected with work.

I. V. Kurchatov had outstanding organizational talent. He was convinced that any important scientific problem could be successfully solved by the correct organization of work. Very few great scientists have been able to combine scientific and organizational work with such brilliance. It is these qualities which have enabled him to organize a huge army of scientists and engineers of the most widely differing specialties, and to direct their energies to the solution of problems in atomic energy in the USSR.

To organize this work, he brought in a few men who formed the nucleus of the Institute which he founded (now the I. V. Kurchatov Institute of Atomic Energy, Order of Lenin). The number of people occupied on the problem (and then scientific institutions, planning and industrial organizations) increased according to an exponential law.

Throughout the development of atomic science and up to his death, Igor' Vasil'evich was a real scientific leader and took a lively interest in all aspects of the work. The most outstanding scientists of widely varying specialties came to his study; he discussed urgent scientific problems in detail with them; he was visited by the heads of the planning organizations with whom he worked out technical tasks; important builders came to see him, future heads of atomic installations, etc. It was usually three o'clock in the morning before the light in Igor' Vasil'evich's study was switched off.

During the building of atomic installations where he was directly responsible, for many months he transferred his working center to the construction site; he looked into all details of the building and assembly.

Although occupied with the solution of current problems requiring urgent investigational work, supervizing the planning, design of equipment, and the commissioning of atomic installations, not for one minute did Igor' Vasil'evich forget the future problems of science. He himself understood deeply and never failed to impress on others, not only scientists but also leaders of the national economy and industry, that the successful and rapid development of technology requires the widest development of science and the encouragement of even those investigations which do not promise an immediate practical result. This is because, in the most difficult days, when Igor' Vasil'evich was

overcoming daily cares connected with the operational solution of urgent scientific and technical problems, he found time to help in the organization of investigations into cosmic rays, the building of accelerators, the development of biology; briefly, in the organization of fields of science which were outside the sphere of his own scientific interests. Igor' Vasil'evich organized a course of lectures on general problems in nuclear theory and he himself was invariably present at these lectures.

During the period when nuclear engineering was being established, Kurchatov and his closest co-workers had to set up the closest connections with a number of industrial plants. The serious problem arose of the correct relationships between the scientists and workers in industry. Difficulties appeared here because, at first, the engineering and technical workers of production and technical organizations were unfamiliar with the scientific principles of the problems which they had to solve; they were not familiar with scientific ideas, which they were required to translate into engineering terms. However, the technical solution of the problems could not be delayed. It was therefore necessary to combine the education of the main personnel with the simultaneous fulfillment of all production tasks. It was clear that at first the main, even purely technical solutions would be suggested by the scientific leaders of the various sections and, of course, primarily by Kurchatov himself. Under these conditions it was essential to exhibit considerable tact in dealings between scientists and engineers. Matters were still further complicated by the fact that it was necessary to change the already accepted and partially established technical solutions, and to insist on a new method being used. Igor' Vasil'evich was able to do this so tactfully and cleverly, and to instruct his co-workers to do the same, that in most cases serious friction was avoided. Problems of authorship or so-called priority were especially delicate. There were cases when scientists came to Igor' Vasil'evich complaining that the industrial workers were claiming the authorship of ideas which had been introduced by the scientists. Igor' Vasil'evich very firmly (at least at first) refuted this kind of pretention. He explained that the tremendous responsibility which rested on the scientists and the leading part which was entrusted to them were incompatible with trivial priority disputes and, furthermore, that such disputes interfered with real productive collaboration between the scientists and production workers. He was firmly convinced that the initial development of the new technology should be controlled by scientists; he understood control in the widest sense of the word, not only providing ideas but also giving the scientists sufficient rights. It was essential, he added, that notice should be taken of the opinion of scientists (and not merely listened to). When necessary, Kurchatov turned to the party leaders and government for help. At the same time, he felt that it would be very dangerous for science to have too much control over technology, and that at certain stages of its development the initiative and management should gradually transfer to the technologists. In particular, when a number of fundamental scientific problems in nuclear engineering were successfully solved and nuclear engineering became an industry, the scientists were to act mainly as consultants and Kurchatov himself became actively engaged in the new and exciting problem of the controlled thermonuclear reaction.

The whole activity of Igor' Vasil'evich and his co-workers in the scientific managment of nuclear engineering brilliantly proved the correctness of these views.

We have already mentioned that the solution of nuclear engineering problems needed a large staff of workers. In particular, the Institute of Atomic Energy headed by Kurchatov rapidly became filled with new people. During the organization period he was very concerned as to how to form these people into a single working group enjoying good relationships; they differed in qualifications, professions, and ages. Before him was the experience in the development of the Leningrad Physicotechnical Institute by his teacher A. F. Ioffe, who had considerable personal charm and unquestionable authority. Igor' Vasil'evich himself modestly felt that he did not have sufficient scientific authority to build up this large group of people into a unit. Looking back we can state that the personal qualities of Igor' Vasil'evich as an administrator played an important part in the formation of the Institute; it has become a first-class scientific institute.

Despite the fact that he was head of a large group of scientists and that he insisted on the purposeful solution of the problems with which the Institute was concerned, he did not restrict the personal initiative of the scientists to the slightest degree, neither the more experienced scientists nor the young scientists. Unlike some managers, he was not guilty of the fault of "omniscience." On the contrary, he was not afraid to show his ignorance of some particular problem, and he was happy to learn where and when possible. This still further increased his authority with those around him. Even though he was the director, he did not mind sitting in the auditorium to listen to a course of lectures on radioelectronic methods in nuclear physics, which was given by one of the young scientists of his Institute.

He respected the interests of the people with whom he came into contact. He devoted much time and energy in helping people, either to help them out of some misfortune, or to help them in their work, and even to arrange

their living accommodations and family life; he concerned himself with encouragement and awards for success in work. He was particularly concerned about all cases which might affect the health of his staff. Igor' Vasil'evich was careful with his promises. But all those who dealt with him knew that he was a man of his word. He did much that he did not have to do. Everyone was familiar with his famous notebook which he always carried with him and in which he wrote his "obligations."

Igor' Vasil'evich loved life in all its aspects. He not only reacted in a lively manner to all important events, but at times he also interested himself in the small but characteristic details of these events. He was able to listen to his colleagues; he himself was a man of few words. When he was able to tear himself away for a rest, he tried, in his own words, to "gather as many impressions as possible." He took great pleasure in telling of his trip in Central Asia, which made a tremendous impression on him. He loved humorous folk tales and expressions and originated some himself. Many were familiar with his phrase "go and work on yourself" (which meant "go to sleep"). When he wanted to finish a conversation politely, he would say: "right, have a rest." He loved giving his friends funny, good-natured nicknames, and he did not mind if the joke sometimes went against himself.

He loved and understood serious music and tried to attend at least a few good concerts. In the last concert he heard (a few days before his death), the Mozart Requiem was played.

I. V. KURCHATOV AND NUCLEAR REACTORS

V. V. Goncharov

Translated from Atomnaya Énergiya, Vol. 14, No. 1,
pp. 10-17, January, 1963
Original article submitted October 18, 1962

Working with Igor' Vasil'evich Kurchatov from the very start of the organization of the atomic energy institute which bears his name today, I have had some connection with the course of problems in the use of atomic energy, and I want to tell of Igor' Vasil'evich's part in the solution of many of the most important problems.

First of all, it must be noted that I. V. Kurchatov's leadership was characterized by direct participation in experiments and by daily discussions of results and of plans for future work.

One of the achievements of fundamental importance for the future development of reactor construction was the establishment, under the guidance of I. V. Kurchatov, of the first nuclear reactor in our country in which a chain reaction was realized. This was preceded by intensive experimental and theoretical work on the fission process, and on the measurement of neutron-nucleus constants, and by other studies which were carried out on a broad front with the active participation of I. V. Kurchatov.

In the first reactor, natural uranium was used as fuel (at that time, enriched uranium was not available), and the moderator was graphite.

Extremely rigid requirements were set for the purity of the uranium and graphite. Suffice it to say, for example, that the admixture of boron in graphite was limited to a few parts per million. The problem was complicated because uranium and graphite of such purity had never been produced, and because they were required in large quantities – up to fifty tons of metallic uranium and hundreds of tons of graphite.

Because of the energetic measures taken by I. V. Kurchatov, a capability for the production of high-purity graphite was developed within a comparatively short time, and its commercial production in the required amounts was arranged. Production of uranium of the required purity was also successfully achieved.

I. V. Kurchatov himself went out into the factories and laboratories, posed questions, was of on-the-spot help in overcoming difficulties, and kept in constant touch with the progress of the work.

Under the direct supervision of I. V. Kurchatov, the successful startup of the first nuclear reactor with natural uranium and graphite moderator was accomplished.

In a foreword to the brochure Nuclear Radiations in Science and Technology, he write: "I remember the emotion with which I and a group of my associates, for the first time on the European continent, achieved a chain fission reaction in the Soviet Union with a uranium-graphite reactor."*

The exceptionally valuable experience obtained from the first reactor and from the nuclear physics studies performed with it, made it possible to pass on to the planning and building of other reactors.

I. V. Kurchatov initiated the creation of an all-around experimental basis within the Institute of Atomic Energy for carrying out tests of experimental fuel elements, construction materials, and coolants without which further development of new power, transport, and research reactors would have been impossible. Such a basis was created, consisting of the RFT research reactor, experimental loops with various forms of coolants and varying test modes, and a "fuel" materials technology laboratory. The reactor was put in use in April, 1952; its thermal power was 10,000 kW, and the maximum thermal neutron flux was $5 \cdot 10^{13}$ neut/cm^2-sec. Graphite and in part water, served as reactor moderator; 10% enriched uranium was used for fuel.

*I. V. Kurchatov, Nuclear Radiations in Science and Technology [in Russian] (Moscow, 1958), p. 5.

One of the difficult problems which arose during the building of the RFT reactor was the creation of fuel elements of complicated construction which had to operate under high specific energy deposition and thermal loading. As investigation showed, the problem was complicated by the fact that uranium pieces underwent violent changes in shape and size under irradiation. This eliminated the possibility of manufacturing fuel elements from enriched metallic uranium operating with high U^{235} burnup.

The complex problem of creating nonswelling and nondeformable fuel elements with maximum lifetime under conditions of stress for RFT and other reactors was successfully solved by the basically new idea of dispersing fissionable material in a diluent.

It is of interest to note that experts in the USA followed the same path in creating dispersed fuel elements for reactors operating with enriched uranium at high specific loading, in particular, for the MTR reactor which went into operation in 1952, as reported by American scientists at the 1955 Geneva conference.

Dispersed fuel elements were successfully used in RFT and other types of reactors in the Soviet Union.

I. V. Kurchatov devoted a great deal of attention to the investigation of the behavior of fuel elements in reactors and to the development of new types of elements.

A rebuilding of the RFT reactor, which was done for the purpose of significantly broadening its experimental possibilities, was successfully accomplished in 1957-1958 with the support of I. V. Kurchatov. After rebuilding, reactor power was increased to 15,000-20,000 kW, maximum neutron flux was raised to $1.8 \cdot 10^{14}$ neut/$cm^2 \cdot$ sec in the uranium and to $(3\text{-}4) \cdot 10^{14}$ neut/$cm^2 \cdot$ sec in the central, water-filled channel. The number of experimental channels for testing fuel elements was considerably increased.

The basis of the reconstruction was a loading of new fuel elements, original in construction and in manufacturing technique, of 90%-enriched uranium, and with highly developed cooling surfaces. Within a fuel element assembly of six concentrically located thin-walled pipes, irradiation of various samples could be done. The walls of the pipes were made of an aluminum-uranium alloy with an aluminum cladding. Fuel elements with the same kind of steel ? were used in a number of other reactors in the Soviet Union.

Tests of a large number of experimental fuel elements in the RFT reactor were of great value in working out and selecting the most reliable and efficient construction of elements for a number of new reactors (those of the First Atomic Power Station, the water-cooled, water-moderated reactors of the Novo-Voronezh atomic power station, the gas-cooled reactor of the Czechoslovakian atomic power station, the reactors of the icebreaker "Lenin," and others).

Extremely interesting phenomena which were of great importance for reactor operation, and which concerned the action of radiation on matter, were discovered under the leadership of I. V. Kurchatov.

Through studies of the physical properties of graphite under conditions of intense neutron irradiation, tremendous changes in the properties were discovered; reduction of thermal and electrical conductivity, changes in volume and mechanical strength. It was further established that latent energy, stored in the crystal lattice, was released by the annealing of irradiated graphite. These studies made it possible to explain the physical nature of the changes in graphite associated with deformations of the crystal lattice and with a shift of its constants, and to solve a number of practical problems which arose in the planning and use of graphite-moderated nuclear reactors.

Most valuable results for the study of graphite properties, particularly the buildup of latent energy and the nature of its release, were obtained after a very bold experiment, pushed by I. V. Kurchatov, involving the dismantling of the pile of the 50,000-kW uranium-graphite IR reactor after four years of use.

I. V. Kurchatov made a tremendous contribution to the development of nuclear power in the USSR.

He deserves great credit for creating the Soviet atomic power station, the first in the world, whose startup was the first step in the development of nuclear power in our country.

I. V. Kurchatov considered that nuclear power might prove to be more economical than thermal in isolated regions of the country despite the fact that the Soviet Union possesses a wealth of natural power resources.

In his appearance before the Twentieth Congress of the Communist Party of the Soviet Union in 1956, he stated, "...although the capital investment per installed power unit in an atomic power station is approximately one and one half times more than that of the corresponding coal-fired station, the cost per kilowatt-hour of power from an atomic

or coal power station may be approximately the same. To a great extent, this arises from the fact that fuel consumption in an atomic power station is negligibly small."*

On the initiative of I. V. Kurchatov, and with his active participation, construction was started on large atomic power stations, so that this grand experiment might allow us to accumulate experience in the construction and use of atomic power stations with mass production of fuel elements and their processing, to discover more technically reliable and more economical means for building atomic power stations, and to determine what portion atomic power should occupy in the over-all power picture of our socialist government. At the present time, assembly has been completed on two large industrial power stations: Beloyarsk and Novo-Voronezh.

The wealth of experience accumulated during the building and operation of the First Atomic Power Station was employed in the construction of the Beloyarsk atomic power station which bears the name of I. V. Kurchatov. Its reactors with nuclear superheated steam are a further development of the reactor of the First Atomic Power Station.

The planning of the Novo-Voronezh atomic power station with water-cooled, water-moderated reactors was carried out under the leadership of I. V. Kurchatov. The great compactness, the reliability, the possibility of achieving more thorough fuel burnup (which has been verified by operating experience with such reactors, for example, in the icebreaker "Lenin"), all point out the prospect for the application of water-cooled, water-moderated reactors in atomic power stations.

Lecturing at the English atomic center, Harwell, in 1956, I. V. Kurchatov said, "From the point of view of the possibility of U^{238} burnup, the nuclear fuel recirculation process is of great interest, i.e., a succession of operating periods in a uranium-water lattice. There are reasons to expect that greater utilization of U^{238} may be achieved by the use of nuclear fuel circulation in a uranium-water lattice... In connection with the possibility of achieving more thorough burnup (including that during a single run), the problem of building fuel elements capable of extended operation under irradiation takes on great practical significance."**

I. V. Kurchatov carefully saw to the experimental work on the building and testing of such fuel elements for water-cooled, water-moderated power reactors.

Fuel elements with calcined-uranium dioxide cores in a zirconium alloy cladding underwent extensive and prolonged tests in reactors. The tests indicated that the elements were capable of operating reliably while achieving thorough burnup – up to 25,000 MW · days per ton of uranium.

I. V. Kurchatov directed the tests on many critical assemblies. The results of these tests were the basis for the development of reactors for various purposes.

Research reactors of various types were built in the Soviet Union under the guidance of I. V. Kurchatov. Among the first, as mentioned, were reactors with graphite moderators.

In many institutes of the Soviet Union and of the people's democracies, the building of water-cooled, water-moderated research reactors assured a firm basis for carrying out research in the fields of reactor construction, neutron physics, radiochemistry, and biology, for producing radioactive isotopes, and also for training scientific and engineering cadres.

New methods of calculation were required for the particular physics of water-moderated reactors. Problems arose in connection with the securing of chain reaction stability and with core construction. At that time, many physicists had doubts about the possibility of safe operation of a reactor in which the entire moderating material was in motion with accompanying density fluctuation of various kinds. They pointed out the danger that the moderator density fluctuations might lead to uncontrolled runaway with serious consequences – rupture of the core or even a small atomic explosion.

As a result of theoretical and experimental studies of a water-moderated reactor, methods were devised which allowed fairly accurate estimation of core dimensions, critical loading, and other parameters.

The VVR-2 reactor, the first water-cooled, water-moderated research reactor in the USSR with enriched uranium and channel-free core, was built at the Institute of Atomic Energy. This reactor served as the prototype for the VVR-S reactor.

---

* "Pravda," February 22, 1956.

** I. V. Kurchatov, Atomnaya Énergiya No.3, 5 (1956).

The first water-cooled, water-moderated research reactor of the swimming-pool type, the IRT reactor, was also built at the Institute of Atomic Energy. Both types of reactor (VVR-S and IRT) received wide distribution. I. V. Kurchatov took energetic measures toward the further improvement of research reactors and toward the creation of new types of reactors intended for the attainment of higher neutron fluxes (above 10^{15} neut/cm^2 · sec) in order to carry out certain physical experiments.

The development of research reactors followed the line of creating reactors which operated at constantly maintained power levels with provision for continuous removal by circulating coolants, of the heat released in the reactor. Relatively recently, there appeared the idea of building reactors of a new type – impulse or pulsed reactors in which extra-high neutron fluxes can be obtained momentarily. Intense bursts for a short period of time can be obtained in such relatively simple and small reactors which have no special cooling system.

I. V. Kurchatov deserves great credit for the creation and construction of pulsed reactors in the Soviet Union with neutron fluxes up to 10^{18} neut/cm^2 · sec, which exceed the maximum neutron fluxes in the most powerful operating reactors by three to four orders of magnitude.

An important role was played by I. V. Kurchatov in the creation of many atomic research centers in our country.

The planning of a network of research reactors in the Soviet Union and the direction of the research at them was done with consideration of such factors as the existence of established scientific schools at the locations, the necessity for the solution of problems vital to the national economy of the Union republics and the autonomous regions, the training of cadres possessing modern research methods.

In 1956, I. V. Kurchatov visited Uzbekistan and afterwards, at one of the meetings at the Institute of Atomic Energy, he stated that if there were an experimental reactor in Tashkent, this would permit the successful solution of problems associated with the further development of cotton growing and the production of mineral fertilizers in Uzbekistan. At a meeting called by the Academy of Science of the UzbekSSR, it was discovered that Uzbekistan had cadres which had already done much in the fields of agriculture and medicine. However, the progress of a number of operations, including the development of the best fertilizers from Kara-Tau phosphate rock and the development of measures to fight saline soils, which are of enormous importance to the republic, has been hindered because of the absence of short-lived radioactive isotopes with lifetimes of tens of minutes. Such short-lived isotopes can only be obtained in a reactor on the spot, and can only be used in experimental work carried out in the immediate vicinity of the reactor. The research reactor VVR-S, which went into operation in 1959, was built in Tashkent with the cooperation of I. V. Kurchatov. He was elected honorary member of the Academy of Science of the UzbekSSR, and, in Tashkent, the national costume was presented to him. I remember how he, with delight, gave his impressions of the trip to Tashkent and Bukhara and of his meeting with the Uzbek scientists, all the while wearing those clothes (robe, sash, and skull-cap).

Attaching great importance to the study of the properties of matter at very low temperatures in a reactor, and taking into account the existence of Georgian schools of cryogenics, I. V. Kurchatov proved to be of great help in the construction of the IRT research reactor in Tbilis, which also went into operation in 1959.

In his last article, "The development of atomic physics in the Ukraine," which was published in Pravda on the day of his death, February 7, 1960, I. V. Kurchatov wrote, "Work on the investigation and peaceful application of the energy from nuclear transformations is being carried on at the Institute of Physics of the Academy of Science of the Ukrainian SSR." He further noted, "In the Institute of Physics, they have completed a group of interesting studies on the scattering and capture of fast neutrons by atomic nuclei which essentially broaden our ideas about the structure of the nucleus and about nuclear transformations. A proton accelerator is being used in this Institute and, in the near future, one of the best nuclear reactors in the Soviet Union will be placed in operation.

With this technical base, they will carry out nuclear physics research, and they will develop various applications of radioactive isotopes in physics and other branches of science, in industry, in agriculture, and in medicine."

The VVR-M reactor, to which I. V. Kurchatov referred, was put in operation in Kiev in March, 1960.

After the construction of a number of research reactors in the Soviet Union, it became necessary to coordinate the scientific research being carried out with them. Through the initiative of I. V. Kurchatov, successful preparations were made in the Academy of Science of the USSR for conducting a broadly coordinated meeting of the directors of all the research reactor centers in the Soviet Union. The meeting was to have been under the direction of I. V.

Kurchatov. His unexpected death made this impossible. The meeting was held in March, 1960 under the direction of Academician A. P. Aleksandrov, and all the basic purposes of I. V. Kurchatov – the determination of the principal direction of scientific activity at each center, the elimination of unnecessary parallelism, the division of the leading institutes according to individual problems, the interchange of experiments between institutes – were reflected in the decisions taken.

It was decided that work on problems in neutron spectroscopy and capture γ-ray spectroscopy, work on problems in neutron thermalization, and other work would be developed mainly at the I. V. Kurchatov Order of Lenin Institute of Atomic Energy; work on problems in the effects of radiation on semiconductors and work on nuclear isometry would be developed in Leningrad at the Physicotechnical Institute of the Academy of Science of the USSR; work on the chemistry of hot atoms would be developed at the Institute of Physics of the Academy of Science of the Georgian SSR; and work on activation analysis would be developed at the Institute of Geochemistry and Analytic Chemistry of the Academy of Science of the USSR.

Activation analysis was taken as a basic area of research for the VVR-S reactor of the Uzbek SSR Academy of Science in Tashkent. This decision was determined by the fact that the Uzbek SSR, like the other Central Asian republics, possessed rich and far from completely explored mineral resources and, therefore, they were very interested in the development of express methods for the analysis of samples into their various components, and also in the development of methods for the detection of micro-impurities. Important results have already been obtained in the field of activation analysis (development of a method for controlling boron impurity in silicon, the production of mass determinations of copper in cores obtained by exploratory drilling, etc.).

Materials analysis through capture γ-ray spectra and through neutron resonance absorption has been developed here along with the usual activation analysis.

These procedures were developed in connection with the study of capture γ-radiation and in connection with neutron spectroscopy studies in the Soviet Union. The experience acquired in other USSR institutes, particularly in the Institute of Atomic Energy, and data on equipment (γ-spectrometers, mechanical neutron choppers, multichannel time analyzers) were passed on to the Institute of Nuclear Physics of the Uzbek SSR Academy of Science.

The study of the action of nuclear radiations on the biologic properties of various agricultural products – cotton, hemp, jute, grapes – has great economic significance for the Uzbek SSR. These studies are also carried out with the help of a reactor.

Extremely interesting and promising results were obtained in the radiation destruction of silkworm pupa within the cocoon.

With its IRT reactor, the Institute of Physics of the Georgian SSR Academy of Science is carrying out work on low-temperature neutron spectroscopy of solids and quantum liquids; it is studying the effect of nuclear radiations on diffusion in single crystals of metals and alloys; it is making observations of the formation of dislocations in ionic crystals; it is investigating the breakdown of solid solutions under the influence of neutron fluxes and the effect of irradiation on the semiconductor properties of materials. A great deal of the work is involved with studies of reactions which involve the participation of hot atoms or recoil atoms.

By instruction from I. V. Kurchatov, scientific workers from the Institute of Physics of the Georgian SSR Academy of Science did preliminary work in the selected fields at the Institute of Atomic Energy even while the reactor was being built. The Georgian scientists received technical documents on mechanical monochromators, cold neutron filters, neutron detectors, time analyzers, all needed for scientific work. Such a system of cadre training and instrumental information was also used in the organization of reactor centers in Tashkent, Minsk, Riga, and other places.

The VVR-M reactor of the Leningrad Physicotechnical Institute of the USSR Academy of Science has been called upon to meet the requirements of the research institutes of one of the most important scientific centers in the Soviet Union – Leningrad.

With the VVR-M reactor of the Ukrainian SSR Academy of Science, great advances are being made in work on neutron spectroscopy, in studies of thermalization processes, and in work on capture γ-rays. Work on solid state physics, in particular with reference to radiation effects on materials, and work in radiobiology are also typical of the work being done with the reactor in Kiev.

The basic directions of the work being done with the IRT reactor at the Institute of Physics of the Latvian SSR

Academy of Science are studies of capture γ-ray spectra and the spectra from short-lived isotopes, studies in solid state physics, including the study of the properties of magnetic materials, and studies in radiobiology.

With the IRT reactor at the Power Institute of the Belorussian SSR Academy of Science, investigations will be carried out in solid state physics (the structure of ferrites and other magnetic materials, and of semiconductors, the dynamics of the condensed state), in nuclear spectroscopy, in the radiation resistance of various organic coolants,etc.

Because of the great benefit derived from the first coordinating meeting, such meetings came to be held yearly.

I. V. Kurchatov was the principal initiator in the creation of the largest scientific center in the world – the Joint Institute for Nuclear Studies in Dubna – and he has promoted, in every way possible, cooperative organizations among the socialist countries and the creation of reactor research centers in them. At the Twentieth Congress of the Communist Party of the Soviet Union, I. V. Kurchatov said, "Through atomic reactors, we shall carry out work in conjunction with the scientists and engineers of the countries in the socialist camp who, with the help of the Soviet Union, will build for themselves atomic reactors for scientific purposes, and who will plan the construction of atomic power stations. Our common effort with the scientists of the countries of the socialist camp will be broadened and deepened, and certainly will lead to outstanding results."*

In 1956, in one of his speeches, he emphasized the great importance of the help which was being given to the socialist countries in the planning and construction of research reactors and in the training of cadres, and he expressed confidence that these cadres would safetly operate the reactors and would carry out research with them. The Soviet Union began to give such help in 1955. Research reactors of various types were put into operation from 1957 on in Rumania, Czechoslovakia, East Germany, Poland, China, Hungary, Bulgaria, and other countries. These countries then had at their disposal modern equipment which enabled them to train national cadres of scientists and engineers and to develop research in various branches of science and engineering.

It then became necessary to discuss and plan the scientific work to be done with the reactors, to make an efficient selection of research goals, and to coordinate them. I. V. Kurchatov expedited these activities in every possible way.

The first such meeting took place in Dubna in the spring of 1959. At it, there was discussed information about the status and course of research work at reactors built in the Joint Institute for Nuclear Studies member-countries. The meeting was faced with the problem of coordinating the efforts of the socialist countries toward the greater development of peaceful uses of atomic energy.

With the support of I. V. Kurchatov, an international conference of scientists and engineers of the socialist countries on the problems of operation and use of research reactors was arranged. This conference, which took place in June, 1960 in Dresden, was an important landmark in a new stage of brotherly cooperation between our countries in the matter of the peaceful use of atomic energy. About 150 scientists and engineers from nine countries participated. At the conference, the experience acquired in a number of socialist countries in the operation of research reactors was reviewed, along with the extension of their experimental possibilities and their use for scientific work. A number of scientific and engineering problems were presented which were to be solved in a short time, since some countries which had the experience and specialization offered to take upon themselves the solution of individual problems. This important meeting offered prospects for strengthening the collaboration between brother scientists in the countries. In turn, yearly meetings began to be held in the various countries, meetings which dealt with reactor research, reactor physics, and the exchange of experiences with the operation and improvement of reactors.

The reactor research centers established with the help of the Soviet Union became full-fledged scientific organizations in the majority of the socialist countries, actively working in timely fields of science and engineering, making their contribution to world science, and meeting the demands of the economy of their countries.

We see how true were the words spoken by I. V. Kurchatov in 1956 in connection with the creation of research reactor centers in the socialist countries, and to what successful results this has led.

I. V. Kurchatov strove for close collaboration with the scientists of all countries. It is well known what a great role in the development of international collaboration of scientists was played by the lecture of I. V. Kurchatov which was given in England, and which dealt with the work being carried on in the USSR in the field of thermonuclear fusion. In a second lecture, he dealt with some problems in the development of nuclear power.

* "Pravda," February 22, 1956.

I. V. Kurchatov more than once played the host to foreign scientists newly arrived in the Soviet Union, showed them the experimental equipment at the Institute of Atomic Energy, as well as the results of investigations, and led joint seminars. For example, F. Joliot-Curie visited him in 1958, he received a delegation of English scientists under the leadership of J. Cockcroft that same year and, in 1959, a group of American scientists, among whom were such outstanding scientists in the field of reactor construction as A. Weinberg and W. Zinn.

Through the initiative of I. V. Kurchatov, and under his guidance, a session of the USSR Academy of Science, was arranged which met in July, 1955, and which was devoted to the peaceful uses of atomic energy. At this session, 80 reports were read in which the results of important investigations being carried on in the Soviet Union were presented for the first time. These reports aroused great interest and proved useful to the scientists of other countries.

I. V. Kurchatov was in charge of the preparation of reports for the International Conference on the Peaceful Uses of Atomic Energy held in Geneva in 1955.

The reports at the July session of the USSR Academy of Science and at the Geneva conference were a great contribution of Soviet science to the problems of the peaceful uses of atomic energy. Among the reports presented at the Geneva conference, an important position was occupied by reports on the First Atomic Power Station, on the course of the development of nuclear power, on a reactor for physical and technical research, by reports about the VVR-2, VVR-S, and TVR research reactors, by reports on reactor theory, and a number of others.

At the conference, at which the representatives of 79 countries were present, the Soviet Union submitted 102 reports. From the tribune of the Twentieth Congress of the Communist Party of the Soviet Union, I. V. Kurchatov declared, "We derived great satisfaction from the fact that, at this conference, the reports of our scientists and engineers received a high rating from the world scientific community."*

Again with the active participation of I. V. Kurchatov, preparations also went forward for the Second International Conference on the Peaceful Uses of Atomic Energy (Geneva, 1958). For the first time, a considerable number of papers were devoted to the problem of thermonuclear fusion. The speech by I. V. Kurchatov in England led to the open discussion of this most important scientific problem.

A great deal of interest was aroused by the Soviet scientists' reports on a number of subjects: the construction of the atomic icebreaker "Lenin," the operating experience with the First Atomic Power Station, the plans for new atomic power stations with uranium-graphite reactors producing high-pressure superheated steam as well as stations with water-cooled, water-moderated reactors, the experimental fast reactors, the building of the intermediate research reactor SM-2 with high thermal neutron flux, the rebuilding of the existing RFT, IR, VVR-2, and TVR reactors, the development of rod-shaped fuel elements for VVER-type reactors, and the reactors of the atomic icebreaker "Lenin," the tubular elements for research reactors, and many more. An especially powerful impression was made by the unexpected news of the start-up, in the Soviet Union, of the first new atomic power station of its kind (100,000 kW).

The high scientific level of the reports presented assured the prestige of the Soviet Union.

The brilliant life and career of that outstanding Soviet scientist and man, I. V. Kurchatov, which are forever engraved in our hearts, will serve for all as an example of unselfish service to the Motherland.

*"Pravda," February 22, 1956.

SPONTANEOUS FISSION AND SYNTHESIS OF FAR TRANSURANIUM ELEMENTS

G. N. Flerov, E. D. Donets, and V. A. Druin

Translated from Atomnaya Énergiya, Vol. 14, No. 1,
pp. 18-26, January, 1963
Original article submitted August 30, 1962

The possibility of spontaneous fission of nuclei was predicted theoretically in 1939 on the basis of a model representing the nucleus as a drop of charged liquid [1]. Immediately after the publication of that article, intensive research was started in the laboratories of many countries to investigate the spontaneous fission of uranium and thorium, the heaviest elements known at that time. At the Leningrad Institute of Physics and Technology of the Academy of Sciences of the USSR Professor I. V. Kurchatov's laboratory developed a highly sensitive procedure by means of which K. A. Petrzhak and G. N. Flerov were able, for the first time in 1940, to observe spontaneous fission fragments of U^{238} [2].

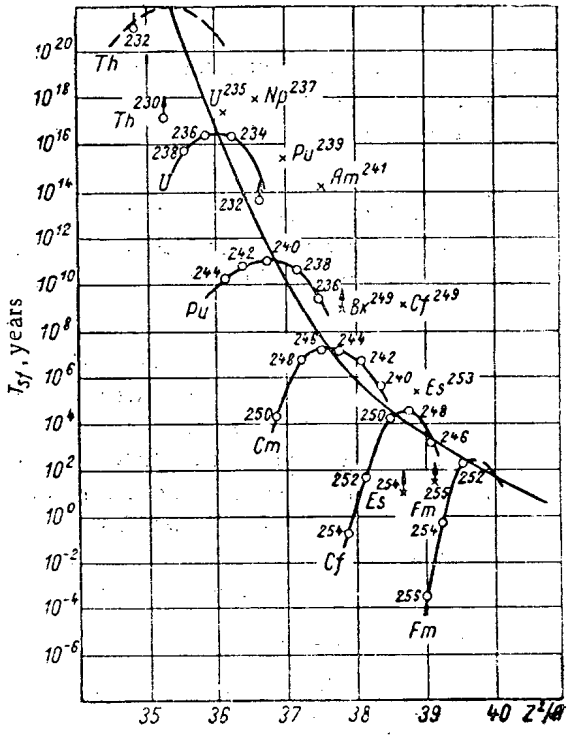

Fig. 1. Period of spontaneous fission T_{sf} as a function of the fissility parameter Z^2/A.

The experimental discovery of the fission of U^{238} from the ground (unexcited) state greatly heightened the interest in the study of this new form of radioactive decay of nuclei. Investigations were conducted along two main lines: to explain the mechanism of spontaneous fission, and to find new nuclei in which it took place. It was found that many transuranium elements obtained artificially in reactors or accelerators undergo spontaneous fission.

Some Laws Governing the Spontaneous Fission of Nuclei

By 1952 a large amount of experimental material on spontaneous-fission periods had been collected, and this enabled Seaborg to publish the first systematic study of these data [3]. He constructed a graph of the spontaneous fission period T_{sf} as a function of the fissility parameter Z^2/A, which in the liquid drop model represents the ratio of the Coulomb energy tending to force the protons apart to the stabilizing surface energy of the nucleus. This systematization was later refined and extended [4,5]; its present form is shown in Fig. 1. We can observe three basic features in the behavior of the spontaneous-fission periods of the various elements: 1) a general tendency for T_{sf} to decrease as Z^2/A increases; 2) the "parabolic" shape of the curves on which the values of T_{sf} lie for the various isotopes of one element; 3) a value of T_{sf} in nuclei with an odd number of neutrons or protons which is 10^3 to 10^6 times the T_{sf} value of an even-even nucleus for a given Z^2/A value. The first of these features agrees qualitatively with the predictions based on the hydrodynamic model, while the latter two cannot be explained from the viewpoint of this nuclear model. The development of the theory of spontaneous fission is closely related to that of the general theory of nuclear structure and nuclear reactions. The various models to represent nuclear structure were also used to explain features of the T_{sf} versus Z^2/A graph. Evidently, for a correct understanding of what happens in the fission process we must consider not only the collective properties of the nucleus, but also the behavior of the individual nucleons when the nucleus as a whole is deformed. As was shown by Nilsson [6], the energy of the individual nucleons changes considerably as the nuclear deformation increases, and this may produce an appreciable change in the hydrodynamic fission barrier. Johansson [7] used the Nilsson diagram for an analysis of

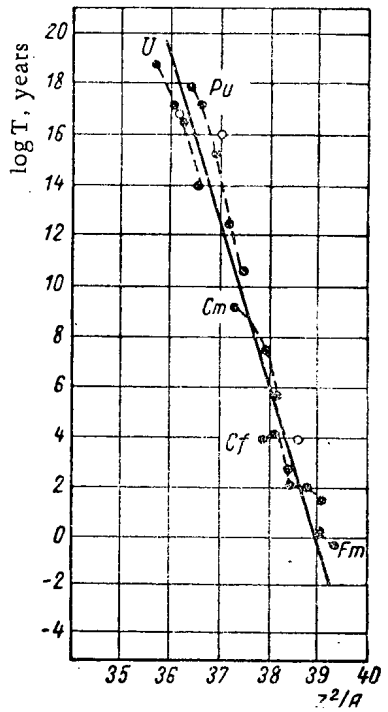

Fig. 2. Graph of experimental values of T_{sf} as a function of Z^2/A after single-particle corrections are applied [7].

effective barriers; the analysis indicated that the graph of T_{sf} as a function of Z^2/A can be made considerably more regular by taking single-particle corrections to the hydrodynamic barrier into account. The dispersion of the points is considerably reduced, and they are grouped about a straight line (Fig. 2).

Despite the substantial theoretical advances in the understanding of spontaneous fission, the theory is still only qualitative. In particular, it is very difficult to give a theoretical estimate for the lifetimes of the far transuranium elements. For such estimates, therefore, we resort to various semi-empirical formulas and to the extrapolation of experimentally observed relationships to the range of the unknown nuclei. The Swiatecki [8] and Dorn [9] formulas are widely used. These formulas were based on the fact that the experimental values of the nuclear masses in the ground state do not agree with the points on the smooth mass surface which were calculated on the basis of the hydrodynamic model, using the quantity δm, and that the spontaneous-fission periods determined experimentally disagree with those expected from this model when the quantity δT is used.

Swiatecki observed a well-defined correlation between δT and δm. This seems natural today, since we already know that the hydrodynamic formula for the masses ignores the shell structure of the nuclei, the fluctuations in the pairing energies, the nonuniformity of the angular and radial charge distributions, etc., but all these energy effects influence the nucleus lifetime for spontaneous fission. By applying empirical corrections $K\delta m$ to the observed spontaneous-fission periods, Swiatecki obtained a smooth curve of $T_{sf} + K\delta m$ versus Z^2/A for even-even nuclei with $K = 5 - (Z^2/A - 37.5)$.

Dorn made a slight change in the Swiatecki formula by adding a $\sqrt{Z}/A$ term, thereby smoothing the curves even more. An analytic expression of the Swiatecki-Dorn formula for periods of spontaneous fission is the following:

$$\left.\begin{matrix}\lg T_{\text{even-even}}\\ \lg T_{\text{odd A}}\\ \lg T_{\text{odd-odd}}\end{matrix}\right\} = \left\{\begin{matrix}-30{,}06\\ -23{,}46\\ -18{,}56\end{matrix}\right\} - 7{,}8\theta + 0{,}35\theta^2 + 0{,}0736\theta^3 + 1389\frac{\sqrt{Z}}{A} - (4-0)\,\delta m,$$

where $\theta = Z^2/A - 37.5$, T_{sf} is expressed in seconds, and δm is expressed in MeV. To estimate the spontaneous-fission periods of unknown nuclei, δm may be defined as the difference between Cameron's tabulated mass value [10] and a point on the smooth mass surface:

$$M = 1000A - 8{,}3557A + 19{,}12A^{2/3} + 0{,}76278\frac{Z^2}{A^{1/3}} + 25{,}444\frac{(N-Z)^2}{A} + 0{,}420\,(N-Z).$$

Figure 3 shows the spontaneous-fision periods calculated by the Swiatecki-Dorn formula for a number of isotopes of curium, californium, fermium, and elements 102 and 104. For comparison purposes, experimental points have been shown by crosses, and broken curves have been drawn through them. It can be seen that satisfactory agreement with the formula is found in the case of californium isotopes, while in the case of fermium the position and behavior of the broken curve differ considerably from those of the solid curve. For heavy isotopes of curium, the formula predicts a sharp increase in the probability of spontaneous fission, and in the case of elements 102 and 104, the periods of spontaneous fission decrease somewhat more slowly in the $N > 152$ range than those of californium and fermium. In [11], analyzing the curve of emission of various transuranium elements from the "Mike" thermonuclear explosion, Dorn showed that the formula yields lower values of T_{sf} for very heavy isotopes (for example, Fm^{254} and Fm^{255}). According to his conclusions, the emission curve can be explained only if we assume that in the region far from the beta stability curve spontaneous fission cannot take place more rapidly than beta disintegration, i.e., that the Swiatecki-Dorn formula is not valid for neutron-enriched nuclei. We cannot at present determine the range of N values for

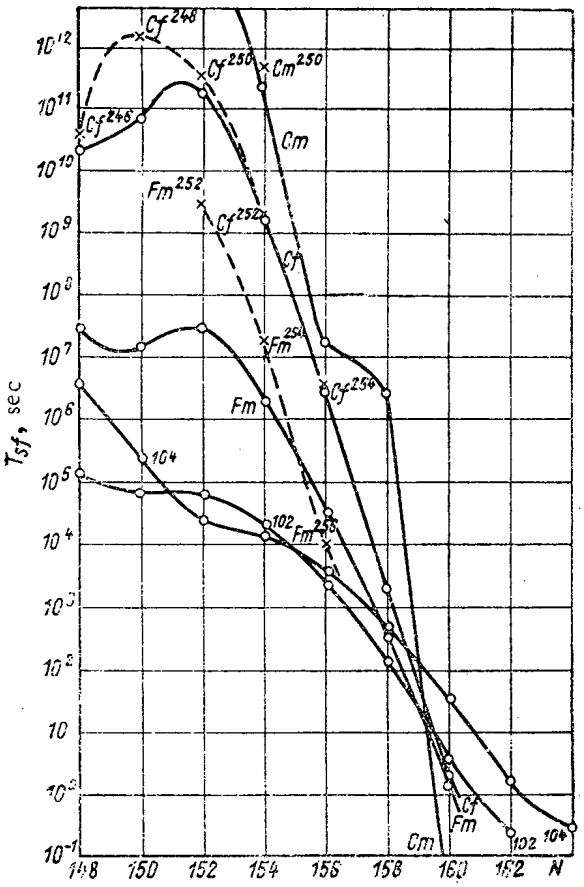

Fig. 3. Values of T_{sf} calculated by the Swiatecki-Dorn formula as a function of the number of neutrons N in the nucleus: —○— calculated values; - -×- - experimental data.

which this formula is valid. If we consider the new, still undiscovered elements immediately adjacent to those we have studied, the most reliable method of estimating their spontaneous-fission lifetimes still appears, up to the present time, to be the extrapolation of empirical curves of T_{sf} versus Z and A. For this purpose we may use, for example, curves of T_{sf} as a function of the number of neutrons N in the nucleus when Z is constant (Fig. 4), or of T_{sf} as a function of the number Z of protons in the nucleus when N is fixed (Fig. 5). Simple graphical extrapolation yields values of T_{sf} for elements 102 and 104 which differ considerably from the calculated values. In particular, a lifetime of 0.01-1 sec may be expected for the isotope 104^{260} on the basis of Figs. 4 and 5, while the Swiatecki-Dorn formula yields a value of one hour for the period.

A very important question in predicting the properties of elements is just how much the subshell with N = 152 affects the fission barrier for high values of A.

For very high A values, the parameter Z^2/A becomes considerably smaller than $(Z^2/A)_{N=152}$. According to the position of the hydrodynamic model, such nuclei should be more stable with regard to fission. The competition from the shell effect reduces the value of T_{sf}, but the importance of this effect may be considerably less beyond N = 152, and we may then expect a rise in the right-hand branches of the curves in Fig. 4. It is difficult to predict where this rise will begin. Johansson [7], analyzing the behavior of neutron levels up to the value of N = 160, concludes that the heavier isotopes of californium and fermium will have longer lifetimes than might be expected from graphical extrapolation. For example, the extrapolated value of T_{sf} for Fm^{258} is a few minutes, but Johansson estimates it at one hour. The value of T_{sf} similarly obtained for Cf^{256} is between one year and one month.

Only experimentation can provide the answers to all these questions. However, the experimental determination of the spontaneous-fission periods of some relatively heavy isotopes of fermium and californium is hampered by serious difficulties in the problem of synthesizing them.

In order to estimate the various possible ways of obtaining such isotopes, we shall first consider the present state of the problem of obtaining new transuranium elements and studying their properties, and we shall try to note some methods which will enable us to advance further into this range.

Synthesis of Transuranium Elements Using Multicharge Ions

The start of work in this direction in the USSR is closely linked with the name of Igor' Vasil'evich Kurchatov. The first reactor, the first cyclotron accelerating multicharged ions, and later the large heavy-ion accelerator at Dubna, were established with his direct participation, guidance, or enthusiastic support. The installation of the 300-cm cyclotron at the Joint Institute of Nuclear Studies, which makes it possible to obtain intense beams of ions in a wide range of Z and A values, opened a wealth of new possibilities for conducting experiments in the synthesis of new elements. Various multicharged ion accelerators have been set up and put into operation in a number of countries during the past few years.

Up to the present time, heavy ions have been successfully used to synthesize all previously known transuranium elements, as well as the new elements 102 and 103 (lawrencium) [12-15].

Judging by the successes achieved with this method, we may consider it the most promising for the synthesis of new elements. Nevertheless, the difficulties encountered in its use are so great that we are forced to analyze and test all processes which are even the least bit likely to extend the possibilities of this method.

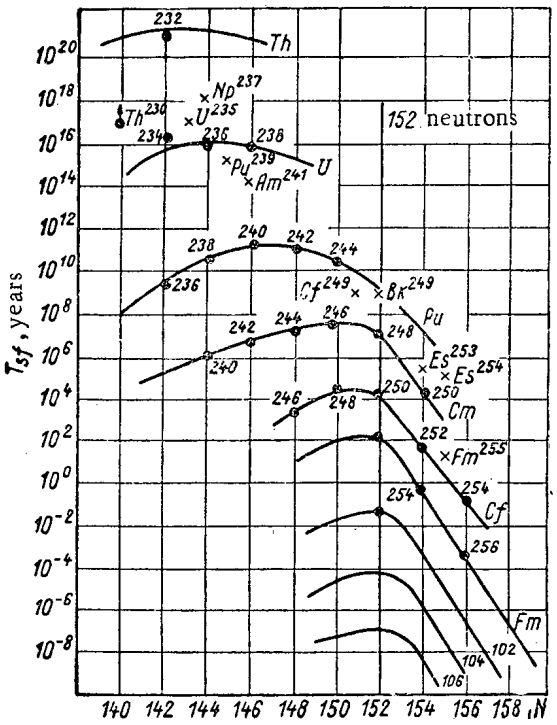

Fig. 4. T_{sf} as a function of the number N of neutrons in the nucleus.

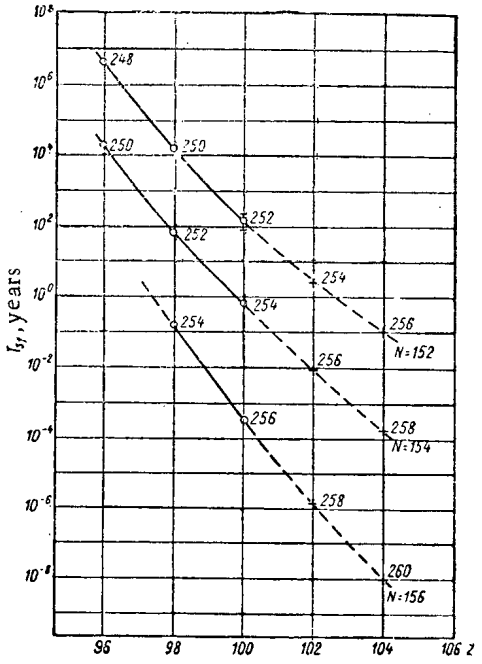

Fig. 5. T_{sf} as a function of the number Z of protons in the nucleus.

The synthesis of a heavy element B_Z^A from a target $A_{Z_1}^{A_1}$ and an accelerated ion $I_{Z_2}^{A_2}$ depends on a nuclear reaction of the type

$$A_{Z_1}^{A_1}(I_{Z_2}^{A_2}, xn)\,B_Z^A.$$

The heavy ion, accelerated to an energy somewhat greater than that of the Coulomb barrier, penetrates into the target nucleus with a cross section close to the geometric cross section and contributes all its kinetic energy to the compound nucleus. Since the nucleons in the compound nucleus are less firmly bound than in the target nucleus and in the nucleus of the heavy ion, part of this energy is expended in unpacking, and the remainder (usually 30-60 MeV), is used to excite the compound nucleus. The nucleus may release this energy by the evaporation of a number of nucleons (usually three to five). However, since we are dealing with heavy nuclei, i.e., nuclei with a low fission barrier, the main form of disintegration of the compound nucleus is fission, which usually predominates over all stages of nucleon evaporation. As a result, the yield cross sections of far transuranium elements are found to be smaller by several orders of magnitude than the geometrical cross sections and usually have values of 10^{-29} to 10^{-33} cm^2.

Sometimes a reaction of the type

$$A_{Z_1}^{A_1}(I_{Z_2}^{A_2}, He_2^4 xn)\,B_{Z-2}^{A-4}$$

is used to synthesize a heavy element. This reaction differs from the previous one in the fact that an alpha particle is emitted when the heavy ion is captured; in other respects, the process is similar. Since this case also includes an evaporation stage, the cross section of B_{Z-2}^{A-4} isotope formation is also smaller by several orders of magnitude than the geometrical cross sections.

Experimenters of today have at their disposal some fairly high-intensity ion beams containing $B^{10,11}$, $C^{12,13}$, $N^{14,15}$, $O^{16,18}$, and $Ne^{20,22}$, and a good supply of target materials from U^{238} to Cf^{252}. The choice of Z_1 for the target and Z_2 for the particle used to synthesize an element with a given $Z = Z_1 + Z_2$ remained uncertain for a long time. The hypothesis was expressed that increasing Z_2 by one, and decreasing Z_1 accordingly should reduce the yield cross section of the element with atomic number Z by a factor of ten. However, an analysis of studies made earlier [16, 17], and of the data obtained in [18] indicates that these estimates were too pessimistic. The transition from the synthesis of Fm^{250} by the $Pu^{241}(C^{13}, 4n)Fm^{250}$ reaction to the synthesis of Fm^{250} by the $Th^{232}(Ne^{22}, 4n)Fm^{250}$ reaction reduces the cross section only by a factor of 20, rather than by four orders of magnitude as was supposed earlier.

Thus, it is possible even today, in theory, to synthesize all the elements up to an including 108. However, when we try to apply this possibility, we encounter difficulties involving not the synthesis itself, but the study of the properties of the newly obtained elements and new isotopes.

Neutron evaporation reactions generally result in the formation of light isotopes of new elements which have a

short alpha disintegration lifetime. For this reason, chemical methods of identification cannot be used. This considerably complicates the entire investigative process and often reduces the reliability of its results.

The method of physical identification of a new alpha-active element with a short lifetime is based on the recording of alpha-activity with a systematically assumed energy. At the same time, all possible background influences must be eliminated. It has been found experimentally that in reactions with heavy ions in mixtures of lead, bismuth, and other elements in the target, alpha-active nuclei in the Ac—Po region may appear, with disintegration properties close to the expected properties of the new elements [13, 19].

Moreover, recent studies [20, 21] analyzing the products of Th + Ne nuclear reactions indicated that such background activity comes about as the result of deep-detachment reactions. The additional background sources may be unknown light isotopes of californium, fermium, etc.

Any further advance toward the synthesis of heavier elements by the alpha-activity recording method will become increasingly difficult, and its results will become less and less reliable. The reason for this is that as we pass to heavier particles, the number of background activities will increase and the cross sections of formation of new elements will decrease. At the present time, experimenters have approached the synthesis of element 104. This is the region in which spontaneous fission may come to predominate over other forms of disintegration.

It has been found considerably simpler to show that a new element has been formed by using its spontaneous fission than by using alpha disintegration or electron capture, since the absence of background makes the method very sensitive. The nuclei produced in the reactions taking place in the mixtures of the target cannot undergo spontaneous fission. To identify a new element it would be sufficient to use the complex study of the excitation functions of the formation of a spontaneously-splitting product (this would give the value of the atomic weight A) and the yields of a given nucleus under crossed irradiation of different targets by particles with varying A_1 and Z_1 values (to determine the atomic number Z of the product under consideration). However, in practice this has been found more complex than might have been expected.

It was shown in [22] that when heavy ions (Ne^{22}, O^{16}, B^{11}, etc.) interact with nuclei of uranium, we obtain a spontaneously splitting isotope with an anomalously small half-life (about 0.015 sec). A study of the excitation function for the formation of this isotope in various reactions led the authors to conclude that this synthesis takes place because some of the nucleons of the incident nucleus are transmitted to the target nucleus, and that it has an atomic number not exceeding 97. The maximum cross section of the $U^{238} + Ne^{22}$ reaction is approximately $2 \cdot 10^{-32}$ cm^2. On the other hand, the cross section of the $U^{238} + B^{11}$ reaction is several times the above value in experiments with neon. The authors suggest the hypothesis that the observed effect is caused by spontaneous fission from the isomeric state. Indeed, if U^{238} is irradiated with B^{11} ions, we obtain known isotopes with elements with $Z \leq 97$. All of these have in the ground state a lifetime considerably greater than 0.015 sec, while the spontaneous-fission periods T_{sf} of these isotopes are found to be not less than 10^7 years. It follows from this that the spontaneous fission of the resulting nuclei has been made easier by a factor of more than 10^{16}.

Thus far no direct evidence exists as to whether this isomeric is a unique case or whether the phenomenon is widespread in nature and isomers with various lifetimes may be found in the reactions concerned. An extensive study of these nuclei will make it possible to obtain further information on the mechanism of "ordinary" spontaneous fission.

Thus, the problem of synthesizing and identifying transfermium elements by their spontaneous fission from the ground (unexcited) state is found to be related to the obtaining of the heaviest isotopes; this would make it possible to make not only physical studies of the new elements, but chemical studies as well, and would considerably increase the reliability of the identification.

After these preliminary remarks, we shall now consider a number of possible reactions which would enable us, in theory, to synthesize a nucleus with a number of neutrons considerably exceeding the "magic" number N = 152; this could not be achieved by neutron evaporation reactions even if the heaviest targets were used. For example, if Cm^{248} is irradiated with C^{13} ions, we cannot obtain isotopes of element 102 with a weight of more than 257; irradiation with N^{15} cannot produce isotopes of element 103 heavier than 259, and these isotopes, as is indicated by the systematic study, should have short lifetimes.

Incomplete-Fusion Reactions Using Heavy Particles. If Ar_{18}^{40} or Ca_{20}^{8} is used as the bombarding particle, we may hope that in the reaction involving boundary interaction with the target nucleus there will be capture of a considerable portion of the incident particle, and the nucleus will remain near the ground state.

As an example, let us consider reactions to synthesize a number of heavy isotopes of fermium, using the interaction of Ar^{40} with uranium:

$$U^{238} + Ar^{40} \longrightarrow Fm^{256} + Ne^{22};$$
$$U^{238} + Ar^{40} \longrightarrow Fm^{258} + Ne^{20};$$
$$U^{238} + Ar^{40} \longrightarrow Fm^{260} + Ne^{18}.$$

Our hopes of success of such reactions are based on the following: First of all, these reactions are threshold reactions, and their thresholds lie above the Coulomb barrier. The reason for this is that oxygen nuclei are captured from the bound state in the Ar^{40} into the bound state in fermium. Consequently, there is an energy range of the bombarding particles within which any considerable excitation of the fermium nuclei will be impossible, from energy considerations, so that there will be neither nucleon evaporation nor fission. In the second place, we have at our disposal data indicating that in reactions with multicharged ions there has been observed a considerable yield of such products, which may be formed, in particular, by a mechanism noted above (for example, $U^{238} + N^{14} \rightarrow Cm^{242-244}$). In the third place, we know reliably [21] that a large cross section is found in the reactions which include the capture of a large number of nucleons of the target nucleus by the incident particle. If the mass and charge of this particle are increased, by accelerating, for example, argon or heavier elements, we may expect the reverse reaction to take place as well: the reaction in which a large number of nucleons from the incident particle are captured by the target nucleus.

In order to check this method, it is most convenient to use the first of the above reactions, in which we obtain the spontaneously splitting isotope Fm^{256} with T_{sf} = 2.7 hours, which should assure a high degree of sensitivity.

Radiative Capture of a Heavy Ion. A second possibility for approaching the region of beta stability may be found in reactions involving the radiative capture of a heavy ion. In these reactions, the emission of a high-energy gamma quantum should reduce the excitation energy of the compound nucleus to a level below the fission threshold. Such reactions should yield products with mass numbers four units greater than those usually obtained in nucleon evaporation reactions. Clearly, the process of emission of one high-energy gamma quantum from a heavy compound nucleus will constitute little competition for the processes of fission and nucleon evaporation. Nevertheless, the fact that in this process there is only one stage of emission of a gamma quantum $[\Gamma_\gamma / (\Gamma_f + \Gamma_n + \Gamma_p + \Gamma_\gamma)]^1$, as compared to the usual four stages of neutron evaporation $[\Gamma_n / (\Gamma_n + \Gamma_f)]^4$, gives some hope that the effective cross section of this process will not be very small.

Unfortunately, at present there are only a very small number of studies [23, 24] devoted to reactions involving radiative capture of a heavy ion, and all of these investigations were carried out on light targets. In this case the cross section is about 10^{-30} cm^2. There is no way of obtaining from this result a cross section corresponding to the region of heavy transuranium elements.

Here, we believe, the simplest procedure is to establish experimentally the cross section for the radiative capture of O^{18} by a U^{238} nucleus to form Fm^{256}:

$$U^{238}(O^{18}, \gamma) Fm^{256}.$$

The sensitivity of this method, when a 100-μA current of O^{18} ions is used, enables us to observe reactions taking place with a cross section of 10^{-35} cm^2. The effect in the case of such a cross section is about ten fissions per hour.

Nucleon Evaporation Reactions Using the Products of Nuclear Reactions as Bombarding Particles. Let us consider in some more detail the data obtained in [21].

When Th^{232} was irradiated with Ne^{22} ions, the authors of the present study observed large-scale emission of the isotopes Ac^{224}, Ac^{225}, Ac^{226}, and Th^{227}. The only mechanism capable of explaining this result is the stripping of a number of nucleons from the target nucleus. At the same time, the authors obtained data indicating that the stripped nucleons, in all probability, were transferred to the incident particle. Thus, when Th^{232} is irradiated with Ne^{22} ions, there is a beam of secondary particles which will include very heavy isotopes of neon, sodium, and magnesium.

Let us estimate the possible intensity of the beam of secondary particles. Starting from the data of the study, it may be expected that the cross section of formation of these particles may be about 10^{-27} cm^2. With a 100-μA current of Ne^{22} ions and a Th^{232} target with a thickness of 10 mg/cm^2, we shall have about 10^6 particles per second. Putting aside the question of the energy distribution of the secondary particles, we note that such a beam is completely

adequate for the study of reactions taking place with a cross section $\geq 10^{-28}$ cm^2, if the reaction products make possible the recording of several events per hour.

A cross-section value of 10^{-28} cm^2 is not too large even for the region of far transuranium elements, since the fissility of the compound nucleus in this case must be considerably reduced by reason of its increase in mass, and the neutron evaporation process can successfully compete with the fission process. In each case, the possibility can be checked without much difficulty; we can do this by irradiating a thick Th^{232} target with Ne^{22} ions of sufficiently high energy. The thorium will not only transform the beam, but will also serve as the target at which the $Th^{232}(Ne^{28},4n)Fm^{256}$ and $Th^{232}(Na^{28}, 4n)Md^{256} \xrightarrow{\text{electron capture}} Fm^{256}$ reactions will take place.

The means of synthesis of enriched neutrons of the far transuranium elements which we have considered above could considerably widen, in our opinion, the possibilities in this direction of the method of multicharged ions.

It remains only to note certain particular cases in which individual heavy nuclei are obtained, and to analyze briefly the reactions involving the evaporation of protons from compound nuclei, since such reactions also lead to the formation of heavy isotopes of transuranium elements.

From the viewpoint of a systematic study of spontaneously splitting nuclei, the synthesis of Cf^{256} and Fm^{258} is of great interest, since the lifetimes of these isotopes, as estimated by different methods, are too contradictory.

The isotope Cf^{256} may be synthesized, in quantities sufficiently large for study, by a reaction of the type $Cf^{254}(O^{18}, O^{16})Cf^{256}$, provided the experimenter has at his disposal at least 10^{10} nuclei of Cf^{254}.

In reactions involving multicharged ions [for example, $Cm^{248}(B^{11}, 4n)Md^{255} \xrightarrow{\text{electron capture}} Fm^{255}$, for which $T_{\frac{1}{2}}$ = 21.5 hours], we can accumulate about 10^9 nuclei of Fm^{255}; if the reaction in which three neutrons are captured by some particle takes place with a cross section of about 10^{-26} cm^2, we can synthesize enough Fm^{258} for study (several disintegrations per hour).

Reactions involving the evaporation of charged particles provide another possibility of obtaining relatively heavy isotopes. For example, $Pu^{242}(Ne^{22}, p3n)103^{260}$ may be such a reaction. There is good reason to expect the isotope 103^{260} to be unstable with respect to electron capture. Electron capture will result in the formation of the isotope 102^{260}, which should be spontaneously fissile.

The $(Ne^{22}, p3n)$ nuclear reaction was used successfully to synthesize element 101, Md^{256}, by irradiating U^{238} [25, 26]. A similar reaction involving the evaporation of a proton and two neutrons may yield still heavier isotopes. In particular, it may be hoped that the $Pu^{242}(Ne^{22}, p2n)103^{261}$ reaction will yield a relatively long-lived isotope of element 103.

A reaction in which a proton and only one neutron are emitted is very unlikely. The reason for this is the small cross section of formation of a compound nucleus in the case of a low-energy incident particle. Experiments indicate that the cross section of the $U^{238}(Ne^{20}, pn)Md^{256}$ reaction is not more than 10^{-36} cm^2. This sets a limit to the use of charged-particle evaporation reactions in synthesizing heavy isotopes.

Conclusion

The further study of the properties of spontaneous fission is closely related to an advance into the region of still undiscovered elements and to the synthesis of heavy isotopes of californium, fermium, and element 102.

Moreover, a study of the phenomenon in which we are interested – the fission of isomers of the transuranium elements and the nuclear reaction in which they are formed – will also provide a great deal of new information on the mechanism of nuclear fission from the ground state.

On the basis of recent studies establishing a relationship between the probability of spontaneous fission and the energy-level distribution of nucleons in the nucleus [7, 27, 28], we may hope to obtain additional information on the structure of nuclei if we study their periods of spontaneous fission.

Furthermore, by studying the rules of variation of the periods of spontaneous fission over a wide range of Z and A values, we may be able to answer the question of how important spontaneous fission is for those isotopes of transfermium elements which ought to be obtained in the very near future.

The synthesis of a new element is a very complex problem. To solve this problem we must develop a large number of different specialized methods, and the choice of any particular method will depend to a great extent on the type of disintegration and the lifetime of the element under study. The more we know about spontaneous fission, the more exactly we will be able to determine T_{sf} for the new element, and the greater will be our chances for a successful solution of the problem of synthesis.

Thus, the problem of the further study of the rules governing spontaneous fission and that of the synthesis of new elements, are inseparably connected, so that progress in one yield will necessarily constitute progress in the other.

LITERATURE CITED

1. N. Bohr and J. Wheeler, Phys. Rev., 56, 426 (1939).
2. K. A. Petrzhak and G. N. Flerov, ZhETF., 10, 1013 (1940).
3. G. Seaborg, Phys. Rev., 85, 157 (1952).
4. B. Foreman and G. Seaborg, J. Inorg. and Nucl. Chem., 7, 305 (1958).
5. V. Druin, I. Brandshtetr, and Ya. Maly, OIYaI Preprint, P-875 (Dubna, 1962).
6. S. Nilsson, Symposium: Deformation of Atomic Nuclei [Russian translation] (IL, Moscow, 1958).
7. S. Johansson, Nucl. Phys., 12 , 449 (1959).
8. W. Swiatecki, Phys. Rev., 100, 937 (1955).
9. D. Dorn, Phys. Rev., 121, 1740 (1961).
10. A. Cameron, Report CRP-690 (1957).
11. D. Dorn, Phys. Rev., 126, 639 (1962).
12. P. Fields et al., Phys. Rev., 107, 1460 (1957).
13. G. N. Flerov et al., DAN SSSR, 120, 73 (1958).
14. A. Ghiorso et al., Phys. Rev. Lett., 1, 18 (1958).
15. A. Ghiorso et al., Phys. Rev. Lett., 6, 473 (1961).
16. T. Sikkeland, S. G. Thompson, and A. Ghiorso, Phys. Rev., 112, 543 (1958).
17. V. V. Volkov et al., ZhÉTF., 37, 1207 (1959).
18. E. D. Donets et al., ZhÉTF., 43, 11 (1962).
19. G. N. Flerov et al., ZhÉTF., 38, 82 (1960).
20. I. Brandshtetr et al., OIYaI Preprint, P-978 (Dubna, 1962).
21. G. Kumpf and E. D. Donets, OIYaI Preprint, P-1071 (Dubna, 1962).
22. S. M. Polikanov et al., ZhÉTF., 42, 1464 (1962).
23. D. Fisher, A. Zucker, and A. Gropp, Phys. Rev., 113, 542 (1959).
24. R. Coleman, D. Herbert, and J. Perkin, Proc. Phys. Soc., 77, 526 (1961).
25. G. Béranova et al., OIYaI Preprint, P-856 (Dubna, 1962).
26. V. A. Druin, OIYaI Preprint, P-874 (Dubna, 1962).
27. J. Wheeler, Symposium: Niels Bohr and the Development of Physics [Russian translation] IL, Moscow, 1958).
28. J. Newton, Progr. in Nucl. Phys., 4, 234 (1955).

All abbreviations of periodicals in the above bibliography are letter-by-letter transliterations of the abbreviations as given in the original Russian journal. *Some or all of this periodical literature may well be available in English translation.* A complete list of the cover-to-cover English translations appears at the back of this issue.

INVESTIGATION OF PROPERTIES OF μ-MESIC ATOMS AND μ-MESIC MOLECULES OF HYDROGEN AND DEUTERIUM AT THE DUBNA 680-MeV SYNCHROCYCLOTRON

V. P. Dzhelepov

Translated from Atomnaya Énergiya, Vol. 14, No. 1,
pp. 27-37, January, 1963
Original article submitted September 14, 1962

The first stages in the development of a new field of physics in our country, the physics of high-energy particles, are linked to the building of the synchrocyclotron at Dubna in 1949. This machine is capable of producing protons of 680 MeV, and pions and muons of energies up to 400 MeV. An important initiating and managing role is credited to the late Igor' Vasil'evich Kurchatov both in the stages of the installation and assembly of this unique accelerator, and in the stages of performing research on the machine. Being in possession of a broad scientific horizon typical of an outstanding scientist and prominent public activist, in harmony with the solution of the country's most pressing and grandiose large-scale problems in practical applications of nuclear energy, Igor' Vasil'evich always took the long forward view and expended intense efforts in cementing the necessary base for the future potentialities in scientific research in the field of the atomic nucleus and elementary particles. The Nuclear Problems Laboratory, where the accelerator was installed, was over a long period a branch of the Institute of Atomic Energy of the USSR Academy of Sciences, over which I. V. Kurchatov presided in the post of Director. The 680-MeV synchrocyclotron, now turned over to the Joint Institute of Nuclear Research, has made it possible to complete a huge volume of research on a variety of topics, with extremely valuable scientific results.*

I. V. Kurchatov consistently felt a passionate urge in science toward what was new, important, of broad scope, and appealed to his disciples to follow in that direction. It is a pleasure for us to report, in this issue of the periodical which is devoted to the memory of our beloved teacher, on one of these new trends in research developed in recent years in work with the Dubna synchrocyclotron, the study of mesoatomic and mesomolecular processes in hydrogen, all the more so in that some of these investigations touch on the problem of the thermonuclear fusion of light elements, to the study of which Igor' Vasil'evich devoted, with the tremendous involvement and energy characteristic of him, the last years of his scientific activities.

Introduction

As a result of the completion of a number of high-precision experiments with μ-mesons (measurement of the gyromagnetic ratio of the μ-meson [1], study of muon scattering on carbon [2], etc.), particularly in recent years, it has been established to a high order of reliability that the μ-meson, possessing a mass 200 times larger than that of the electron, is entirely similar to the electron in its electromagnetic properties. One of the manifestations of this similarity is the fact that negative muons may be captured into atomic orbits and there form mesic atoms and mesic molecules of various elements, in a manner similar to the way electrons form the familiar atomic and molecular systems. The distinguishing features of mesoatomic systems are, however, the fact that the lifetimes of these systems are relatively short and are determined, in the case of the light elements, by the lifetime of the μ-meson ($2.2 \cdot 10^{-6}$ sec), while their dimensions are approximately 200 times smaller than the dimensions of conventional atoms. Mesoatoms and mesomolecules constitute a great new world of particles of matter existing in a very special state. In this article, we shall be dealing with a study of the properties of mesoatoms of the simplest element, hydrogen.

The radius of the first Bohr orbit of the hydrogen mesoatoms is at most $2.5 \cdot 10^{-11}$ cm, and this fact, along with the electroneutrality of these atoms, leads to a whole series of specific physical phenomena.

*The most important of these results have been published in the periodical Atomnaya Énergiya in articles authored by V. P. Dzhelepov and B. M. Pontecorvo, 3, 11, 413 (1957), and D. I. Blokhintsev, 10, 4, 317 (1961).

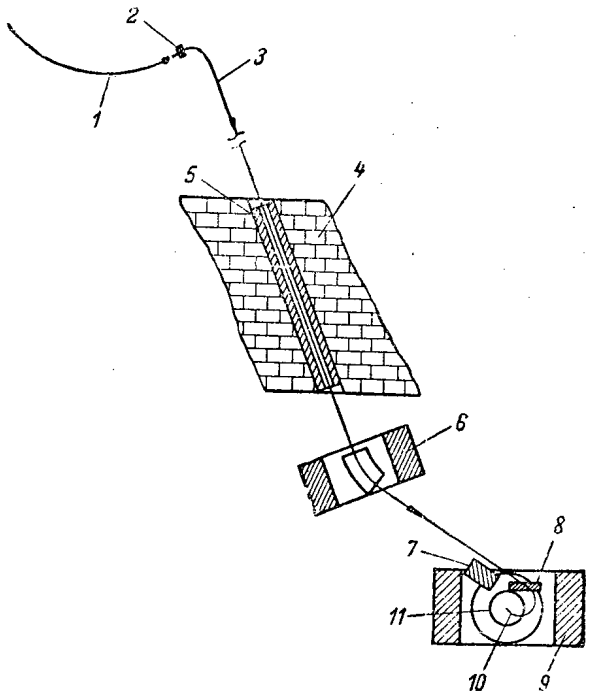

Fig. 1. Arrangement of experimental equipment. 1) Inner proton beam from 680-MeV synchrocyclotron; 2) beryllium target; 3) μ^-- and π^--mesons, of 260 MeV/c momentum; 4) shielding wall; 5) collimator; 6) deflecting and defining magnet; 7) lead shield; 8) copper filter; 9) diffusion-chamber solenoid magnet; 10) stopping of μ^--mesons; 11) diffusion chamber.

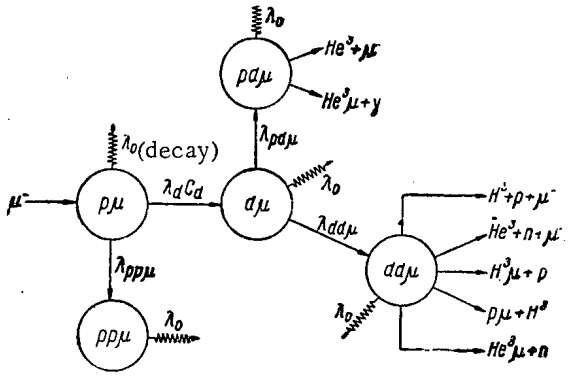

Fig. 2. Scheme of mesoatomic and mesomolecular processes and nuclear reactions between hydrogen isotopes, with μ^--mesons in a hydrogen-deuterium mixture as causal factors.

The most salient and interesting of these phenomena may be termed the catalysis of μ-mesons of nuclear reactions between hydrogen isotopes. The possibility of such a process had been predicted theoretically by the Soviet scientists A. D. Sakharov and Ya. B. Zel'dovich [3], and independently by F. Frank [4] in the West. The phenomenon of muon catalysis was first detected experimentally by L. Alvarez and co-workers [5] in 1957. One characteristic trait of the process is that, in the presence of μ-mesons, nuclear reactions involving hydrogen isotopes may go ahead in "cold" hydrogen while, for example in thermonuclear reactors, plasma must be heated to millions of degrees to bring about fusion. The brief lifetime of the μ-meson, as well as the fact that the meson has a certain probability of forming a helium μ-mesoatom in the p + d and d + d reactions, render impossible the achievement of a sustained nuclear chain reaction by means of μ-mesons. Nevertheless, because of the fact that nuclear reactions brought about by μ-mesons not infrequently take place under conditions entirely distinct from those under which they are observed in accelerator arrangements, the study of μ-meson catalysis may well furnish a source of new information on nuclear reactions at very low energies.

The heightened interest displayed by physicists in μ-mesoatomic processes in hydrogen, as of recent years, is due in large measure to that peculiar part played by these processes in the solution of one of the fundamental problems in the contemporary physics of elementary particles – that of determining the value of the weak muon-nucleon interaction constant from experiments on the capture of muons by protons:

$$\mu^- + p \longrightarrow n + \nu. \qquad (1)$$

In actual practice, this reaction proceeds in hydrogen from the pμ-mesoatom state or the ppμ-mesomolecule state. It has been demonstrated theoretically [6-8] that the probability of reaction (1) depends on the spin state of the original system. As a result of the fact that the μ-meson has half-integral spin ($S_\mu = \frac{1}{2}$),* the ground level of the pμ-mesoatom is split into two sublevels belonging to a hyperfine structure of total spins equal to zero and unity. Similarly, the spin state of the mesomolecule ppμ may be represented as a mixture of singlet and triplet states. This means that a correct interpretation of the rate of reaction (1) as measured in an experiment requires that quantitative data be available on the probability of formation of ppμ-mesomolecules, and that a solution be reached to the problem of what spin state the pμ-mesoatom is in prior to capture. The urgency of the problems referred to has stimulated the development of experimental research at the Joint Institute on mesoatomic processes and on the catalysis of nuclear reactions in hydrogen and deuterium, as well as deeper probing into the theory underlying these phenomena.

*The fact that the spin of the μ-meson is one-half was first established by investigations reported by A. E. Ignatenko et al. [9], performed on the synchrocyclotron of the Nuclear Problems Laboratory at the Dubna Joint Institute.

The article sheds light on the principal results amassed in the first stage of these investigations, as reported at the July 1962 International Conference on the Physics of High-Energy Particles at Geneva [10, 11]. These investigations were completed in the 1960-1962 period by a team of Joint Institute workers including S. S. Gershtein, P. F. Ermolov, Yu. V. Katyshev, E. A. Kushnirenko, V. I. Moskalev, M. Friml, and the author of this article.

Our attention was concentrated on the study of the following phenomena: elastic scattering of $p\mu$-mesoatoms on protons, the jumping of a μ-meson from a proton to a deuteron, the formation of $pp\mu$-mesic molecules, μ-catalysis of (p + d)- and (d + d)-reactions, the probabilities of formation of the corresponding mesic molecules, and the jumping of μ-mesons from protons and deuterons to complex nuclei.

The existing theoretical development of the circle of phenomena discussed is presented in [8, 12-14], and opens up rather broad vistas for comparison of experimental material and theoretically computed data. As the material is presented in its full scope, the amount of harmony between experimental results and theory, as well as the attendant complications, will become evident.

1. Experimental Procedure

The study of mesoatomic and mesomolecular processes in hydrogen is a relatively complicated job. This is due, in the first instance, to the multiplicity of possible phenomena and the need to separate out each of these variants in some reliable manner. The second major difficulty is of a more basic nature. The trouble here is that some of the processes (e.g., formation of mesomolecules) do not present a directly observable effect and the absolute probability of these processes may be determined either by some indirect approach or as a result of the observation of the yields from the corresponding nuclear reactions. We must take cognizance here of the fact that the energies of the reacting particles are very low, and the ranges of the reaction products in condensed-phase material (liquid hydrogen) are also very short. Several processes, e.g., diffusion of $p\mu$-mesic atoms, are in general impossible to observe directly when the hydrogen density is very high.

Analysis shows that most of these difficulties can be coped with successfully when the processes are studied in a gaseous medium. Our investigations therefore involved the use of a diffusion chamber filled with either hydrogen or a mixture of hydrogen and deuterium. The use of ordinary industrial-grade deuterium could not be countenanced in these experiments, since this grade always contains tritium in relatively large quantities (about 10^{-12} at. fract.),and the radioactivity of the tritium results in a complete deterioration of chamber sensitivity. It was mandatory, therefore, to fill the chamber with specially purified deuterium in which the tritium concentration was kept below $5 \cdot 10^{-14}$ at. fract. Special experiments were set up to determine the effect associated with the robbing of μ-mesons by the complex nuclei of the ambient medium, i.e., the vapors of the chamber working fluid (oxygen, carbon). One contributor to improved conditions for identifying events and enhancing chamber efficiency in revealing stopping of μ-mesons was the fact that the chamber was operated in a magnetic field of 7000-Oe intensity.

A diagram showing the layout of the apparatus at the exit of the meson beam from the synchrocyclotron is shown in Fig. 1. Muons and pions of 260-MeV/c momentum, generated by 680-MeV protons from the synchrocyclotron, were employed in the experiments. Since μ-mesons form mesic atoms and mesic molecules under conditions where their speed is close to the speed of the orbital electrons belonging to the atoms, the μ-mesons are slowed down directly prior to their energy into the chamber in a filter installed near the chamber wall, to such a low speed that, on entering the chamber, they are brought to rest in the gas filling the chamber. The filter thickness is made such that the π-mesons present in the beam will be fully absorbed and fail to gain entry into the diffusion chamber.

Under usual operating conditions, one stoppage of a μ-meson was observed in every three to five stereophotographic shots of the chamber sensitive volume. Two hundred thousand stereophotographic shots were taken. They were processed with the aid of a projector and measuring microscope.

2. Scattering Cross Sections: $p\mu$-Mesoatoms on Protons

The multiplicity of processes brought about by μ-mesons in a hydrogen–deuterium mixture may be illustrated graphically by the layout presented in Fig. 2. The initial system (low deuterium concentration in the hydrogen) for the subsequent processes was the $p\mu$-mesic atom existing in the 1S-state and moving at thermal speed. At all stages along the chain of mesoatom transformations listed in the scheme, muon decay acted as a competing process: $\mu^- \rightarrow e^- + \nu + \tilde{\nu}$, proceeding at a rate $\lambda_0 = 0.45 \cdot 10^6$ sec^{-1} (denoted by the broken line).

One of the simplest processes occurring in hydrogen with the participation of $p\mu$-mesoatoms is scattering of the latter on protons. This scattering may be either elastic or inelastic. The latter case results in a transition of the $p\mu$-

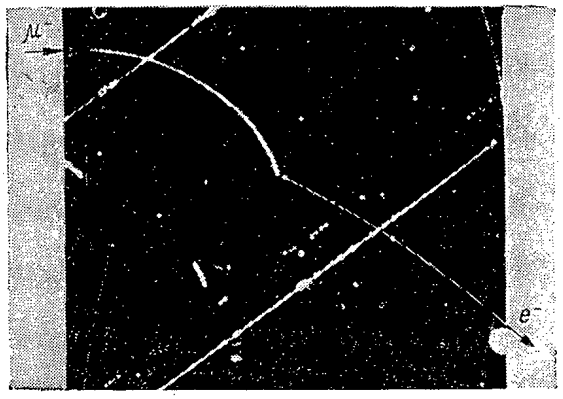

Fig. 3. Formation of $p\mu^-$-mesoatoms in gaseous hydrogen. The slow μ^--meson formed, at the point where it was brought to rest, a $p\mu$-mesic atom, which traversed by diffusion a path of about 1 mm (the gap from the end of the μ^--meson track and the beginning of the electron track). At the end of the diffusion path, the μ^--meson jumped from the proton to a complex impurity atom, and decayed. A "point" (Auger electron) is clearly visible at the start of the decay-electron track.

mesic atom from the energetically higher triplet state to the singlet state.* The spin realignment, according to S. S. Gershtein's calculations [15], is necessarily a rapid process proceeding to completion in $5 \cdot 10^{-10}$ sec at the density of liquid hydrogen. One of the consequences of this spin realignment must be the rapid depolarization of muons which had been longitudinally polarized as a result of decay.

Experiments on the measurement of muon depolarization in liquid hydrogen, carried out with the synchrocyclotron in our laboratory [16], apparently serve to confirm this inference. We note that depolarization is determined, in this experiments, on the basis of measurements of the asymmetry in the angular distribution of electrons from muon decay, by the method of the precession of the spin in a magnetic field.

Another possible effect due to spin realignment should be, again as demonstrated theoretically by S. S. Gershtein, the fact that the elastic scattering cross section for scattering on protons of mesic atoms in the singlet state ($\sigma^0_{p\mu+p}$) turn out roughly two orders of magnitude smaller than the cross sections in the triplet state. This circumstance, in principle, opens the way for the solution of one of the most crucial and pressing problems outstanding in the area of muon-proton interactions, that of determining from experiment the spin state of the $p\mu$-mesoatom from which the capture of the μ-meson by the proton took place.

In order to study elastic scattering, we availed ourselves of the same principle which underlies the measurement of the thermal neutron scattering cross section, namely measuring the diffusion length in hydrogen of the $p\mu$-mesoatom over a finite time interval. Since the formation of mesic molecules may be neglected at low hydrogen densities, the diffusion time is determined principally in terms of the probability of free muon decay and the probability of the muon jumping to complex nuclei. Since the $p\mu$-mesic atom fails to produce any ionizing effect in its motion, the diffusion process of the $p\mu$-mesic atom must be observed, in diffusion chamber photographs, as a displacement of the origin of the track of the decay electron relative to the end of the track of the stopped μ-meson (as a discontinuity or gap between the end of one track and the beginning of the other). Actually, in the course of the first experiment, with the hydrogen pressure in the chamber placed at about 20 atm, such displacements were successfully observed in dimensions of from the half-width of a μ-meson track (0.25 mm) to 1.5 mm. An example of this case is shown in Fig. 3. Further experiments were carried out both at high hydrogen pressure (23 atm) and at low hydrogen pressure (5 atm). The concentration of complex nuclei was varied in several experiments. It was found, however, that the extent, and, consequently, also the frequency of appearance, of the visible displacements is mainly a function of the hydrogen density. One clear illustration of this is the following fact. At a hydrogen pressure of 23 atm, of 320 $(\mu - e)$-decays in 49 cases (i.e., in 15% of the cases) gaps whose dimensions exceeded 0.5 mm were observed, while the number of such gaps amounted to 50% at 5 atm hydrogen pressure, even though the concentration of complex nuclei in the second experiment was almost triple that in the first experiment. The elastic scattering cross section for $p\mu + p \rightarrow p\mu + p$ was found from the expression

$$\sigma_{p\mu+p} = \frac{1,1\bar{v}}{\overline{r^2}N(\lambda_0 + \lambda'_z C_z)}, \qquad (2)$$

where $\bar{v}$ is the mean velocity of the relative motion of $p\mu$ and H_2 ($\bar{v} = 2.7 \cdot 10^5$ cm/sec); r^2 is the root mean square of the gaps computed from the distribution of the number of events over the gap lengths; N is the number of protons per cubic centimeter; $\lambda_0 + \lambda'_Z C_Z$ is the sum of the rates of free muon decay and jumping to carbon and oxygen nuclei at

*The energy of the hyperfine structure triplet level in the $p\mu$-mesic atom, with total spin F = 1 is 0.2 eV higher than the energy of the singlet state with F = 0. The reverse transition (from singlet to triplet) is impossible then, on account of the low value of the energy of the mesoatom's motion compared to the energy difference in the F = 0 and F = 1 levels.

a concentration C_Z determined in subsequent experiments (cf. section 5). The expression (2) takes cognizance of the fact that, in real hydrogen, scattering occurs not on free protons, but on H_2 molecules. The value of the cross section $\sigma_{p\mu + p}$, determined with the aid of expression (2) on the basis of experimental data for $\bar{r}^2$, λ_Z', and C_Z, was found to be $(1.7^{+0.4}_{-0.5}) \cdot 10^{-19}$ cm^2. A comparison reveals that this value is roughly 20 times greater than that predicted by theory for the value of the scattering cross section of mesic atoms in the singlet state, which is $\sigma^0_{p\mu + p} \leqslant 10^{-20}$ cm^2 [17]. This fact greatly complicates the situation and offers no direct proof (as might be anticipated on the basis of muon depolarization data for liquid hydrogen) of the existence of fast transitions of $p\mu$-mesoatoms from the F = 1 state to the F = 0 state. Two avenues are open in interpreting the large value of the $(p\mu + p)$-scattering cross section: either the F = 1 → F = 0 transitions actually proceed at a slower pace and then scattering in the triplet state (which, as noted above, is considerable) introduces its contribution to the globally measured cross section, or else the true parameters of the mesomolecular potentials determining the principal characteristics of the processes occurring in the $p\mu + p$ system will differ from those assumed in the theoretical treatment. In our later discussion, with the aim of achieving a correct grasp of the experimental facts and drawing a more definite conclusion on the true rapidity of the transitions occurring in the $p\mu$-mesic atom between the hyperfine structure states (determining the spin state of the $p\mu$-mesoatom), we will have to make a detailed analysis, based on a large volume of statistical data, of the distribution pattern over the lengths of the ranges (gaps) of $p\mu$-mesoatoms in order to explain the possible existence in these mesic atoms of two components with large and small values of $\bar{r}^2$ corresponding to scattering in the singlet and triplet states, on the one hand; on the other hand, we will have to carry out a combined theoretical analysis of the most fundamental processes pertaining to the $p\mu + p$ system, such as scattering, depolarization of μ-mesons, formation of $pp\mu$-mesic molecules, etc., and we will have to find the parameters of the μ-mesomolecular potentials satisfying these processes. The investigations of this problem at the Dubna Joint Institute for Nuclear Research progressed in both the directions outlined.

3. Probability of Jumping of a μ-Meson from a Proton to a Deuteron, and Formation of $pp\mu$-Mesomolecules

When a slight deuterium admixture is present in hydrogen, the diffusing $p\mu$-mesoatom may pass close by a deuteron. Owing to the fact that the K-level of the $d\mu$-mesoatom is situated 135 eV below the K-level of the $p\mu$-mesoatom, jumping of the μ-meson from the proton to the deuterium,

$$p\mu + d \longrightarrow d\mu + p\,, \tag{3}$$

is highly favored. The difference in the binding energies of the μ-meson on the K-shells of the corresponding mesoatoms in process (3) goes over into the kinetic energy of the relative motion of the nuclei exchanging the μ-meson. The probability of process (3) is proportional to the concentration of deuterium but, as shown by theory, even at a deuterium concentration of roughly 1% in hydrogen, the probability of this process begins to dominate over all other rivals in this system of processes. It is evident from Fig. 2 that the $d\mu$ system is the initial system for the formation of $dd\mu$- and $pd\mu$-mesic molecules in which nuclear fusion is later realized. It is therefore obvious that an experimental determination of the absolute probability of process (3) (the rate value which we designate by the symbol λ_d) is of first-ranking significance.

If we remember that, as a result of the transition (3), the $d\mu$-mesic atom acquires a relatively high energy (about 45 eV) and may range over a path of roughly 1 mm in liquid hydrogen,* then the attempt to find the value of λ_d from liquid-hydrogen experiments with very slight deuterium admixtures will appear to be not at all hopeless. However, the path turns out to be a closed one. This is chiefly due to the fact that process (3) suffers competition in liquid hydrogen by the relatively intense process of formation of $pp\mu$-mesic molecules:

$$p\mu + \mathrm{H\ (hydrogen\ atom)} \longrightarrow pp\mu + e^-\,. \tag{4}$$**

It is precisely the mutual superposition of these processes which thwarts a direct experimental determination, in liquid hydrogen, of the absolute probability of process (3) from the number of observed events featuring such gaps. The use of a diffusion chamber offers tremendous advantages in such experiments, since the lower density of hydrogen renders

*L. Alvarez et al. [5], in liquid hydrogen bubble chamber experiments involving slight natural impurities of deuterium (1 deuteron per 10,000 hydrogen atoms), observed gaps of precisely this dimension.

**In process (4), the binding energy of mesic molecules (approximately 100 eV) is imparted to the electron of the hydrogen atom as a result of an electric dipole transition. In the $pp\mu$ system, the catalysis reaction is extremely improbable under ordinary conditions [12].

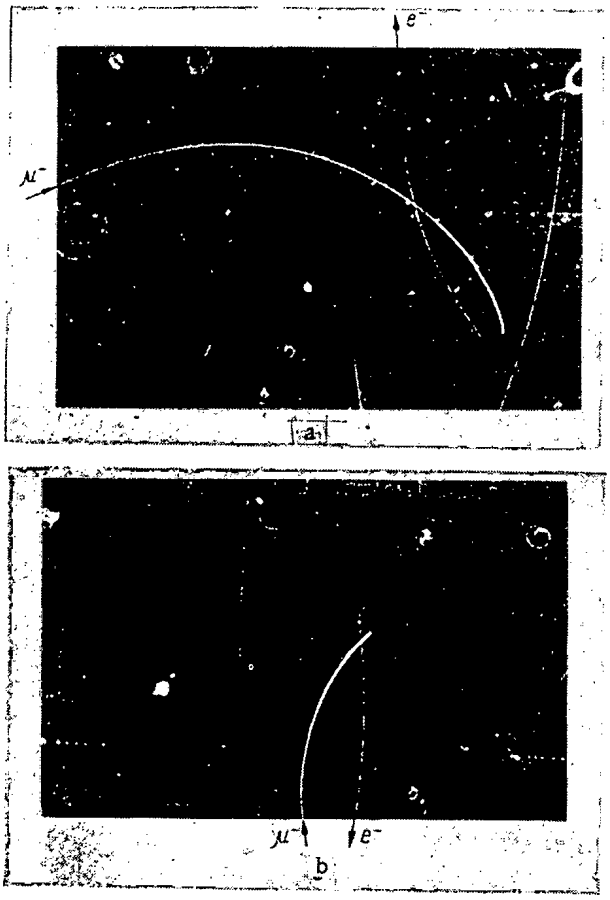

Fig. 4. Formation of dμ-mesoatoms in gaseous hydrogen with deuterium impurity. Large gaps (8 - 10 mm) from the end of the μ^--meson track to the beginning of the decay-electron track are due to the range of the dμ-mesoatom, formed as a result of the transition $p\mu + d \rightarrow d\mu + p$. A point (Auger electron) is seen at the beginning of the decay-electron track, in case b.

the formation of ppμ-molecules far less likely, and the gaps of interest to us, due to the range of dμ-mesic atoms, acquire dimensions tens of times larger than the dimensions of those due to diffusion of pμ-mesic atoms. We set up an experiment at 23 atm hydrogen pressure and the optimum deuterium concentration of 0.44% arrived at in special experiments. In that experiment, about 800 events were found, of which about half were conventional ($\mu - e$)-decay events, and the remaining showed apparent gaps stretching from the end of the track of the muon brought to rest to the beginning of the electron track, reaching 17 mm.* Two examples of such events are shown in Fig. 4. The observation of large-gap events has made it possible to reliably determine the probability of a muon jumping from a proton to a deuteron. Under the conditions prevailing in our experiments, the value found was $\lambda'_d = (1.5^{+0.5}_{-0.3}) \cdot 10^6\ \text{sec}^{-1}$. On this basis, we obtain the value $\lambda_d = (1.2^{+0.4}_{-0.2}) \cdot 10^{10}\ \text{sec}^{-1}$ ** for the probability of the transition (3) reduced to the density of liquid hydrogen, and the deuterium concentration $C_d = 1$. This value is in excellent accord with theoretical values computed and reported in [18, 14], equal to $1.3 \cdot 10^{10}\ \text{sec}^{-1}$. It has already been noted that the transition process $p\mu + d \rightarrow d\mu + p$ is characterized by the highest probability among all the mesoatomic processes occurring in hydrogen and deuterium. Its cross section, computed on the basis of the known value of the rate λ_d, is $\sigma_d = (4.2 \pm 1.2) \cdot 10^{-18}\ \text{cm}^2$ at the temperature of liquid hydrogen.

A knowledge of the absolute value of the rate λ_d, which, as we have indicated, plays an important part in μ-catalytic phenomena, is particularly valuable for the precise reason that the road is opened up for the determination of another important quantity, the probability of formation of the mesic molecule ppμ in liquid hydrogen. This last probability is very important to have on hand in order to determine the relative fraction of muons experiencing nuclear capture by a proton [process (1)] from the mesomolecule state. Let $\lambda_{pp\mu}$, for purposes of determination, consist in the use of the ratio $(\lambda_0 + \lambda_{pp\mu})/\lambda_d$, the value of which has been determined and reported in several papers [5, 19, 20] in studying the yield of the $d\mu + p \rightarrow He^3\mu + \gamma$ reaction in liquid hydrogen. According to these papers, the most accurate measurements are those carried out most recently by L. Lederman's group [20], a value of $(1.06 \pm 0.11) \cdot 10^{-4}$. The value which we found for λ_d leads, under these conditions, to the $\lambda_{pp\mu}$ value of $(0.8^{+0.4}_{-0.2}) \cdot 10^6\ \text{sec}^{-1}$. It must be stressed that the values we determined for rates λ_d and $\lambda_{pp\mu}$ were confirmed in that paper [20], where the work was carried out with much the same precision and accuracy, but by use of a completely different procedure (measurement of the time dependence of the γ-quantum yield from the $d\mu + p \rightarrow He^3\mu + \gamma$ reaction at different deuterium concentrations, and using electronic techniques). Both our data and the data reported in [20] are in perfectly satisfactory agreement with the theoretical values of these process rates, as computed by Ya. B. Zel'dovich and S. S. Gershtein.

Armed with these experimental data, we are now in a position to state that, at the density of liquid hydrogen,

*Under the prevailing experimental conditions, the pμ-mesic atoms display ranges from 0.25 mm to a maximum of 1.5 mm (cf. section 2).

**This means that the μ-meson jumps from the proton to the deuteron in a time $1/\lambda_d \sim 0.8 \cdot 10^{-10}$ sec under conditions where the number of hydrogen nuclei and deuterium nuclei are equal, and $C_d = 1$.

only about 30% of the μ-mesons (35% according to our data, and 25% according to the data reported in [20]) decays, or is captured from the pμ-mesoatom orbit, while the remaining fraction is captured from the ppμ-system.

4. μ-Meson Catalysis of the Nuclear Reactions d + d and p + d

Because of the high probability of the μ-meson jumping from a proton to a deuteron, almost all the μ-mesons succeed in making the transition to the deuterons even when the concentration of deuterium in the hydrogen is very low. In the same manner, in turn, as pμ-mesic atoms approaching close to hydrogen atoms form the mesic molecule ppμ, dμ-mesic atoms, as a result of the same mechanism, may succeed in forming pdμ-mesic molecules, and even ddμ-mesic molecules, when the deuterium concentration is high. In these systems the nuclei of the deuterium atoms or deuterium and hydrogen atoms approach to a distance on the order of the mesoatomic radius ($\sim 10^{-11}$ cm), with the result that the width of the Coulomb barrier narrows down to a width far smaller than that found in conventional molecules, where the distance separating the nuclei of the atoms is $\sim 10^{-8}$ cm. Since the tunneling coefficient of the particles is strongly dependent on the width of the Coulomb barrier, the nuclear fusion reaction takes place at an appreciably high probability in mesic molecules. This is precisely the gist of the catalytic action of negative muons in fusion reactions involving light nuclei, which usually take place only when high energies (e.g. in thermonuclear reactions) are imparted to the participating particles.

Catalysis of the d + d Reaction. As is evident from Fig. 2, the ddμ-mesic molecule may participate in two types of nuclear reactions. In reactions of the first type, the μ-meson is either liberated or proves to be bound in a neutral system with a proton or triton, and may bring about a nuclear reaction again sometime in the future. A typical feature of the reactions of the second type is the bond linking the μ-meson to the helium nucleus. This type of mesic atom is no longer electrically neutral, and is incapable of approaching to within a close distance of other nuclei and surrendering its μ-meson, or of causing a new nuclear fusion reaction. The μ-meson caught in the He^3 orbit will either decay or, as has been demonstrated in experiments on muon capture in pure He^3 carried out in our laboratory by B. Pontecorvo, R. M. Sulyaev et al. [21], has a very low probability of being absorbed by the He^3 nucleus (as a result of weak interaction) with the formation of H^3 and a neutrino.* The capture of muons, resulting in the formation of μ-mesic atoms of helium, constitutes one of the principal hindrances to the realization of a sustained nuclear chain reaction between hydrogen isotopes by means of μ-meson catalysis. The most probable reactions in the ddμ-mesic molecule are, according to theory, the first two reactions, so that the μ-meson proves to be free. The other three reactions account for 2% of the events.

Only the first reaction,

$$dd\mu \longrightarrow H^3 + p + \mu^-, \tag{5}$$

has been studied to date in our experiments.

The principal task before us is the determination of the probability of formation of ddμ-mesic molecules (the reaction rate $\lambda_{dd\mu}$). An experiment was carried out at a deuterium pressure of about 16 atm. Of 10,000 stoppages of μ-mesons, 27 cases of the reaction (5) were recorded. This reaction was easily identified from the range of the proton or triton and from the presence of a decay-electron at the point where the triton-proton particle emerges. A typical photograph showing such an event is seen in Fig. 5. Since, according to theoretical estimates, the probability of the nuclear reaction in the ddμ-mesic molecule exceeds by several orders of magnitude the probability of muon decay, the nuclear reaction will take place in all the ddμ-mesic molecules formed. This is the set of circumstances which enabled us to determine the rate $\lambda_{dd\mu}$ of interest from the observed yield of reaction (5). In so doing, we allowed for the fact that the probability of the reaction $dd\mu \rightarrow He^3 + n + \mu^-$ is equal to the probability of reaction (5).

The rate $\lambda_{dd\mu}$ so calculated, reduced to liquid-deuterium density, is found to be

$$\lambda_{dd\mu} = (0{,}44 \pm 0{,}14) \cdot 10^6 \text{ sec}^{-1}.$$

There are no other experimental data currently available in the literature on the value of the rate $\lambda_{dd\mu}$, except for the estimate $\lambda_{dd\mu} > 0.1 \cdot 10^6$ sec^{-1} obtained from liquid-deuterium bubble-chamber experiments [22].

If we compare the value we found from experiment for the probability of formation of ddμ-mesic molecules and the theoretically computed counterparts, then we find that $\lambda^{exp}_{dd\mu}$ is approximately one order of magnitude greater

*According to experimental evidence [21], the probability of nuclear capture of the μ-meson by the He^3 nucleus is $(1.41 \pm 0.14) \cdot 10^3$ sec^{-1}.

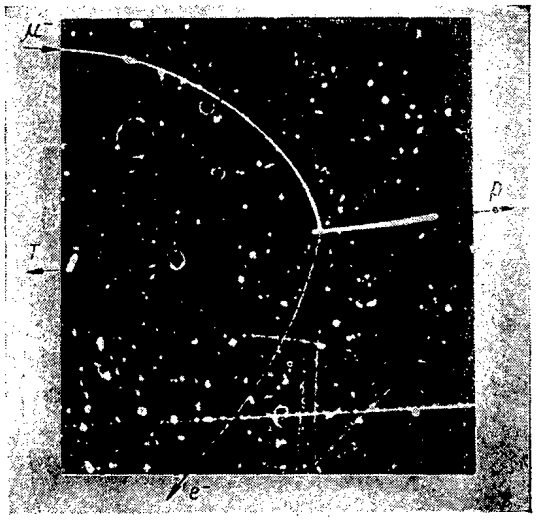

Fig. 5. μ^--Catalyzed fusion of two deuterium nuclei. When a $d\mu$-mesic atom collides with a deuteron, a $dd\mu$-mesic molecule is formed, with an ensuing nuclear fusion reaction $dd\mu \rightarrow T + p + \mu^-$. Almost all of the energy of the reaction (~4 MeV) is carried off by the tritium nucleus and the proton, flying off in opposite directions. Such a low energy is imparted to the μ^--meson in the process (several kiloelectronvolts, i.e., of the order of the binding energy of the mesic atom) that the particle cannot travel any appreciable distance from the point where the reaction took place, and decays with the emission of a fast electron.

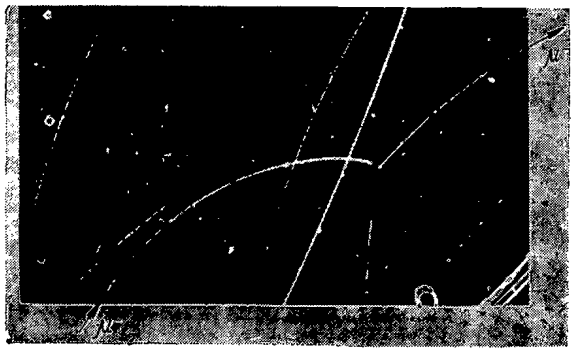

Fig. 6. Fusion reaction involving a proton and a deuteron; reaction catalyzed by a μ^--meson. After being brought to rest, the μ^--meson formed the mesic atom $p\mu$, and later a mesic atom $d\mu$. In the encounter between the $d\mu$-mesic atom and a proton, the $pd\mu$-mesic molecule was formed, leading to the nuclear fusion reaction $pd\mu \rightarrow He^3 + \mu^-$. 5.5-MeV energy were liberated in the reaction; most of this energy (~5.3 MeV) was carried off by the μ^--meson, so that the latter was reejected. The gap stretching between the μ^--meson tracks corresponds to the range of the neutral mesic atom $d\mu$. The point at the start of the track traveled by the ejected μ^--meson is a track left by the He^3 nucleus which took a slight recoil (~0.2 MeV) in the reaction.

than $\lambda^{th}_{dd\mu}$ [12, 14]. It is worthwhile to point out, however, that the latter value was computed with no cognizance taken of the existence in the $dd\mu$-mesic molecule of a rotational level K = 1 and binding energy close to zero [12]. It is possible that the presence of such a level will result in resonance effects accompanying the formation of the $dd\mu$-mesic molecules, as well as an increase in the probability of the nuclear reaction in flight.

In future catalysis-reaction experiments in deuterium, the most interesting point to uncover will be whether the rate of the reaction $dd\mu \rightarrow He^3 + n + \mu^-$ actually differs little from the rate of reaction (5) which we studied, as well as the determination of the sticking probability of muons to helium nuclei.

Catalysis of the p + d Reaction. The catalysis of (p + d)-reactions is, at the present time, a relatively well-investigated process, when compared to the other mesoatomic phenomena. It has been established [5, 23] that two reactions proceeding in the mesic molecules $pd\mu$ are (cf. Fig. 2)

$$pd\mu \rightarrow He^3\mu + \gamma \qquad (6)$$

and

$$pd\mu \rightarrow He^3 + \mu^-. \qquad (7)$$

The probability of a gamma quantum being emitted here is approximately 15 times greater than the probability of conversion of a μ-meson. On being liberated in reaction (7), the μ-meson carries off 5.3-MeV energy, i.e., almost all the energy of the reaction. The yield of nuclear reactions (6) and (7) is determined by the probabilities of the processes: the probability $\lambda_{pd\mu}$, of the formation of the $pd\mu$-mesic molecule, and the probability of a nuclear reaction occurring in that mesic molecule.

Since the probability of the mesic molecules forming is proportional to the density of the hydrogen, while the speed of the nuclear reaction in the mesic molecule is independent of density, a comparison of the yields, e.g., of reaction (7), at different hydrogen densities, affords us an idea of the value of $\lambda_{pd\mu}$. With this in mind, we set up an experiment to determine the yield of reaction (7) at a hydrogen pressure of about 20 atm under conditions of almost complete saturation of process (3) ($C_d \simeq 5\%$). Of 12,000 muons stopped, only five events of reaction (7) were detected, so identified by measuring the momentum of the converted μ-meson.

Figure 6 presents a photograph of one such event. Results reported in [19], obtained in liquid-hydrogen bubble-chamber experiments, were used to determine the value of $\lambda_{pd\mu}$, along with our own experimental data. It was found that, at the density of liquid hydrogen,

$$\lambda_{pd\mu} = \left(0{,}5\ ^{+0{,}6}_{-0{,}4}\right) \cdot 10^6\ \text{sec}^{-1}.$$

Recently, in experiments completed by two teams of American physicists {one of the teams [20] using a target with liquid hydrogen and a slight admixture of deuterium measured the distribution in time of gamma photons from reaction (6), while the other group [22] used a liquid-hydrogen bubble chamber with a high deuterium concentration to determine the muon yield from reaction (7)}, values for the probability $\lambda_{pd\mu}$ which differed by several times were obtained, and were far in excess of the values we found. At the present time, it is difficult to account for such a considerable discrepancy in the results. The problem calls for further study at several angles. There are grounds for supposing that the reason lies in inaccurate interpretation of data directly obtained from experiments performed under greatly disparate conditions. It may turn out that there exists some nontrivial density effect which has so far escaped scrutiny, and which affects the determination of the probability of formation of pdμ-mesic molecules in experiments involving gaseous and liquid hydrogen and deuterium. On the other hand, an interpretation of the time distribution of gamma photons from reaction (6), from which the authors of [20] determine the probability $\lambda_{pd\mu}$ and the time of the nuclear reaction in the pdμ-mesic molecule, may prove to be ambiguous because of the existence of several nuclear reaction times in various spin states of the mesic molecule [24].

We see, accordingly, that the protons and deuterons are bound by μ-mesons into the mesic molecules ppμ, pdμ, and ddμ, with a probability comparable to the probability of muon decay. The relatively low probability of formation of mesic molecules, compared to the probability of process (3), is related to the mechanism, referred to above, operating in the formation of the mesic molecules which has, as its result, the transmission of the excess energy to a third particle, the atomic electron. In the transition process $p\mu + d \rightarrow d\mu + p$, the energy is distributed between the heavy particles, and the rate of this transition is therefore four orders of magnitude [$\sim 1/\alpha^2 \sim (137)^2$] greater.

It must be noted that, in tritium-enriched hydrogen and deuterium, we may encounter formation of the mesic molecules pTμ, dTμ, and TTμ, and catalysis of the corresponding nuclear fusion reactions by the mesic molecules formed. These processes are imperfectly studied at the present time, with meager experimental information available.

5. Jumping of Muons from Protons and Deuterons to Complex Nuclei

Probability of the Transitions λ_Z^p and λ_Z^d. If nuclei of charge greater than two are present in hydrogen, then the effective process at work will be the irreversible transition of muons from the hydrogen or deuterium orbit to the mesoatomic orbits of these nuclei. Since there is always some oxygen and carbon impurity present in the hydrogen and deuterium used in diffusion-chamber experiments, in proportions of approximately one impurity atom per 500 hydrogen atoms, we must have some knowledge of the probability of a muon jumping to the nuclei mentioned. This value was determined for each experiment by comparing the number of stars produced by nuclear capture of a muon by oxygen and carbon in the particular experiment to the number of such muon-produced stars in a specially setup experiment where the transition of muons to those nuclei was close to 100%. The experiments showed that the probabilities of muon transition from protons or deuterons to carbon nuclei or oxygen nuclei are relatively large. We found that, within the limits of experimental error, these probabilities are the same for the nuclei of both elements, in the neighborhood of $1.5 \cdot 10^{10}$ sec^{-1}, i.e., $\lambda_Z^{p,d} \simeq 1.5 \cdot 10^{10}$ sec^{-1}. If we take into account the results of recently completed experiments on the observation of jumping of muons from protons and deuterons to Ne^{20} nuclei, with the resulting rate $\lambda_{Ne} \sim 10^{10}$ sec^{-1}, it will apparently become possible to draw an inference of even more sweeping generality, viz., that the probabilities of muons jumping from hydrogen to light nuclei vary, but not drastically, from nucleus to nucleus. Experimental λ_Z values are found to be in satisfactory accord with theoretical data [25].

Auger Electrons. A theoretical paper has shown [25] that the high probability of a muon jumping from a proton to nuclei of $Z > 2$ is due to the intersection of mesomolecular terms in the pZμ system.* A detailed discussion of the term diagram shows that the muon jumps most commonly to the mesoatomic levels of the carbon and oxygen nuclei with principal quantum numbers $n = 4$ and $n = 5$, respectively. The upshot is that succeeding cascade transitions of the mesic atoms to the ground state, at a transition rate close to 100%, must be accompanied by the escape of one or several Auger electrons carrying away several kiloelectron-volts energy.

Our experiments support this theoretical inference, and are in agreement with the proposed transition mechanism. Actually, in experiments using "pure" hydrogen, as well as in experiments using hydrogen with some deuterium impurity, in about 60% of the ($\mu - e$)-decay events where the starting point of the decay-electron track is separated by a gap from the end of the muon track, a rather conspicuous "point," i.e., a clustering of droplets 0.3 to 0.6 mm

*This mechanism accounts, in particular, for the low value of the experimentally observed cross section for jumping of muons to helium nuclei [26, 19]; there is no intersection of terms in helium mesic atoms.

across, is observable at the start of the electron track (cf. Fig. 3, Fig. 4b). These are the tracks of the low-energy Auger electrons. The frequency with which they appear and their associated energy (an idea of which may be derived from the size of the tracks left behind) correspond to the values anticipated theoretically.

It is worthy of note that another explanation for these points, interpreting them as tracks of protons obtained in the jumping of muons directly from hydrogen to the 1S state of the oxygen [or carbon mesic atom and carrying off the entire energy associated with the transition ($p\mu + O \rightarrow O\mu + p$)] has not been substantiated. Two reasons are advanced in explanation: first, theoretical estimates predict a very low rate for the transition of a μ-meson directly into the 1S state of the mesic atom of a complex nuclei nucleus; secondly, in the transition these protons would receive an energy of about 100 keV, and would leave tracks of length about 1.5 mm under a chamber pressure of 5 atm. We did observe points whose maximum dimensions fail to exceed 0.5 to 0.6 mm.

Summary

While the problem of hydrogen μ-mesic atoms was first probed into theoretically as far back as about 15 years ago, the intensification of experimental research on this topic does not date back past the recent half-decade, for practical purposes. At the same time, we find this to be one of the most vigorously developing new fields in muon physics in the recent period. One brilliant piece of evidence in support of this view is, for instance, the fact that while only two or three experimental papers, including the well-known paper by L. Alvarez and colleagues reporting the detection of μ-catalysis, were available in the literature at the start of our experiments on hydrogen mesic atoms at the Dubna synchrocyclotron facilities, at the present time research on various aspects of this very problem is under way at virtually all the large synchrocyclotrons throughout the world. It may be seen that, as a result of those experiments performed at Dubna, the principal characteristics of the most important mesoatomic processes occurring in hydrogen and deuterium have been determined quantitatively; a number of phenomena are being studied first (e.g., scattering of $p\mu$-mesoatoms on protons). The values found for the probabilities of a μ-meson jumping to deuterium, of formation of the mesic molecule $pp\mu$, and jumping to complex nuclei, are in excellent accord with calculations, and provide confirmation of the correctness of the mechanisms invoked in theoretical treatments to explain the processes. Disagreement has cropped up in some instances between empirical results and data derived from theoretical analysis (the larger experimental value of $\lambda_{dd\mu}$), and the results of measurements performed in different laboratories have been at variance in some cases. This is entirely to be expected in the study of new phenomena. However, there is every reason for assuming that the further development of experiment and theory will make it possible to overcome these difficulties, to probe still deeper into the secrets of the world of mesic atoms, and to reveal new characteristic properties and regularities in this peculiar state of matter.

LITERATURE CITED

1. G. Charpak et al., Phys. Lett., 1, 16 (1962).
2. A. Citron et al., Phys. Lett., 1, 175 (1962).
3. Ya. B. Zel'dovich, DAN SSSR, 95, 493 (1954); Ya. B. Zel'dovich and A. D. Sakharov, ZhÉTF, 32, 947 (1957).
4. F. Frank, Nature, 160, 525 (1947).
5. L. Alvarez et al., Phys. Rev., 105, 1127 (1957).
6. Ya. B. Zel'dovich and S. S. Gershtein, ZhÉTF., 35, 821 (1958).
7. H. Primakoff, Rev. Mod. Phys., 31, 802 (1959).
8. S. Weinberg, Phys. Rev. Lett., 4, 575 (1960).
9. L. B. Egorov, A. E. Ignatenko, and D. Chultem, ZhÉTF., 37, 1517 (1959).
10. V. P. Dzhelepov et al., ZhÉTF., 42, 439 (1962).
11. V. P. Gelepov et al., Intern. Conf. on High-Energy Physics, Geneva (CERN, 1962), p. 484.
12. Ya. B. Zel'dovich and S. S. Gershtein, Uspekhi fiz. nauk, 71, 581 (1960).
13. L. Wolfenstein, Proc. 1960 Ann. Intern. Conf. on High-Energy Physics, Rochester (Publ. Univ. Rochester, 1960) p. 529.
14. S. Cohen, D. Judd, and R. Riddell, Phys. Rev., 119, 397 (1960).
15. S. S. Gershtein, ZhÉTF., 34, 463 (1958).
16. A. E. Ignatenko et al., ZhÉTF., 35, 894 (1958).
17. S. S. Gershtein, ZhÉTF., 36, 1309 (1959).
18. V. B. Belyaev et al., ZhÉTF., 37, 1652 (1959).
19. M. Shiff, Nuovo Cimento, 22, 66 (1961).
20. E. Bleser et al., Phys. Rev. Lett., 8, 128 (1962).
21. I. Falomkin et al., Phys. Lett., 1, 318 (1962).

22. J. Fetkovich et al., Phys. Rev. Lett., 4, 570 (1960).
23. A. Ashmore et al., Proc. Phys. Soc., 71, 161 (1958).
24. S. S. Gershtein, ZhÉTF., 40, 698 (1961).
25. S. S. Gershtein, ZhÉTF., 43, 706 (1962).
26. O. A. Zaimidoroga et al., ZhÉTF., 41, 1804 (1961).

All abbreviations of periodicals in the above bibliography are letter-by-letter transliterations of the abbreviations as given in the original Russian journal. *Some or all of this periodical literature may well be available in English translation.* A complete list of the cover-to-cover English translations appears at the back of this issue.

LONGITUDINALLY POLARIZED PROTON BEAM IN THE SIX-METER SYNCHROCYCLOTRON

M. G. Meshcheryakov, Yu. P. Kumekin, S. B. Nurushev, and G. D. Stoletov

Translated from Atomnaya Énergiya, Vol. 14, No. 1, pp. 38-40, January, 1963
Original article submitted October 16, 1962

Quantitative investigations of the spin dependence of the nuclear interaction at high energies are connected with the performance of experiments on the scattering of protons on protons and neutrons in high-power accelerators. The data thus obtained can be complete only if longitudinally polarized proton beams are used in experiments along with unpolarized and transversely polarized beams [1].

The program of complete experiments on the scattering of protons on protons, which is carried out by means of the six-meter synchrocyclotron of the Joint Institute of Nuclear Studies, includes experiments with the use of longitudinally polarized proton beams. The present article describes an experiment where a longitudinally polarized beam of protons with an energy of 612 MeV was obtained, and it also provides an analysis of its characteristic. The outline of the experiment was proposed by S. B. Nurushev in 1959 [2]. In contrast to the well-known methods for producing longitudinally polarized proton beams at lower energies [3,4], the polarizing scattering in our experiment took place in the vertical plane outside the synchrocyclotron chamber. This made it possible to obtain a longitudinally polarized beam in the horizontal plane, while the polarization vector could be directed parallel as well as antiparallel to the proton pulse in the beam.

The experimental layout is shown in the figure. The unpolarized proton beam that was brought out of chamber 1 of the synchrocyclotron was deflected upward at the angle $\psi = 2°$. The magnetic field's horizontal component that was necessary for this deflection was provided at the beginning of the extracted beam's channel in the region of the accelerator's scattered magnetic field by means of special magnetic adapters 2. A detailed calculation of the dimensions of the adapters and the determination of their optimum position relative to the synchrocyclotron magnet are given in [2]. After collimation (collimator 3) and focusing by means of quadrupole lenses 4, the slightly upward deflected primary beam entered the horizontal magnetic field of magnet 5, where the beam was deflected downward through an angle of 8° in the vertical plane. The graphite diffuser 6, which served as the polarizer, was mounted at the place where the beam intersected the median plane of the accelerator. The collimator 8 separated protons which were scattered at the angle $\theta = 6°$, whose trajectories were in the horizontal plane. The scattering angle could be changed by varying the deflection angles of the primary beam, which made it possible to regulate the degree of polarization of the secondary beam. The $\theta = 6°$ value corresponds to the maximum of the product $\frac{d\sigma}{d\omega}(\theta)P_1(\theta)$, where $\frac{d\sigma}{d\omega}(\theta)$ is the differential cross section of the elastic scattering of protons on carbon nuclei, while $P_1(\theta)$ is the polarization in this process [5]. Thus, the optimum conditions for the performance of experiments on triple proton scattering were secured.

Secondary protons whose polarization vector had the direction of the normal to the scattering plane entered the vertical magnetic field of magnet 9 after leaving collimator 8. In order to intensity the magnetic field, magnet 9 was provided with additional adapters, which also secured partial focusing of the beam. Due to the presence of the anomalous magnetic moment in the protons, the proton spin will precess in such a magnetic field with a velocity different from the velocity of changes in the direction of the proton pulse vector. In this, the precession angle χ relative to the direction of the pulse vector is related to the beam's deflection angle φ in the magnetic field by the expression

$$\chi = \frac{\mu_p - 1}{\sqrt{1-\beta^2}}\varphi,$$

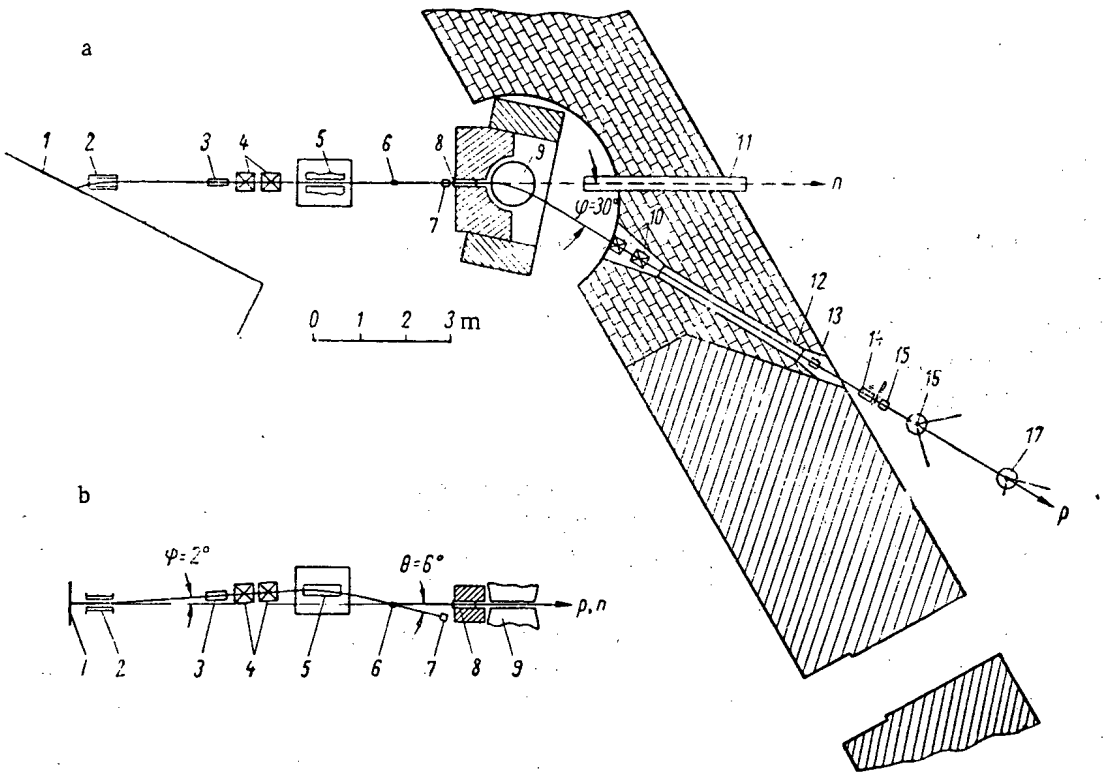

Experimental layout for producing longitudinally polarized beams of protons with an energy of 612 ± 9 MeV. a) Plan view; b) side view.

where μ_p is the proton magnetic moment in nuclear magnetons, and β is the proton velocity in units of the velocity of light.

As a result of precession, there appears the longitudinal polarization component $P_{long} = P_1 \sin \chi$. For $\chi = 90°$, the beam will have only the longitudinal polarization component. The given relationships make it possible to choose such a deflection angle φ as to obtain a completely longitudinally polarized beam for an initial energy of the primary beam equal to 660 MeV.

The longitudinally polarized beam obtained as a result of deflection through the angle $\varphi = 30°$ was focused by means of quadrupole lenses 10 and was directed to the recording devices 16 and 17 through collimator 12. Ionization chambers 7 and 13 served as monitors of the primary unpolarized beam and of the longitudinally polarized beam. For the geometry shown in the figure, the polarization vector of the obtained beam was directed in opposition to the proton pulse. If the angle of primary deflection is made to be $\psi = -2°$, and the unpolarized beam is then deflected upward through an angle of 8° in magnet 5, the direction of longitudinal polarization will be reversed. In practice, such an operation can be completed in 15-20 min. The flux density secured in the beam was equal to $2 \cdot 10^6$ protons per $cm^2 \cdot sec$.

The energy of the longitudinally polarized beam was determined by measuring the proton ranges in copper (devices 14 and 15); it was equal to $E_{long} = 612 \pm 9$ MeV. This value is in agreement with the primary-beam energy $E_0 = 663 \pm 7$ MeV, which was measured by using the same method and allowing for the energy loss in the carbon polarizer, which had a thickness of 23 g/cm^2. The energy $E_{long} = 612 \pm 9$ MeV, and the deflection angle $\varphi = 30°$, correspond to the precession angle $\chi = 89 \pm 2.5°$. In this, the degree P_{long} of longitudinal polarization is virtually equal to the degree P_1 of polarization that occurs in the scattering of the primary beam in polarizer 6. The P_1 value was measured in a separate experiment, where the primary deviation of the beam and the scattering in polarizer 6 were effected in the horizontal plane, while all the other geometric conditions remained unchanged. The value $P_1 = 0.43 \pm 0.03$ which we obtained was in agreement with data from [5].

By analyzing secondary p + p-scattering by means of polarimeters 16 and 17, which consisted of polyethylene diffusers and combined scintillation counters, it was found that the vertical and horizontal transverse polarization components were absent in the longitudinally polarized beam. This was indicated by the fact that, within the limits

of the measurement accuracy, which was ±0.02 with respect to absolute magnitude, no asymmetry in the distribution of protons repeatedly scattered at an angle of 21° was observed either in the horizontal or in the vertical planes.

The determination of the spatial position of the trajectories of the primary and secondary beams, and the choice of the best focusing conditions were performed with respect to self-recordings of transverse beam cross sections along the entire channel and by measuring the beam intensities. At the location of polarizer 6, the beam cross section had a circular shape with a diameter of 30 mm.

The density distribution of the proton flux in the longitudinally polarized beam between polarimeters 16 and 17 was investigated by means of a special device, which consisted of two scintillation counters and an ÉPP-09 automatic electronic potentiometer. The scintillators had the shape of small cylinders with a diameter of 3 mm and a length of 50 mm, and they were placed vertically and horizontally in the plane perpendicular to the direction of the beam. The counters could be moved, one in the horizontal direction, and the other in the vertical direction. The photomultiplier current for each counter was recorded on the strip chart of the ÉPP-09 potentiometer in dependence on the counter position with respect to the beam axis. The horizontal and vertical scales were printed simultaneously. The curves thus obtained indicated that no significant asymmetry in the density distribution of protons in the beam was present.

It should be noted that, simultaneously with the longitudinally polarized proton beam, the polarized beam of neutrons which were generated as a result of the exchange interaction of protons in the carbon polarizer emerged from the adjacent collimator 11. For neutrons emitted with an energy of 610 MeV, the precession angle χ_n in the magnetic field of magnet 9 was approximately 95°.

The authors hereby extend their thanks to L. P. Moskaleva for her help in measuring the intensity of the longitudinally polarized proton beam.

LITERATURE CITED

1. L. Wolfenstein, Phys. Rev., 96, 1654 (1954).
2. S. B. Nurushev et al., OIYaI reprint, R-278 (1959).
3. J. Simons, Phys. Rev., 104, 416 (1956).
4. A. England et al., Phys. Rev., 124, 561 (1961).
5. L. S. Azhgirei and Huang Tieh-ch'iang, ZhÉTF., 44, No. 1 (1963).

All abbreviations of periodicals in the above bibliography are letter-by-letter transliterations of the abbreviations as given in the original Russian journal. *Some or all of this periodical literature may well be available in English translation.* A complete list of the cover-to-cover English translations appears at the back of this issue.

ON THE THEORY OF ROTATIONAL SPECTRA*

A. Bohr, Institute for Theoretical Physics, University of Copenhagen, Copenhagen, Denmark
and B. R. Mottelson, NORDITA, Copenhagen, Denmark
Translated from Atomnaya Énergiya, Vol. 14, No. 1,
pp. 41-44, January, 1963
Original article submitted September 13, 1962

It is a great pleasure to contribute to this issue of "Atomic Energy" commemorating the scientific achievements of the late Igor Vasilievitch Kurchatov. We would also like to take the opportunity to pay a special tribute to Academician Kurchatov's contributions to international scientific cooperation, which have meant so much for the fruitful collaboration between members of our Institutes and physicists of the Institute for Atomic Energy in Moscow.

In the course of the last few years, a large body of empirical data on nuclear rotational spectra has been accumulated, as a result of great ingenuity and refinement in the experimental techniques.**

The rotational description implies, as a first approximation, a number of simple relations between the states in a given rotational band. Thus the energies vary as $I(I+1)$ (for $K \neq 1/2$), and the transition intensities are proportional to the square of a vector addition coefficient.*** It is found that these relations are usually rather well satisfied, often with an accuracy of the order of one percent.

The great accuracy of the experimental data, moreover, has permitted a quantitative study of the deviations from the simple rotational rules, in a number of cases. For the interpretation of these data, one needs a systematic scheme for enumerating the various correction terms implied by the rotational description. Such a scheme may be based on a series expansion of the different matrix elements, as powers of the total angular momentum. The simple rotational rules appear as the leading order terms in such an expansion. In the regions where the rotational description is most applicable, the series converges rapidly, and thus one obtains an accurate description in terms of a few parameters. These parameters depend on the detailed structure of the rotating systems, but it is often possible on the basis of simple models to estimate their relative orders of magnitude.

The details of the derivations and the more systematic enumeration of terms will be discussed in a forthcoming publication; in the present note we shall confine ourselves to a few examples that seem to be of particular interest in the analysis of the present data.

I. Energy Terms

The rotational energy may be considered a function of the components I_1, I_2, and I_3 of the angular momentum in the intrinsic coordinate system. (The nuclear symmetry axis is the intrinsic 3-axis.) For a band with $K = 0$, the axial symmetry implies that the energy must be a function of $I_1^2 + I_2^2$ and thus has the form

$$E_{\text{rot}} = AI(I+1) + BI^2(I+1)^2 + CI^3(I+1)^3 + \ldots \qquad (1)$$

*The publishers wish to express their appreciation to the authors for supplying a copy of their original manuscript.

**See, for example, the compilations by B. S. Djelepow and L. K. Peker, Decay Schemes of Radioactive Nuclei, Moscow 1958; Nuclear Data Sheets, K. Way et al. Editors, Washington, D. C., and the analyses by B. R. Mottelson and S. G. Nilsson, Mat. Fys. Skr. Dan. Vid. Selsk. 1, No. 8 (1959), and by C. J. Gallagher, Jr., and V. G. Soloviev, Mat. Fys. Skr. Dan. Vid. Selsk. 2, No. 2 (1962).

***We are here restricting ourselves to the case of nuclei with approximate axial symmetry. The effect of small departures from axial symmetry in the nuclear shape is included in the higher order terms considered below. For a nucleus with major deviations from axial symmetry, the power series considered here would converge poorly. One should then develop an expansion based upon the appropriate rotational model.

The empirical data have been found to fit this formula with good accuracy. The coefficient B is typically of order -10^{-3} A, and C $\sim 3 \times 10^{-6}$ A.*

For $K \neq 0$, one obtains, in addition to (1), terms resulting from the fact that the nuclear wave function is a symmetric combination of terms with $I_3 = \pm K$. (The additional terms which are associated with a coupling between the two parts of the wave functions may be thought of as resulting from fluctuations away from axial symmetry in the intrinsic structure.)

For the first few values of K, these terms have the form

$$E'_{K=\frac{1}{2}} = (-1)^{I+\frac{1}{2}}\left(I+\frac{1}{2}\right)\times\ [A_1 + B_1 I(I+1) + \ldots];$$

$$E'_{K=1} = (-1)^{I+1}\, I(I+1)\ \times [A_2 + B_2 I(I+1) + \ldots];$$

$$E'_{K=\frac{3}{2}} = (-1)^{I+\frac{3}{2}}\left(I-\frac{1}{2}\right)\left(I+\frac{1}{2}\right)\times\left(I+\frac{3}{2}\right)[B_3 + C_3 I(I+1) + \ldots];$$

$$E'_{K=2} = (-1)^{I}\,(I-1)\,I\,(I+1)(I+2)\times [B_4 + C_4 I(I+1) + \ldots].$$

The parameters are labelled by the index 2K, since they arise from operators proportional to $(I_1 + iI_2)2K$, which couple the K and $-K$ components of the state.

The leading terms in E' for $K = 1/2$ is the familiar "decoupling term", and usually A_1 is of order A in (1). Similarly, one expects $B_1 \sim B_3 \sim B$. Although A_2 appears as a coefficient of a second-order term in I, it is expected usually to be much smaller than A, as follows from a consideration of simple models, such as two particles coupled to an axially symmetric rotor. Such models suggest that, apart from special situations involving degeneracies in the intrinsic motion, a more reasonable estimate is $A_2 \sim B$. Similarly, one may expect in most cases $B_2 \sim B_4 \sim C$.**

While the expansion in I is expected to be valid for not too high values of I, there may occur, for large I, modifications in the intrinsic structure which cannot be expressed by such a simple power series in I. An example is provided by the expected breakdown of the pairing correlation at the critical angular momentum I_C.***

In situations where two near lying bands are strongly coupled, the usual expansion may not be appropriate. It is then necessary to treat this particular coupling explicitly, while all other perturbations may be included in the usual expansion of the various operators.****

E2-Intensity Rules

For transition matrix elements, one can proceed in a similar manner as for the energy, taking due account of the tensorial character of the operator. The most systematic evidence is available on E2 intensity rules.

E2-transitions within a band are expected to be rather accurately described by the leading order term [$B(E2; I_1K \rightarrow I_2K) \sim < I_1\ K\ 20 |\ I_2K >^2$] which is obtained from the I-independent transition operator. The coupling between rotational and intrinsic motion implies, as for the energy, I-dependent terms in the transition moment, but their effect is relatively small, due to the collective character of the leading term. Usually, the leading order intensity rule is therefore expected to be accurate to about a percent or better. The best available experiments have an accuracy of 5 - 10 percent, and so far no definite evidence for departure from the leading order intensity rule has been established.*****

*We are indebted to O. B. Nielsen for making available to us the results of his analysis of rotational energies in even-even nuclei, to appear shortly.

**The existence of a term of the type B_3 has recently been identified in the Coulomb excitation of Tb^{159} (A = 11.61 keV, B = −5.8 eV, B_3 = 8.0 eV. (Diamond, Elbek, Stephens and Perlman, to be published).

***B. R. Mottelson and J. Valatin, Phys. Rev. Letters 5, 511 (1960).

****For an example of this situation, see the spectrum of W^{183}, discussed by A. Kerman, Mat. Fys. Medd. Dan. Vid. Selsk. 30, No. 15 (1956).

*****Estimates of the expected correction terms to the intensity rules have also been made by P. Hemmer (private communication. See M. C. Olesen and B. Elbek, Nucl. Phys. 15, 134 (1960), and B. Elbek (to appear).

For K = 1/2 and K = 1, additional I-independent terms may occur, which couple the $\pm$ K components in the wave function. Thus, for K = 1/2, we obtain

$$B\left(E2;\ I_1K=\tfrac{1}{2}\rightarrow I_2K=\tfrac{1}{2}\right) = \frac{15}{16\pi}\left[Q_0\left\langle I_1\tfrac{1}{2}20\,|\,I_2\tfrac{1}{2}\right\rangle + q_1(-1)^{I_1+\frac{1}{2}}\left\langle I_1-\tfrac{1}{2}21\,|\,I_2\tfrac{1}{2}\right\rangle\right]^2, \tag{3}$$

where Q_0 is the usual intrinsic quadrupole moment, and q_1 (which is related to the wave function of the last odd particle) is of single-particle magnitude. Thus, the correction term in (3) may amount to as much as 10 percent. For K = 1, the corresponding correction term is expected in most cases to be appreciably smaller.

E2-transitions between bands may be much more sensitive to higher order terms, partly because the leading terms are smaller, and partly because certain of the admixed terms are proportional to the large collective matrix element, Q_0. We shall not attempt to enumerate all the correction terms, but confine ourselves to the leading order terms involving Q_0. These may be regarded as resulting from a coupling of the two bands considered.

For Δ K = 1 (excluding K = 1/2$\leftrightarrow$K = 3/2), the leading order collective admixture gives rise to corrections which have the same I-dependence as those obtained from an I-independent operator, and thus simply amount to a renormalization of the intrinsic matrix element. In the case of K = 1/2$\leftrightarrow$K = 3/2), a special term arises (associated with the ΔK = 2 combination (K = $-$ 1/2$\leftrightarrow$K = 3/2)), and one obtains

$$B\left(E2;\ I_1K=\tfrac{1}{2}\rightarrow I_2K=\tfrac{3}{2}\right) = \left\{\left[M_1+M_2'(-1)^{I_1+\frac{1}{2}}\left(I_1+\tfrac{1}{2}\right)\right]\times\left\langle I_1\tfrac{1}{2}21\,|\,I_2\tfrac{3}{2}\right\rangle + (M_2+M_2')(-1)^{I_1+\frac{1}{2}}\times\left\langle I_1-\tfrac{1}{2}22\,|\,I_2\tfrac{3}{2}\right\rangle\right\}^2 \tag{4}$$

involving the three intrinsic matrix elements M_1, M_2, and M_2^1.

For ΔK = 2, the generalized intensity rule has the form

$$B(E2;\ I_1K\rightarrow I_2K+2) = \left[(M_2+M_2')\langle I_1K22\,|\,I_2K+2\rangle + M_2'\sqrt{(I_1-K)(I_1+K+1)}\times\langle I_1K+121\,|\,I_2K+2\rangle\right]^2. \tag{5}$$

For transitions between two different bands with the same K, the leading term containing the collective matrix element, Q_0, is of second order in I, as for ΔK = 2. To this approximation one obtains

$$B(E2;\ I_1K\rightarrow I_2K) = \langle I_1K20\,|\,I_2K\rangle^2\times\{M_0+M_0'[I_1(I_1+1)-I_2(I_2+1)]\}^2. \tag{6}$$

(For K = 1/2$\leftrightarrow$1/2 and K = 1$\leftrightarrow$1, additional terms are present).*

The most systematically studied E2 intensities for transitions between bands are those between the ground-state band in even-even nuclei (K = 0+) and the systematically occurring K = 2+ bands (γ-vibrations). It is found that the M_2^1 term in (5) makes a significant correction to the observed intensities, typically of order 20 percent for the lowest values of I. (Such an effect is produced by $M_2^1 \sim 0.03\, M_2$). The corrected intensity rule (5) is found to account for the available experimental measurements on these intensities.**

*Correction terms of the type M_0^1 in (6) have also been considered by Z. Bochnacki (private communication).

**O. B. Nielsen, Rutherford Jubilee Intern. Conf., 1961 (London, 1962).

III. K-Forbidden Transitions

It is a characteristic feature of the intensity rules obtained from I-independent operators that the matrix element vanishes for ΔK greater than the multipolarity λ. Such K-forbidden transitions are indeed observed to be significantly retarded (compared to "allowed" transitions) typically by a factor of 10^2 for each order of K-forbiddenness.

For the K-forbidden transitions, one may, however, write down the power series expansion in I in the same manner as for the allowed transitions. The principal difference is that the leading order term already involves an I-dependent transition operator, proportional to $(I_1 + i\, I_2)^{\Delta K - \lambda}$. To this order, the intensity rules take the form

$$B(\lambda; I_1 K \rightarrow I_2 K + \Delta K) = M^2_{\Delta K} \langle I_1 K \; + \Delta K - \lambda; \; \lambda\lambda \,|\, I_2 K + \Delta K \rangle^2 \quad \times \frac{(I_1 - K)!}{(I_1 + K)!} \frac{(I_1 + K + \Delta K - \lambda)!}{(I_1 - K - \Delta K + \lambda)!} . \qquad (7)$$

The accuracy of (7) is expected to be governed by the same considerations as apply to the usual "allowed" transitions discussed above. Thus, in cases where higher order terms involve relatively large intrinsic matrix elements, one may expect a significant improvement by employing generalized intensity rules, similar to those discussed above for the E2 case.*

In any discussion of intensity rules, it must be borne in mind that when the leading order intrinsic matrix element is very small, the transition strength may be sensitive to small admixtures in the wave function and, therefore, the power series expansion in I may appear to converge poorly. This seems to be the case for many of the low-energy E_1 transitions in odd-A nuclei, which are observed to be hindered by factors of the order of $10^3 \times 10^6$ compared to single-particle estimates; for these the leading order intensity rules are often found to fail by a large factor. The appropriate intensity rule would depend on the mechanism responsible for the observed E_1-transition moment. So far, there appears to be no adequate analysis of these effects.

The I-dependent terms in the energy and transition moments may be regarded as a result of the Coriolis force acting on the intrinsic motion. The procedure outlined above provides a systematic enumeration of the various terms which may occur to any given order in I. Such a description is phenomenological in the sense that the coefficient of each term is left as an adjustable parameter. These coefficients may in turn be calculated from a knowledge of the intrinsic nuclear structure. Thus, the I-independent terms may be obtained directly from the intrinsic states in a static nuclear field; the higher order effects result from the rotation of the field and can be obtained in a manner analogous to the estimate of the moment of inertia on the basis of the cranking model.

Part of this work was carried out during a visit to the California Institute of Technology, Pasadena, California. We wish to thank members of the Physics Department for their generous hospitality.

* Recently, the M1 transitions from the K = 7/2+ band to the K = 1/2+ band in Tm^{169} have been found to have relative intensities in agreement with (7) to within 15%. (Private communication from P. Alexander and F. Boehm).

ON DELAYED PROTONS

N. A. Vlasov

Translated from Atomnaya Énergiya, Vol. 14, No. 1,
pp. 45-47, January, 1963
Original article submitted September 27, 1962

It is known that there are radiators of delayed neutrons among the isotopes of light nuclei (Li^9, N^{17}, C^{16}) and fission fragments with excess neutrons. The emission of neutrons occurs after the β-decay into excited levels with the energy $E^* > B_n$ (B_n is the neutron binding energy in the final nucleus) and is, consequently, possible under the condition that the decay energy E_β is greater than B_n.

Among the isotopes with excess protons, there may be such where the β^+-decay energy exceeds the proton binding energy B_p in the final nucleus. In the decompositon of these nuclei into excited levels, delayed neutrons, which until now have not been observed [1], may be emitted. The possibility of producing and observing delayed neutrons is indicated and estimated in the present communication.

Possible Radiators of Delayed Protons that are Produced in the (He^3, 2n) Reaction

Target	Product	Reaction energy, MeV	E_β, MeV	B_p, MeV	Period, sec
C^{12}	O^{13}	—16	17,1	1,94	0,01
O^{16}	Ne^{17}	—22,3	13,4	0,60	0,05
Ne^{20}	Mg^{21}	—18,9	12,0	2,45	0,3
Mg^{24}	Si^{25}	—18,9	11,6	2,29	0,4
Si^{28}	S^{29}	—19,5	12,4	2,72	0,4
S^{32}	Ar^{33}	—16,5	10,8	2,28	0,7
Ar^{36}	Ca^{37}	—13,5	11,2	1,86	—
Ca^{40}	Ti^{41}	—15,5	11,6	1,60	0,4

On the basis of the tables of nuclear masses which were calculated by using semiempirical equations, for instance in [2], one can indicate the regions containing possible radiators of delayed nucleons on an N(Z) diagram (N is the number of neutrons, and Z is the number of protons). Such a diagram for light nuclei with even Z values from 10 to 30 is given in Fig. 1. The $E_\beta > B_n > 0$ band corresponds to possible radiators of delayed neutrons and contains 7-15 isotopes for each element, while the $E_\beta > B_p > 0$ band corresponds to possible radiators of delayed protons and contains four to six isotopes of each element. It is obvious that, besides the known radiators of delayed neutrons, it is possible that there are many radiators which have not yet been detected. Generally speaking, their production is difficult due to the fact that neutrons are more readily emitted than protons in nuclear reactions. Thus, the latest of the detected radiators of delayed neutrons, C^{16}, was obtained [3] in the $C^{14}(t,p)C^{16}$ reaction, where both initial nuclei are radioactive. It is simpler to produce nuclei with excess protons.

The probability that a proton will be emitted by an excited nucleus due to the Coulomb barrier is lower than the probability that a neutron with the same energy will be emitted. If the neutron width Γ_n exceeds the radiation width Γ_γ even when $\Delta E_n = E^* - B_n > 50$ keV, the condition $\Gamma_p > \Gamma_\gamma$ will be satisfied for considerably greater energy margins $\Delta E_p = E^* - B_p$. Thus, for a copper nucleus, $\Delta E_p \simeq 3$ MeV, while $\Delta E_p \simeq 7$ MeV for a tin nucleus [4]. This is the reason why the detection of delayed-proton radiators among the isotopes of heavy and even medium elements is not very probable. However, the detection of such radiators among the isotopes of light elements is highly probable.

One of the simplest methods for producing nuclei with excess protons is the bombardment of certain targets with He^3 nuclei, which are at the present time accelerated in some cyclotrons. The table lists the possible radiators of delayed protons that can be obtained in the (He^3, 2n) reaction. The characteristics of the reactions and of the nuclei were borrowed from [2, 5, 6].

For all the nuclear products enumerated in the table, $E_\beta > 10$ MeV, while the proton binding energy in the nucleus formed after β-decay is $B_p < 3$ MeV and, therefore, the probability of decomposition into levels $E^* > B_p$ is sufficiently high. The probability $P(B_p)$ of the emission of a delayed proton can be estimated by means of the equation which G. R. Kipin [7] used for estimating the probability of the emission of delayed neutrons:

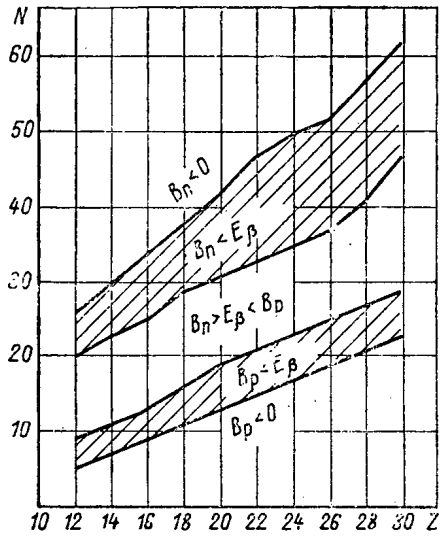

Fig. 1. Regions which possibly contain radiators of delayed nucleons in an N(Z) diagram for even elements of light nuclei.

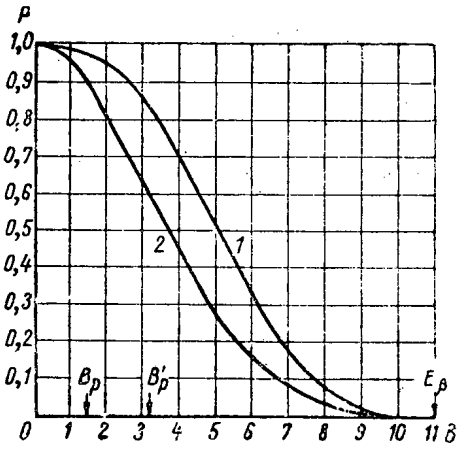

Fig. 2. Probability of the emission of a delayed proton for the decay energy E_β = 11 MeV in dependence on the effective binding energy B for two values of the constant a in the level density distribution. The arrows correspond to the $Ti^{41} \rightarrow Sc^{41}$ decay.

$$P(B) = \frac{\int_B^{E_\beta} \frac{\Gamma_p}{\Gamma_\gamma + \Gamma_p} \Phi(E)\, \varrho(E)\, dE}{\int_0^{E_\beta} \Phi(E)\, \varrho(E)\, dE}.$$

Here, $\Phi(E)$ is the dependence of the probability of β-decay on the energy, which can be given as $\Phi = (E_\beta - E)^5$, and $\rho(E) = \text{const}\, e^{2\sqrt{aE}}$ is the density of levels of the final nucleus [8]. The width ratio $\frac{\Gamma_p}{\Gamma_p + \Gamma_\gamma}$ (under the conditions considered here, $\Gamma_n = 0$) changes rather sharply with energy and, therefore, it can be assumed that

$$\frac{\Gamma_p}{\Gamma_p + \Gamma_\gamma} = 0 \quad \text{for} \quad E < B'_p = B_p + \Delta E_p;$$

$$\frac{\Gamma_p}{\Gamma_p + \Gamma_\gamma} = 1 \quad \text{for} \quad E > B'_p,$$

i.e., P(B) can be estimated by using not the physical magnitude of the binding energy B_p, but a certain effective value B'_p that exceeds B_p by ΔE_p, which corresponds to the equality of widths $\Gamma_p = \Gamma_\gamma$. Then, the probability of decay to a level with the energy E > B can be calculated by using the equation

$$P(B) = \frac{\int_B^{E_\beta} (E_\beta - E)^5 e^{2\sqrt{aE}}\, dE}{\int_0^{E_\beta} (E_\beta - E)^5 e^{2\sqrt{aE}}\, dE}.$$

Figure 2 shows the thus-calculated probability P(B) for E_β = 11 MeV. The two curves correspond to the two values of the constant a in the expression for the density of levels: a_1 = 3 MeV^{-1} (curve 1) and a_2 = 1 MeV^{-1} (curve 2). For small B values, P(B) does not depend heavily on the a value. For the case of the $Ti^{41} \rightarrow Sc^{41}$ decay, $B'_p \simeq 3$ MeV, and P(3) = 0.60 according to the one curve, and P(3) = 0.83 according to the other curve. The same curves can be used for estimating the probability of the escape of a proton with the energy $E_p > E = B - B_p$. For the other isotopes given in the table, the estimates are less favorable. Finally, the actual probability can differ significantly from the probability calculated on the basis of the statistical theory, since the density of levels is small for light nuclei. The above curves illustrate only the high probability of detecting radiators of delayed protons among the enumerated and other similar isotopes of light elements.* None of the nuclear products given in the table has been obtained until now. The cross sections of the (He^3, 2n) reaction and of other reactions in which these nuclei could be produced apparently are small in comparison with the cross sections of the simpler reactions that yield radioactive isotopes and, therefore, it is rather difficult to detect them with respect to β- or γ-activity. It is relatively simpler to detect delayed protons, and their presence can be used for studying new nuclei with excess protons and nuclear reactions leading to their formation. From this point of view, the observation of delayed protons is of methodological interest.

*V. I. Gol'danskii pointed out [9] that, in the β-decay of the predecessors of delayed protons, the superallowed transition would occur with the greatest probability and, on the basis of this, he estimated the probability of the emission of delayed protons by certain nuclei.

For the observation of delayed protons, it is necessary to have a pulse source of He^3 nuclei, which are accelerated to an energy in excess of 20 MeV (or a source of other particles, which are accelerated to higher energies), and a proton detector, which is connected periodically during the intervals between radiation pulses.

LITERATURE CITED

1. V. L. Karnaukhov and N. I. Tarantin, ZhÉTF., 39, 1106 (1960).
2. A. Cameron, Canad. J. Phys., 35, 1021 (1957); P. Seeger, Nucl. Phys., 25, 1 (1961).
3. S. Hinds et al., Phys. Rev. Lett., 6, 113 (1961).
4. V. Weisskopf and D. Eving, Phys. Rev., 57, 472 (1940).
5. E. Almguist and D. Bromley, AECL, No. 950 (1959).
6. V. J. Goldansky, Nucl. Phys., 19, 482 (1960); A. I. Baz', V. I. Gol'danskii, and Ya. Zel'dovich, Usp. Fiz. Nauk., 72, 211 (1960).
7. G. R. Kipin, Atomnaya énergiya, 4, 3, 250 (1958); see also A. Pappas, Transactions of the Second International Conference on the Peaceful Uses of Atomic Energy (Geneva, 1958). Selected Reports by Scientists from Abroad [in Russian] (Atomizdat, Moscow, 1959), Vol. 2, p. 308.
8. J. Blatt and V. Weiskopf, Theoretical Nuclear Physics [Russian translation] (IL, Moscow, 1954).
9. V. I. Gol'danskii, DAN SSSR, 146, 1309 (1960).

All abbreviations of periodicals in the above bibliography are letter-by-letter transliterations of the abbreviations as given in the original Russian journal. ***Some or all of this periodical literature may well be available in English translation.*** **A complete list of the cover-to-cover English translations appears at the back of this issue.**

THE ISOTOPE EFFECT IN ELASTIC SCATTERING OF PROTONS ON NUCLEI

A. K. Val'ter and A. P. Klyucharev

Translated from Atomnaya Énergiya, Vol. 14, No. 1,
pp. 48-56, January, 1963
Original article submitted September 13, 1962

Before proceeding to our exposition of the material, the authors would very much like to aknowledge, with deepfelt appreciation, the crucial role played by the late Igor' Vasil'evich Kurchatov in the successful completion of the investigation herein described.

Important contributions to the success of the project were made by the use of linear proton accelerators, the use of targets containing various isotopes, and the processing of experimental data on high-speed electronic computers.

The late I. V. Kurchatov took a lively and indefatigable interest, backed up by effective and vigorous efforts in the rapid development and implementation of linear accelerators at Khar'kov. We must acknowledge his valuable contributions toward the production of an ample supply and variety of enriched materials. Finally, it was through the approval and support of the late Igor' Vasil'evich that the electronic digital computer belonging to the Institute of Atomic Energy of the USSR Academy of Sciences was made available to us (and which was, by the way, the first such computer for our Institute) for the processing of experimental results.

Igor' Vasil'evich displayed an intense interest in the entire program since its inception in 1955. The last occasion on which he took active part in the discussion of new results was in February 1960, less than a month before his untimely demise.

The problem of elastic scattering of nucleons on atomic nuclei has attracted and continues to attract, at the present time, the attention of many investigators. Over the past two decades, the arsenal of nuclear research techniques has been strengthened by the addition of charged-particle accelerators, which have made it possible to obtain intense beams of monoenergetic protons over a wide range of energies. This in turn has made it possible to carry out a study in depth of the interactions of protons with atomic nuclei.

Until very recently, elastic scattering of protons on atomic nuclei was studied over a wide range of energies on targets of natural isotope composition [1-10]. Results were obtained which contributed to the formulation of several general regularities present in the scattering picture. It was demonstrated, for example, that elastic scattering of protons on atomic nuclei at energies higher than the Coulomb potential barrier displays a diffraction character, and that the position of the extreme points in the differential cross section as a function of scattering angle is determined by the mass number of the scatterer at the specified energy and is shifted in the direction of smaller angles with increased energy [11, 12]. This is clearly illustrated in Figs. 1a,1b for the energies 40 and 9.8 MeV, respectively, in diagrams borrowed from references [13, 14].

The value of the differential cross section calculated within the framework of the presently accepted optical model is in satisfactory accord with the experimentally obtained value over a significant range of angles and energies [15, 16]. The largest deviations of calculated values from experimental values is observed in the region of large angles and increases, as a rule, as the mass number of the scatterer decreases. Except for the very lightest nuclei, the angular distributions of elastically scattered protons at energies exceeding the Coulomb barrier are qualitatively the same for all the elements in the periodic table. However, for neighboring elements in the Z = 24-29 region, the scattering picture is markedly altered at lower energies. For example, Bromly and Wall [17], who studied elastic scattering of protons of 5.25-MeV energy on copper nuclei (Z = 29), found that there are two peaks in the 40-50° and 130-140° regions, straddling a minimum (cf. Fig. 1c) in the angular dependence of the ratio of the measured cross section $\sigma(\theta)$ to the Coulomb scattering cross section $\sigma(\theta)_{\text{Rutherford}}$. At the same time, the nickel atom neighboring on copper (Z = 28 for nickel) yields a different scattering picture: the maximum is found at low angles, with the

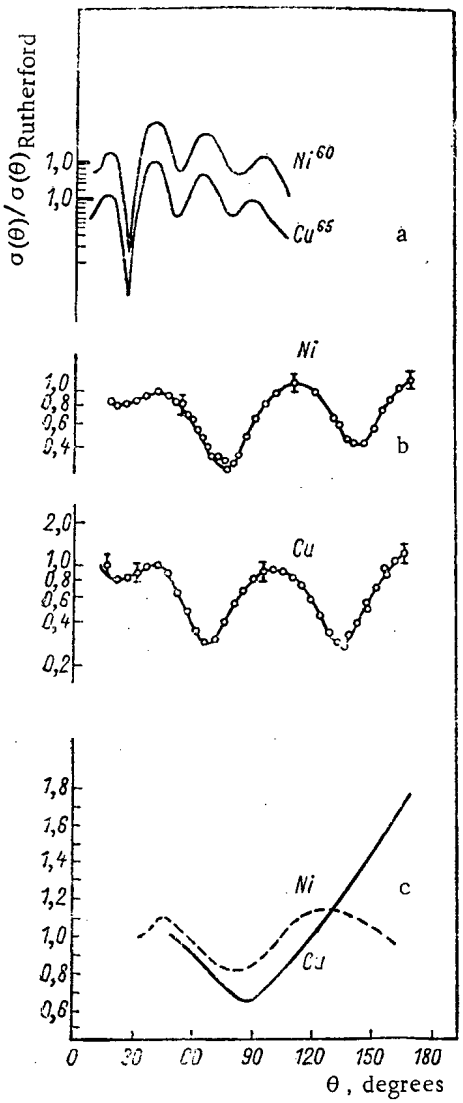

Fig. 1. Ratio of experimentally measured scattering cross section $\sigma(\theta)$ to the Coulomb scattering cross section $\sigma(\theta)_{Rutherford}$ as a function of scattering angle.

minimum in the 80-90° region, and a continuous increase is evident at large angles. Later on, Kondo et al. [18], studying elastic scattering of protons (5.7 MeV) on targets consisting of even-Z nuclei (titanium, chromium, iron), demonstrated that the angular distribution of elastically scattered protons is similar to the distribution in scattering on even nickel.

We infer from the findings of these experiments that the angular dependence of $\sigma(\theta)/\sigma(\theta)_{Rutherford}$ differs qualitatively for even-Z nuclei and odd-Z nuclei at energies below the top of the Coulomb potential barrier.

All of the investigations were conducted on targets of natural isotopic composition, so that the differential scattering cross sections were averaged relative to cross sections of nuclei included in the composition of the targets. Even-even nuclei predominate in even-Z targets; targets with odd-Z nuclei in this region of the periodic table consist of odd-even nuclei. The study of proton scattering on targets of natural isotope composition therefore yields a scattering pattern typical, or even or odd mass number of the target nucleus. It is difficult to suppose that the parity of the mass number would so affect the nature of the scattering.

Low-energy investigations thus turned out to be more sensitive to the effect exerted by the individual properties of the nuclides on the elastic scattering of protons.

A Study of Elastic Scattering of Protons on Separated Isotopes

Elastic scattering of protons on separated isotopes at energies 5.4 MeV [19-20] and 19.6 MeV [21] was carried on using the linear accelerators of the Khar'kov Physics and Engineering Institute of the Academy of Sciences of the Ukrainian SSR, and at 6.8-MeV energy [22] using the cyclotron at the Kiev Institute of Physics of the Academy of Sciences of the Ukrainian SSR, the purpose of the investigation being a more detailed study of the scattering process.

Techniques were first elaborated for production of targets in the form of thin free metal foil made of enriched isotopes. In the process, workers were plagued with some difficulties related in the first instance to the scanty supply of "raw material" available, and secondly to the fact that this raw material usually involved a chemical compound rather than pure metal. Some of these techniques have been described in contributions by the authors and co-workers [23, 24].

The techniques worked out for studying the elastic scattering process are not highly involved, and we need not be detained, therefore, in a reexamination of those techniques at this time. We shall confine our remarks to the point that reliable discrimination of the particles due to inelastic processes is what counts here. The methods we employed to record the protons were the scintillation counter method and the nuclear emulsion stack method, and relatively small thicknesses of target material enabled us to single out and record groups of elastically scattered protons in our work. The geometry of the experiment is shown in Fig. 2. The measured angular distributions of elastically scattered protons are in agreement with theoretical results based on optical-model calculations run on an electronic computer.

Results of the Measurements

Calcium. Scattering was studied for two calcium isotopes (Ca^{40} and Ca^{48}) with doubly magic numbers 20 and 28. Unfortunately, the calcium targets suffered partial oxidation during the experiment. We were therefore obliged to limit our comparison to data obtained at large angles, where it might be possible to reliably distinguish groups of protons scattered by calcium. But enough such data was found to infer a substantial difference in the angular distributions (Fig. 3). The solid-line curves in Fig. 3 were drawn through experimental data points; the broken curves

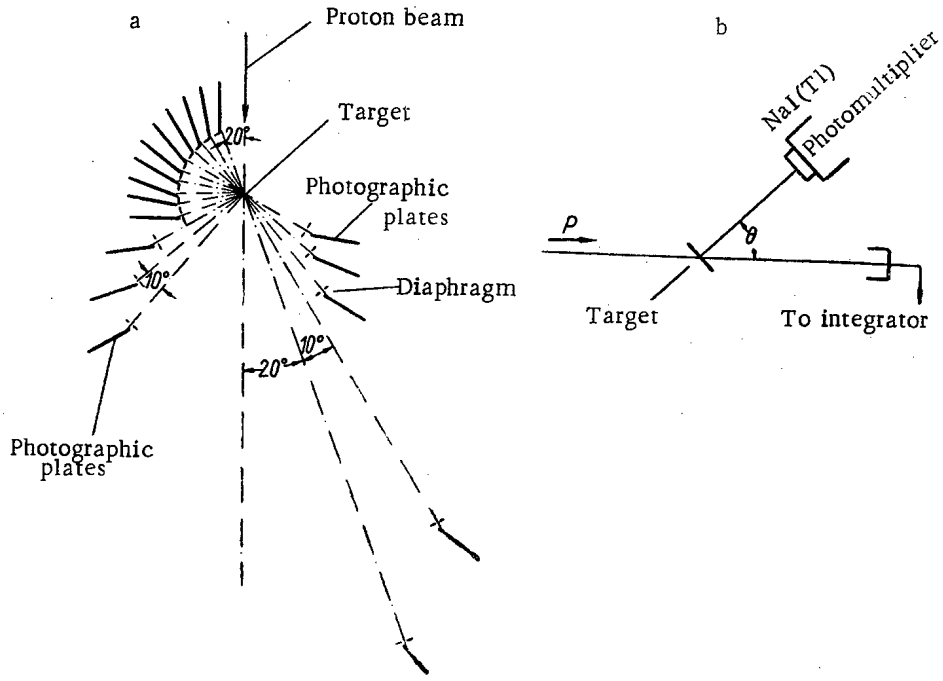

Fig. 2. Scheme of the experiment: a) Using the nuclear emulsion technique; b) using the scintillation counter technique.

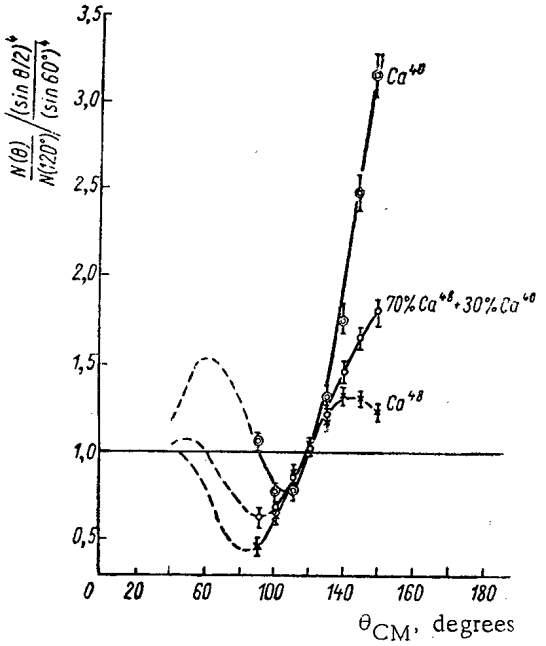

Fig. 3. Angular dependence of ratio $\sigma(\theta)/\sigma(120°)$ in case of Ca^{40} and Ca^{48} at E_p = 5.45 MeV.

correspond to the hypothetical low-angle variation of the angular distribution. The even-even Ca^{40} nucleus yields a scattering pattern typical for nuclei of odd mass number M, while the even-even Ca^{48} nuclide also evinces an angular dependence similar to the dependence for nuclei of odd M (in the large-angle region a pronounced peak is evident in the angular distribution).

Chromium. Cr^{52} and Cr^{53} targets were bombarded by 5.4 and 6.8 MeV protons. The angular dependence for this case is shown in Fig. 4. Scattering on Cr^{52}, which is an even-even nuclide magic with respect to neutrons, is similar to scattering on Ca^{40} at 5.4-MeV energy, while the angular dependence for the even-odd nuclide Cr^{53} is, on the other hand, similar to the dependence for nuclei of odd mass number. The data obtained at 6.8-MeV energy only emphasize the difference in the elastic scattering of protons by these nuclides, but the appearance of a hump in the large-angle curve in the case Cr^{52} points to a tendency for this difference to smooth out as the energy is increased. The continuous curves indicate the angular distribution computed on the basis of the optical model. It is not difficult to see that the best agreement between experimental and theoretical data is observed for odd chromium, while a sharp difference in the large-angle variation of the angular dependence is detected in the case of Cr^{52}.

Nickel. Scattering was studied on the four nickel nuclides Ni^{58}, Ni^{60}, Ni^{62}, and Ni^{64} at proton energies 5.4 and 6.8 MeV. The results obtained appear in Fig. 5. At 5.4-MeV energy, the angular distribution for the first three nuclides is qualitatively the same, and similar to the angular relationships for Ca^{40} and Cr^{52}. However, even in the case of Ni^{62}, we find the scattering intensity at large angles to be markedly lower than the intensity for Ni^{58} and Ni^{60}. As for Ni^{64}, despite the even mass number, the angular dependence proved to be similar to that applying to the case

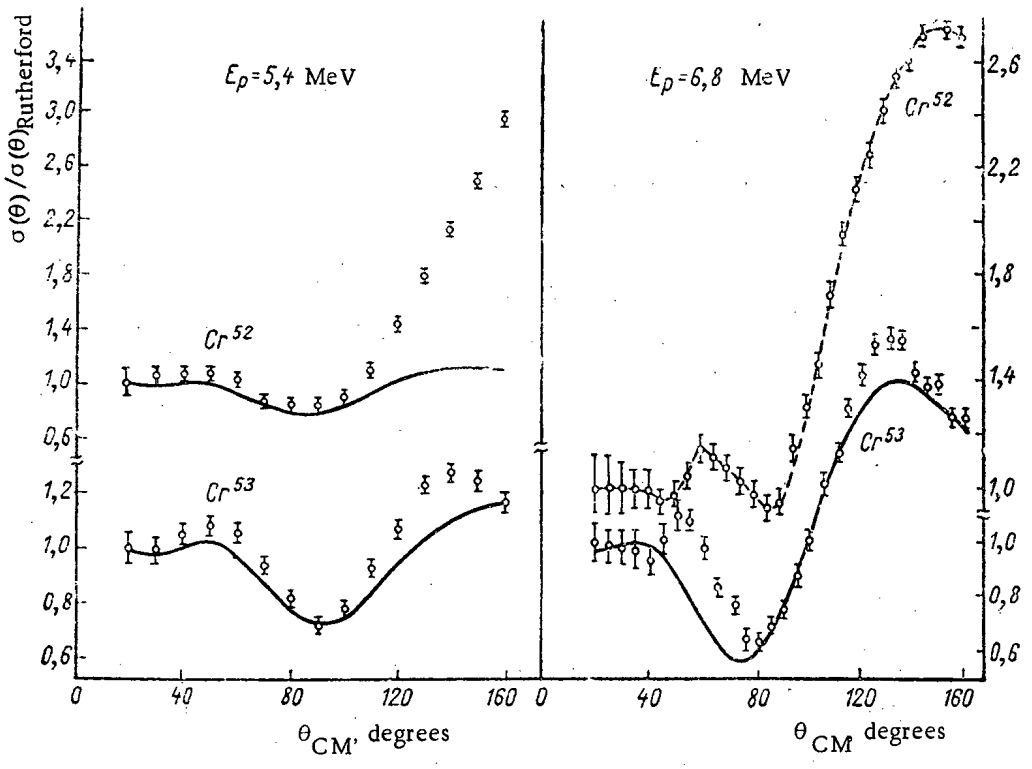

Fig. 4. Angular dependence of the $\sigma(\theta)/\sigma(\theta)_{Rutherford}$ ratio for Cr^{52} and Cr^{53}.

Thresholds of (p,n)-Reaction

Nuclide	Threshold of (p,n)-reaction, MeV		Data source
	calc.	exptl.	
Ca^{40}	15,0	—	—
Ca^{48}	0,52	—	—
Ti^{46}	8,0	—	—
Ti^{47}	3,57	—	—
Ti^{48}	4,90	—	—
Ti^{49}	1,43	—	—
Ti^{50}	3,06	—	—
V^{50}	0,25	—	—
V^{51}	1,53	1,56	[28]
Cr^{52}	5,63	—	—
Cr^{53}	1,83	—	—
Mn^{55}	1,01	1,02	[28]
Fe^{56}	5,4	—	—
Fe^{57}	1,29	—	—
Fe^{58}	3,08	—	—
Co^{59}	1,87	—	—
Ni^{58}	10,48	—	—
Ni^{60}	7,17	—	—
Ni^{62}	4,77	4,7	[28]
Ni^{64}	2,45	2,5	[28]
Cu^{63}	4,2	4,2	[28]
Cu^{65}	2,13	(2,7)	[28]
Zn^{64}	8,00	—	—
Zn^{66}	5,97	6,05	[28]
Zn^{68}	3,81	3,4	[28]

of odd nuclides. At 6.8-MeV proton energy, Ni^{58} and Ni^{60} much the same way as Cr^{52}, while Ni^{62} presents the same scattering pattern as an odd nuclide. The theoretically computed curves are in excellent agreement with experimental curves for Ni^{64} at 5.4 MeV and for Ni^{62} at 6.8 MeV. A striking discrepancy is observed for the lighter nuclides, particularly for Ni^{60} at 5.4 MeV. At a higher energy, the optical model reflects in a satisfactory manner the qualitative variation of the angular relationship for Ni^{58} and Ni^{60}.

Cobalt, Copper, and Zinc. Scattering on cobalt, Cu^{65}, Zn^{64}, and Zn^{68} at 5.4-MeV proton energy was studied. The angular relationship resulting is shown in Fig. 6. Despite the fact that both zinc nuclides are of even mass number, scattering turned out to be similar to the case of scattering by such odd nuclides as cobalt and Cu^{65}.

The curves computed for 5.4-MeV energy turned out to be in excellent accord with empirically plotted curves for Cu^{65} and Zn^{68}, while a fairly pronounced large-angle discrepancy was observed for Zn^{64}.

Angular scattering results for scattering on Cu^{63} and Cu^{65} at 6.8-MeV proton energy were measured and computed theoretically. The curves are similar (both nuclides having odd mass numbers) and exhibit satisfactory agreement with the experimental curves both in general shape and in absolute values (Fig. 7).

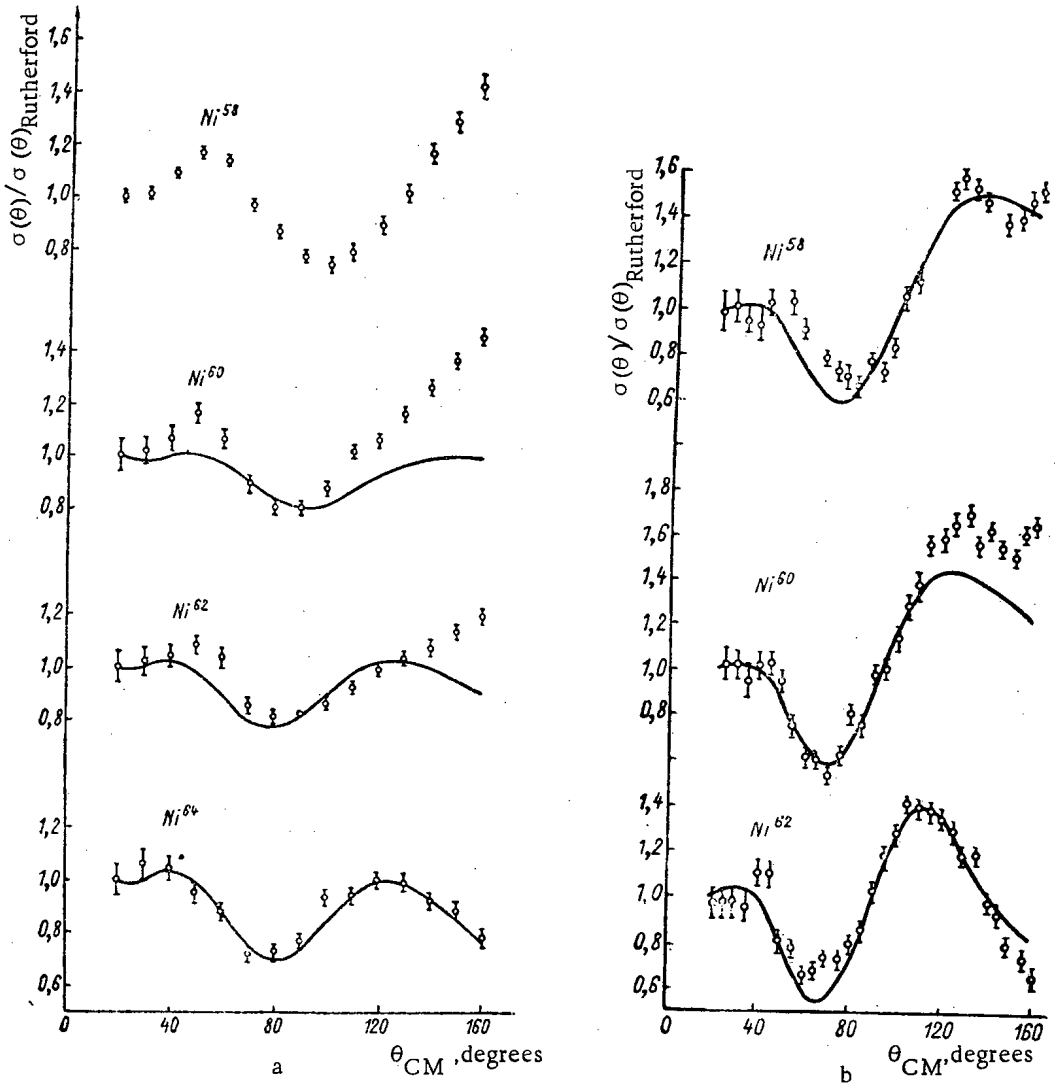

Fig. 5. The same as Fig. 4, for nickel isotopes at E_p = 5.45 MeV (curve a), and E_p = 6.8 MeV (curve b).

Discussion of the Results

The results mentioned above make it possible to draw several inferences on the nature of elastic scattering of protons on atomic nuclei at low energies. It is evident, first of all, that the angular dependence of the ratio of the measured cross section to the Coulomb scattering cross section is qualitatively different for nuclides of odd and of even mass number, while the number of neutrons is close to a magic number in even nuclei.

The scattering picture is sharply altered when the number of nucleons in the nucleus is changed by one unit (independently on the nucleon charge state). The parity of the mass number is accordingly of vital importance in scattering. An odd nucleon strongly smears out the nuclear surface, apparently, and causes an appreciable increase in the probability that an impinging particle will be absorbed in the surface layer of the nucleus. The same effect is observed in nuclides far removed from the magic region, with even mass number and paired nucleons above the closed nucleon shells.

However, an increase in absorption results in an increase in the scattering. In measuring the intensity of scattered protons together with protons scattered elastically in the Coulomb field of the nucleus and in the field of the nuclear forces, we inevitably come to record protons of the same energy and passing through the stage of the compound nucleus, the (p,p)-process with capture. In our preliminary paper on the study of elastic scattering of 5.4-MeV protons by some elements, which was published in 1956 [25], we expressed the conjecture that the high value of the $\sigma(\theta)/\sigma(120°)$ ratio at large angles is related to the capture of the impinging proton by the target nucleus and the formation of the compound nucleus N^{13} with the excitation energy in the resonance region. Greenless et al. [26],

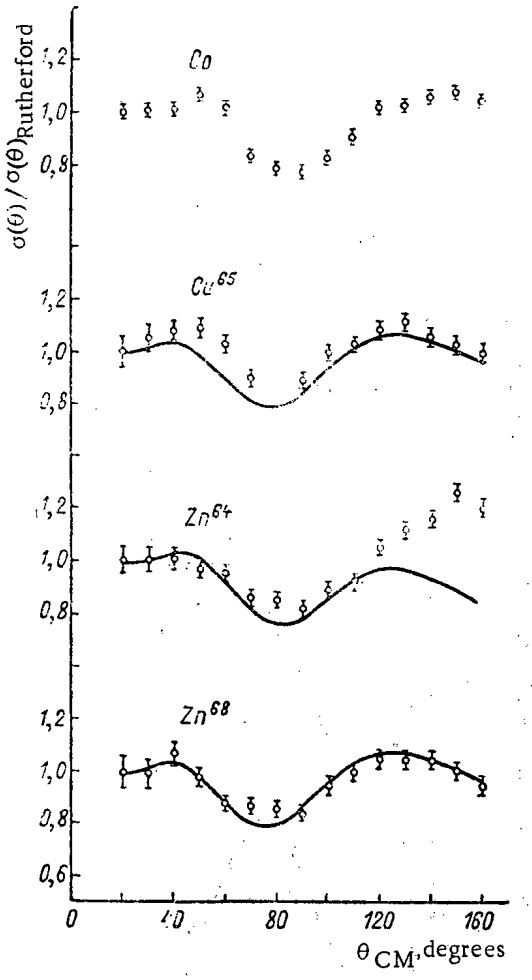

Fig. 6. Same as in Fig. 4, for cobalt, Cu^{65}, Zn^{64}, and Zn^{68} at E_p = 5.45 MeV.

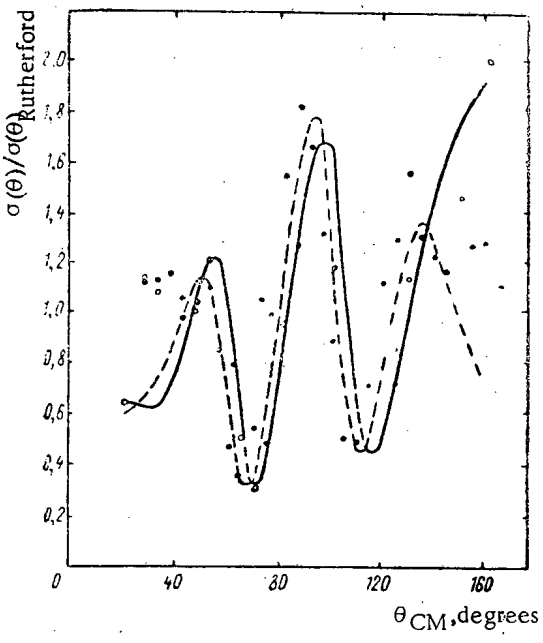

Fig. 8. Same as in Fig. 4, for Co^{59} and Cu^{65} at E_p = 19.6 MeV: O(—), Co^{59}; ●(---), Cu^{65}.

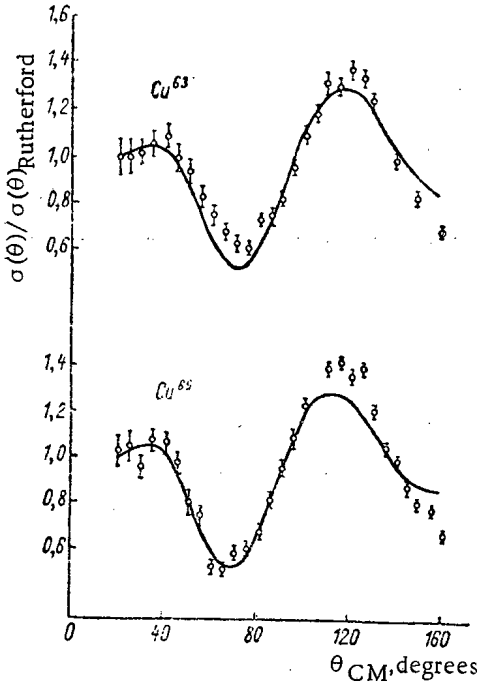

Fig. 7. Same as in Fig. 4, for copper nuclides at E_p = 6.8 MeV.

detected a nonmonotonic energy dependence of the angular distribution of protons elastically scattered on magnesium, and this may likewise be related to the formation of the compound nucleus. At energies below the Coulomb barrier, the probability of decay of the compound nucleus through the elastic channel is always greater than the probability of decay through inelastic channels for charged particles.

The (p,p)-process with capture will predominate if the threshold of the (p,n)-reaction is greater than the energy of the incident particle. Otherwise, a powerful competitor will appear in the (p,p)-process in the form of a reaction with neutron yield. This imparts considerable interest to a comparison of the thresholds of (p,n)-reactions and the behavior of the angular distribution of elastically scattered protons.

In the above table, we list values of the thresholds of (p,n)-reactions computed from the values cited in [27] and values found experimentally for the nuclides in the region we studied. The inference we may make from the table is that all nuclei of odd mass number have low thresholds, just as neutron-enriched isotopes of even nuclei. Nuclides of even mass number but of low N − Z difference have a high threshold, as a rule. This is due to the binding energy of the last neutron in the nucleus.

Let us compare these data with the results of measurements of the angular distributions of elastically scattered protons. The maximum in the large-angle angular distribution is given by all nuclides for which the threshold of the (p,n)-reaction is lower than the energy of the primary protons: Ca^{48}, Cr^{53}, Ni^{64}, Cu^{65}, and Zn^{68}, but this does not apply to Ni^{62} and

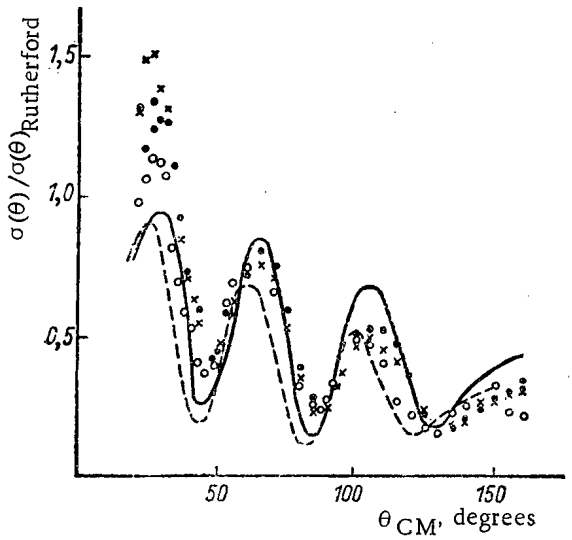

Fig. 9. Same as in Fig. 4, for cadmium nuclides at E_p = 19.6 MeV: ●, Cd^{111}; ×, Cd^{113}; ○, Cd^{116}.

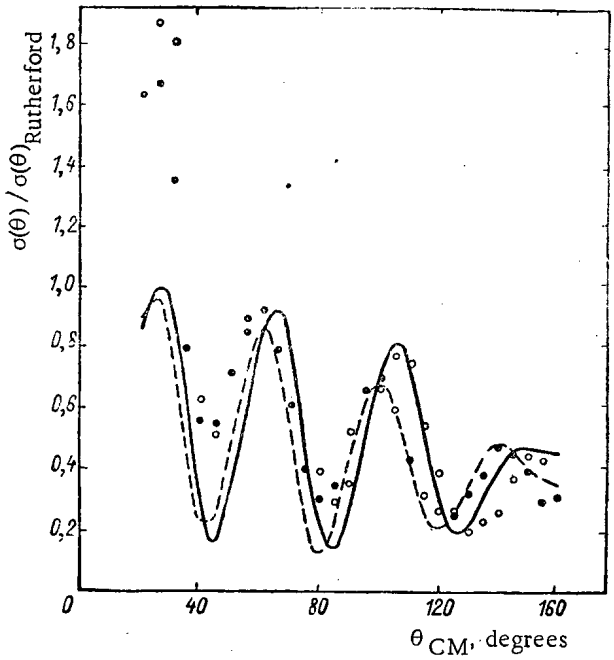

Fig. 10. Same as in Fig. 4, for tin nuclides at E_p = 19.6 MeV: ○(—), Sn^{116}; ●(---), Sn^{124}.

Zn^{64}. This maximum is not present in the case of Ni^{62} despite the fact that the threshold is below the energy of the bombarding particles, but the value of the $\sigma(\theta)/\sigma(\theta)_{Rutherford}$ ratio in the large-angle region is significantly lower than is the case for Ni^{58} and Ni^{60} at 5.4-MeV energy. But even at 6.8-MeV energy, this nuclide scatters protons in the same manner as an odd nucleus. It is possible that the probability of the (p,n)-reaction for Ni^{62} close to the threshold is not high, and increases appreciably as the energy is increased.

Consequently, the "anomalous" increase in the ratio $\sigma(\theta)/\sigma(\theta)_{Rutherford}$ in the large-angle region in the case of nuclides of even mass number is due to a considerable extent to elastic scattering of protons with the formation of a compound nucleus. As the energy increases, the role of the inelastic channels in the decay of the compound nucleus is enhanced, in particular the role of the (p,n) channel, when the energy of the primary protons exceeds the (p,n) reaction threshold. Now this leads to a decrease in the probability of decay of the compound nucleus through the (p,p) channel with capture.

The preceding discussion implies clearly that the theoretical treatment of the experimental results on elastic scattering of protons on atomic nuclei, based on the optical model with no allowance for competing processes, is valid only in those cases where the binding energy of the neutron in the nucleus is not great and the threshold of the (p,n)-reaction is small compared to the energy of the particle scattered.

Of course, a certain contribution to the attenuation of the (p,p)-reaction is creditable to the inelastic channels bearing a yield of charged particles, for example (p,p')-scattering, the value of which varies as the energy. This may apparently account for the humps in the curves of the angular distribution at large angles, in the case of Zn^{64} at 5.4 MeV, and in the case of Ni^{58} and Ni^{60} at 6.8 MeV.

As the energy is increased, the relative contribution of protons scattered with capture to the over-all intensity of the (p,p)-process will decrease because of the growing probability of other inelastic channels open to the decay of the compound nucleus, and the pattern of elastic scattering will approach more and more closely a diffraction pattern. The "isotope effect" in proton scattering at high energies exerts a much less prominent effect at high energies than at low energies.

We studied elastic scattering of 19.6-MeV protons on the following separated isotopes: tritium, He^3 and He^4, Li^6 and Li^7, N^{14}, O^{16}, cobalt, Cu^{63}, Cu^{65}, Ge^{73} and Ge^{74}, Cd^{111}, Cd^{113} and Cd^{116}, Sn^{116}, Sn^{117}, Sn^{118}, Sn^{119}, Sn^{120}, Sn^{122} and Sn^{124}, Pb^{207}, Pb^{208}, and bismuth [21].

The experimental and theoretically computed results for cobalt, Cu^{65}, and various nuclides of cadmium and tin appear in Figs. 8-10. The scattering in these cases is typically diffractive in nature. The optical model is in this case a fully satisfactory description of the elastic scattering of protons on atomic nuclei. The discrepancies in the low-angle region may be due to large experimental errors associated with certain difficulties encountered in low-angle measurements.

At low energies, the extent of agreement between experimental and theoretical data is also considerable for those nuclides having a (p,n)-reaction threshold lower than the energy of the bombarding particles. For these nuclides, the smearing-out of the nuclear surface and the absorption width are greater than for nuclei of even mass number and are close to magic neutron number. This is in accord with the supposition we advanced earlier on the smearing-out of the nuclear surface and the enhanced absorption of impinging particles by these nuclei. It is of course a bit premature to draw any categorical inference from the data. An extended systematic study of the process of elastic scattering of nucleons on separated energies at various energies will be required, with improved experimental accuracy and with allowances for the contribution of the compound nucleus to the scattering picture.

LITERATURE CITED

1. E. Rhoderik, Proc. Roy. Soc., A201, 348 (1950).
2. R. Lelevier and D. Saxon, Phys. Rev., 87, 40 (1952).
3. L. Goldman, Phys. Rev., 89, 349 (1953).
4. B. Cohen and R. Neidigh, Phys. Rev., 93, 282 (1954).
5. I. Dayton, Phys. Rev., 95, 754 (1954).
6. I. Dayton and Q. Schrank, Phys. Rev., 107, 1602 (1957).
7. I. Beyster, M. Wall, and E. Salmi, Phys. Rev., 104, 1319 (1956).
8. W. Waldorf and N. Wall, Phys. Rev., 107, 1602 (1957).
9. M. V. Pacetshnik, N. I. Putsherov, and M. A. Totsky, Comptes rendus du Congress Internationale de Physique Nucleare (Paris, 1958), p. 598.
10. N. I. Pucherov, Ukrains'ki fiz. zh., 4, 313 (1959).
11. A. I. Akhiezer and I. Ya. Pomeranchuk, Usp. fiz. nauk., 39, 153 (1949).
12. B. Kinsey and T. Stone, Phys. Rev., 103, 975 (1956).
13. M. Brussel and J. Williams, Phys. Rev., 114, 525 (1959).
14. H. Hinz, Phys. Rev., 106, 1201 (1957).
15. A. Glassgold, W. Cheston, M. Stein, and G. Erickson, Phys. Rev., 106, 1207 (1957).
16. A. Glassgold and P. Kellog, Phys. Rev., 107, 1372 (1957).
17. D. Bromly and N. Wall, Phys. Rev., 102, 1372 (1957).
18. M. Kondo et al., J. Phys. Soc. Japan, 13, 231 (1958).
19. A. P. Klyucharev and N. Ya. Rutkevich, ZhÉTF, 38, 286 (1960).
20. N. Ya. Rutkevich, V. Ya. Golovnya, A. K. Val'ter, A. P. Klyucharev, DAN SSSR, 130, 1008 (1960).
21. R. A. Vanetsian, A. P. Klyucharev, and E. D. Fedchenko, Atomnaya énergiya, 6, 661 (1959).
22. A. K. Val'ter et al., ZhÉTF., 38, 1419 (1960).
23. A. D. Bondar' et al., Pribory i tekhn. éksp., No. 3, 134 (1960).
24. A. D. Bondar' et al., Pribory i tekhn. éksp., No. 3, 137 (1960).
25. A. P. Klyucharev, L. I. Bolotin, and V. A. Lutsik, ZhÉTF., 30, 573 (1956).
26. G. Greenless et al., Proc. Phys. Soc., A70, 331 (1957).
27. V. A. Kravtsov, Usp. fiz. nauk., 65, 451 (1958).
28. J. Blaser et al., Helv. phys. acta, 24, 3 (1951).

All abbreviations of periodicals in the above bibliography are letter-by-letter transliterations of the abbreviations as given in the original Russian journal. *Some or all of this periodical literature may well be available in English translation.* A complete list of the cover-to-cover English translations appears at the back of this issue.

COLLECTIVE INTERACTIONS AND THE PRODUCTION OF A HIGH-TEMPERATURE PLASMA

E. K. Zavoiskii

Translated from Atomnaya Énergiya, Vol. 14, No. 1,
pp. 57-65, January, 1963
Original article submitted October 15, 1962

Introduction

The problem of producing a high-temperature plasma and the problem of containing such a plasma cannot be treated independently. It is difficult to think of a plasma confinement device that is not affected by the method used to produce the plasma. Indeed, the plasma heating process determines directly confinement parameters such as heating time, the time-rate-of-change of the electron and ion temperatures during the plasma production process, the oscillation spectrum, the presence of trapped magnetic fields and impurities, plasma currents, etc. Because of the complexity of the problem, however, at this stage we must consider methods of heating plasma separately from methods of containing plasma. Below we shall be interested primarily in the plasma heating problem.

It is now clear that the description of a plasma in terms of a system of charged particles that interact with each other via binary Coulomb collisions is an inadequate one. Collective interactions play an extremely important role in plasmas produced under actual experimental conditions. Among these interactions we think first of the interaction of a beam of charged particles with a plasma, an interaction that has been studied in detail both theoretically and experimentally. It has been found that a beam in the plasma rapidly loses the energy associated with the ordered motion because of collective interactions. The possibility of using this effect for plasma heating seems to be worth investigating. However, in actual experiments the beams are generally formed outside the plasma and for this reason are characterized by low densities, as is the plasma into which they are injected. Obviously, charged particle beams need not be injected into the plasma from outside; under certain conditions they are produced inside the plasma [1]. In this case a beam can generally excite plasma oscillations and have an important effect on the nature of the plasma processes. This was first pointed out by R. Z. Sagdeev [2], who showed that the excitation of collective electron motions can explain the damping of shock waves in a collisionless plasma.

L. I. Rudakov has proposed that the dissipation of oscillation energy by virtue of this mechanism is possible not only for the shock wave, but also for an ordinary wave, if the wave amplitude is sufficiently great.

Thus, the important problem of studying collective processes in a plasma can be reduced to the search for conditions under which charged particle beams capable of exciting plasma oscillations can be produced by electomagnetic fields. If an effective method for transferring the energy of an external electromagnetic field to a flux of charged particles can be found, this would represent a solution to the problem of heating a collisionless plasma with a high degree of efficiency.

Obviously the importance of collective processes in a plasma is not limited to this one aspect of the problem; as far as obtaining a high-temperature plasma is concerned, however, these effects are evidently the most important so long as plasma stability is not considered.

The problem of heating a plasma by randomizing the energy of ordered motion through collective processes has certain wider ramifications. Let us assume that strong external electromagnetic fields cause rapid ordered plasma motion which, in turn, leads to the appearance of an instability on a scale which is much smaller than the characteristic dimensions (for example, the radius of the plasma column). If the growth time of these instabilities and the time during which the external electromagnetic fields are applied are both small, and if the oscillations arising as a result of the instability relax quickly to a thermal level, then this process will result in the thermalization of the ordered velocity without having a noticeable effect on plasma loss from the trap. The plasma temperature that can be achieved under these conditions is determined by the ordered velocity of the ions, i.e., the magnitude of the external fields. The difference between this method of heating and that described above, which is based on the

development of beam-type instabilities, lies in the difference in the nature of the mechanisms producing the instabilities in the plasma; in turn, these differences lead to important differences in the space and time scales of the instabilities.

Conditions for the Excitation of Electron Plasma Oscillations

The interaction of a beam of charged particles with a plasma has been studied in detail both theoretically and experimentally, and has been described by many authors. Although most of the experiments have been carried out with the beams injected into the plasma from outside, the criteria for excitation of collective oscillations are approximately the same as for the case in which the beams are produced in the plasma by external electromagnetic fields. The excitation of oscillations requires that v_e, the ordered velocity of the electrons with respect to the ions, be greater than the thermal velocity $v_{eT} = \sqrt{\frac{2T_e}{m}}$. Under these conditions, Langmuir oscillations are excited in the plasma in a time of order $\tau \simeq \frac{1}{\omega_0}\sqrt{\frac{M}{m}}$, where $\omega_0^2 = \frac{4\pi ne^2}{m}$, with wavelengths of order v_e/ω_0. The energy of the plasma oscillations is thermalized at the same time. If the plasma is located in an external magnetic field H and $\omega_0 >> \omega_{eH}$, where $\omega_{eH} = \frac{eH}{mc}$, the magnetic field has little or no effect on the development of the instabilities.

Using these general considerations, we now consider the concrete problem of exciting electrostatic oscillations in a plasma by means of external electromagnetic fields [3]. Assume that the plasma column is located in a longitudinal magnetic field described by

$$H = H + H_{\sim} e^{-\alpha t} \sin \omega t. \tag{1}$$

The electron current density in the plasma is then

$$j = -ev_\varphi n = -\frac{c}{4\pi}\frac{\partial H_{\sim}}{\partial r}, \tag{2}$$

where r is the distance from the axis of the column. Using Eq. (2), we find criteria for the appearance of a collective electron friction

$$\frac{H_{\sim}^2}{8\pi n T_e} > \frac{\omega_0^2}{|k|^2 c^2}, \tag{3}$$

where $k = \left|\frac{1}{H_{\sim}}\frac{dH_{\sim}}{dr}\right|$ is the wave vector, which depends on the plasma density n, the magnetic field H, and the orientation of the field with respect to $H_{\sim}$. If $H_{\sim}$ is parallel to H, then when $H_{\sim}/H << 1$, neglecting wave damping, we have

$$k^2 = \frac{\omega^2}{v_A^2}\frac{1}{1-\frac{\omega^2}{\omega_{ei}^2}}, \tag{4}$$

where

$$v_A = \frac{H}{\sqrt{4\pi nM}}; \quad \omega_{ei}^2 = \frac{e^2H^2}{mMc^2}.$$

Thus, the relation in (3) can be written in the form

$$\frac{H_{\sim}^2}{8\pi n T_e} > \frac{\omega_{ei}^2}{\omega^2}\left|\left(1-\frac{\omega^2}{\omega_{ei}^2}\right)\right|. \tag{5}$$

The relation in (5) gives the threshold value of the amplitude of the ac field required for the excitation of electrostatic oscillations in the plasma.

It should be noted that when $\omega > eH/Mc$, the wave vector k (i.e., the fraction of kinetic energy of the electrons in wave energy) falls off rapidly with increasing $\theta = \angle \mathbf{k}; \mathbf{H}$; when $\theta > \sqrt{\frac{m}{M}}$ the energy obtained by the electrons from the external high-frequency field becomes small compared with the energy of the electromagnetic field in the wave. This result has a simple meaning: In oblique propagation of waves in a magnetic field, the electric field of the wave is highly damped by the electrons, which can move easily along the fixed magnetic field; for this reason

the drift velocity of the electrons in the wave v_φ is reduced, and this means that the kinetic energy of the electrons is reduced.

We now consider the question of how rapidly the energy of the Langmuir oscillations can be thermalized, and whether the excitation of these oscillations has an appreciable effect on the loss of plasma from the confinement system. It follows from the theory [4] that the electron velocity distribution in a monochromatic beam in a plasma is converted into a smooth essentially Maxwellian function in a time of the order of ten Langmuir periods. Thus, if $\omega \ll \omega_0$, the thermalization of the energy of electrostatic oscillations will occur very rapidly as compared with the period of the external field. Hence, particle loss from the plasma due to oscillations with amplitude appreciably greater than the amplitude of thermal (equilibrium) oscillations will occur only during the heating time τ. If $\tau < \frac{r}{\sqrt{\frac{2(T_e + T_i)}{M}}}$, this loss is small. This result has been verified experimentally.

We now consider the development of electron heating in a plasma as a function of time. To avoid complications, we assume that the plasma is located in a fixed magnetic field and that at time t = 0 an additional sinusoidal field is applied in accordance with Eq. (1), where $\alpha = 0$. If the frequency of the external field $\omega \ll \omega_0$ and the amplitude $H_\sim$ satisfy the condition for excitation of electrostatic oscillations (3), absorption of plasma wave energy will continue up to the time at which the thermal velocity of the electrons becomes comparable with the ordered velocity of the electrons in the wave. Since the time required for excitation and thermalization of the energy of the Langmuir oscillations is much smaller than the period of the high-frequency field $2\pi/\omega$, the temperature of the electrons will increase along with the growth in energy density $H^2_\sim/8\pi$; heating is terminated in approximately the time required for penetration of the high-frequency field over the entire depth of the plasma column, i.e., a time of order r/v_A.

At this point the electron temperature that is established is determined by the amplitude of the variable field and other plasma parameters in accordance with Eq. (3), so long as we neglect the plasma cooling resulting from various energy loss mechanisms. Thus, the plasma heating rate is very high and it is not necessary to use a long heating pulse. In most cases in practice one requires a time of the order of one period of the external magnetic field. If the heating is applied over a section of a long plasma cylinder, the time required for heating the electrons to the peak temperature is determined by the electron thermal conductivity along the plasma.

The method of plasma heating described here is now called turbulent heating; it can be used to produce a plasma with hot electrons. The next question then concerns the possibility of heating the ions. Obviously one cannot rely on the transfer of energy from electrons to ions via binary Coulomb collisions because the electron-ion collision cross section is very small at high electron temperatures T_e. Several possible methods of ion heating associated with turbulent electron heating are discussed below.

Excitation of Ion Plasma Oscillations

The turbulent electron heating mechanism considered above can be used to produce conditions for the excitation of ion plasma oscillations by virtue of the two-stream instability for ions moving along the fixed magnetic field. As shown by B. B. Kadomtsev [5], the ion two-stream instability can arise only when the electron temperature is greater than the ion temperature and is greater than the energy of the directed ion motion. This requirement can be explained simply: If the electrons are cold, the electrostatic fields produced by the ion instability are rapidly compensated by the electrons, since the electrons can move freely along the magnetic field. However, at electron temperatures such that

$$T_e > \frac{Mv_i^2}{2} > T_i \tag{6}$$

this compensation of the ion fluctuation charges by virtue of the high pressure of the electron gas is no longer possible, and the ion-beam instability can develop freely. Hence, turbulent heating of electrons allows thermalization of opposing ion streams and thus makes it possible to obtain a plasma with both hot electrons and hot ions.

According to Eq. (6), the limiting ion temperature which can be achieved by means of the two-stream instability depends only on the electron temperature if the ions have a sufficiently high relative velocity with respect to each other.

Magnetic Compression of a Turbulently Heated Plasma

It is well known that magnetic plasma compression [6] can be used to increase temperature and density; moreover, under conditions compression reduces appreciably the loss of particles from the confinement system due to binary

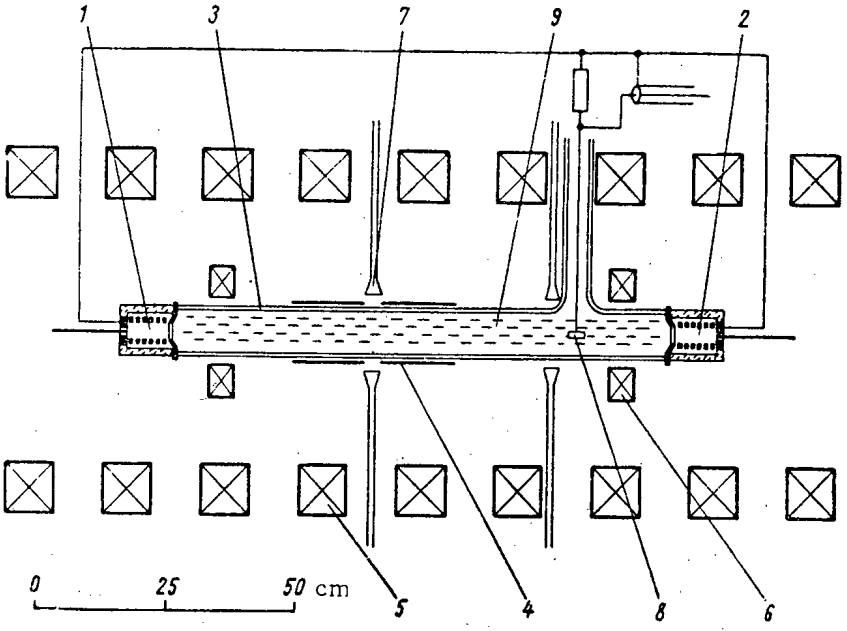

Fig. 1. Diagram of the experimental apparatus used to study turbulent heating, containment of a turbulently heated plasma in a magnetic mirror system, and the ion two-stream instability. 1) and 2) Plasma guns (the current pulse in the guns is approximately 3-4 μsec); 3) quartz tube 3.6 cm in diameter and 110 cm long; 4) oscillation circuit mounted on tube 3; 5) coils of the main solenoid producing the fixed magnetic field; 6) mirror coils providing a mirror ratio up to 5; 7) microwave probes at 3 and 0.8 cm; 8) probe for measuring ion temperature [8]; 9) section of plasma from which light is emitted into two monochromators furnished with photomultipliers. The magnetic probe is located at the axis of the tube 3 at the center of circuit 4 or at its edge. Operation of circuit 4 with a small delay time with respect to guns 1 and 2 in the region of the circuit causes appearance of opposing plasma jets with densities of $\sim 2 \cdot 10^{13}$ electrons per cm^3 and proton energies up to 100 eV. At time delays greater than 50 μsec the ions essentially lose all their ordered velocity.

Coulomb collisions. If the radial compression of the plasma occurs by virtue of a magnetic field that increases linearly in time, the maximum compression time without particle loss due to collisions is [6]

$$t < \frac{1{,}17 \cdot 10^{11} T^{3/2} \alpha_0^{1/2}}{n} \text{ sec.} \tag{7}$$

Here, T is the initial plasma temperature in keV: $\alpha_0 = H_f / H_0$, where H_0 and H_f are the initial and final magnetic field strengths. It is evident from Eq. (7) that turbulent heating, which can yield appreciable initial temperatures T_e and T_i can, even with small α_0, be used in conjunction with slow compression to obtain long confinement time of a hot plasma; this statement holds so long as dangerous instabilities do not develop.

In turbulent heating the energy transferred by the wave to the plasma is determined only by the strength of the variable magnetic field, and is given by

$$T_v = \frac{\xi H_\sim^2}{8\pi n}, \tag{8}$$

where, as shown experimentally (cf. below), the maximum value of the constant $\xi = 0.5$ [3]. It is convenient to use a shock-excited circuit to obtain high $H_\sim$; this circuit may consist of one wide turn (inductance in the circuit) and a capacity connected in parallel. It is easily shown that the magnetic field at the axis of such a turn is

$$H_\sim = \frac{5 \cdot 10^6 \cdot U}{\nu R^2 (1 + \bar{\lambda})}, \tag{9}$$

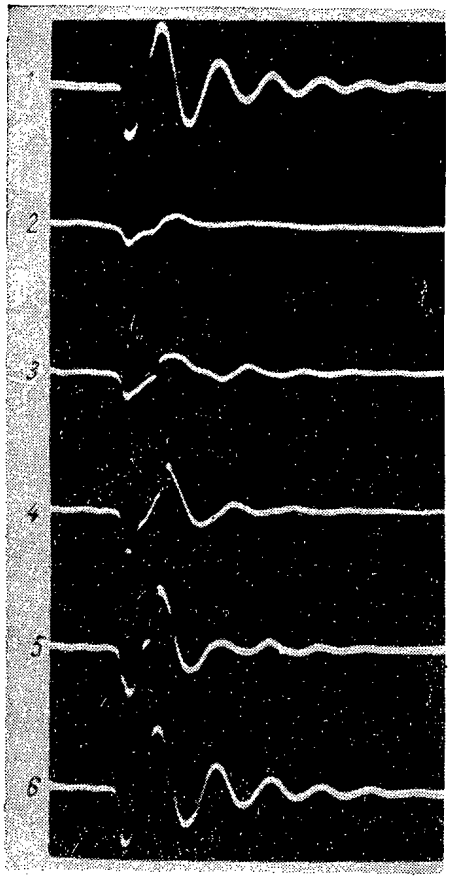

Fig. 2. Oscillograms of the voltage on the magnetic probe located at the axis of the plasma column at the center of the oscillation circuit for different values of the fixed magnetic field. Oscillation circuit frequency $\nu = 1.2 \cdot 10^7$ cps, $H_\sim = 600$ Oe, working gas is hydrogen, $p = 10^{-3}$ mm Hg, $n \simeq 1.7 \cdot 10^{13}$ cm^{-3}. The probe readings indicate that the wave is damped in the plasma very strongly in the region in which $\omega \simeq \omega_{ei}$. Wave damping is not due to ionization or other binary collision processes, since the gas pressure is low and the frequency of field variation is very high.

where U is the voltage (in volts) across the circuit capacity; ν is the natural frequency of the circuit; R is the radius of the turn; $\bar{\lambda}$ is the ratio of stray inductance of the circuit to useful inductance. In Eq. (9), the frequency ν is related to the radius of the plasma column in the following way: The radius r must represent at least a quarter wavelength, i.e.,

$$r \geq \frac{v_A}{4\nu}. \tag{10}$$

In addition to Eq. (10), we must impose the following obvious limitation on ion temperature:

$$r = b\rho_i, \tag{11}$$

where ρ_i is the ion Larmor radius and b is a factor greater than unity. We use Eqs. (8)-(11) to perform an approximate calculation of the electron and ion temperatures. We assume that $\nu = 10^7$; $U = 3.5 \cdot 10^5$ V; $R = 1.2r = 6$ cm; $r = 2.5\rho_i$; $\bar{\lambda} = 0.5$. Then, with $n = 2 \cdot 10^{13}$ cm^{-3} and $H \simeq H_\sim$, we have from Eqs. (8)-(11), $T_e = 5.8 \cdot 10^3$ eV, $T_i \leq 5 \cdot 10^3$ eV, and from Eq. (7) the time for magnetic field compression with $\alpha_0 = 10$ is found to be

$$t \leq 0{,}2 \text{ sec.}$$

With this long compression the turbulent heating can provide a final plasma temperature of about 50 keV.

If we assume that the natural frequency of the shock-excited circuit is

$$\nu = \frac{8 \cdot 10^2}{R\sqrt{C_1(1+\bar{\lambda})}}, \tag{12}$$

where C_1 is the capacity of the circuit per unit length of turn in farads, then, introducing the notation $H = aH_\sim$ and $R = \varkappa r$, from Eqs. (8), (9), and (12) (with the condition $r = v_A/4\nu$) we find

$$T_e = \frac{0{,}126\xi}{\varkappa^2(1+a^2)(1+\bar{\lambda})C_1} \ (^\circ\text{K}); \tag{13}$$

$$n = \frac{0{,}9 \cdot 10^{23}(1+a^2)C_1^2U^2}{r^2} \ (1/\text{cm}^3); \tag{14}$$

$$q_1 = \pi r^2 nkT_e = \frac{0{,}5 \cdot 10^7 \xi C_1 U^2}{\varkappa^2(1+\bar{\lambda})} \ (\text{erg/cm}). \tag{15}$$

where q_1 is the energy generated per unit length of plasma column, i.e., the energy obtained by the plasma from the oscillatory circuit due to turbulent heating. It is interesting to note that (13), the temperature reached by the plasma in turbulent heating under the most convenient conditions, is inversely proportional to the running capacity C_1 and is independent of the voltage across the capacity and the natural frequency of the circuit.

Experiments on Collective Interactions in a Plasma

These experiments were carried out with the following purposes: 1) investigation of turbulent heating [1,3]; 2) containment of a turbulently heated plasma in a magnetic mirror system [7]; 3) examination of the effect of the ion beam instability in turbulent heating of electrons by oppositely directed plasma jets [8]. In all of these cases, the experimental apparatus was very much the same, so that we describe one case only [7].

A diagram of the apparatus is shown in Fig. 1. The plasma is produced in a quartz tube 3 by injection of plasma jets from the guns 1 and 2 which contain titanium buttons saturated with hydrogen or deuterium. The guns

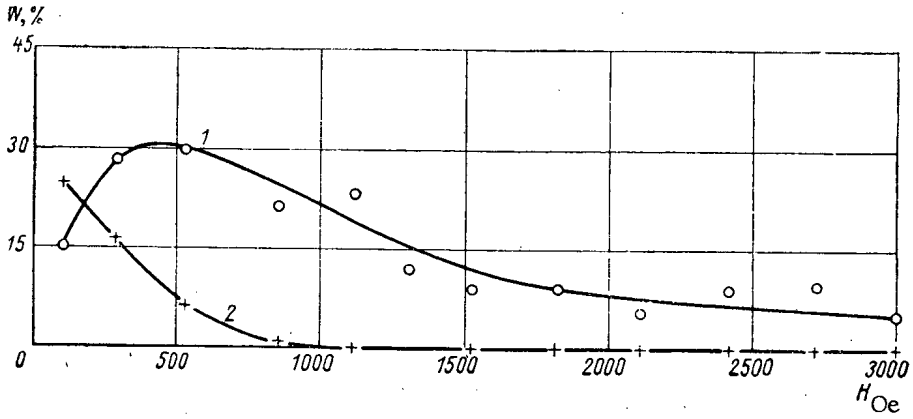

Fig. 3. The energy absorbed in a collisionless plasma as a result of turbulent heating as a function of the fixed magnetic field H and the angle between H and $H_{\sim}$. Curve 1) $\theta = 0$; curve 2) $\theta = 8°$; $H_{\sim} = 500$ Oe; $\nu = 1.4 \cdot 10^7$ cps. According to the linear theory, the peak of wave absorption lies at $\omega = \omega_{ei}$, in which case H = 310 Oe, which is in satisfactory agreement with experiment at $\theta = 0$. For $\theta > 1.5°$, the linear theory does not give wave absorption but it is observed experimentally even when $\theta = 8°$ for fields $H \lesssim H_{\sim}$. This effect is related to the existence of a nonlinearity in the process. Under the conditions of these measurements the area of a cross section of the plasma column represents approximately 0.6 of the cross-sectional area of the coil of the oscillation circuit; hence, a unit volume of plasma, according to curve 1, absorbs at peak approximately half the energy of the magnetic field per unit volume, i.e., in Eq. (8), $\xi \simeq 0.5$.

are operated simultaneously and produce two plasma jets which start to move toward each other in the fixed magnetic field produced by the coils of solenoid 5 (300-600 Oe); these jets penetrate each other. Control experiments show that in the course of time the velocities of the jets are reduced, and that the tube 3 is gradually filled by a nonmoving plasma. Thus, one apparatus can be used with plasma jets, for the examination of ion beam instabilities, as well as with a fixed plasma. Spectroscopic measurements have shown a small amount of impurities in the plasma. For operation with helium (in certain cases with hydrogen [1, 3]), the guns are replaced with copper or molybdenum electrodes; the gas discharge is then formed by discharging a condenser bank of $5 \cdot 10^4$ pF charged to 20-30 kV. The oscillation circuit 4 on the quartz tube 3 filled with plasma is a copper cylinder 30 cm long and 4-5 cm in diameter, split into two equal halves along the axis. To one side is connected the capacity of $C = 10^4$ pF; a controlled spark gap is connected to the other. The capacity can be charged to a maximum of 60 kV, making it possible to produce at the axis of the cylinder a magnetic field of $H_{\sim} \simeq 1.2$ kOe at a frequency of 10^7 cps. The oscillation circuit has a low quality factor so that the amplitude of the current is reduced by a factor of 2 in a time of approximately two oscillation periods, i.e., $2 \cdot 10^{-7}$ sec. The measurement of $H_{\sim}$ inside the plasma is accomplished by means of a magnetic probe shielded from the electric fields.

To measure the wave damping in the plasma caused by the excitation of Langmuir oscillations by the electrons accelerated by the electric field of the wave, we produce a plasma by one of the indicated methods in tube 3; then we fire the discharge gap of the oscillation circuit. We measure $H_{\sim}$ in the plasma and the damping of the oscillation circuit caused by energy losses in the plasma. Microwaves at 3 and 0.8 cm are used to determine the plasma density while monochromators and photomultipliers are used to study the emission of individual spectral lines.

Since the quality factor of the oscillation circuit is low, the time during which the high-frequency magnetic field operates on the plasma is much smaller than the time required for ionization of the neutral particles. Furthermore, because of the high electric field in the wave (resulting from the appreciable $H_{\sim}$), the electrons rapidly acquire high velocities and the Joule losses in the wave are insignificant. For this reason the electron temperature of the plasma can be found by a "calorimetric" method: we determine the plasma density before and after turbulent heating and determine the electron temperature from the energy lost by the electrons to ionization.

Another reliable method of determining electron temperature is the measurement of the plasma containment time in the mirror device [7].

We present below the basic results of these experiments.

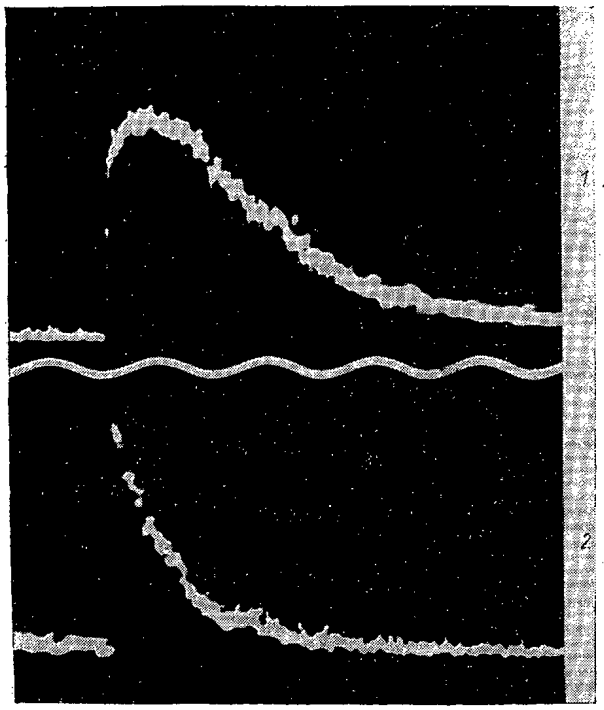

Fig. 4. Containment of a turbulently heated hydrogen plasma with small helium impurity in a magnetic mirror system. Upper trace shows emission in time of the He II 4865 A line with mirror system switched on. The sharp rise in emission of the line in both cases corresponds to the time at which oscillation circuit is triggered. Primary magnetic field H = 600 Oe; field in the mirrors = 3000 Oe. Below we show emission of same line under same conditions but with magnetic mirror switched off. The signal gain is three times higher than in first picture. Period of sinusoid shown in the figure is 10 μsec; $H_{\sim}$ = 1.2 kOe; $n = 1.7 \cdot 10^{13}$ cm^{-3}. Plasma is produced by injection of plasmoids from guns. Initial gas pressure in tube $p \leq 10^{-6}$ mm Hg. Fuzziness in emission on first pattern is related to gradual ionization of helium atoms and accumulation of He II in the plasma. Sharp drop in emission in the second trace is related to fast cooling of electrons at the ends of the tube.

1. It has been established that there is a high degree of strong collisionless absorption of electromagnetic waves in the region $\omega \simeq \omega_{ei}$ (Figs. 2 and 3). It is found that the wave damps out appreciably even in a distance of the order of a half wavelength in the plasma. It is shown that the absorption is related to the transfer of energy from the wave to the plasma electrons, and that the electron temperature corresponds approximately to the expected theoretical value (8), where $\xi = 0.5$. The experiments were carried out at $\omega/2\pi \simeq 10^7$ cps and $H_{\sim} \leq 1.2 \cdot 10^3$ Oe in a plasma density of $10^{12} \leq n \leq 2 \cdot 10^{13}$. A maximum electron temperature of approximately 800 eV was obtained. The region of strong wave absorption occupies a wide range of magnetic fields. This region increases as the intensity of the high-frequency field is increased. The wave absorption effect exhibits a threshold: it disappears at low values of the ratio $H_{\sim}/H$, in accordance with theory (5). The measured dependence of wave absorption on angle θ is also found to be in accordance with theory (Fig. 3).

2. Turbulent heating of electrons in a plasma to temperatures of the order of 600-800 eV allows us to study the stability of a plasma obtained in this way in a mirror device [7]. The measurements show that this plasma is contained for a time approximately equal to the time required for one electron-electron collision (Fig. 4). Turbulent heating does not lead to any dangerous instability. It is interesting to note that the plasma is contained for a time at least an order of magnitude greater than the time required for the development of the interchange instability.

3. In experiments on the excitation of an ion two-stream instability with two colliding plasmoids, it has been shown that turbulent heating of the electrons leads to the complete thermalization of the directed ion velocities [8]. The experiments were carried out in hydrogen with directed ion energies along the magnetic field with a maximum value of 100 eV and plasmoid densities of approximately $2 \cdot 10^{13}$ cm^{-3} and $T_i \simeq 5$ eV. The proton energy, 100 eV, corresponds to a mean free path for Coulomb collisions several times greater than the dimensions of the experimental apparatus. The maximum recorded ion temperature after turbulent heating is 50 eV. Ions with higher energies escape to the chamber walls. The maximum electron temperature in these experiments is estimated as 200-400 eV.

Thus, these experiments have verified the possibility of using collective motions of electrons and ions for plasma heating.

4. The experiments described above to examine the ion two-stream instability [8], were carried out in a fixed magnetic field no greater than 0.6 kOe. It was later discovered that for values H = 1-3 kOe and $0.6 \leq H_{\sim} \leq 1.2$ kOe there is an appreciable heating of ions to 25-30 eV, even when the ions in the plasma have no directed velocities. This condition is produced when the turbulent heating is carried out with a very long time delay with respect to the time at which the guns are triggered and the Coulomb scattering of the plasma jets brings the plasmoids to rest. It has been found that the ion temperature exhibits a well-defined peak, which depends on the fixed magnetic field, and that this peak is shifted linearly toward higher fields with increasing $H_{\sim}$. In magnetic field $H \geq 3.5$ kOe (with $H_{\sim}$ = 1.2 kOe), the heating of ions is terminated just as when $H \leq 0.6$ kOe. We note that for fixed magnetic fields 0.3 to

1 kOe there is a maximum of turbulent electron heating for a hydrogen plasma while in the region $H \geq 3.5$ kOe (with $H_{\sim} = 1.2$ kOe) the electrons are no longer heated. Thus, the ion temperature increases when the turbulent heating of electrons is reduced and the ion heating vanishes when the turbulent heating is terminated. According to the linear magnetohydrodynamic calculation [9], the energy of the electrons in the wave has a maximum in the region $\omega \simeq \omega_{ei}$, and falls with increasing ω_{ei}/ω, while the ion energy has a minimum in the range $\omega_{ei}/\omega \simeq 1$, and is independent of the magnetic field when $\omega_{ei}/\omega \gg 1$. If we accept the latter, then the following conclusion can be drawn regarding the observed effect: The ions are heated as a consequence of thermalization of the ordered ion velocity of the wave and thermalization can be realized only with relatively hot electrons.

One expects that this effect is related to the development of a relatively fine scale plasma instability in the strong electromagnetic wave by virtue of fast mixing of the plasma and strong damping of the turbulence, as noted in the introduction.

Conclusions

Turbulent heating appears to be a simple method for obtaining a plasma with a high electron temperature. Based on the use of collective motion in the plasma, it has certain advantages compared with heating methods based on binary Coulomb collisions. This advantage is especially important when the temperature is increased, in which case the Coulomb cross section becomes smaller.

In a plasma with hot electrons produced by turbulent heating, conditions arise in which ion electrostatic oscillations can be excited. Hence, we have two-stream motion of the ions with high relative velocities; turbulent heating allows us to produce a plasma with hot electrons and ions. It is of interest to study magnetic compression of such a plasma in this connection, since the appreciable initial temperature makes it possible to obtain a high temperature plasma by means of slow and relatively weak compression.

The hot plasmas obtained by means of turbulent heating open a number of new possibilities for the investigation of plasma stability in various confinement systems.

In conclusion, I wish to thank M. V. Babykin, A. A. Vedenov, E. P. Velikhov, L. I. Rudakov, R. Z. Sagdeev, and V. A. Skoryupin for interesting discussions of the work described here.

LITERATURE CITED

1. M. V. Babykin et al., Report No. 209, International Conference on Plasma Physics and Controlled Nuclear Fusion (Salzburg, 1961).
2. A. A. Vedenov, E. P. Velikhov, and R. Z. Sagdeev, Nuclear Fusion, 1, 82 (1961).
3. M. V. Babykin et al., ZhÉTF., 43, 411 (1962).
4. J. Dawson, Report No. 163, International Conference on Plasma Physics and Controlled Nuclear Fusion (Salzburg, 1961).
5. B. B. Kadomtsev, Plasma Physics and the Problem of a Controlled Thermonuclear Reaction [in Russian] (Izd. AN SSSR, Moscow, 1958), Vol. 4, p. 364.
6. R. Post, International Conference on the Peaceful Uses of Atomic Energy, Geneva, 1958.
7. M. V. Babykin et al., ZhÉTF., 43, 1547 (1962).
8. M. V. Babykin et al., ZhÉTF., 43, 1976 (1962).
9. D. A. Frank-Kamenetskii, ZhÉTF., 39, 669 (1960).

All abbreviations of periodicals in the above bibliography are letter-by-letter transliterations of the abbreviations as given in the original Russian journal. *Some or all of this periodical literature may well be available in English translation.* A complete list of the cover-to-cover English translations appears at the back of this issue.

BRITISH RESEARCH IN CONTROLLED THERMONUCLEAR FUSION

Sir John Cockcroft

Translated from Atomnaya Énergiya, Vol. 14, No. 1,
pp. 66-71, January, 1963
Original article submitted August 30, 1962

British research on controlled thermonuclear fusion began in the 1940's at Liverpool. Craggs and his group produced a high-current spark discharge in deuterium and looked hopefully for neutrons, but were disappointed. Cousins and Ware [1], working under G. P. Thomson, passed currents of up to 15,000 A in a toroidal discharge and observed the pinch effect which had in argon and hydrogen been studied 10 years earlier by Tonks. They found that the pinch discharge wandered backwards and forwards across the torus, thus demonstrating one of the modes of instability of pinched discharges. At Oxford, Thonemann and his colleagues started work first on linear discharges and later on the toroidal discharges, and also observed the pinch effect. Most of this work was published in 1951-1952.

During the period 1952-56, the work at Imperial College was moved to the Associated Electrical Industries research laboratories at Aldermaston to enable its scope to expand,and the Oxford work was moved to Harwell. Carruthers and Davenport observed kink instabilities in a 10-cm internal diameter glass torus [2]. The era of larger scale torus construction then began, starting with a 30-cm diameter metal torus built to study the pinch effect with much higher currents. In this torus currents of about 10 kA were passed for about 10^{-3} sec. Spectroscopic measurements were started, and from the Doppler broadening of spectral lines, ion temperatures of about 10^5 °K were estimated.The kink instability was found.in this torus and it was found necessary to apply an axial B_z field to stabilize the discharge and prevent it whipping about and touching the walls.

These results were sufficiently promising to begin work in 1955 on the construction of a 1-m diameter torus later called ZETA, with the objective of increasing the gas currents to about 100,000 A. One of the reasons for going to a larger diameter torus was to reduce the influence of impurities from the metal walls in the discharge. At the same time, the A.E. I. group with Ware started the construction of the "Sceptre" torus of 30-cm bore at Aldermaston.

In April, 1956, we had the famous visit from Bulganin and Kruschev accompanied by Igor' Kurchatov. I had not met Kurchatov before, but was greatly impressed by his intelligence and by his eagerness to talk about collaboration in atomic energy work, and we had a very animated discussion at the top of the Athenaeum staircase where he was able to go much further than I could reciprocate, having had no idea of the way the discussion would go. He suggested that he should deliver a lecture at Harwell, and I agreed to arrange this. On April 25, Kurchatov delivered his lecture in the Harwell Conference Room, describing work at the Atomic Energy Institute in Moscow on a linear unstabilized pinch discharge. Peak currents, ranging from 100 kA to 2 million A had been passed through straight tubes of diameters up to 50 cm in a variety of gases from hydrogen up to xenon. Theoretical calculations prior to the experimental work had suggested that the increase of temperature due to the compression in the pinch effect should take temperatures up to a level where the D − D reaction should produce powerful bursts of neutrons. High-speed photography produced pictures showing the rapid contraction of the discharge and subsequent oscillations, and in 1952, soon after the experiments with pinch discharge were started, it was found that the discharge in deuterium became a source of neutrons. Neutrons were always observed in short pulses with a steep front. Although it was thought at first that the behavior of the neutrons could be explained by a controlled thermonuclear mechanism, serious doubts began to appear when it was found that the neutrons appeared at currents well below that calculated to produce a thermonuclear reaction. It was found that no neutrons appeared during the first contraction. They appeared at the second contraction, and it was thought that instabilities were producing electric fields along the axis of the discharge tube which could speed up deuterons by a direct process and so lead to neutron production by the D − D reaction in the classical, non-thermonuclear way.

By September, 1957, ZETA had been built and operated for a month or so, and a conference was held at Princeton in October at which our results, as well as USA results in this field were described. With currents of 200,000 A, Doppler width measurements of impurity ion spectra suggested ion temperatures of up to 5 million degrees and neutron

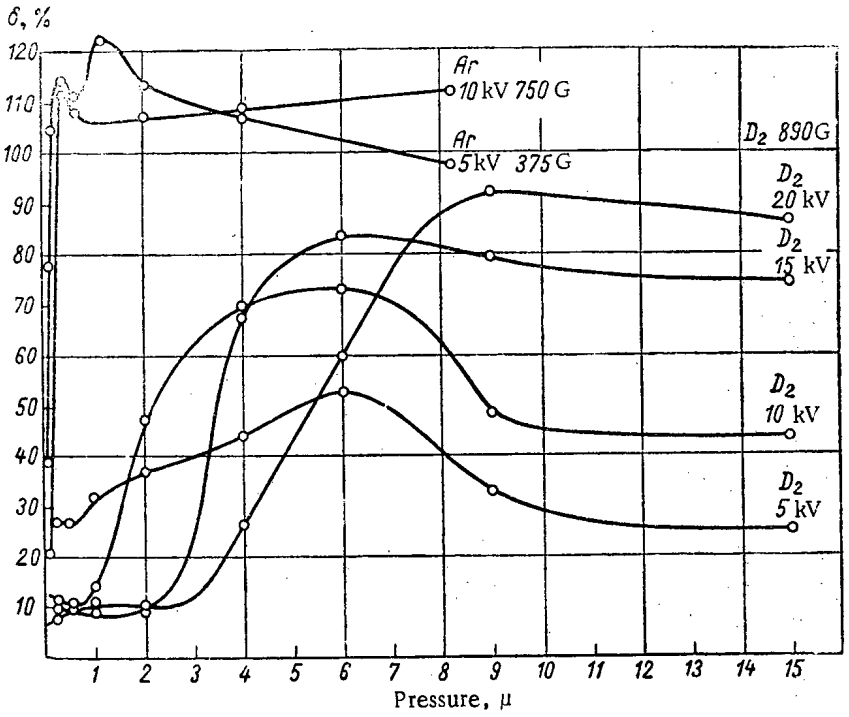

Fig. 1. Ratio δ of the radiation energy to the complete energy contribution in the plasma as a function of pressure.

production was observed for the first time in stabilized pinch discharges. Soon after this, the Harwell results and some USA results were published in a note in Nature. This first lifting of the veil on British and American research aroused tremendous interest in the press, and led to too much optimism about prospects of fusion power in the near future.

The point of greatest popular interest was whether the neutrons observed were due to a "true controlled thermonuclear reaction." The note published in Nature [3] stated specifically that "the neutron flux so far obtained was insufficient to obtain a sufficient accuracy of measurement to show that a thermonuclear process was responsible for the neutrons." We emphasized time and time again that many years of intensive work would be required to obtain a laboratory thermonuclear device which would produce more energy than it consumed, and that after this it would take many more years to develop a full-scale power producing unit [4]. We were not believed.

All of this was a precursor to the very exciting 1958 Geneva Conference on the Peaceful Uses of Atomic Energy when, for the first time, C.T.R. work was fully discussed between East and West, and a dazzling display of model C.T.R. devices actually working was produced by the Americans, unveiling for the first time the Princeton Stellarator, the Livermore Mirror Machine, the Los Alamos Scylla, the Oak Ridge DCX, while the Russian scientists had models of their OGRA, and ALPHA – a similar machine to ZETA – constructed in the remarkably short time of 6 months – a terrific feat. In spite of this wealth of revelation, the elusive "true thermonuclear reaction" was not claimed or produced. By this time, we had become much more aware of the ways in which D–D fusion reactions could be produced by other mechanisms.

One of the great advantages of this declassification of C.T.R. work was that it enabled us to follow up my discussions with Igor' Kurchatov in London, and I was invited by him to visit his Atomic Energy Research Institute in Moscow in November, 1958. Together with Dr. Thoneman, Mr. Pease, and other colleagues, we flew to Moscow in the fast T.U. jet on November 8, 1958, and I was warmly welcomed by Kurchatov and members of the Academy of Sciences. During the following week we studied the work of the Kurchatov Institute on Controlled Fusion, and were greatly impressed by the variety of devices being studied, especially the high density of equipment and the great enthusiasm of the workers. This was quite clearly a reflection of the enthusiasm and drive of Kurchatov. We were entertained to lunch at his house in the grounds of the Institute, where I met Mrs. Kurchatov, a sister of Professor Sinelnikov, whom I knew well during the time he worked with Kapitza in Cambridge. My colleagues were also able to visit the Electrotechnical Institute in Leningrad while I visited Dubna.

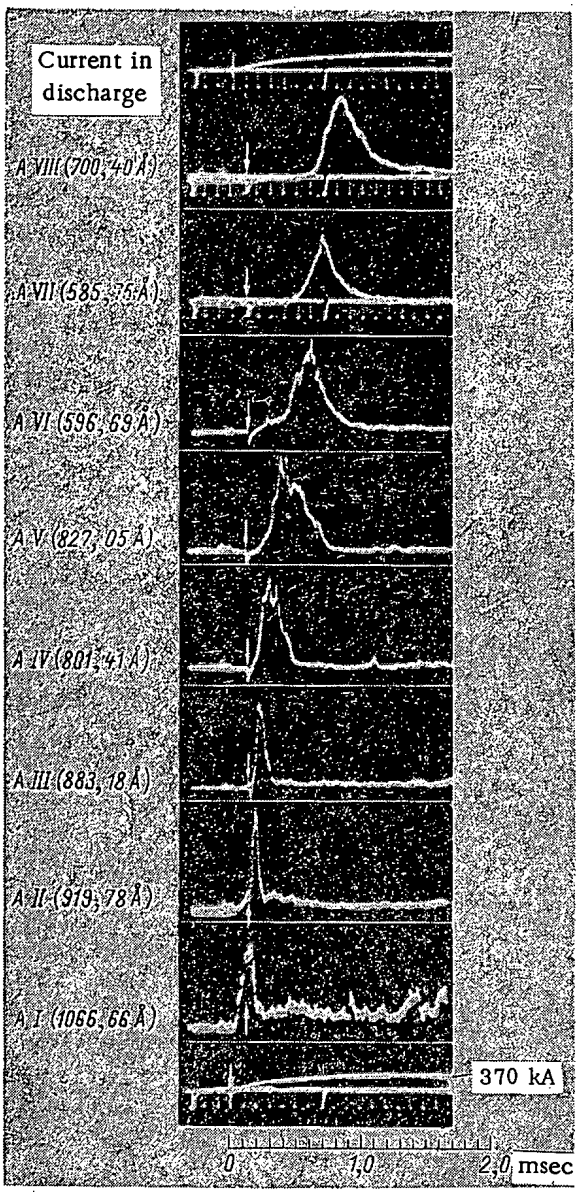

Fig. 2. Variation of intensities of the spectral lines for ionization of argon ions in a deuterium plasma. Pressure D_2 = 0.5 μ Hg; argon addition 10%; battery with energy 3 MJ; V = 10 kV; B_Z = 800 G.

Our visit to Russia was returned by a visit of the USSR delegation to Harwell in April, 1959 and, in turn, a delegation of Harwell/Culham physicists led by Dr. John Adams has been to Russia very recently for discussions on USSR and U.K. work. The initiative of Igor' Kurchatov of April, 1956 has therefore borne fruit and is contributing to international collaboration in this field.

Three years after the Geneva conference, there was another stocktaking at the Salzburg conference, last August. During the preceding 3 years there had been a marked development of techniques for finding out what was going on in the high-temperature discharges. Radiation losses in the infrared from plasma are measured by an infrared spectrometer viewing the plasma from 10 cm away, and are now using a semiconducting detector of n type indium antimonide, making use of cyclotron resonance. This has the advantage of a microsecond response time, and enables time resolved measurements of radiation to be made in the wavelength region 0.1-2 mm. Electrostatic analyzers measure the spectrum of electrons hitting the walls of the discharge tube. Vacuum ultraviolet spectrometers have enormously increased the selection of spectral lines available for diagnostics; moreover, accurate measurements of line widths and of continuous intensities are now possible in this spectral region [A (VIII), Xe (IX)].

During the same period, ZETA had been reconstituted. To get rid of troublesome power arcs at the walls, a corrugated stainless steel liner had been fitted, the stainless steel being so thin that the liner did not short circuit the discharge appreciably. This also enabled the interior to be baked out and a better vacuum, of the order of 10^{-6} mm Hg to be obtained. A larger condenser bank was installed, allowing currents of up to 900,000 A to be passed and results were given at Salzburg for several hundred thousand discharges of between 200 and 600 kA with B_Z fields of 1800 gauss with no electrical breakdowns of the torus.

As a result of the improvement in diagnostic techniques and better behavior of ZETA, many more measurements could be made and two main sources of energy loss were identified. One mechanism of loss is through radiation loss from impurity ions. This radiation is almost all in the ultraviolet < 1600 A. Figure 1 shows that the radiation loss varies between 10% and 100% of the input energy as the initial gas pressure increases.

At low pressures of less than about 1 millitorr, Gibson and Mason detected the plasma close to the walls by probe measurements, so the plasma crosses the lines of force which ought, on a simple classical picture, to result in slow diffusion across the lines. The electron density close to the walls was shown to be about $3 \cdot 10^{13}$ cm^{-3}. The energy of electrons reaching the walls was measured by an electrostatic analyzer. They had a Maxwellian temperature distribution with energies ranging from 15-50 eV, depending on pressure and contamination. High electron temperatures were observed at low pressures. At 5 millitorr they had only a few eV, and only a small proportion of the energy was lost in this way. The plasma diffusion was observed together with electrical field fluctuations. The fields are of the order of 50 V/cm, and are principally transverse to B. The well-known E × B diffusion of plasma as a whole takes place. This mass motion has also been observed spectroscopically, the Doppler width of spectra of tracer elements fit a model in which (under the conditions of the experiment), the random motion of the ion corresponds to a temperature of 100 eV common to all ions, and a mass velocity of about 10^6 cm/sec in agreement with electric field measurements [5].

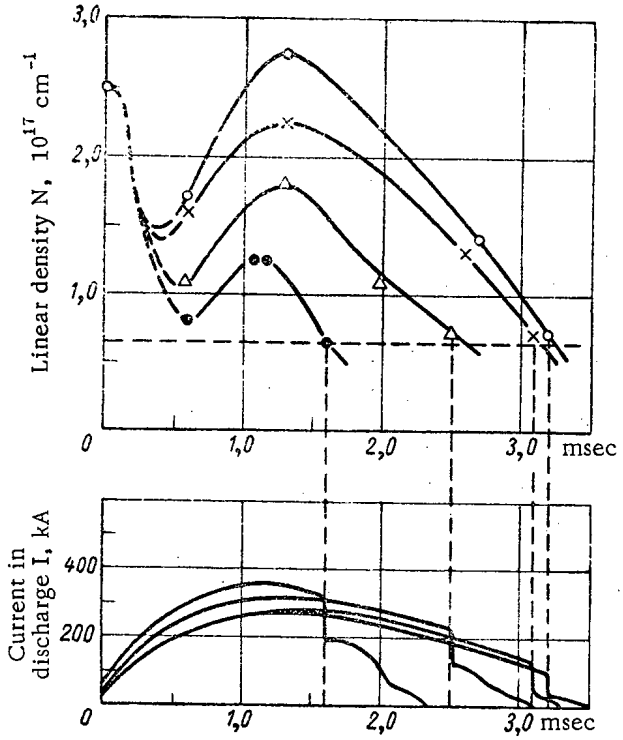

Fig. 3. Variation of linear density of the plasma determined according to spectroscopic data as a function of time. θ_p is the ratio of the component B_θ to the initial value B_z of the stabilizing magnetic field. ○) 4.9; ×) 3.8; △) 3.0; ●) 1.9.

Still more striking evidence was provided by spectroscopic analysis of the life history of impurity ions in plasma. Figure 2 shows the successive excitation of spectral lines of added tracer elements. The intensity rises to a maximum and then decreases as the next ion species is produced. These measurements provide evidence for the variation of plasma density, and show that in addition to the so-called pump-out effect – loss of plasma to the walls – there is an injection of cold gas from the walls through evaporation and unipolar arcs, so that the total amount of gas in the plasma rises to a maximum and then falls again (Fig. 3). When the plasma line density falls to $6 \cdot 10^{16}$ cm^{-1}, there is an abrupt termination of current and simultaneously a runaway of electrons leading to x-ray emission and a large part of the total energy in the torus at the end of the pulse is dissipated by this mechanism. Electron temperatures in the plasma have been measured by microwave, infrared, and ultraviolet spectroscopic techniques, and are between 2 and $4 \cdot 10^5$ °C. The general result of 2 years work with ZETA was therefore a marked growth of understanding of plasma physics, but little progress toward high temperatures.

The United Kingdom atomic energy work on C.T.R. is in future to be transferred to the new Culham Research Establishment, directed by Dr. John Adams. This laboratory is to be a completely open research establishment and scientists from any country will be welcome there; the Establishment will especially hope to receive scientists from the Kurchatov Institute.

Among the equipment to be installed for plasma research will be an improved version of the Phoenix device described at Salzburg and developed by AWRE, Aldermaston. Phoenix is an injection mirror machine. In this machine neutral hydrogen atoms produced by dissociation of 90-keV H_3^+ ions are fired into the machine. In the process of molecular dissociation, a small proportion of neutral atoms are formed at higher excited levels, and these atoms are then ionized by the Lorentz force on entering the mirror magnetic field. The probability of ionization depends on the vector product of the speed of the particles and the intensity of the magnetic field. The effect of the Lorentz ionization is to increase the initial rate of plasma buildup several hundred times.

Another device to be installed at Culham is the cusp geometry experiment. In this experiment, the plasma is generated and preheated by two colliding shock waves, and is then adiabatically compressed by rapidly developing a cusp field around it. Plasma densities greater than 10^{16} ions/cm^3 have been obtained so far at relatively low temperatures of 200,000°C. So far, no large-scale instabilities have been observed in the equilibrium phase when the magnetic pressure and plasma pressure are about equal.

Work on the theta pinch is also to be transferred to Culham using a new low induction 1-MJ jet condenser bank. The plasma in the first device has been found to rotate with peripheral speeds of up to $2 \cdot 10^7$ cm/sec, and this leads to instabilities in which the plasma splits into two cylinders which rotate about a common axis.

All this work and the work of many other laboratories shows that plasma physics continues to be a field of research of great interest. In pursuing this, we have a clear long-term goal of tremendous importance to mankind, and we have now the advantage of unhindered international cooperation. For his contributions and interest in this field we will always remember Igor' Kurchatov.

LITERATURE CITED

1. Cousins and Ware, Proc. Phys. Soc., B64, 159 (1951).
2. Carruthers and Davenport, Proc. Phys. Soc., B70, 49 (1957).
3. Nature, 181, 217 (1958).
4. J. Cockcroft, New Scientist, 3, No. 63 (1958).
5. Jones and Wilson, Saltzburg Paper No. 57 (1961).

CYCLOTRON INSTABILITY IN OGRA

V. I. Pistunovich

Translated from Atomnaya Énergiya, Vol. 14, No. 1,
pp. 72-81, January, 1963
Original article submitted November 12, 1962

Introduction

It is now known that a plasma with an anisotropic velocity distribution function (ions or electrons) can be unstable. The effect of a temperature anisotropy on the excitation of transverse oscillations in a uniform plasma has been studied in a number of papers [1-3], and it has been shown that the plasma becomes more stable as the pressure is reduced. If the plasma pressure is smaller than the magnetic pressure $\left(\beta = \frac{8\pi nT}{H^2} \ll 1\right)$ the thermal velocity of the ions (electrons) v_T is much smaller than the Alfvén velocity v_A, and only a small fraction of the particles have velocities of the order of the wave phase velocity. Only particles that fall into resonance with the wave that can effectively exchange energy with it and excite oscillations. Thus, when $\beta = \frac{v_T^2}{v_A^2} \ll 1$, the plasma is essentially stable with respect to the excitation of transverse oscillations.

When $\beta \ll 1$, it is of interest to consider longitudinal oscillations. It has been shown in [4,5] that a uniform anisotropic plasma can be unstable against the excitation of longitudinal oscillations for small values of β, with the instability developing at frequencies close to the ion cyclotron frequency (electron) and its harmonics (the so-called cyclotron instability).

In the present work we consider the cyclotron instability of a uniform anisotropic plasma in connection with certain observations in Ogra which have indicated the existence of high electric fields at the cyclotron frequencies of the molecular and atomic ions. The maximum value of the growth rate for the instability for a cold plasma (electron temperature $T_e = 0$) is determined by the most unstable perturbation; it is shown that increasing T_e leads to a stabilization of the plasma with respect to perturbations of this kind. We also carry out a qualitative comparison of the experimental results obtained with Ogra and the predictions of the theory for an infinite plasma.

Theory

We consider a fully ionized uniform plasma in a fixed magnetic field $\mathbf{H}_0$. The dispersion equation for the longitudinal oscillations in such a plasma is obtained by solving the kinetic equation together with Maxwell's equations. In analyzing longitudinal oscillations, we make use of the condition that $|\operatorname{rot}\mathbf{E}| \ll |\operatorname{div}\mathbf{E}|$, where $\mathbf{E}$ is the electric field of the perturbation. In this case, only one equation remains in the set of Maxwell equations:

$$\operatorname{div}\mathbf{E} = 4\pi \sum_{\alpha=1}^{2} e_\alpha n_\alpha, \tag{1}$$

where $\alpha = 1, 2$ (electrons, ions); e_α, m_α, and n_α are, respectively, the charge, mass, and density of particles of type α. We introduce the following notation: $f_\alpha(t, \mathbf{r}, \mathbf{v})$ is a small correction to the equilibrium distribution function $f_{0\alpha}(\mathbf{v})$; v, θ, and v_z are the cylindrical coordinate system in velocity space; $\omega_{H\alpha}$ and $\omega_{p\alpha}$ are the cyclotron frequency and plasma frequency, respectively. The z axis is chosen in the direction of the external magnetic field. Then we have

$$\frac{\partial f_\alpha}{\partial t} + v\cos\theta\frac{\partial f_\alpha}{\partial x} + v\sin\theta\frac{\partial f_\alpha}{\partial y} + v_z\frac{\partial f_\alpha}{\partial z} - \omega_{H\alpha}\frac{\partial f_\alpha}{\partial\theta} = -\frac{e_\alpha}{m_\alpha}\mathbf{E}\frac{\partial f_{0\alpha}}{\partial \mathbf{v}}. \tag{2}$$

$$\operatorname{div} \mathbf{E} = 4\pi \sum_{\alpha=1}^{2} e_\alpha \int f_\alpha d\mathbf{v}. \tag{3}$$

We solve (2) and (3) by integrating along the trajectory of the unperturbed motion, assuming that the potential ψ, which is defined by

$$\mathbf{E} = -\nabla\psi, \tag{4}$$

varies in space and time in accordance with $e^{ikr-i\omega t}$. Using the familiar recursion relations for the Bessel functions, after some simple calculations we obtain the dispersion equation for longitudinal plasma oscillations, the equilibrium distribution of which is described by the function $f^0_\alpha(\mathbf{v})$, normalized to unity $\left(\int f^0_\alpha d\mathbf{v} = 1\right)$:

$$k^2 = -2\pi \sum_{\alpha=1}^{2} \omega^2_{p\alpha} \int_0^\infty v\,dv \sum_{m=-\infty}^{\infty} J^2_m\left(\frac{k_x v}{\omega_{H\alpha}}\right) \int_{-\infty}^{\infty} \frac{dv_z}{\omega - m\omega_{H\alpha} - k_z v_z} \left(\frac{m\omega_{H\alpha}}{v}\frac{\partial f^0_\alpha}{\partial v} + k_z \frac{\partial f^0_\alpha}{\partial v_z}\right). \tag{5}$$

The dispersion equation (5) can be obtained from the general expression for the dielectric tensor $\varepsilon_{\alpha\beta}$ by setting ε_{zz} equal to zero [5].

We now consider the case in which the plasma contains fast ions (half of these move along a helix in the direction of the magnetic field, and the other half against the magnetic field) and of electrons, characterized by the temperature T_e, i.e.,

$$f^0_i = \frac{\delta(v - v_0)}{4\pi v_0}\left[\delta(v_z - v_1) + \delta(v_z + v_1)\right];$$
$$f^0_e = \frac{1}{(2\pi)^{3/2} v_T^3} e^{-\frac{v^2+v_z^2}{2v_T^2}}, \quad v_T = \sqrt{\frac{T_e}{m_e}}. \tag{6}$$

Since we are interested in perturbations with wavelengths appreciably greater than the electron Larmor radius ρ_e (it will be shown below that the wavelength of the most unstable oscillation is of the order of the ion Larmor radius ρ_i), in the summation of (5) for the electrons it is sufficient to take only the m = 0 ($k_x\rho_e \ll 1$) term. For the ions in the frequency region $\omega \simeq m\omega_{Hi} \mp k_z v_z$, the basic contribution is due to the resonance terms, whose denominators vanish. Hence, the sum can be replaced by the mth term. Carrying out the integration over velocity in (5), and writing $\frac{\omega}{\sqrt{2}k_z v_m} \gg 1$, we have

$$1 + \beta^2 = \frac{\omega^2_{pe}}{\omega^2} - i\varepsilon\frac{\omega}{\omega_{pe}} + \frac{\omega^2_{pi}}{2}\left\{\frac{mk_x}{k_z^2 v_0}\frac{\partial J^2_m(t)}{\partial t} \times \left[\frac{1}{\omega - m\omega_{Hi} - k_z v_1} + \frac{1}{\omega - m\omega_{Hi} + k_z v_1}\right] + \right.$$
$$\left. + J^2_m(t)\left[\frac{1}{(\omega - m\omega_{Hi} - k_z v_1)^2} + \frac{1}{(\omega - m\omega_{Hi} + k_z v_1)^2}\right]\right\}, \tag{7}$$

where $\varepsilon = \sqrt{\frac{\pi}{2}}\frac{\omega^3_{pe}}{k_z^3 v_T^3} e^{-\frac{\omega^2}{2k_z^2 v_T^2}}$; $\beta = \frac{k_x}{k_z}$, $t = \frac{k_x v_0}{\omega_{Hi}}$; $J_m(t)$ is the Bessel function of mth order $\omega^2_{pe} = \frac{4\pi e^2 n_e}{m_e}$.

It follows from Eq. (7) that waves propagating along the magnetic field ($k_x = 0$) are stable. The so-called oblique waves ($\beta \neq 0$) are unstable.

We consider the frequency region $\omega \simeq m\omega_{Hi} - k_z v_1$ for $\beta \ll 1$ and $T_e = 0$. Equation (7) assumes the form

$$1 + \beta^2 = \frac{\omega^2_{pe}}{\omega^2} + \frac{\omega^2_{pi} J^2_m(t)}{2(\omega - \omega_{Hi} + k_z v_1)^2} \equiv F(\omega). \tag{8}$$

It then follows that the plasma can be unstable when

$$1 + \beta^2 < F(\omega) \tag{9}$$

for any values of ω. The function $F(\omega)$ has a minimum at $\omega = \omega_1$, where

$$\omega_1 = \frac{m\omega_{Hi} - k_z v_1}{1 + \sqrt[3]{\frac{m_e}{2M} J_m^2(t)}}. \tag{10}$$

Consequently, the criterion for the development of an instability (9) is

$$1 + \beta^2 < \frac{\omega_{pe}^2}{(m\omega_{Hi} - k_z v_1)^2} \left[1 + \sqrt[3]{\frac{m_e}{2M} J_m^2(t)} \right]^3. \tag{11}$$

We determine the growth rate of the instability. We first introduce the new variable

$$x = m - \frac{\omega}{\omega_{Hi}} - \frac{k_z v_1}{\omega_{Hi}} \tag{12}$$

and the following notation: $\delta = \frac{\omega_{pe}}{\omega_{Hi}}$; $h = \frac{k_z v_1}{\omega_{Hi}}$; $\nu = \frac{m_e}{2M} J_m^2(t)$; $s^2 = \frac{\delta^2}{1+\beta^2}$. Then, Eq. (8) assumes the form

$$\frac{1}{(m-h-x)^2} = \frac{1}{s^2} - \frac{\nu}{x^2} \tag{13}$$

or $m - h - x = \frac{1}{\sqrt{s^{-2} - \frac{\nu}{x^2}}}$ when $\omega > 0$. The maximum value of the growth rate is obtained by taking $\nu/x^2 \ll s^{-2}$, expanding the square root in the small parameter, and solving the cubic equation

$$x^3 + (s - m + h)\, x^2 + \frac{\nu}{2} s^3 = 0. \tag{14}$$

From the condition $s - m + h < 3s \sqrt[3]{\frac{\nu}{4}}$ we find

$$\operatorname{Im} \omega = \frac{\sqrt{3}}{2} \left[s \sqrt[3]{\frac{m_e}{4M}} J_m^{2/3}(t) - \frac{s - m + h}{3} \right] \omega_{Hi}. \tag{15}$$

It is evident that the growth rate is a maximum when

$$s = m - h \tag{16}$$

and this maximum is

$$(\operatorname{Im} \omega)_{\max} = \frac{\sqrt{3}}{2} \sqrt[3]{\frac{m_e}{4M}} \frac{\delta}{\sqrt{1+\beta^2}} J_m^{2/3}(t)\, \omega_{Hi}. \tag{17}$$

The growth rate is reduced when $\nu/x^2 \gtrsim s^{-2}$ and $s - m + h > 3s \sqrt[3]{\frac{\nu}{4}}$:

$$\operatorname{Im} \omega = \sqrt{\frac{m_e}{2M}} \frac{m-h}{\sqrt{s^2 - (m-h)^2}} \frac{\delta}{\sqrt{1+\beta^2}} J_m(t)\, \omega_{Hi}. \tag{18}$$

It follows from Eq. (16) that the most unstable waves are those for which

$$\frac{k_x}{k_z} = \sqrt{\frac{\delta^2}{(m-h)^2} - 1}. \tag{19}$$

The physical picture for the development of the cyclotron instability is the following: As the plasma density increases, so that the electron Langmuir frequency becomes comparable with the ion cyclotron frequency and greater [when Eq. (11) is satisfied], a resonance occurs between the frequency of rotation of the ions and the longitudinal (Langmuir) oscillations of the electrons. This means that any small perturbation of the plasma density increases rapidly. (The field increases threefold in a time $\tau \simeq 30\omega_{Hi}^{-1}$ sec.) The oscillations of the plasma density cause strong longitudinal electric fields. As is evident from (19), at the outset waves that propagate at a small angle with respect to the magnetic field ($k_x \ll k_z$) are excited; then, more oblique waves propagate ($k_x \simeq k_z$).

It follows from the expression for the maximum growth rate (17) that the most unstable wave is the one for which m = 1, and for which the wavelength is of the order of the ion Larmor radius ($\lambda_x \approx \pi\rho_i$), since the Bessel function $J_m(t)$ for $m \neq 0$ reaches a maximum value for m = 1 and $t = k_x\rho_i \simeq 2$. For a fixed value of t, the growth rate (17) falls off monotonically as m increases beyond the value of two.

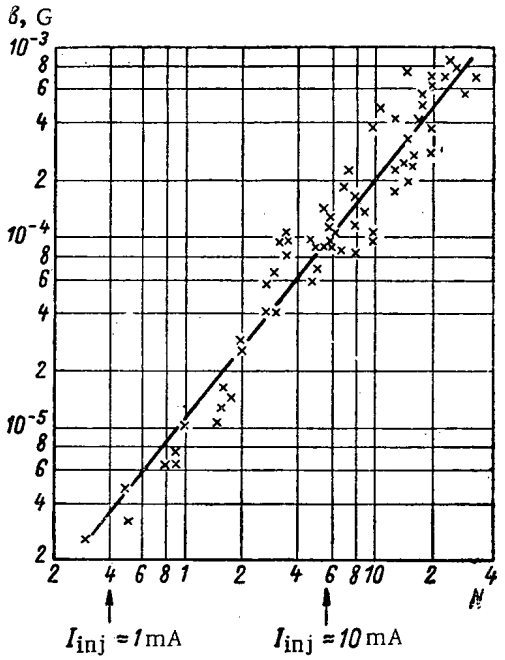

Fig. 1. The magnetic field measured by the loop antenna at frequency f_1 = 2.2 Mc as a function of the density of fast ions N [E = 160 keV; I_{con} = 1.5 kA; I_{inj} = 0.5-110 mA; p = (1-6) · 10^{-7} mm Hg; U_c = 0].

The velocity v_1 does not affect the maximum value of the growth rate ($k_z v_1 \ll \omega_{Hi}$), but merely shifts the boundary of the instability (11). Also, for the experimental conditions in Ogra, the term $k_z v_1 \ll \omega_{Hi}$. Hence, in all the following expressions, we eliminate the term $k_z v_1$.

We now consider the case in which $\beta \gg 1$ and $x \lesssim \sqrt{\nu} s$. In place of Eq. (13) we have

$$\frac{1}{(m-x)^2} = \frac{1}{s^2} - \frac{\nu}{x^2} + \frac{m\beta}{\eta}\frac{\mu}{x}, \qquad (20)$$

where

$$\eta = \frac{k_z v_0}{\omega_{Hi}}; \quad \mu = \frac{m_e}{2M}\frac{\partial J_m^2(t)}{\partial t}.$$

Solving Eq. (20), we have

$$\operatorname{Im}\omega = \frac{\sqrt{\nu}\, ms}{\sqrt{s^2-m^2}}\sqrt{1-\frac{\mu^2}{4\nu}\frac{m^4 s^2\beta^2}{\eta^2(s^2-m^2)}}\,\omega_{Hi}. \qquad (21)$$

Thus, as $\beta = k_x/k_z$ increases, the growth rate is reduced.

We now examine the effect of the electron temperature ($T_e \neq 0$) on the development of the cyclotron instability. When $\beta \ll 1$, we have from Eq. (7)

$$\frac{1}{(m-x)^2} = \frac{1}{s^2} - \frac{\nu}{x^2} + i\frac{\varepsilon(m-x)}{\delta^3}. \qquad (22)$$

Since $\varepsilon \ll 1$ when $k_z v_T \ll \omega_{pe}$, assuming that

$$\varepsilon \simeq \sqrt{\frac{\pi}{2}}\left(\frac{\omega_{pe}}{k_z v_T}\right)^3 e^{-\frac{\omega_{pe}^2}{2k_z^2 v_T^2}},$$

in place of Eq. (17) we obtain the following value for the growth rate:

$$\operatorname{Im}\omega = \frac{\sqrt{3}}{2}\sqrt{\frac{m_e}{4M}}\frac{\delta J_m^{2/3}(t)}{\sqrt{1+\beta^2}}\omega_{Hi} - \frac{\varepsilon m\omega_{Hi}}{12(1+\beta^2)^{3/2}}. \qquad (23)$$

As T_e increases, the growth rate diminishes. The magnitude of the thermal spread of the electrons for which the growth rate of the instability becomes vanishingly small is approximately

$$k_z v_T \simeq m\omega_{Hi}.$$

On the other hand, if the ions move along the magnetic field with velocities satisfying the relation

$$v_1 - u \leqslant v_z \leqslant v_1 + u,$$

i.e., if there is some thermal spread u, the instability vanishes if the following condition is satisfied:

$$1 - \frac{m^2\omega_{Hi}^2}{\omega_{pe}^2} > \frac{m_e}{2M}\frac{m^2\omega_{Hi}^2}{k_z^2 u^2} J_m^2\left(\frac{k_x v_0}{\omega_{Hi}}\right) \qquad (24)$$

where $\beta^2 \ll 1$ and $k_z v_1 \ll m\omega_{Hi}$.

Similarly, using the dispersion equation (5), we can show that if the ion velocity distribution is of the form

$$f_i^0 = \frac{1}{(2\pi)^{3/2} v_\perp^2 v_\parallel} e^{-\frac{v^2}{2v_\perp^2} - \frac{v_z^2}{2v_\parallel^2}},$$

while the electrons are cold (T_e = 0), then making the approximation $T_\perp / T_\parallel > 10$ and $\omega - m\omega_{Hi} \gg \sqrt{2} k_z v_\parallel$, we obtain results which, to within a numberical factor, agree with those given above [(11), (17), (18)]. Thus, in making a qualitative comparison of the theory and experimental results, we can use the results of calculations obtained in which

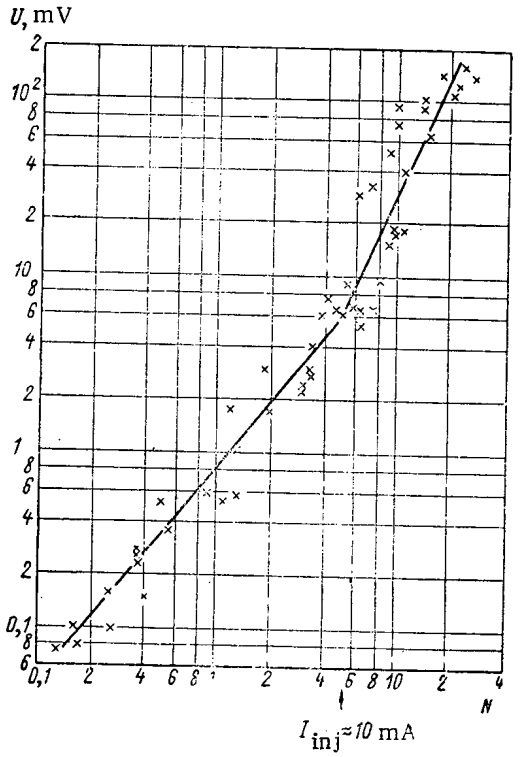

Fig. 2. The signal received by the rod antenna at frequency f_1 = 2.2 Mc as a function of N [E = 160 keV; I_{con} ~1.5 kA; I_{inj} = 0.5-110 mA; p = (1-6) · 10^{-7} mm Hg; U_c = 0].

the ion distribution function is assumed to be a δ-function if the relation $T_\perp / T_\parallel > 10$ is satisfied in Ogra, where $T_\perp$ is the mean kinetic temperature of the transverse ion motion.

Experimental Results

Earlier measurements of the electric fields at the cyclotron frequencies of molecular and atomic ions carried out in Ogra by means of a spectrum analyzer [6] showed a nontrivial dependence of the amplitude of the high-frequency field on the density of fast particles [7]. The intensity of the field at the H_2^+ ion cyclotron frequency as a function of density exhibited a rise for injection currents $I_{inj} \geq 10$ mA as compared with currents ≤ 10 mA; on the other hand, there was no singularity in the dependence of the total density of fast ions or the density of atomic ions on current in this region.

In order to interpret the nature of the field oscillations at the cyclotron frequencies, we carried out a number of special experiments. Using a loop antenna located in the central region of the Ogra chamber, we measured the magnetic component of the field. The dependence of the magnetic field at the cyclotron frequency for the molecular ions (f_1 = 2.2 Mc) on the density of fast ions N (in relative units) is shown in Fig. 1. In this same mode of operation we obtain the dependence on N of the signal measured by a rod antenna (Fig. 2). It is evident from these figures that the magnetic component of the high-frequency field increases in approximate proportion to the density over the entire range of variation. However, at injection currents greater than approximately 10 mA, the electrical component of the field exhibits a sharp rise. This may indicate that at some critical value of N the electric component of the field in the plasma becomes greater than the magnetic component, i.e., in addition to the electromagnetic wave, there are electric fields (the so-called longitudinal oscillations) associated with oscillations of the plasma density. The linear growth of magnetic field with increasing density indicates the bunching of ions. It is known that the radiation produced by charges moving in a circle is proportional to the charge density if the charges are phased (coherent radiation).

We now estimate the magnetic field produced by ions moving in a circle in free space. The magnetic field due to a single particle is

$$H \simeq \frac{c\omega_H \varrho_H}{cR^2} \sin\theta,$$

where ω_H and ρ_H are, respectively, the gyration frequency and the radius of the circle traversed by the charge e; R is the distance from the center of the circle to the point of observation; θ is the angle between the axis of rotation and the line connecting the center of the circle to the point of observation. If $\omega_H = 1.4 \cdot 10^7$ sec^{-1}, ρ_H = 25 cm, R = 10^2 cm, $\theta = \pi/2$, the field due to a single H_2^+ ion is

$$H \simeq 10^{-15} \text{ gauss.}$$

In incoherent radiation due to many particles, $\sqrt{\overline{H^2}} \sim \sqrt{N_t}$, where N_t is the total number of radiated particles. If $N_t = 10^{14}$ (the number of H_2^+ ions in Ogra), $\sqrt{\overline{H^2}} \simeq 10^{-8}$ gauss. The measured values of magnetic field for ion densities of approximately 10^7 cm^{-3} are found to lie in the range $5 \cdot 10^{-5}$ to $8 \cdot 10^{-4}$ gauss, which is four or five orders of magnitude greater than the value obtained by the estimate given above, which applies for free space. Actually, the ions move in a volume enclosed by metal. Hence, in computing the magnitude of the oscillating electromagnetic field produced by the ions, one should take account of the actual boundary conditions. The solution of this problem would involve considerable mathematical difficulty; on the other hand, the measured values of the field differ from the estimate given above by several orders of magnitude, and it would be difficult to attribute the effect to the boundary conditions alone. For this reason, these calculations were not carried out. The large discrepancy can be

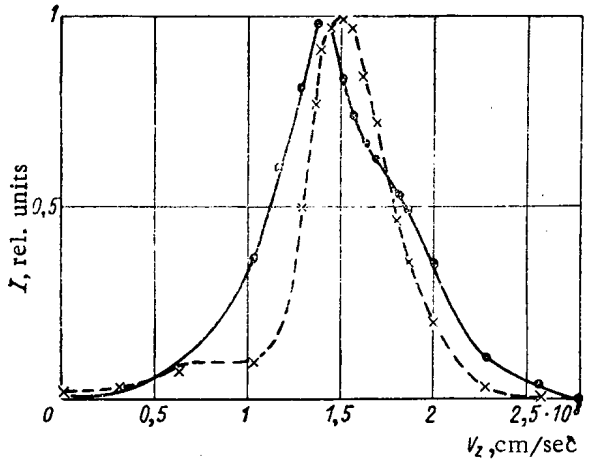

Fig. 3. The distribution of H_2^+ ions over longitudinal velocity measured in the central region: solid line, I_{inj} = 100 mA; broken line, I_{inj} = 2 mA.

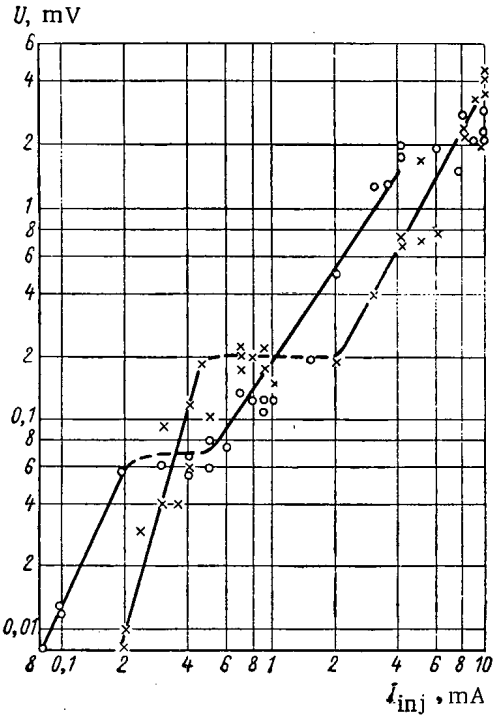

Fig. 4. The signal picked up by the rod antenna as a function of the injected current [E = 160 keV; I_{con} = −1.5 kA; p = (0.8-3) · 10^{-7} mm Hg; U_C = 0]. ○, f_1 = 2.2 Mc; ×, f_2 = 4.4 Mc.

explained qualitatively if one assumes that the ions form bunches and radiate coherently. The current of molecular ions injected into Ogra does not have frequency components beyond 0.8 Mc. Furthermore, it is possible to operate the ion source so that the current spectrum contains no frequencies above 2 Mc. However, it is found that even under these conditions the antennas record signals at the frequency f_2 = 4.4 Mc. In order to understand how molecular ions in Ogra can form bunches, and to explain the observed dependence of high-frequency electric and magnetic fields on ion density, we must postulate some mechanism which is responsible for the excitation of intense oscillations at the ion-cyclotron frequency. Such a mechanism is the cyclotron instability described above. As far as the anisotropy of the plasma formed by injection of the molecular ion beam in Ogra is concerned, we have qualitative information regarding the ion distribution for H_2^+ measured over longitudinal velocity v_z by Yu. A. Kucheryaev and D. A. Panov, who used a collimated radial probe located in the central portion of Ogra (Fig. 3). If we assume that the transverse ion temperature $T_\perp$ is equal to the kinetic energy $Mv_\perp^2/2$ while the longitudinal temperature $T_\parallel$ is equal to the half-width of the spread in longitudinal ion velocity, then for H_2^+ with I_{inj} = 100 mA, we find $T_\perp / T_\parallel \geq 26$. This means that the cyclotron instability can develop in Ogra if (11) is satisfied.

Since the cyclotron frequency for H_2^+ ions is f_1 = 2.2 Mc, the inequality in (11) is satisfied at an electron density $n_e > 6 \cdot 10^4$ cm^{-3}. To examine the existence of instability boundaries of the plasma in Ogra, measurements were made of the electric fields, at small injection currents (Fig. 4). In this case, with I_{inj} = 0.1 mA and a chamber pressure p = 1 · 10^{-7} mm Hg, the plasma density is approximately 10^5 cm^{-3} [8]. Measurements at frequencies f_1 = 2.2 Mc and f_2 = 4.4 Mc indicate that when the current is increased from 0.1 mA there is first a strong increase in the signal at the fundamental frequency f_1, and then at the proton cyclotron frequency f_2. An especially sharp rise is observed at the frequency f_2 when the current is changed from 0.2 to 0.3 mA, in which case the signal increases by approximately a factor of 6. In spite of the large spread in the experimental points (Fig. 4), it is evident that after the initial growth of the signal there is little change, although the plasma density continues to increase in linear fashion. Then the field increases again, but at a smaller rate.

In Fig. 5 we show a typical oscillogram of the signal spectrum observed on the rod antenna. Similar spectra can be observed by connecting to the analyzer any other pickup unit located in Ogra. The magnitude of the electric field can be estimated by means of a method suggested by D. A. Panov. In particular, if we regard the antenna as a metal surface on which there is induced a charge with surface density σ, the electric field component normal to the surface is $E = 4\pi\sigma$, where $\sigma = U/\omega_H SR$ (here U is the voltage measured in the experiment across a resistance R; ω_H is the field frequency; S is the surface area). In the case of the rod antenna we have $E = 5 \cdot 10^2 U$. For the observed values of the signal U = 0.1 V, we find E = 50 V/cm ($I_{inj} \approx 120$ mA, $p \approx 3 \cdot 10^{-7}$ mm Hg). This value is more than two orders of magnitude greater than the electric field E = H = 0.24V/cm obtained by meausrements with the rod antenna. Thus, the estimate of the electric field given above supports the conclusion based on the experimental

Phase Velocities and Wavelengths (Grid Potential $U_c = 0$)

i_{inj}, mA	Antenna number	$I_{con} = -1,5$ kA			$I_{con} = -0,1$ kA		
		$\Delta\varphi$, degrees	λ, m	v_φ, 10^8 cm/sec	$\Delta\varphi$, degrees	λ, m	v_φ, 10^8 cm/sec
80	13—16	—	—	—	45	24	54
	13—1	—	—	—	30	24	54
	5—12	—	—	—	170	1,4	3,1
60	6—1	<30	>12	>27	—	—	—
	5—12	100	2,4	5,4	—	—	—
50	13—6	0—180	⩾6	⩾13	0—90	⩾12	⩾27
	13—1	—	—	—	0—60	⩾12	⩾27
	6—1	<30	>12	>27	<30	>12	>27
	5—12	120	2	4,5	120	2	4,5
30	13—6	90±45	8—24	18—54	—	—	—
	13—1	60	12	27	30	24	54
	1—6	—	—	—	<30	>24	>54
	5—12	100—120	2,4—2,0	5,4—4,5	60	4	9
20	13—6	0—90	⩾12	⩾27	45—180	⩾6	⩾13
	13—1	—	—	—	30—120	⩾6	⩾13
	1—6	—	—	—	<30	>12	>26
	5—12	60	4	9	60—70	4—3,4	9—7,6
10	13—6	90±30	9—18	20—40	180	6	13
	13—1	60	12	27	120	6	13
	1—6	30	12	27	30—90	4—12	9—27
	5—12	0; 60	none; 4	none;9	60	4	9
5	13—6	270	4	9	180	6	13
	1—6	70	5,1	11	—	—	—
	5—12	60	4	9	0	none	none

results that longitudinal density waves are excited in Ogra. In order to determine the spectral composition of these waves, we have carried out experiments with a series of foil antennas (13 elements in all) located along the axis and in the azimuthal direction (Fig. 6). The antennas are copper sheets 1 cm in radius located at a distance of 6 cm from the chamber walls. The signal from each antenna is transmitted from the measuring instrument by means of a matched cable. In these experiments we measured the distribution of electric field in the plasma along the axis and in the azimuthal direction, and recorded the phase shifts between two antennas, at the frequency $f_1 = 2.2$ Mc. The experiment showed that in Ogra there are both traveling and standing density waves; the amplitudes and wavelengths depend upon the mode of operation (injection current, pressure, grid voltage [8]). In the azimuthal direction the waves travel in the same direction as the fast ions. It is evident from Fig. 7 that the signal on antenna 12 leads the signal on antenna 5. The direction of propagation of the wave along the axis is not unique and depends upon the injection current and the pressure. In certain modes of operation it is possible to observe two wave groups: one travels toward the center and the other away from the center (Fig. 8). Thus, there are waves that propagate at an angle with respect to the external magnetic field H_0. The observed phase shifts indicate the existence of a complicated wave pattern in the plasma which changes with time.

The phase shifts were measured by means of a two-beam oscilloscope DÉO-1 to which the signals at 2.2 Mc from the two antennas are applied through a narrow band amplifier. The oscilloscope is triggered by one of the signals (in the table and in the figures the number of this antenna is indicated at the beginning).

On the screen of the oscilloscope one can see the stationary pattern of two sinusoidal signals shifted in phase with respect to each other. If the phase shift changes with time a sine wave remains on one pattern (the signal triggering the oscilloscope), while the other pattern becomes smeared, indicating the superposition on one frame of many single-shot measurements of phase shift. This result indicates the existence of a whole spectrum of waves at the cyclotron frequency.

The measured phase shifts and the computed wave lenths and phase velocities are given in the table. The wavelength is computed from the relation $\lambda = \frac{2\pi}{\Delta\varphi} x$, where $\Delta\varphi$ is the phase shift; x is the distance between the antennas, and it is assumed that the wave propagates in one direction. To compute λ and the phase velocity v_φ when $\Delta_\varphi \leqslant 60°$, in general it is necessary to take account of the existence of two traveling waves moving in opposite directions.

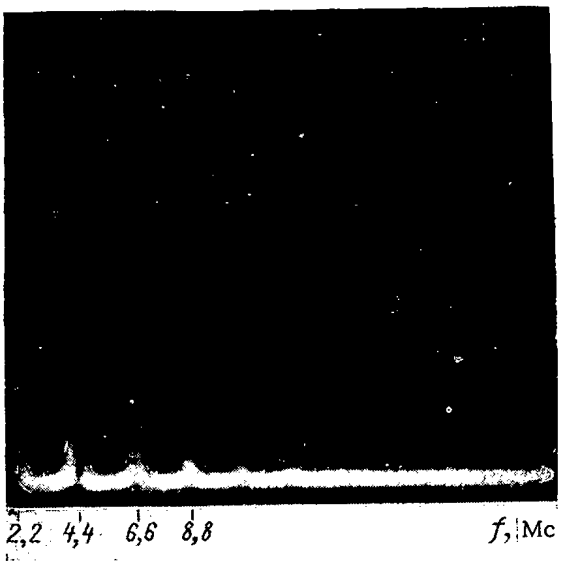

Fig. 5. Oscillogram showing the spectrum of the electric field (E = 160 keV; I_{con} = −0.1 kA; I_{inj} = 100 mA; p = 3.5 · 10^{-7} mm Hg; U_c =.0).

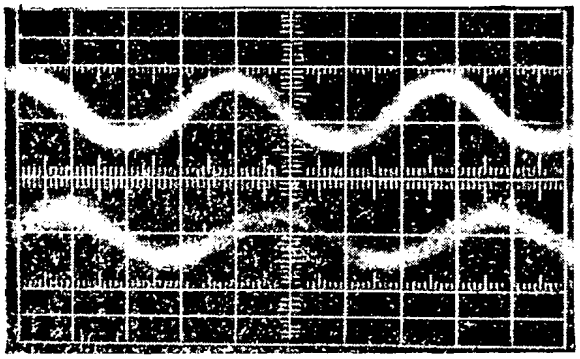

Fig. 7. Oscillogram showing the phase shift between signals at antennas numbers 12 and 5 (the upper beam corresponds to No. 12, the lower to No. 5): E = 160 keV; I_{con} = −1.5 kA; I_{inj} = 20 mA; p = 1.5 · 10^{-7} mm Hg; U_c = 0.

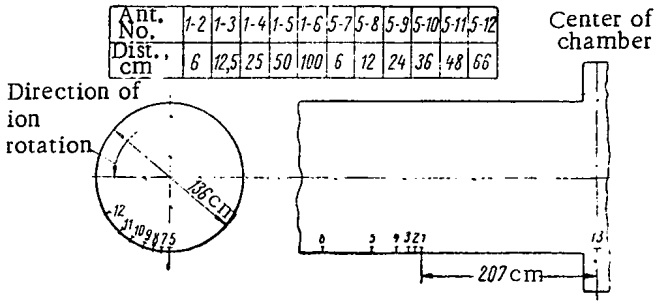

Fig. 6. Location of the foil antennas in Ogra.

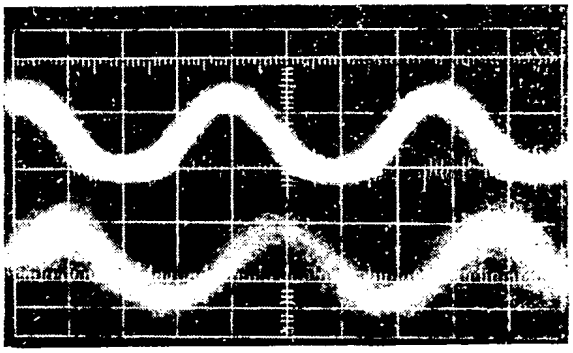

Fig. 8. Oscillogram showing the phase shift between signals at antennas numbers 6 and 13 (the upper beam corresponds to No. 6, the lower to No. 13): E = 160 keV; I_{con} = −1.5 kA ; I_{inj} = 20 mA; p = 1.5 · 10^{-7} mm Hg; U_c = 0.

In spite of the large spread of experimental points and poor accuracy in the phase-shift measurements (20°), using the table we can establish certain features of these phenomena. First of all, as the current is reduced the length of the wave propagating along the axis is reduced from approximately 24 to 4-6 m, while the wavelength in the azimuthal direction increases from 1.4 to 4 m (at small currents the azimuthal phase shift cannot be detected). In other words, as the plasma density increases, waves with greater obliqueness ($k_x/k_z \neq 0$) are excited, in qualitative agreement with Eq. (19) which, strictly speaking, applies to an infinite plasma.

Second, to within the experimental errors the observed azimuthal wavelengths are found to be approximately an integral fraction of the circumference (l = 4 m) at the radius at which the antennas are located. As the injection current is changed the wavelength changes in discrete steps.

Third, from the table and the oscillogram (cf. for example Fig. 8), it follows that as the current is increased one not only excited individual waves, as at small currents, but a whole spectrum of waves with different phase velocities.

The measurements of the amplitude of the electric fields along the axis and in the azimuthal direction show that standing waves also occur in Ogra (Fig. 9). With an injection current of 5 mA, the wavelengths of these waves along the axis is smaller than at 50 mA, as for the wavelengths of the traveling waves. The electric field in most modes of operation does not vary greatly in azimuth (within 20%), i.e., we have primarily traveling waves. When a positive potential is applied to the grids located in the mirrors the magnitude and wavelength of traveling and standing waves are both reduced.

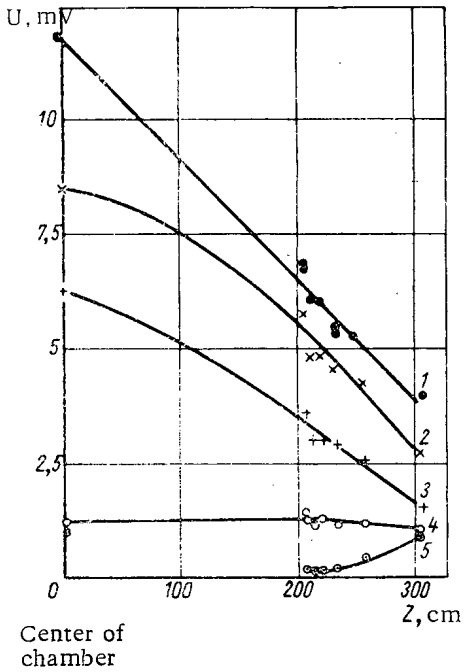

Fig. 9. Distribution of electric field along the axis of the chamber at frequency f_1 = 2.2 Mc [E = 160 keV; I_{con} = −0.1 kA; p = (1.6-2) · 10^{-7} mm Hg; U_c = 0] for the following values of I_{inj}, mA: 1) 50; 2) 30; 3) 20; 4) 10; 5) 5.

Conclusions

The experimental results reported here indicate that a cyclotron instability can and does develop in Ogra. Furthermore, at the present time, as far as we know there is no other possible explanation for the anomalous magnitude and the dependence of electric field (at the cyclotron frequency) on plasma density observed experimentally. The presence of density waves with different phase velocities can cause electron heating and electron loss. In this regard, the fact that the electrons can interact with the electric waves seems to be indicated by experiments with an electron beam carried out by Yu. A. Kucheryaev and D. A. Panov [9]; these experiments indicate that an electron beam passing through a plasma along the magnetic field loses or gains energy by virtue of interaction with waves at the cyclotron frequencies corresponding to H_2^+ and H_1^+ ions.

On the one hand, the effect of the cyclotron instability can cause ions to form bunches as a result of nonlinear effects, and these can lead to a more effective interaction, with the dissipation and exchange of energy. On the other hand, the existence of electric fields perpendicular to the magnetic field can cause ion drift across the magnetic field when the phase velocity of these waves is approximately equal to the ion velocity. As is evident from the table, this situation can arise in certain modes of operation. For a more detailed explanation of the effect of the cyclotron instability on ion loss and electron loss, it will be necessary to carry out further investigations.

The author wishes to take this opportunity to thank I. N. Golovin for his continued interest in this work and for a number of valuable comments offered in discussions of the experimental results, E. P. Velikhov for help in carrying out the calculations, and A. N. Karkhov and V. F. Nefedov for help in carrying out the measurements with Ogra. Fruitful discussions of the experiments and the results of the calculations with colleagues working with Ogra were very helpful in determining the physical pattern of these effects.

LITERATURE CITED

1. A. A. Vedenov and R. Z. Sagdeev, Collection: Plasma Physics and the Problem of a Controlled Thermonuclear Reaction [in Russian] (Izd. AN SSSR, Moscow, 1958), Vol. 3, p. 278.
2. R. Z. Sagdeev and V. D. Shafranov, ZhÉTF, 39, 181 (1960).
3. A. V. Timofeev, ZhÉTF., 39, 397 (1960).
4. E. Harris, Phys. Rev. Lett., 2, 2, 34 (1959).
5. K. N. Stepanov and A. B. Kitsenko, ZhTF., 31, 167 (1961).
6. A. N. Karkhov, PTÉ, No. 5, 115 (1961).
7. A. E. Bazhanova, V. T. Kariukhin, A. Karkhov, and V. I. Pistunovich, Report No. 212, International Conference on Plasma Physics and Controlled Nuclear Fusion, Salzburg, 1961.
8. G. F. Bogdanov, I. N. Golovin, Yu. A. Kucheryaev, and D. A. Panov, Report No. 210, International Conference on Plasma Physics and Controlled Nuclear Fusion, Salzburg, 1961.
9. U. A. Kucheryaev and D. A. Panov, J. Nucl. Energy, Part C (in press).

SCREW AND FLUTE INSTABILITIES IN A LOW-PRESSURE PLASMA *

B. Lehnert

Royal Institute of Technology, Stockholm
Translated from Atomnaya Énergiya, Vol. 14, No. 1,
pp. 82-91, January, 1963
Original article submitted October 4, 1962

1. Introduction

Under certain conditions, a plasma can be confined in a magnetic field in the directions across the field lines. In the particular situation where the plasma pressure is small compared to the magnetic energy density, the magnetic field is only slightly affected by the plasma and will become close to a vacuum field. Any transverse plasma motion which produces noticeable distortions of the field would then increase the field energy far beyond the energy content of the plasma. Such a motion therefore becomes energetically impossible.

However, even in a low-pressure situation there exist other types of motion by which the plasma may escape the confinement. For these types the particles drift across the field in a way to leave the latter unchanged at the same time, i.e., without producing any electromagnetic induction effects. The mechanism which makes this possible is due to an electric field and an associated transverse drift which arise from a charge separation in the plasma.

There are two ways in which this can be established in a plasma of nonuniform density. First, a separation occurs when the density distributions of ions and electrons drift at different speeds across the magnetic field, at the same time as there is a transverse density gradient in the plasma. Such conditions prevail in the "flute" instability phenomenon first discussed by Rosenbluth and Longmire [1].

Secondly, a charge separation will also occur when the ion and electron distributions move at different speeds along the magnetic field. Then, there should also exist a density gradient, both in the longitudinal and in the transverse directions. An example of this is given by a "screw"-shaped disturbance which may become unstable on account of the longitudinal motion. This phenomenon has been analyzed in detail by Kadomtsev and Nedospasov [2]. Further discussions on the corresponding instability mechanism are due to Hoh and Lehnert [3] and Kadomtsev [4].

The purpose of the present paper is to treat some simple cases which demonstrate the close connection between the screw and flute instability phenomena. The paper also gives a survey of different mechanisms which influence the space charge formation, such as drift motions from gravitation and centrifugal fields and from the magnetic gradients, effects of magnetic compression and Coriolis force, and finite Larmor radius effects. A short discussion on the influence of viscosity is also included.

2. Starting Points

The present analysis is based on the following conditions:

1. A plasma is originally assumed to be in a stationary, unperturbed state where it is confined by a static magnetic field $\mathbf{B}$.

2. Possibly, a stationary gravitation field $g = -\nabla \Phi_g$ will be present, and the plasma may rotate around an axis of symmetry at the constant and homogeneous angular velocity Ω. We limit the discussion to such configurations where g is perpendicular and Ω is parallel to $\mathbf{B}$.

3. The angular velocity Ω is much smaller than the gyro frequencies $\omega_i = eB/m_i$ and $\omega_e = eB/m_e$ of ions and electrons (m_i is the ion mass and m_e is the electron mass).

4. In the unperturbed state the plasma is uniform in the direction along the magnetic field lines. The surfaces of constant density and of constant particle energy are perpendicular to g, to the centrifugal force arising from Ω, and to ∇B in the cases to be discussed.

5. The center of mass of the plasma is at rest in a frame which follows the unperturbed motion. Ohmic

*This paper is presented by Academician Kh. Al'fven (translated from the English).

dissipation is very small and can be neglected as far as the motion of small perburations of the equilibrium state are concerned.

6. Superimpose small perturbations on the stationary state. The densities n_i and n_e, and the velocities $\mathbf{v}_i$ and $\mathbf{v}_e$, of ions and electrons will then be changed from their unperturbed values, $n_{i0} = n_{e0} = N$, and $\mathbf{v}_{i0}$ and $\mathbf{v}_{e0}$. The perturbations become $\tilde{n}_i = n_i - N$, $\tilde{n}_e = n_e - N$, $\tilde{\mathbf{v}}_i = \mathbf{v}_i - \mathbf{v}_{i0}$ and $\tilde{\mathbf{v}}_e = \mathbf{v}_e - \mathbf{v}_{e0}$. Analogously, the pressure tensors are π_{i0} and π_{e0} in the unperturbed state, and $\pi_i = \pi_{i0} + \tilde{\pi}_i$ and $\pi_e = \pi_{e0} + \tilde{\pi}_e$ in the perturbed state. Finally, the electric field changes from its unperturbed value $\mathbf{E}_0$ to $\mathbf{E} = \mathbf{E}_0 + \tilde{\mathbf{E}}$. The perturbations are small enough for corresponding nonlinear effects to be neglected.

7. The gyro periods $2\pi/\omega_i$ and $2\pi/\omega_e$ are assumed to be much shorter than the characteristic times during which the perturbations change appreciably. Likewise, the Larmor radii a_i and a_e of ions and electrons should be much smaller than the characteristic lengths $\tilde{L}_c$ of the perturbations.

8. The particle density is high enough for the plasma to become electrically quasi-neutral in the sense that $|\tilde{n}_i - \tilde{n}_e| \ll |\tilde{n}_i + \tilde{n}_e|$. We assume the dielectric constant ε_0 in vacuo to be much smaller than Nm_i/B^2.

9. The macroscopic motion which results from the perturbations is situated in planes perpendicular to the magnetic field, i.e., $\tilde{\mathbf{v}}_i = \tilde{\mathbf{v}}_{i\perp}$ and $\tilde{\mathbf{v}}_e = \tilde{\mathbf{v}}_{e\perp}$. (Subscripts $\perp$ and $\parallel$ are used throughout this paper to denote the directions perpendicular to and parallel with $\mathbf{B}$.)

10. The velocities $\mathbf{v}_{i0\parallel}$ and $\mathbf{v}_{e0\parallel}$ along the field lines either vanish or obey the conditions $\operatorname{div}\mathbf{v}_{i0\parallel} = \operatorname{div}\mathbf{v}_{e0\parallel} = 0$. They are sustained by a longitudinal electric field $\mathbf{E}_{0\parallel} = eN\eta(\mathbf{v}_{i0\parallel} - \mathbf{v}_{e0\parallel})$, which is very small since the resistivity η is assumed to approach zero according to condition 5.

11. Since the electron mass m_e is much smaller than the ion mass m_i, we neglect all inertia forces on electrons, but not those which act on ions.

12. Assume the plasma pressure to be small compared to the magnetic energy density. Restrict the treatment to such perturbations by which ionized matter moves across the magnetic field and leaves the latter unchanged at the same time. Thus, we decouple the disturbances from such transverse modes which are of magnetohydrodynamical character and would change the magnetic field energy (cf. Rosenbluth et al. [5]). Consequently, we neglect the induced magnetic field, but $\operatorname{rot}\mathbf{B} \simeq 0$ and $\partial B/\partial t = 0$, and express $\mathbf{E} = -\nabla\Phi$ in the terms of an electrostatic potential Φ.

3. Basic Equations

Conservation of mass and charge is expressed by

$$\frac{\partial n_\nu}{\partial t} = \operatorname{div}(n_\nu \mathbf{v}_\nu), \tag{1}$$

where we use subscript ν to indicate ions (ν = i) and electrons (ν = e) throughout this paper.

The balance of forces acting on an element of the ion or electron gas is determined by

$$\begin{aligned} n_\nu m_\nu \left[\frac{\partial \mathbf{v}_\nu}{\partial t} + (\mathbf{v}_\nu \cdot \nabla)\mathbf{v}_\nu\right] &= q_\nu n_\nu (\mathbf{E} + \mathbf{v}_\nu \times \mathbf{B}) + \\ + n_\nu m_\nu \mathbf{g} - \operatorname{div}\pi_\nu + \frac{1}{2} n_\nu m_\nu \nabla(\boldsymbol{\Omega} \times \boldsymbol{\varrho})^2 + & \\ + 2n_\nu m_\nu \mathbf{v}_\nu \times \boldsymbol{\Omega}. & \end{aligned} \tag{2}$$

Here, q_ν is the electric charge and $\boldsymbol{\rho}$ is a vector describing the position of the fluid element with respect to the origin which is supposed to be situated on the axis of rotation.

Form the vector product between Eq. (2) and $\mathbf{B}$, and solve the resulting equation for $n_\nu \mathbf{v}_{\nu\perp}$. After some deductions the result becomes

$$\begin{aligned} n_\nu \mathbf{v}_{\nu\perp} = n_\nu \mathbf{E} \times \frac{\mathbf{B}}{B^2} + & \\ + n_\nu m_\nu \left[\mathbf{g} + \frac{1}{2}\nabla(\boldsymbol{\Omega} \times \boldsymbol{\varrho})^2 + 2\mathbf{v}_\nu \times \boldsymbol{\Omega}\right] \times & \\ \times \frac{\mathbf{B}}{q_\nu B^2} - \operatorname{div}\pi_\nu \times \frac{\mathbf{B}}{q_\nu B^2} - n_\nu m_\nu \frac{\partial \mathbf{v}_\nu}{\partial t} \times \frac{\mathbf{B}}{q_\nu B^2}. & \end{aligned} \tag{3}$$

The contribution $(\mathbf{v}_\nu \cdot \nabla)\mathbf{v}_\nu$ to the inertia term of Eq. (3) has been neglected on account of conditions 5, 6, and 11.

It should be mentioned that Furth [6] has recently investigated instabilities due to finite resistivity and finite current-carrier mass. Such effects will not be included here.

4. The Unperturbed State

Choose a frame of reference where the center of mass is at rest, as specified in condition 5. Since $m_e \ll m_i$, this implies that the ion gas is nearly at rest in this frame ($\mathbf{v}_{i0} \simeq 0$). The unperturbed equation (2) for ions then reduces in the transverse direction to

$$\mathbf{E}_{0\perp} \simeq -\frac{m_i g}{e} + \left(\frac{1}{eN}\right) \operatorname{div} \boldsymbol{\pi}_{i0} - \\ - \left(\frac{m_i}{2e}\right) \nabla (\boldsymbol{\Omega} \times \boldsymbol{\varrho})^2 \tag{4}$$

for the unperturbed electric field. A corresponding relation for the electron gas involves the velocity $\mathbf{v}_{e0}$. It represents the electric current which balances the gravitation, centrifugal,and pressure forces in the unperturbed state.

5. The Perturbed State

The equation (1) of continuity can be written as

$$-\frac{\partial n_\nu}{\partial t} = \operatorname{div} (n_\nu \mathbf{v}_{\nu\perp}) + \mathbf{v}_{\nu 0\parallel} \cdot \nabla n_\nu \tag{5}$$

when use is made of conditions 9 and 10. We now introduce the unperturbed electric field (4) and the perturbation $-\nabla \tilde{\Phi} = \mathbf{E} - \mathbf{E}_0$ into Eq. (3). Further, perform an iteration process where the expression for $\mathbf{v}_{\nu\perp}$ given by Eq. (3) is substituted into the inertia term of the same equation. Such a process is allowed on account of condition 7. In combination with Eq. (5), the result then becomes

$$-\frac{\partial n_\nu}{\partial t} - \mathbf{v}_{\nu 0\parallel} \cdot \nabla n_\nu = \operatorname{div} (n_\nu \mathbf{v}_{\nu\perp}) = \\ = \left[\nabla \left(\frac{n_\nu}{B^2} \times \mathbf{B}\right]\right] \cdot \nabla \tilde{\Phi} + \left(\frac{1}{eB^2}\right)(m_\nu - m_i)\left[\mathbf{g} + \frac{1}{2}\nabla (\boldsymbol{\Omega} \times \boldsymbol{\varrho})^2\right] \times \\ \times \mathbf{B} \cdot \nabla n_\nu + 2\left(\frac{m_\nu}{q_\nu}\right) \operatorname{div}\left[\left(\frac{n_\nu}{B^2}(\mathbf{v}_\nu \times \boldsymbol{\Omega}) \times \mathbf{B}\right]\right] + \left(\frac{2}{q_\nu B^3}\right)(\mathbf{B} \times \nabla \mathbf{B}) \cdot \operatorname{div} \boldsymbol{\pi}_\nu - \\ - \left(\frac{1}{q_\nu B^2}\right) \mathbf{B} \cdot \operatorname{rot} (\operatorname{div} \boldsymbol{\pi}_\nu) + \operatorname{div}\left(n_\nu \operatorname{div} \boldsymbol{\pi}_{i0} \times \frac{\mathbf{B}}{eNB^2}\right) - \\ - \operatorname{div}\left\{\left(\frac{n_\nu m_\nu}{q_\nu B^2}\right)\left[\nabla \frac{\partial \tilde{\Phi}}{\partial t} + \frac{\partial}{\partial t}\left(\frac{1}{q_\nu n_\nu} \operatorname{div} \boldsymbol{\pi}_\nu\right)\right]\right\} + \operatorname{div}\left\{\left(\frac{n_\nu m_\nu^2}{e^2 B^2}\right)\left[2\left(\frac{\partial \mathbf{v}_\nu}{\partial t} \times \boldsymbol{\Omega}\right) - \frac{\partial^2 \mathbf{v}_\nu}{\partial t^2}\right]\right\}, \tag{6}$$

where use has been made of conditions 3, 4, 7, 9, 11, and 12.

The second term of the left-hand member of Eq. (6) produces a longitudinal convection of the surfaces of constant density and is the driving force of the screw instability phenomenon. In the right-hand member of the same equation the first term represents the electric field drift across the surfaces of constant density. It includes magnetic compression effects. The driving forces of the flute instability phenomenon are included in the second and fourth terms of the same member. They represent transverse drifts of the surfaces of constant density due to the gravitation field, the centrifugal force, and the magnetic gradient, respectively. The main influence of Coriolis force comes from the third term. Finite Larmor radius effects from the pressure tensor and effects of viscous dissipation arise from the fifth term. The unperturbed pressure tensor is balanced by a part of the unperturbed electric field which produces a drift and a convection of the density distributions, as given by the sixth term. Acceleration of the guiding center drift and inertia effects associated with the Larmor motion are represented by the seventh term. The first part of this term can also be considered to represent electric polarization phenomena due to the inertia of ions. Finally, the last term of Eq. (6) contains higher order contributions which can be neglected on account of conditions 3 and 7.

We shall now make a closer examination of the screw and flute instabilities in a number of special cases. The study which follows does not make any pretention to give an exhaustive analysis of all possible types of screw and flute instabilities of the system. Its purpose is merely to demonstrate how the mechanisms of these phenomena operate and to draw the attention to such effects which may enhance or suppress their growth rate. The theory will be developed in terms of localized perturbations.

6. Screw and Flute Instabilities in a Rotating Plasma of Small Thermal Energy

Assume a homogeneous magnetic field which is in the z direction of a cylindrical coordinate system (r, φ, z). Put $\mathbf{g} = 0$, and assume the thermal energy and the Larmor radii of ions and electrons to be small enough for all pressure terms in Eq. (6) to be neglected. A discussion on finite Larmor radius effects will be postponed to section 8. Further, introduce

$$\Lambda_\nu = 1 + 2m_\nu \frac{\Omega}{eB}, \tag{7}$$

where Ω is the z component of $\boldsymbol{\Omega}$ (positive or negative).

Equation (6) can now be rearranged into the form

$$\begin{aligned} -\Lambda_\nu \left(\frac{\partial n_\nu}{\partial t} + \mathbf{v}_{\nu 0\parallel} \nabla n_\nu \right) &= \Lambda_\nu \operatorname{div}(n_\nu \mathbf{v}_{\nu\perp}) = \\ &= \boldsymbol{\varkappa} \cdot \nabla \tilde{\Phi} + \left(\frac{1}{2eB^2} \right) (m_\nu - m_i) [\nabla (\boldsymbol{\Omega} \times \boldsymbol{\varrho})^2 \times \mathbf{B}] \times \\ &\times \nabla n_\nu - \operatorname{div} \left[\left(\frac{N m_\nu}{eB^2 \Lambda_\nu} \right) \nabla \frac{\partial \tilde{\Phi}}{\partial t} \right]. \end{aligned} \tag{8}$$

Combination of equations (8) for ions and electrons yields, after some straightforward deductions,

$$\begin{aligned} &\left(\frac{\varkappa}{r} \right) \left(\frac{\partial}{\partial t} + v_{i0z} \frac{\partial}{\partial z} \right) \frac{\partial \tilde{\Phi}}{\partial \varphi} - \\ &- \left(\frac{\partial}{\partial t} + v_{e0z} \frac{\partial}{\partial z} + \frac{\Omega^2}{\omega_i} \frac{\partial}{\partial \varphi} \right) \cdot \left[\left(\frac{\varkappa}{r \Lambda_i} \right) \frac{\partial \Phi}{\sigma \Phi} + \right. \\ &\left. + \operatorname{div} \left(\frac{N}{\omega_i B \Lambda_i^2} \nabla \frac{\partial \tilde{\Phi}}{\partial t} \right) \right] = 0, \end{aligned} \tag{9}$$

where $\varkappa = dN/Bdr$ and we have put $\Lambda_e = 1$, since $\overline{m}_e \ll \overline{m}_i$. Poisson's equation leads to $n_i \simeq n_e$ in Eq. (8) on account of condition 8. Equations which are analogous to Eq. (9) can be deduced for the density perturbations $\tilde{n}_\nu$.

Considerable simplification is achieved if we now restrict ourselves to perturbations with a weak radial dependence. Therefore, study normal modes where all perturbed quantities vary as $\exp[i(m_\varphi \varphi + k_z z + \omega t)]$. The disturbance then has the form of radial, screw-shaped spokes. This is a special case which does not contain all modes which are possible for a screw-shaped disturbance. However, it still gives an illustration of the main mechanism which determines its growth. From Eq. (9) a dispersion relation is obtained:

$$\omega = -\frac{1}{2}\alpha \pm \frac{1}{2}\alpha (1 - \Gamma)^{1/2}, \tag{10}$$

where

$$\alpha = k_z v_{e0z} + m_\varphi \frac{\Omega^2}{\omega_i} + 2r\varkappa\Omega \frac{\Lambda_i B}{N m_\varphi} \tag{11}$$

and

$$\begin{aligned} \frac{1}{4}\alpha^2 \Gamma = \omega_i k_z \varkappa (v_{i0z} - v_{e0z} \Lambda_i^{-1}) \frac{B \Lambda_i^2 r}{N m_\varphi} - \\ - r\varkappa \Lambda_i \Omega^2 \frac{B}{N}. \end{aligned} \tag{12}$$

Relations (11) and (12) are independent of r when $N = \text{const} \cdot r^{\text{const}}$.

For $\Gamma > 1$, the system is unstable and the perturbations oscillate with an exponentially increasing amplitude. For $\Gamma < 1$, it is stable against the present type of disturbances and the amplitude of the oscillations is limited. The Coriolis force is represented by the last term of Eq. (11). It will always have a stabilizing influence on the disturbances discussed here, provided that it gives a contribution which definitely exceeds that of $k_z v_{e0z}$.

The result can be illustrated by the following limiting cases:

1. In the absence of rotation we have

$$\Gamma = 4\omega_i k_z (v_{i0z} - v_{e0z}) r \frac{\left(\frac{dN}{dr} \right)}{N m_\varphi (k_z v_{e0z})^2};$$

$$\alpha = k_z v_{e0z}. \tag{13}$$

Here the quantity $\frac{1}{|k_z(v_{i0z} - v_{e0z})|}$ is the time required by the ion and electron density distributions to move one wavelength $2\pi/k_z$ relative to each other along the z axis. In most cases of interest, this time is much longer than the gyro period $2\pi/\omega_i$ of an ion. Usually we also have $|v_{e0z}| >> |v_{i0z}|$.

For not-too-flat density distributions N, the modulus of Γ becomes strongly positive. Then, there will always exist a screw-shaped disturbance with such signs of k_z and m_φ that Γ becomes positive and the system is unstable. With $(v_{i0z} - v_{e0z}) < 0$, $dN/dr < 0$, $m_\varphi > 0$, and $k_z > 0$, we have $\Gamma > 0$, and a left-handed screw instability occurs. A similar result has earlier been obtained by Kadomtsev and Nedospasov [2] for a partially ionized gas. The driving mechanism of the screw-instability in the present fully ionized case is identical with that of the partially ionized gas. The analysis of this section can therefore be taken as a simple illustration of the way in which this kind of instability is produced.

It has to be observed that the screw instability takes its energy from the longitudinal velocities v_{i0z} and v_{e0z} which have been assumed as given constraints. Thus, the system is not isolated and energy is extracted from external sources.

For very flat density distributions, the modulus of Γ may become less than unity and the present perturbations are stable. The stabilization is then due to a scrambling mechanism produced by the longitudinal motion of electrons, somewhat similar to a situation earlier discussed in connection with flute disturbances [7].

2. In absence of longitudinal motions and with $\Omega << \omega_i$ according to condition 3, Eqs. (11) and (12) instead reduce to

$$\Gamma = -\frac{Nm_\varphi^2}{r\left(\frac{dN}{dr}\right)}; \quad \alpha = 2\Omega r \frac{\left(\frac{dN}{dr}\right)}{Nm_\varphi}. \tag{14}$$

When the density distribution is very flat and decreases in radial direction, Γ becomes strongly positive. A "gravitation" instability will then be produced by the centrifugal force. The growth rate is given by the characteristic time $\left[\frac{N}{\Omega^2 r \frac{dN}{dr}}\right]^{\frac{1}{2}}$, as expected from earlier results by Kruskal and Schwarzschild [8] and by Rosenbluth and Longmire [1]. However, when the second term in Eq. (11) has to be retained, certain modes may still become stable on account of the same scrambling mechanism as mentioned in case 1.

For a steep density distribution the modulus of Γ becomes less than unity. The assumed type of flute disturbances is then stabilized by the Coriolis force even when the density decreases in radial direction [9].

It should be noted that the present problem can be solved exactly by combination of Eqs. (1) and (2) and without imposing the restrictions of conditions 3 and 7. With $m_e = 0$ and vanishing thermal energies of ions and electrons, the dispersion relation becomes

$$\omega^3 - \left(\frac{m_\varphi N \omega_i}{rN'}\right)\omega^2 - \Omega\left[2(\omega_i + 2\Omega) + \frac{m_\varphi^2 \Omega N}{rN'}\right]\omega + m_\varphi \Omega^2 (\omega_i + 2\Omega) = 0, \tag{15}$$

where $N' \equiv dN/dr$. The three roots ω_1, ω_2, and ω_3 of this equation can easily be found. In the limit where $|\Omega/\omega_i| << 1$, we obtain $\omega_1 \approx m_\varphi N \omega_i / rN'$. Further, ω_2 and ω_3 become equal to the solutions (14) and (10). Thus, the exact solution leads to the same stability condition as already deduced in Eqs. (14) and (10).

7. Magnetic Compression Effects Produced by an Inhomogeneous Magnetic Field

Consider a cylindrically symmetric plasma column which is confined by the magnetic field from a line current situated at the axis of the column. Perturbed as well as unperturbed quantities are assumed not to vary in the direction along the magnetic field lines. Restrict the situation to perturbations which have a characteristic length that is much smaller than the characteristic lengths of the unperturbed plasma and of the magnetic field.

We shall only study effects of lowest order and assume the pressure tensor to be given by a scalar and isotropic pressure. Thus,

$$\operatorname{div} \pi_v = \nabla_\perp p_v \tag{16}$$

according to condition 4. For adiabatic changes of state it follows that

$$\left(\frac{\partial}{\partial t}+\mathbf{v}_\nu\cdot\boldsymbol{\nabla}\right)\left(\frac{p_\nu}{n_\nu^{5/3}}\right)=0. \tag{17}$$

Without losing the essential features of the present problem we can achieve a considerable simplification by assuming the unperturbed plasma pressures $p_{\nu 0}$ and the density N to be adiabatically distributed in the sense that $p_{\nu 0} = \text{const} \cdot N^{5/3}$. The relation between the pressure and density perturbations is then immediately deduced from Eq. (17) and becomes

$$\tilde{p}_\nu = c_\nu \tilde{n}_\nu; \quad c_\nu = \frac{5}{3}\frac{p_{\nu 0}}{N} \tag{18}$$

for all points in space.

Introduce a cylindrical coordinate system (r, φ, z) with z along the axis of the configuration. Further, insert expressions (18) and (16) into Eq. (6). After some straightforward deductions, and by application of conditions 4, 8, 9, 11, and 12, we arrive at

$$\left[\boldsymbol{\nabla}^2\frac{\partial^2}{\partial t^2}-(u_{Biz}-u_{Bez})\boldsymbol{\nabla}^2\frac{\partial^2}{\partial z\,\partial t}+G_{ie}\frac{\partial^2}{\partial z^2}\right]\tilde{\Phi}=0, \tag{19}$$

where

$$\mathbf{u}_{B\nu}=\frac{2c_\nu(\mathbf{B}\times\boldsymbol{\nabla}B)}{q_\nu B^3}\ ; \tag{20}$$

$$G_{ie}=-\omega_i\left(\frac{B^2}{N}\right)(u_{Biz}-u_{Bez})\left(\frac{d}{dr}\right)\left(\frac{N}{B^2}\right). \tag{21}$$

Normal modes of the special form $\exp[i(k_z z + \omega t)]$ yield a solution analogous to Eq. (10), where now

$$\alpha=k_z(u_{Biz}-u_{Bez}); \quad \frac{1}{4}\alpha^2\Gamma=G_{ie}. \tag{22}$$

Consider two cases:

1. For a magnetic field gradient which is much smaller than the density gradient, the sign of Γ will be determined by the sign of $(u_{Biz} - u_{Bez})(dN/dr)$. When the magnetic field gradient and the density gradient point in opposite directions, as in "cusped geometry," Γ becomes negative and there is always stability. When the two gradients point in the same direction, as in "mirror geometry," there is still stability for sufficiently small values of dN/dr. At larger values of dN/dr, where Γ far exceeds unity, the system becomes unstable. Oscillations will then occur at an exponentially increasing amplitude. The characteristic time of the growth rate becomes $\left[N/\omega_i(u_{Biz}-u_{Bez})\frac{dN}{dr}\right]^{\frac{1}{2}}$, which is analogous to the rate found in section 6 (case 2) for a rotating plasma.

2. For a magnetic field gradient which is comparable to or even exceeds the density gradient, a magnetic compression mechanism will affect the results. Observe that the solution of Eq. (6) for small values of the thermal energy is $n_\nu/B^2 = \text{const}$ to lowest order. From this is easily understood that the surfaces of constant density will no longer move with the first-order macroscopic and particle velocities [10]. This changes the driving forces of the instability. This result is obvious if we for a moment assume N/B^2 equal to the same constant all over the plasma. For any motion at the velocity $\mathbf{E}\times\mathbf{B}/B^2$, the surfaces of constant density would then remain unaffected.

When dN/dr and dB/dr point in opposite directions, there is always stability; also in this case. However, if dN/dr and dB/dr point in the same directions, stability is now secured by the magnetic compression effect, as soon as $\left|\frac{B}{(dB/dr)}\right| < \left|2\frac{N}{(dN/dr)}\right|$. For the present magnetic field this implies that N should decrease more slowly than $1/r^2$ in the radial direction.

8. Finite Larmor Radius Effects

We shall now return to the gravitation instability produced by a field **g** and a centrifugal force which both are at right angles to a homogeneous magnetic field. Finite Larmor radius effects will be taken into account. We further allow the characteristic length of the density distribution to become short compared to the characteristic wavelengths

$\tilde{L}_c$ of the perturbations. As shown by Marshall [11] (see also [12, 13]), the pressure tensor has the transverse components (ν = i, e)

$$\pi_{\nu xx} = p_{\nu\perp} - \frac{1}{4} eBn_\nu a_\nu^2 \left(\frac{\partial v_{\nu y}}{\partial x} + \frac{\partial v_{\nu x}}{\partial y} \right), \tag{23}$$

$$\pi_{\nu yy} = p_{\nu\perp} + \frac{1}{4} eBn_\nu a_\nu^2 \left(\frac{\partial v_{\nu y}}{\partial x} + \frac{\partial v_{\nu x}}{\partial y} \right), \tag{24}$$

$$\pi_{\nu xy} = \pi_{\nu yx} = \frac{1}{4} eBn_\nu a_\nu^2 \left(\frac{\partial v_{\nu x}}{\partial x} - \frac{\partial v_{\nu y}}{\partial y} \right), \tag{25}$$

in a coordinate system (x, y, z) with z along $\mathbf{B}$. The quantity $a_\nu^2 = \frac{2K_{\nu\perp}}{m_\nu \omega_\nu^2}$ is the square of the mean Larmor radius. Since a_e^2 is usually much smaller than a_i^2, we neglect the higher-order corrections to the electron pressure tensor in the coming discussion.

In the present analysis we shall treat two cases. The first concerns a plasma rotating around an axis along the magnetic field $\mathbf{B}$ which is in the z direction of a cylindrical coordinate system (r, φ, z). Possibly, a gravitation field $\mathbf{g}$ may be present in the r direction. We study the plasma in a frame of reference as specified in condition 5. Here the ions are approximately at rest, since $m_i >> m_e$. In this frame, the equation of motion of an ion can be rewritten in a form identical with that in the nonrotating system, provided that the magnetic field $\mathbf{B}$ is substituted by the field $\mathbf{B}^* \equiv \mathbf{B} + \frac{2m_i\boldsymbol{\Omega}}{e}$, and the electric field $\mathbf{E}$ by $\mathbf{E}^* \equiv -\nabla\left(\Phi - \Omega r A_\varphi - \frac{m_i \Omega^2 r^2}{2e} \right)$, where A_φ is the φ component of the magnetic vector potential [14]. We can therefore use expressions (23)-(25) for the ion pressure tensor in the rotating system if $\mathbf{B}$ is replaced by $\mathbf{B}^*$.

The second case concerns a plane configuration where a plasma is supported by a magnetic field against gravity in the y direction of a rectangular coordinate system (x, y, z). Here, results are easily obtained from the first case by putting $\frac{\partial}{\partial r} = \frac{\partial}{\partial y}$ and $\frac{1}{r}\frac{\partial}{\partial \varphi} = -\frac{\partial}{\partial x}$.

In the unperturbed state, the transverse ion and electron pressures are assumed to be given by the scalar quantities $p_{i0\perp}$ and $p_{e0\perp}$. According to condition 4, both the perturbed and unperturbed components of the pressure tensor are constant along the magnetic field lines. For the sake of simplicity, we study a linear unperturbed density distribution where second and higher derivatives of N vanish. Regions close to the axis of symmetry are excluded from the analysis. We further restrict ourselves to perturbations with a negligible radial dependence. Thus, we are going to discuss only such flute disturbances which have the form of "long spokes" extended in the radial direction.

Since the magnetic field and $\boldsymbol{\Omega}$ are constant, the adiabatic invariance of the equivalent magnetic moment, $K_{i\perp}/B^*$, of the ions implies that the transverse energy of the thermal motion can be written as

$$K_{i\perp} = K_{i0\perp}(1 + 0_\varepsilon). \tag{26}$$

Here, 0_ε denotes the deviations from adiabatic invariance which ε are at least of first order in $a_i/\tilde{L}_c$. Assume $K_{i0\perp}$ to be constant in space.

Under the present conditions, Eqs. (23)-(25) now yield

$$\hat{\mathbf{B}} \cdot \mathrm{rot}\,(\mathrm{div}\,\pi_i) = \left(\frac{m_i K_{i0\perp}}{2eB^*} \right) [N \nabla^2 (\mathrm{div}\,\mathbf{v}_i) + 2(\nabla^2 \mathbf{v}_i) \cdot \nabla N]. \tag{27}$$

Since $p_{i\perp} = n_i K_{i\perp}$, it is seen from Eqs. (26) and (3) that $\mathrm{div}\,\mathbf{v}_i = 0$ to lowest order. Only the second term of the right-hand member of Eq. (27) therefore remains in second order, and

$$\left(\frac{1}{eB^2} \right) \mathbf{B} \cdot \mathrm{rot}\,(\mathrm{div}\,\pi_i) = -\left(\frac{a_i^2}{2\Lambda_i^2 B r^3} \right) \left(\frac{dN}{dr} \right) \frac{\delta^3 \tilde{\Phi}}{\partial \varphi^3}, \tag{28}$$

where Λ_i is defined by Eq. (7).

With $\mathbf{v}_{\nu 0\|} = 0$, $\nabla B = 0$, and expression (28) inserted into Eq. (6), we obtain two equations for ions and electrons which, after some straightforward deductions, combine to

$$\left[\frac{1}{r^2}\frac{\partial^4}{\partial t^2\,\partial\varphi^2}-\frac{u_g+u_f-u_K+u_a}{r^3}\frac{\partial^4}{\partial t\,\partial\varphi^3}-\right.$$
$$\left.-C\frac{\partial^2}{\partial t\,\partial\varphi}+\frac{G_{ie}}{r^2}\frac{\partial^2}{\partial\varphi^2}-\frac{u_a(u_g+u_f)}{r^4}\frac{\partial^4}{\partial\varphi^4}\right]\tilde{\Phi}=0. \tag{29}$$

Here

$$u_g=-\frac{\left(g+\frac{\Omega^2}{r}\right)}{\omega_i},\quad u_f=\frac{K_{i0\perp}N'}{Nm_i\omega_i},$$

$$u_K=\frac{K_{i0\perp}N'}{eBN},\quad u_a=\frac{\omega_i a_i^2 N'}{2N\Lambda_i^2},\quad C=\frac{2\Omega N'}{rN},$$

$$\text{and } G_{ie}=-\frac{u_g\omega_i N'}{N}.$$

Further, g denotes the component of the gravitation field in the radial direction of a rotating plasma or in the y direction of a plane configuration, and N' stands for dN/dr or dN/dy.

For perturbations of the form $\exp[i(m_\varphi\varphi+\omega t)]$, the solution of Eq. (29) becomes analogous to Eq. (10) with

$$\alpha=\frac{m_\varphi(g+\Omega^2 r)}{\omega_i r}-\frac{m_\varphi u_a}{r}+2\frac{\Omega N' r}{Nm_\varphi};$$
$$\frac{1}{4}\alpha^2\Gamma=-\frac{(g+\Omega^2 r)N'}{N}. \tag{30}$$

The contribution from the last term of Eq. (29) does not affect the result (30) to the present order. When g = 0 and either Ω or u_a are essential, the value of ω will not depend on the coordinate if it is required that rN'/N = const or N'/rN = const, respectively.

For a plane configuration with perturbations of the form $\exp[i(k_x x+\omega t)]$, the corresponding solution for $\Omega = 0$ is

$$\alpha=k_x\left(\frac{\frac{1}{2}\omega_i a_i^2 N'}{N}-\frac{g}{\omega_i}\right);\quad \frac{1}{4}\alpha^2\Gamma=-\frac{gN'}{N}. \tag{31}$$

The stability condition is $\Gamma < 1$. The result (31) has first been derived by Rosenbluth et al. [5] from the Boltzmann equation, and later by Roberts and Taylor [13], from a macroscopic single-fluid model.

At this stage, attention should be drawn to a curiosity which is involved in the present results. In Eq. (29) we observe that the velocities u_f, u_K, and u_a are all equal in a plane configuration where $\Omega = 0$, as well as in a rotating plasma when $\Omega \ll \omega_i$. We have in fact used different notations for these velocities only to indicate that they arise from different effects in Eq. (6). Thus, suppose that we for a moment could neglect the off-diagonal part of the pressure tensor which gives rise to u_a, i.e., to the contribution of Eq. (27). Suppose also that we neglect the inertia effects of the Larmor motion. By these assumptions we drop both the fifth term and the second part of the seventh term in the right-hand member of Eq. (6). This corresponds to dropping both u_a and u_K in Eq. (29), and yields a result which happens to be formally identical with Eq. (31).

However, if we now improve our treatment and take the rate of change of momentum due to the Larmor motion into account, the term u_K will enter into Eq. (29), whereas u_a is still missing. Since the terms u_f and u_K cancel, we now arrive at a result different from Eq. (31), namely where the first term in the expression for α is missing [15].

Finally, if we also take the off-diagonal terms in the pressure tensor into account, the velocity u_a enters as well. We then recover the stability criterion which was found for $u_K = 0$ and $u_a = 0$ and which corresponds to Eq. (31).

The ratio between the first and the second term in the expression (31) for α is

$$\vartheta=\frac{K_{i\perp}N'}{Nm_i g}. \tag{32}$$

There is always stability when the density gradient points in the same direction as the gravitational or centrifugal fields. In cases where this condition cannot be fulfilled, we examine the following special situations:

1. In a plane configuration with $\Omega = 0$ and for flat density gradients $|\vartheta|$ becomes much less than unity. Equations (31) then reduce to an earlier result by the author [7, 15]. The stability condition is

$$\Gamma = -\frac{4\omega_i^2 N'}{N k_x^2 g} < 1 \tag{33}$$

which can be fulfilled for sufficiently small density gradients.

2. For a plane configuration with a steep density gradient, $|\vartheta|$ may become very large and the first term in the expression (31) for α then dominates. This term arises from the off-diagonal elements of the pressure tensor. From Eq. (32) we see that this is the case when the ion Larmor energy $K_{i\perp}$ is much larger than the work performed by the gravitation field across the characteristic distance (N/N') of the density distribution. The stability condition reduces to

$$\Gamma = -\frac{16 g N}{N' \omega_i^2 k_x^2 a_i^4} < 1, \tag{34}$$

as found by Rosenbluth et al. [5]. This condition can be fulfilled for sufficiently steep density gradients and large Larmor radii.

3. For a rotating plasma with $g = 0$, the result (30) tends to Eq. (14) in the limit of zero Larmor radius. When the Larmor radius is finite there is still a stabilizing contribution from Coriolis' force in addition to that arising from finite Larmor radius effects. The former is represented by the last term in the expression (30) for α and the latter by the second term. The ratio between these terms is $4\Omega r^2 / m_\varphi^2 W_i a_i$, where W_i is the thermal velocity of ions. When the thermal velocity W_i does not exceed the velocity Ωr of rotation, and $a_i \ll r$, we then see that the stabilizing effect is almost entirely provided by Coriolis' force for all modes with low values of m_φ.

It has to be emphasized that the present analysis only concerns a special type of perturbation. Its purpose is merely to give some simple illustrations to the effects involved in Eq. (6). As shown by Taylor [16], perturbations of the form $r^m \exp(im\varphi + i\omega t)$ provide unstable solutions to Eq. (9) in the case where $v_{i0z} = 0$, $v_{e0z} = 0$. Whether the Coriolis force may stabilize a rotating plasma or not depends upon the boundary conditions of the particular eigenvalue problem to be considered. This question is out of the scope of a localized perturbation analysis.

9. Viscous Effects Due to Collisions

In the previous section we have investigated off-diagonal contributions to the pressure tensor which are present in a collisionless case. We shall now examine the contributions to the same tensor which originate from collisions between identical particles. This produces viscous shear forces acting on the fluid motion, which is generated by the perturbations. To lowest order like-particle collisions do not create any diffusion of the plasma across the magnetic field.

Study the same gravitation instability as in the plane case of the previous section. To get a rough estimation of the influence of viscous forces, we exclude very steep density gradients as well as finite Larmor radius effects in the off-diagonal elements of the pressure tensor. According to condition 9, the viscous shear stresses are situated in the transverse plane alone. Following Kaufman [17], we introduce the corresponding dynamic viscosity (ν = i, e):

$$\mu_\nu = \frac{n_\nu k T_\nu \tau_{\nu\nu}}{(1 + 4\omega_\nu^2 \tau_{\nu\nu}^2)}, \tag{35}$$

where T_ν is the temperature and $\tau_{\nu\nu}$ is the self-collision time. The divergence of the pressure tensor becomes

$$\operatorname{div} \pi_\nu = \nabla p_{\nu\perp} - \mu_\nu \left[\frac{4}{3} \nabla (\operatorname{div} \mathbf{v}_\nu) - \operatorname{rot}^2 \mathbf{v}_\nu \right] \tag{36}$$

when condition 4 is taken into account. Since $\omega_e \gg \omega_i$, we neglect the viscous contribution from electrons henceforth.

Assume viscous dissipation to be relatively small and substitute the lowest-order approximation of $\mathbf{v}_\nu$ from Eq. (3) into Eq. (36). In this approximation, $\operatorname{div} \mathbf{v}_\nu = 0$. After some straightforward deductions, it is then found from Eq. (36) that

$$\left(\frac{1}{eB^2}\right) \mathbf{B} \cdot \operatorname{rot} (\operatorname{div} \pi_i) = -\left(\frac{\mu_i}{eB^2}\right) \nabla^4 \tilde{\Phi}, \tag{37}$$

when the spatial variations of the perturbations are assumed to be much steeper than those of unperturbed quantities.

From a combination of Eq. (6) for ions and electrons and expression (37) inserted, we easily obtain

$$\left[\nabla^2 \frac{\partial^2}{\partial t^2} + u_g \nabla^2 \frac{\partial^2}{\partial x\, \partial t} + G_{ie} \frac{\partial^2}{\partial x^2} - \right.$$
$$\left. - \lambda_i \nabla^4 \left(\frac{\partial}{\partial t} + u_g \frac{\partial}{\partial x} \right) \right] \tilde{\Phi} = 0, \tag{38}$$

where $\lambda_i = \frac{\mu_i}{m_i N}$ is the kinematic viscosity of the ion gas and u_g and G_{ie} are defined in connection with Eq. (29) for $\Omega = 0$.

With perturbations of the form $\exp[i(k_x x + k_y y + \omega t)]$ a dispersion relation similar to Eq. (10) is obtained, where now

$$\alpha = -\frac{k_x g}{\omega_i} - i\lambda_i (k_x^2 + k_y^2) \tag{39}$$

and

$$\frac{1}{4}\alpha^2 \Gamma = -\frac{k^2 g N'}{N (k_x^2 + k_y^2)} + i k_x \lambda_i \frac{g (k^2 + k^2)}{\omega_i}, \tag{40}$$

with $i = \sqrt{-1}$. The corresponding expression for ω is independent of r when $N'/N = \text{const.}$

The growth rate is suppressed by viscous dissipation, mainly from the effect of the second term of Eq. (39). The dissipative terms of Eqs. (39) and (40) will only have a small influence on the present results when the gyro frequency ω_i of ions is much larger than the self-collision frequency $1/\tau_{ii}$ of ions. This is the situation in many cases of practical interest and the influence of viscosity on the development of a flute disturbance is then only of minor importance, at least in the special situation treated here.

10. Conclusion

The problems of this paper have demonstrated the close connection between the driving mechanisms which produce screw and flute instabilities. These mechanisms are present both in fully and in partially ionized gases. For the latter, Kadomtsev and Nedospasov [2] have found that a screw-shaped disturbance in the positive column becomes unstable at a certain critical magnetic field. Their analysis is in excellent agreement with experiments. The existence of a critical magnetic field depends on the special conditions of a partially ionized gas. In any case, the driving mechanism of the screw instability is the same also in a fully ionized gas, as demonstrated by the simple example of section 6.

The theory presented here is based on the fluid equations derived from moments of the Boltzmann equation. One of the merits of such an approach is the physical survey-ability of the involved equations. Another is that results can be derived with a relatively simple mathematical formalism.

As an alternative approach we could have started from the perturbation theory for the guiding center drift of individual particles. In fact, this drift also comes out explicitly from Eq. (6)[18]. A correct application of such a theory should include the flux and acceleration of the guiding center as well as of the Larmor motion. In the present problems this leads to rather involved calculations in which the approximations have to be examined thoroughly.

Even if the fluid model seems to be easier to handle in the present problems than the equations of the guiding center drift, there still exist difficulties in the present approach. These arise mainly from the determination of the pressure tensor. Whenever there may be doubts about the results, one should return to a direct treatment in terms of the Boltzmann equation.

LITERATURE CITED

1. M. N. Rosenbluth and C. L. Longmire, Ann. Phys., 1, 120 (1957).
2. B. B. Kadomtsev and A. V. Nedospasov, J. Nucl. Energy, Part C, 1, 230 (1960).
3. F. C. Hoh and B. Lehnert, Phys. Rev. Lett., 7, 75 (1961).
4. B. B. Kadomtsev, Nuclear Fusion, 1, 286 (1961).
5. M. N. Rosenbluth, N. A. Krall, and N. Rostoker, Nuclear Fusion, Suppl., Part 1, 143 (1962).
6. H. Furth, Int. School of Physics, "Enrico Fermi," XXV Course, Advanced Plasma Theory, Varenna, Italy; Nuovo Cimento, Suppl. (1962).
7. B. Lehnert, Phys. Fluids, 4, 525, 847 (1961).

8. M. D. Kruskal and M. Schwarzschild, Proc. Roy. Soc., A223, 348 (1954).
9. B. Lehnert, Phys. Fluids, 5, 740 (1962).
10. B. Lehnert, Phys. Fluids, 5, 432 (1962).
11. W. Marshall, Harwell Report AERE, T/R 2419 (1958).
12. W. B. Thompson, Reports on Progress in Physics (edited by A. C. Stickland) (Inst. of Physics and the Physical Society, 1961), Vol. 24, p. 363.
13. K. V. Roberts and J. B. Taylor, Phys. Rev. Lett., 8, 197 (1962).
14. B. Lehnert, Progress in Nuclear Energy: Series XI, Vol. 2, Plasma Physics and Thermonuclear Research (edited by J. L. Tuck) (Pergamon Press, 1962).
15. B. Lehnert, Phys. Rev. Lett., 7, 440 (1961).
16. J. B. Taylor, J. Nuclear Energy, Part C (1962).
17. A. Kaufman, Phys. Fluids, 3, 610 (1960).
18. B. Lehnert, Nucl. Fusion, Suppl., Part I, 135 (1962).

All abbreviations of periodicals in the above bibliography are letter-by-letter transliterations of the abbreviations as given in the original Russian journal. *Some or all of this periodical literature may well be available in English translation.* A complete list of the cover-to-cover English translations appears at the back of this issue.

THE INITIAL STAGES OF THE EVOLUTION OF THE UNIVERSE

Ya. B. Zel'dovich

Translated from Atomnaya Énergiya, Vol. 14, No. 1,
pp. 92-99, January, 1963
Original article submitted October 6, 1962

1. The Expanding Universe

The expanding universe theory is the only cosmological theory completely based on physical laws that have been firmly established by laboratory experiment.

In this theory, it is assumed that, at a definite instant of time, the density of mass was infinite. An initial velocity distribution is predicated, for which the relative velocity of every two particles is proportional to the distance between these particles, and this velocity is in the direction of increasing distance; this type of velocity distribution ensures an expansion of material as viewed from every point.

The velocity distribution varies with time corresponding to the action of the gravitational forces. The density of material is the same in the whole of space at any instant of time and depends on the time according to the same law. The velocity distribution is given in such a way that there is no privileged (distinguishable) point. The given initial velocity distribution contains a single constant K, which is essentially the difference between the kinetic and potential energies of a part of the material we imagine separated out, and the subsequent behavior of the universe depends on this constant: For a negative K, the expansion reaches a certain limiting value and is then replaced by a contraction, while for positive K and for K = 0 the expansion will continue indefinitely (although with a decreasing rate).

Astronomical observations show that, at the present time, the universe is in a state of expansion. The rate of this expansion and its kinetic energy have been established with satisfactory accuracy, even though the value of the velocity considered correct only 15 years ago was five to seven times the contemporary value.

For the calculation of the potential energy, however, it is necessary to know the mean density of material in the whole of space, including the material between the galaxies. The amount of material in the stars can approximately be estimated by observation; to estimate the quantity of atomic and molecular hydrogen in intergalactic space is very difficult.

It therefore is not directly possible even to determine the sign of K or, consequently, the future of the universe. This indeterminancy, however, has practically no effect on our representation of the past of the universe. The expansion observable at the present time is almost certainly evidence of the fact that the density of material was very high in the past. The rate of expansion in the far distant past is obtained from the gravitational equations, i.e., from the condition that the kinetic energy in the past must have been just sufficient to generate the state observable at the present, and so it is practically independent of K. We therefore also obtain the completely definite expression

$$\rho = \frac{1}{6\pi\gamma t^2} = \frac{0{,}8\cdot 10^6}{t^2} \qquad (1)$$

for the density of material in the past, where the density ρ is in g/cm^3 and the time t is in sec; the time zero is taken to be the time of infinite density; γ is the Newtonian gravitational constant.*

*The formula relates to material in which the pressure is essentially lower than the energy density ρc^2, where c is the velocity of light. We give an elementary derivation of the formula, and consider a sphere of radius R and mass M. The equation of motion of a particle at the boundary is

$$\frac{d^2R}{dt^2} = -\gamma\frac{M}{R^2}.$$

It is easily verified that this equation has the solution $R = (9\pi Mt^2/2)^{1/3}$. This expression can be used to obtain the

What had occurred before the time of infinite density when there was negative time $t < 0$? What was the genesis of the state of infinite density with the corresponding velocity distribution?

This question evidently lies beyond the limits of physical analysis; however, a completely rela problem is that of the theoretical investigation of the processes that have been occurring from the instant of infinite density up to the present, and the comparison of theoretical conclusions with observational results.

Certain aspects of this problem will be considered below.

The hydrodynamic criterion described above in classical language was actually first obtained by the Soviet scientist A. A. Fridman in 1922-1924, in the course of a rigorous solution of the equations of general relativity.

2. The Theory of Neutron Matter

In his consideration of the fate of stars, L. D. Landau in [1] noted that, for a compression, after a certain definite density has been attained, any material must be converted into neutrons with a small admixture of electrons and protons.

In fact, if the nuclear density of matter is reached (10^{14} g/cm^3), then the electrons must have a high energy even for a temperature of absolute zero. The electrons fill all states (levels) up to the so-called Fermi energy E_f, which, in the case in question, is 400 MeV. For such energies, it is clear that protons are converted into neutrons:

$$e^- + p \longrightarrow n + \nu.$$

The neutrino ν that is formed freely leaves a star. The process continues until the remaining electrons no longer have an energy E_f of the order of 20 MeV; for nuclear density, this corresponds to 1-2% of electrons (relative to the number of neutrons). There will be the same number of protons.

We note that in this state the neutrons become stable; the usual decomposition

$$n \longrightarrow p + e^- + \nu$$

is not possible, since all the levels, into which an electron formed by such a process can fall, are occupied. In all the reasoning, both here and in the following sections, the Pauli principle is of decisive importance. This principle states that it is impossible to have two electrons in identical states. The electrons (as well as the protons, the neutrons, and the neutrinos) are subject to the Fermi statistics.

Would it not be possible to assume that, in the first stage of the expansion of the universe, the material in the extremely high-density state consists of cold neutrons with a small admixture of electrons and protons?

In the course of the expansion, for example in the first 10 sec, the density, as given by formula (1), will fall to 8000 g/cm^3. For this density, small by nuclear standards, the decomposition of neutrons is already possible. The half-life of a neutron is about 10 min. In each second, 0.1% of the neutrons decompose; in 100 sec, 10% of the neutrons have decomposed. The protons being formed are subjected to extremely strong radiation from the remaining neutrons. Actually, after 100 sec, the density of the matter reaches 80 g/cm^3, of which 70 g/cm^3 is neutrons. At room temperature, the thermal-neutron capture cross section for hydrogen is 0.33 barn and $\sigma v = 0.33 \cdot 10^{-24} \cdot 1.2 \cdot 10^5 = 7 \cdot 10^{-20}$ cm^3/sec. For a neutron density of 1 g/cm^3 (which corresponds to $6 \cdot 10^{23}$ neutrons/cm^3), the probability w of a neutron-proton combination is

$$w = 7 \cdot 10^{-20} \cdot 6 \cdot 10^{23} = 4 \cdot 10^4 \text{ sec}^{-1}.$$

The life for this capture time is

$$\tau = \frac{1}{w} = 2{,}5 \cdot 10^{-5} \text{ sec}.$$

For a neutron density of 70 g/cm^3, the capture time is less. The cross section for the reaction $d + n = T + \gamma$ is only one-thousandth of that for the reaction $p + n = d + \gamma$, but even this reaction occurs, since the expansion takes place slowly. The expansion from a density of 100 g/cm^3 to 1 g/cm^3 takes 800 sec; the expansion from 1 g/cm^3 to 0.01 g/cm^3 takes 8000 sec.

---

density $\rho = \frac{M}{\frac{4\pi}{3} R^3}$ of the mass in the volume. Here, the mass is contracted, i.e., the result is independent of the value of M taken for the calculation. We thus obtain the formula for ρ given above.

Thus, if the original state were made up of cold neutrons, then in the decomposition the protons would have been rapidly converted into tritium (through deuterium). Energy would have been given out which would have raised the temperature, and the tritium would have been consumed as a result of the thermonuclear reaction

$$d + T = He^4 + n, \quad T + T = He^4 + 2n.$$

In any case, there would be practically no free hydrogen left.

This conclusion is in clear contradiction to everything we know concerning the state of matter in the initial formation of the stars. At this period, matter no doubt consisted mainly of hydrogen.

Thus, the suggestion concerning the cold neutrons at superhigh density is contradicted by observation, and it cannot be considered.

3. The Hot-Matter Theory and the Production of the Elements

Gamov, in [2], and after him Alpher and Herman in [3,4], introduced a theory according to which the matter in its initial stage was at a very high temperature. According to this theory, even when the expansion has proceeded rather far (for example after 700 sec, when the general density will be 1 g/cm^3), the density will be almost completely due to light quanta (or, more precisely, the x-ray quanta), corresponding to a temperature of 50 keV (i.e., $6 \cdot 10^8$ deg).

Thus, the substance sometimes unfortunately called material, i.e., the neutrons, makes up only an insignificant part of the total density – from 10^{-3} to 10^{-8} g/cm^3 according to different estimates.*

The authors' original aim in developing their theory was to describe the presently observed distibution of various elements and isotopes in nature.

Evidence for the rules for the propagation of the elements is based on the fact that there was a period of irradiation of the nuclei by neutrons. In fact, nuclei formed with a large cross section by the capture of neutrons (and the subsequent β-decay) were, in this period, more common than nuclei capable of being converted, by the capture of a neutron, into other types of nuclei.

It is assumed at present, however, that the synthesis of heavy elements by the irradiation of nuclei by neutrons takes place in the stars, and in particular during the explosions of supernova.

The theory of Gamov, Alpher, and Herman, according to which the elements were formed in the prestar stage when the universe was expanding from the high-density state, is thus untenable because it is impossible to go from nuclei with $A \leq 4$ to nuclei with $A \geq 9$ by an increase in the number of neutrons, i.e., an increase in the number of neutrons cannot yield beryllium, boron, carbon, etc., from helium (He^4). This is because there is no nucleus with A = 5 (no He^5 or Li^5); for A = 8, the β-decay of Li^8 yields Be^8 and there is thus an immediate conversion into $2He^4$.

In stars, the synthesis of nuclei takes place under high-density conditions, when the reaction $3He^4 \rightarrow C^{12}$ is possible. Under the conditions of prestar expansion when neutron decomposition was occurring, deutrons were formed, the thermonuclear reaction between deutrons yielded He^4, and the density and temperature dropped far enough for the formation of C^{12} and He^4 to become possible.

The analysis of processes occurring in the prestar stage is necessary not from the point of view of describing the spread of the elements, but from the point of view of the composition of the matter from which stars of the first generation were formed.

4. Processes in Hot Matter

We therefore assume that the temperature was high in the early stages. As was shown by Hayashi in [5], the higher the temperature, the more rapidly will thermodynamic equilibrium be established.

It follows from the gravitation equations that there is a definite relation between the density and the time: $\rho = a/t^2$. We may therefore say that the characteristic time of the expansion is $t \simeq \sqrt{\frac{a}{\rho}}$.

At high temperatures, the energy density ε is proportional to T^4, where T is the temperature. For example, for

* When the density depends basically on the radiation, then in the expression relating the density to the time the numerical coefficient is changed, and we have

$$\rho = \frac{3}{32\pi\gamma t^2} = \frac{0{,}45 \cdot 10^6}{t^2}.$$

light quanta $\varepsilon_\gamma = 1.35 \cdot 10^{14} T^4$ (ε in erg/cm^3, T in keV). The corresponding density ρ_γ is

$$\varrho_\gamma = \frac{\varepsilon_\gamma}{c^2} = 1{,}5 \cdot 10^{-7} T^4.$$

In addition to the quanta, there must also be an equilibrium number of electrons and protons. Their concentration is proportional to $e^{-mc^2/T}$, where mc^2 is the energy of a motionless electron (510 keV). For $T > mc^2$, the density of the energy of the electrons and protons is of the same order as that of the quanta, and also depends on the temperature ($\sim T^4$); it is equal to

$$\varrho_e = 1{,}75 \varrho_\gamma.$$

The electrons and protons, in their turn, are in particular, in thermodynamic equilibrium with the neutrons and antineutrons because of the process

$$e^+ + e^- = \nu + \nu.$$

Here,

$$\varrho_\nu = 1{,}75 \varrho_\gamma.$$

The concentration of electrons is proportional to T^3 and the mean energy of an electron is $\sim T$. The cross section of the reactions for the weak interaction is proportional to E^2. Therefore, the time needed for the establishment of equilibrium is $t_e \sim 1/T^5$; it is thus obvious that for high temperature $t_e \ll t$, the time of expansion. Later, in the course of the expansion, the processes involved in the establishment of equilibrium become slower. After this, during the expansion, the energies of the neutrinos and quanta decrease independently; the interchange of energy between them stops. The relation between the energies also remains practically the same for independent expansion, since all the relativistic particles (those moving with the velocity of light) have their energy decreased as time passes in the expanding space.

We may therefore assume that, from the time when the temperature and density are still high, there remain neutrinos of the second kind* and quanta of the gravitational field.

On the whole, it must be assumed that, for a total density $\rho < 100$ g/cm^3 we have

$$\varrho = \alpha \varrho_\gamma,$$

where ρ is the total density of all forms of relativistic particles, ρ_γ is the density of electromagnetic quanta, and α is in the interval $1 + 1.75 < \alpha < 1 + 1.75 + 1 + 1.75$.**

Taking $\alpha = 4$, we obtain the final law for the variation of the temperature from the relations

$$\varrho = \frac{0{,}45 \cdot 10^6}{t^2}, \quad \varrho_\gamma = 1{,}5 \cdot 10^{-7} T^2 \text{ and } \varrho = 4\varrho_\gamma:$$

$$T = \frac{950}{\sqrt{t}}.$$

What happens to nucleons in such a boiling cauldron of quanta, electrons, positrons, neutrinos, and antineutrinos? The reactions

$$n \rightleftarrows p + e^- + \bar{\nu}, \quad \nu + n \rightleftarrows p + e^-,$$
$$e^+ + n \rightleftarrows p + \bar{\nu}$$

occur. For high temperatures, the rates of all processes are high compared with the rate of expansion, and so thermodynamic equilibrium is established. The number of nucleons is negligible in comparison with the number of e^+ and e^-, ν and $\bar{\nu}$; with good accuracy the number of particles and antiparticles are therefore identical. Under these conditions, the equilibrium relation between the neutrons and protons is

$$\frac{n}{p} = e^{-c^2 \Delta m / T},$$

*The existence of two different kinds of neutrinos, related to electrons and μ-mesons, respectively, was recently proved experimentally [6].

**The lower limit corresponds to γ and ν_e, the upper limit to γ, ν_e, to gravitons, and ν_μ.

where Δm is the difference between the mass of a neutron and that of a proton (note that we are considering the mass of a proton and not the mass of an atom of hydrogen). We have $c^2\Delta m = 1300$ keV. For lower temperatures, the concentration and energy of the e^+ and e^-, and also of the ν and $\bar{\nu}$ decrease, and, starting at a certain time, the ratio of the concentrations of n and p ceases to follow a regular law. It has been found by calculation [5] that the ratio becomes constant and equal to $n/p = 1/4$ (which corresponds to an effective temperature of ~900 keV) a few seconds after t = 0. After this, the neutron concentration decreases only as a result of spontaneous decay and capture $n + p = d + \gamma$.

5. Difficulties in Gamov's Theory

If the nucleon density is sufficiently high, then practically all the neutrons surviving to the end of the fast processes will turn into duterium and, further, by thermonuclear reactions, into He^4. The initial state with a ratio $n/p = 1/4$ leads to the relation $He^4/p = 0.5/3$, i.e., to 40% He^4 and 60% hydrogen by weight (see [5]). Such a state is inadmissible.

It is believed that $He^4/H = 0.2$-0.3 in the sun at the present, i.e., that 17-23% of the total weight is He^4. After $5 \cdot 10^9$ years of maintaining the observed brightness, about 5% by weight of the hydrogen will be consumed and converted into He^4, so that the initial state must have corresponded to not more than 12-18% He^4. If the age of the sun is $5 \cdot 10^9$ years, then it must have been formed from gas in which there was already helium produced by reactions in the stars of the preceding generation.

It is pointed out in [7] (with a reference to [8]) that there are stars with $\log He^4/H$ (for atoms) equal to -2.22, and this corresponds to 2.5% He^4 by weight. We cannot make any estimate of the reliability of these results. It is essential that the mechanism that permits the consumption and destruction of the helium (but still leaves the He^3 [9]) be very improbable.

It is evident that the theory of the prestar evolution must lead to a state with the amount of hydrogen maintained at not less than 90% by weight and the He^4 at not more than 10% by weight; in particular, the assumption of 100% pure hydrogen is completely permissible.

In order that the quantity of helium be decreased, the destruction of some of the neutrons is necessary. What process can cause this result? There is, first of all, the process inverse to that of the decay of duterium to protons and neutrons under the action of quanta contained in the state of radiation in thermodynamic equilibrium: $\gamma + d \rightleftharpoons n + p$.

The rate of this process is easily found: We find the rate of change of the relative weight concentration of deuterium:

$$z = \frac{2D}{N + P + 2D}.$$

Using the notation $x = \frac{N}{N + P + 2D}$ for the concentration of neutrons and $y = \frac{P}{N + P + 2D}$ for the concentration of protons, we obtain

$$\frac{dz}{dt} = \sigma v 6 \cdot 10^{23} \varrho_m xy - f(T)\, z - \varphi(T)\, \varrho_m z^2.$$

The first term on the right-hand side describes the formation of deutrons, the second describes the photodecay. The last term gives the decrease in the concentration of deuterium due to the thermonuclear reactions $d + d = t + p$ and $d + d = He^3 + n$.

The first two terms must precisely compensate one another if the concentrations x, y, and z are for thermodynamic equilibrium (below D_e and z_e refer to the equilibrium deuterium concentration):

$$\frac{NP}{D_e} = \frac{4}{3} \frac{(mT)^{3/2}}{2^3 \pi^{3/2} \hbar^3} e^{-Q/T} = \psi(T);$$

$$\frac{xy}{z_e} = \frac{NP}{D_e} \frac{1}{2} (N + P + 2D) = \frac{NP}{D_e} \frac{1}{2} \cdot 6 \cdot 10^{23} \varrho_m = 3 \cdot 10^{23} \varrho_m \psi(T).$$

Hence, $f(T) = 2\sigma v \psi(T)$. In the expression for $\psi(T)$ the quantity Q is the deutron binding energy (Q = 2200 keV), and m is the mass of the nucleon.

The rate of the thermonuclear reaction d + d is well known [10]. It can be approximated by the formula

$$\varphi(T) = 7{,}8 \cdot 10^9 (1 + 0{,}042 T^{3/4})\, T^{-2/3} e^{-18{,}8/T^{1/3}}$$

(according to the sum of two channels). At high temperatures, the equilibrium between formation and decay is rapidly established; the time necessary for the establishment of equilibrium is $\tau_e = [f(T)]^{-1}$. This time must be compared with the time of expansion t. We give the following results:

t, sec	T, keV	τ_e, sec
100	95	10^{-6}
200	67	$3 \cdot 10^{-2}$
300	55	50
400	48	20,000
500	4	10^7

The time for the establishment of equilibrium varies extremely rapidly. It can be assumed approximately that, for t < 320 sec, neutrons are not captured by protons, since the deuterium formed here does not decay.*

At this time, as the result of spontaneous decay, the relative concentration of neutrons has been lowered to $0.20e^{-320/1000} = 0.145$, which for total capture would give 29% He^4 by weight.

For t > 320 sec, on the other hand, we will neglect the photodecay of deuterium. We will consider the competition between the decay of neutrons and the capture of their protons. We will also assume that all the neutrons captured by protons are subsequently transformed into He^4.

For the neutrons we obtain

$$\frac{dx}{dt} = -wx - \sigma v 6 \cdot 10^{23} \varrho_m y x = \\ = -0{,}001x - 4 \cdot 10^4 \varrho_m y x.$$

We use the symbol ρ_1 for the density of nucleons at the instant when the total density (as determined by the radiation) is 1 g/cm^3, i.e., at the time t_1 = 670 sec. From the expansion law we obtain

$$\varrho_m = \varrho_1 \left(\frac{t}{t_1}\right)^{-3/2} = \frac{1{,}7 \cdot 10^4 \varrho_1}{t^{3/2}}.$$

The concentration y of protons will be taken to be equal to 0.8 (it varies only slightly), and the probability of neutron decay will be assumed to be $w = 10^{-3}$.

We integrate the equation from t = 320 sec, x = 0.145.** We thus find the proportion of neutrons captured by protons and the amount of He^4 formed as a function of the natural parameter ρ_1. For a first approximation we take $x = 0.20e^{-wt} = 0.20e^{-t/1000}$, and then calculate the amount of helium (by weight)***:

$$(He^4) = 2 \cdot 0{,}20 \sigma v \cdot 6 \cdot 10^{23} \overline{y} \int_{320}^{\infty} e^{-wt} \varrho_m(t)\, dt.$$

*Here we decrease the amount of deuterium formed, since a part of the deuterons do not decay but take part in the (d + d)-reaction. The He^3, tritium, and He^4 nuclei formed are much more durable than the deuterons and are not subject to decay.

**Corresponding to the previous footnote, a more accurate criterion for the temperature for which we must take capture into account is obtained by comparing the rate of capture (the first term in the equation for dz/dt) with the rate of thermonuclear reaction calculated for the equilibrium concentration of deuterium. This temperature, and the corresponding time, depend on ρ_m and so on ρ_1. For $\rho_1 = 0.6 \cdot 10^{-8}$ calculation yields T = 52 keV and t = 320 sec; for $\rho_1 = 10^{-5}$ we obtain T = 74 keV and t = 160 sec; while for $\rho_1 = 4$ we obtain T = 104 keV and t = 80 sec.

***By using the fact that we always have $(He^4) \leq 0.29$, we obtain the better approximation

$$(He^4) = 0{,}29 \frac{2{,}5 \cdot 10^7 \varrho_1}{1 + 2{,}5 \cdot 10^7 \varrho_1}.$$

Substituting the expression for $\rho_m(t)$, we obtain

$$(He^4) = 2 \cdot 0{,}2 \cdot 5{,}6 \cdot 10^8 \varrho_1 \times$$

$$\times \frac{e^{-0.001 \cdot 320}}{\sqrt{320}} \int_0^\infty \frac{e^{-0{,}320}}{(1+\theta)^{3/2}} d\theta, \text{ where } \theta = \frac{t-320}{320};$$

$$(He^4) = 0{,}29 \cdot 2{,}5 \cdot 10^7 \varrho_1,$$

where $0.29 = 2 \cdot 0.2 \cdot e^{-0.001 \cdot 320}$. If $(He^4) = 0.1$, then $\rho_1 = 1.4 \cdot 10^{-8}$, while for $(He^4) = 0.05$ we obtain $\rho_1 = 0.7 \cdot 10^{-8}$.

The Gamov theory thus leads to the necessity for a very low nucleon density (about 10^{-8} g/cm^3) at the time when the density of all forms of radiation is 1 g/cm^3.

To what results will such a small density lead?

At the present, the density of nucleons is estimated to be $\rho_m = 10^{-29}$ g/cm^3. With expansion, the density of radiation will decrease proportionally to $\rho_m^{4/3}$. Thus, if the density of nucleons decreases in the proportion $10^{-8}/10^{-29}$ (that is to $1/10^{21}$ times its value), then the radiation density will be divided by $(10^{21})^{4/3} = 10^{28}$, and will become 10^{-28} g/cm^3.

Thus, according to Gamov's theory, the radiation density at the present time must be 10 times the density of matter. It is difficult to reconcile such a conclusion with the results concerning the age of the universe [11, 12].

About 25% of the radiation density is due to electromagnetic radiation (see the coefficient α in section 4), while the remaining density is from neutrinos and gravitons. Thus, the density of electromagnetic radiation is $2.5 \cdot 10^{-29}$ g/cm^3, i.e., $2.5 \cdot 10^{-29} c^2 = 2 \cdot 10^{-8}$ erg/cm^3 = 13,000 eV/cm^3. This corresponds to a radiation temperature of 30°K.

For comparison, we note that the intergalactic density of starlight corresponds to an energy density of 10^{-3} eV per cm^3. Considering collisions of relativistic electrons with light quanta, V. L. Ginzburg and S. P. Syrovatskii in [13] estimated the maximum electromagnetic-radiation density to be of the order of 10 eV/cm^3. If this value is taken as a starting point, then for all forms of radiation (the coefficient α), we find $\rho_{rad} = \frac{4 \cdot 10 \cdot 1{,}6 \cdot 10^{-12}}{9 \cdot 10^{20}} = 7 \cdot 10^{-32}$ g per cm^3, for $\rho_m = 10^{-29}$ g/cm^3, and hence for $\rho_{rad} = 1$, we have $\rho_m = \rho_1 = 10^{-29} (7 \cdot 10^{-32})^{-3/4} = 2.5 \cdot 10^{-5}$, which from the formula in the previous footnote yields $(He^4) = 29\%$ by weight. In reality, if we take into account the thermodynamic reaction for $t < 320$ sec, the value is somewhat larger.

Thus, the results on the helium content and on the radiation density at the present time yield the conclusion that the true Gamov hypothesis concerning the hot matter in the early stages of the evolution of the universe is somewhat improbable.

In the light of the above, the determination of the helium content in the slowly evolving stars becomes of great importance, as does the question of the density of the various forms of energy (electromagnetic and neutrino energy).

Gamov's theory is thus not naturally possible in the framework of the expanding universe.

6. The Proton-Matter Theory

We can assume, for the initial state of the universe, a mixture of protons, electrons, and neutrinos in equal quantities (the same number of each type of particle).

The idea is that the neutrinos form a Fermi distribution and fill the whole space with an energy less than the Fermi energy E_f, depending on the density.

After this, the Pauli principle forbids the conversion of matter into neutrons by the reaction

$$e^- + p = n + \nu,$$

since the states for ν, the energy in this reaction, are occupied.

The neutrinos stabilize the protons at high densities, and for low densities the protons stabilize themselves.

This idea cannot be applied to stars because of the loss of neutrinos. In a homogeneous universe, however, the neutrinos cannot escape. The constancy of the neutrino density throughout space means that when a neutrino leaves a given point it is replaced by a neutrino arriving from another point. No answer is given to the question of where

the neutrinos come from, just as there is no consideration in Gamov's theory of the source of the nucleons of the high temperature. In posing the question stated in section 1, we consider the period of expansion and must specify certain quantities that are to be conserved during the expansion or, to be more precise, we specify the characteristic conditions of this expansion.

In addition to the entropy, according to contemporary thought, the "lepton number," which is the sum of the number of e^- and ν minus the number of e^+ and $\bar{\nu}$, must also be conserved; this quantity is conserved in β-decay processes. The proposed variant corresponds to the conservation of the entropy equal to zero and of a lepton number equal to two (relative to one nucleon).

In the light of recent results concerning the existence of two forms of neutrinos [6] (the "electron" and "muon" types), we assume here the presence initially of electron neutrinos ν_e forbidding the capture of electrons.

For a quantitative treatment, it is essential that for equal densities, the Fermi energy of neutrinos is greater than the Fermi energy of electrons. According to Landau's theory [14], a neutrino is described by a two-component wave function, and is a "spiral" particle. This means that for a given direction of momentum, the spin of a neutrino can have only one direction – the opposite direction to that of the momentum – whereas the spin of an electron can have two directions. For the same momentum, the Fermi number of states of an electron is double the number of states of a neutrino, and so for a given number of particles per unit volume, the Fermi momentum of a neutrino is $\sqrt[3]{2}$ times the momentum of an electron. In the relativistic case, the energy is equal to the momentum multiplied by the velocity of light. For a proton density of 10^{14} g/cm^3, i.e., $6 \cdot 10^{37}$ protons/cm^3, and for equal numbers of e^-, ν, and p, the Fermi energy of electrons is 400 MeV and the Fermi energy of neutrinos is 500 MeV. The possibility of conversion into neutrons is completely excluded.

For still higher densities of matter in the composition under consideration, some reactions are possible, for example $\nu_e = e^- + \mu^+ + \nu_\mu$, the formation of hyperons [15], and even the partial conversion of protons into neutrons, when the Fermi energy of the protons becomes sufficiently high.

However, for densities many times greater than nuclear density, the time of relaxation for all processes is greatly shortened, and becomes much shorter than the time of expansion. Thus, when, in the course of expansion, the nuclear density is reached, then the composition of the matter will be at equilibrium, i.e., the matter will consist of protons, electrons, and neutrinos.

The assumption made leads to the conclusion that the first generation of stars, at the beginning of their evolution, consist of pure hydrogen; all the remaining elements appear as the result of subsequent processes in the depths of the stars.

What is the fate of the neutrinos? In the expansion up to the present neutron density 10^{-29} g/cm^3, the Fermi energy of the neutrinos decreases proportionally to $\sqrt[3]{\rho}$ and becomes equal to $2 \cdot 10^{-6}$ eV. The number of neutrinos in unit volume is equal to the number of nucleons, as before. For nuclear density, the energy of the neutrinos is of the same order as that of the electrons and nucleons; at the present, after expansion, the neutrino energy is negligibly small compared with that of the nucleons (the latter energy is 10^{15} times as large as the former). At the present, the energy of the original neutrinos is also negligibly small compared with the energy of those neutrinos that were formed later during nuclear reactions in the stars. The present article has discussed the question of the nuclear processes in an expanding universe. We therefore only mention some considerations concerning the mechanism that forms the stars.

We will assume that at the initial instant the matter was strictly homogeneous. Gravitation will have a tendency during the passage of time, to strengthen density inhomogeneities. However, as has been shown by E. M. Lifshits in [16], the thermodynamic fluctuations of the density in homogeneous matter are too small; at the end of the time preceding the start of the present stage of the evolution, the inhomogeneities due to fluctuations would not have reached a significant amplitude.

The assumption that, in the prestar era, matter consisted of cold hydrogen, obviates this difficulty. During the expansion, the hydrogen is subject to phase transitions: the transition from a metal into solid, molecular hydrogen [17] with a density of about 1 g/cm^3; the explosion of solid hydrogen with the formation of the gas phase with a density less than 0.07 g/cm^3. These phase changes enormously increase the nonuniformity of the density in comparison with that caused by the thermodynamic fluctuations.

The attainable inhomogeneity can be great enough for the subsequent action of gravitational instability to lead to the separation out of stars [18].

Conclusions

1. We have considered the difficulties of Gamov's theory, according to which the temperature was so high in the prestar stage of evolution of the universe that the radiation density was many orders greater than the nucleon density.

2. The proposal was made that the matter consisted of a cold mixture of protons, electrons, and neutrinos.

3. The choice between these assumptions depends on the results of measuring the helium content in old stars and on the size of the intergalactic radiation density.

Three years have passed since the death of Igor' Vasil'evich Kurchatov. He was a great, vibrant man who loved life, who was scientifically talented, who devoted his life to Soviet science and to our country, and he was a close friend. Both in practical and theoretical work we will remember what we were taught by Igor' Vasil'evich: to attack the most important basic problems and to be honest, bold, and passionate in work and in life.

LITERATURE CITED

1. L. D. Landau, DAN SSSR, 17, 301 (1937).
2. G. Gamov, Rev. Mod. Phys., 21, 367 (1949).
3. R. Alpher and R. Herman, Rev. Mod. Phys., 22, 153 (1950).
4. R. Alpher and R. Herman, Ann. Rev. Nucl. Sci., 2, 1 (1953).
5. C. Hayashi, Progr. Theor. Phys., 5, 224 (1950).
6. G. Danby et al., Phys. Rev. Lett., 9, 36 (1962).
7. M. Minnaert, Monthly Notices Roy. Astron. Soc., 117, 315 (1957).
8. G. Righini et al., Contrib. Oss. Asiago, No. 51 (1954).
9. G. Wallerstein, Phys. Rev. Lett., 9, 143 (1962).
10. B. N. Kozlov, Atomnaya énergiya, 12, 3, 238 (1962).
11. A. Peres, Progr. Theor. Phys., 24, 149 (1960).
12. Ya. B. Zel'dovich, and Ya. A. Smorodinskii, ZhÉTF., 41, 907 (1961).
13. V. L. Ginzburg and S. P. Syrovatskii, The Origin of Cosmic Rays [in Russian] (Izd. AN SSSR, Moscow, 1963) (in press).
14. L. D. Landau, ZhÉTF., 32, 407 (1957).
15. V. A. Ambartsumyan and G. S. Saakyan, Astron. Zh., 37, 173 (1960).
16. E. M. Lifshits, ZhÉTF., 16, 587 (1946).
17. A. A. Abrikosov, Astron. Zh., 31, 112 (1954).
18. Ya. B. Zel'dovich, ZhÉTF., 43, 5, 1982 (1962).

All abbreviations of periodicals in the above bibliography are letter-by-letter transliterations of the abbreviations as given in the original Russian journal. *Some or all of this periodical literature may well be available in English translation.* A complete list of the cover-to-cover English translations appears at the back of this issue.

THE AGE OF NUCLEI AND THE NUCLEAR SYNTHESIS TIME

V. A. Davidenko

Translated from Atomnaya Énergiya, Vol. 14, No. 1,
pp. 100-104, January, 1963
Original article submitted November 12, 1962

In this paper we examine methods of determining the age of nuclei, discussed with I. V. Kurchatov in 1947.

To obtain more accurate determinations, a plan was developed, together with I. V. Kurchatov, for measuring the neutron cross sections and lifetimes of a number of nuclei, but these measurements were not carried out; the work was not completed adequately and was not published. However, some of the aspects of this discussion are still of interest.

The time which has elapsed since active synthesis of nuclei ceased is denoted by the age of elements. Its value is determined experimentally from changes in isotopic abundances in meteorites and in the Earth's crust, taking place as a result of decay of long-life radioactive nuclei [1-5].

The use of this method naturally implies determination of the time which has elapsed since the last large-scale phenomenon in that part of the universe closest to us occurred, as a result of which the "primary" distribution of nuclei in meteorites and the earth's crust was established, and then remained almost unchanged. But this does not mean that that part of the nuclei which is determined could not have been formed long before this time, or that the concept of the "age of elements" has a literal meaning. It would be more correct to speak of the age of natural radioactive nuclei, because it is this age which is determined by experiment.

Bearing this in mind, we will examine methods of determining the age of nuclei based on the "inner" relationships of the isotope table.

The determinations are carried out on the assumption that the relative isotopic abundances, observed on the earth, correspond to the initial distribution established by the end of nuclear synthesis. Furthermore, it is assumed that the duration of the active synthesis phase was negligibly small compared with the lifetime of natural radioactive nuclei and, therefore, that the initial abundances of these nuclei were those which might be expected from their position in isotope systematics [6].

Fast nuclear synthesis corresponds closest to these conditions but, as will be noted in paragraph 3, there are indications that the bulk of nuclei appeared as a result of slow neutron synthesis with a characteristic time $\simeq 10^5$ years. However, this does not refute our assumptions.

1. There are two odd-odd radioactive nuclei, K^{40} and Lu^{176}, located in the same position with respect to neighboring nuclei. Both nuclei are "screened" both on the neutron-excess isobar side and the neutron-deficient isobar side by stable nuclei, and may be formed during nuclear synthesis for the most part only as a result of (n,γ)-reactions from K^{39} and Lu^{175}. Therefore, the nuclear abundances of K^{40} and Lu^{176} may be perfectly equal.

Unfortunately, we do not have a sufficiently accurate knowledge of the values of the cross sections of (n,γ)-reactions, based on fast neutrons for K^{39}, K^{40}, Lu^{175}, and Lu^{176} nuclei, to select correctly the most probable value of the initial relative abundance of K^{40}, but for an estimate of this value we may assume that by the end of nuclear synthesis the K^{40}/K^{39} ratio was the same as the Lu^{176}/Lu^{175} ratio. Thus, the age of potassium is determined from the relationship

$$t_{\mathrm{K}} = \frac{1}{\lg 2}\frac{T_{\mathrm{Lu}}T_{\mathrm{K}}}{T_{\mathrm{Lu}}-T_{\mathrm{K}}}\left[\lg\left(\frac{\mathrm{Lu}^{176}}{\mathrm{Lu}^{175}}\right)_t - \lg\left(\frac{\mathrm{K}^{40}}{\mathrm{K}^{39}}\right)_t\right],$$

where T_{Lu} and T_K are the half-lives of Lu^{176} and K^{40}, equal to $2.4 \cdot 10^{10}$ and $1.25 \cdot 10^9$ years, respectively; Lu^{176}/Lu^{175} and K^{40}/K^{39} are the ratios of the observed isotopic abundances, equal to: 2.6% Lu^{176}, 97.4% Lu^{175}, 0.0119% K^{40}, and 93.08% K^{39}, respectively. Substituting the numerical values, we obtain $t_K = 10.2 \cdot 10^9$ years. Therefore, the initial ratio of the potassium isotopic abundances is

$$\left(\frac{K^{40}}{K^{39}}\right)_{t=0} = \left(\frac{K^{40}}{K^{39}}\right)_t 2^{\frac{t_K}{T_K}} = 0{,}036,$$

i.e., this ratio was 280-fold greater than the present value.

The authors of [7] took the mean values of the (n, γ)-cross sections of K^{39} and K^{40} as 8 and 100 mbarn, respectively, and found that initially the value of K^{40} was 260-fold greater than at present.

This estimate is more probably the upper age limit of potassium, because the K^{39} nucleus is "magic" (20 neutrons) and, in contrast to K^{40}, Lu^{175}, and Lu^{176} is more resistant to neutron burnup, with the result that the K^{40}/K^{39} ratio is less than the Lu^{176}/Lu^{175} ratio. Despite this, the figure of $10.2 \cdot 10^9$ cannot be far from the true value, because the equation for t depends only slightly on the initial abundance ratio if a markedly decayed isotope is taken for the calculation.

2. U^{235} and U^{238} isotopes were formed mainly as a result of α-decay of their precursors with atomic weights A equal to 4n + 3 and 4n + 2, i.e., by a different mechanism to that of stable nuclei. Therefore, in this case we cannot justify the determination of the initial U^{235}/U^{238} ratio from stable isotope systematics. Furthermore, two opposing factors could have a marked effect on the initial abundances of uranium isotopes: on the one hand, in the presence of neutrons, U^{235} and its α-precursors must burn up more rapidly than U^{238} and its α-precursors; on the other hand, the latter had a higher neutron excess and therefore were formed more rapidly and could be burned before the β-conversions of the former had even finished. Therefore, the initial U^{235}/U^{238} ratio must be very sensitive to the fast neutron synthesis time.

Despite these reservations, we may compare uranium with its nearest elements: ytterbium and mercury, which have exactly the same number and distribution of β-stable isotopes.

With respect to the position in the β-stability band, Yb^{173} and Hg^{201} nuclei correspond to uranium-235, and Yb^{176} and Hg^{204} to uranium-238. Their ratios are equal to $Yb^{173}/Yb^{176} = 1.28$ and $Hg^{201}/Hg^{204} = 1.93$, respectively. Here, there is no justification for either averaging or extrapolation, but it is interesting to note that in a detailed calculation of the probabilities of formation of uranium isotopes under the synthesis conditions in type I supernova stars, the authors of [7] found, for the initial abundances $U^{235}/U^{238} = 1.64$, i.e., the mean of the two previous values: 1.28 and 1.93. In accordance with this ratio, the age of uranium is $6.6 \cdot 10^9$ years.

The age values of potassium ($10.2 \cdot 10^9$ years) and uranium ($6.6 \cdot 10^9$ years) are fairly close, but, for reasons indicated in our reservations, both values are not fully reliable. The true age of the nuclei (if we disregard the theory that uranium is younger than potassium) is evidently intermediate between these figures.

It would be very interesting to measure the relation between the (n, γ)-cross sections and the energy for potassium and lutetium isotopes and calculate more accurately the age of potassium. In this case, a knowledge of the cross sections of lutetium isotopes would be helpful for selecting more accurately the neutron spectrum, and the role of the other processes in the formation of K^{40} could be taken into account, as follows: the three other odd-odd V^{50}, La^{138}, and Ta^{180} nuclei do not have stable (n, γ)-precursors and could be formed only by other, ineffective processes. The relation between the relative abundances of these nuclei and Z is linear. The short extrapolation from V^{50} to K^{40} indicates that the contribution of these processes in the initial abundance of K^{40} must be about 0.27% with respect to K^{41}.

3. It is known that elements with odd Z have only one or two stable isotopes, only isotopes with an even number of neutrons being stable (K^{40}, V^{50}, La^{138}, Lu^{176}, and Ta^{180} nuclei are not exceptions, because they are radioactive).

If the relative abundances of pairs of odd-even isotopes are plotted on a graph, a distinct relation between them and the Z values is quite evident (see figure). The heavy and light isotopes are located on a straight line or smooth curve (dotted line).

In the case of slow synthesis, a law of this type could be obtained as a result of a steady change in the ratio of the mean (n, γ)-cross sections of the investigated isotope pairs with an increase in the Z value, and in the case of

Absolute Abundance of Synthesized Isotopes and Their (n, γ)-Precursors, According to Suess and Urey [8] and, in Brackets, According to Goldschmidt

Synthesized isotopes and their absolute abundances	Ratio of abundance of isotope pairs	(n,γ)-precursors and their absolute abundances		Ratio of sum of absolute abundances of precursors
		with small Z	with high Z	
Cl^{35} 6670 (3800) Cl^{37} 2180 (1240)	3,06	S^{34} 15 700 (4 800) S^{36} 51 (15,5)	Absent Ar^{36} 126 000 (—)	0,125
K^{39} 2940 (6400) K^{41} 219 (480)	13,4	Ar^{38} 24 000 (—) Ar^{40} —	Absent Ca^{40} 47 500 (55 000)	<0,51
Cu^{63} 146 (316) Cu^{65} 66 (143)	2,2	Ni^{62} 1000 (1680)* Ni^{64} 318 (530)	Absent Zn^{64} 238 (176)	1,8 (2,4)
Ga^{69} 6,86 (11,5) Ga^{71} 4,54 (7,7)	1,3	Zn^{68} 90,9 (67,0) Zn^{70} 3,35 (2,5)	Absent Ge^{70} 10,4 (39,0)	6,6 (1,6)
Br^{79} 6,78 (21,7) Br^{81} 6,62 (21,2)	1,02	Se^{78} 16 (3,55) Se^{80} 33.8 (7,5)	Kr^{78} 0,175 (—) Kr^{80} 1,14 (—)	0,46
Rb^{85} 4,73 (4,9) Rb^{87} 1,77 (1,9)	2,7	Kr^{84} 29,3 (—) Kr^{86} 8,94 (—)	Sr^{84} 0,106 (0,224) "screened"	3,3
Ag^{107} 0,134 (1,65) Ag^{109} 0,126 (1,54)	1,06	Pd^{106} 0,184 (0,49) Pd^{108} 0,18 (0,48)	Cd^{106} 0,0109 (0,032) Cd^{108} 0,0079 (0,023)	1,04
In^{113} 0.0046 (0,097) In^{115} 0,105 (0,22)	0,044	"screened" Cd^{114} 0,256 (0,75)	Sn^{112} 0,0134 (0,29) "screened"	0,052 (0,39)
Sb^{121} 0,141 (0,412) Sb^{123} 0,105 (0,308)	1,35	Sn^{120} 0,43 (9,5) Sn^{122} 0,063 (1,37)	Te^{120} 0,0042 (0,0002) "screened"	6,9
Eu^{151} 0,089 (0,134) Eu^{153} 0,098 (0,146)	0,91	Nd^{150} 0,0806 (0,185) Sm^{150} 0,049 (0,086) Sm^{152} 0,176 (0,302)	Absent Gd^{152} 0.00137 (0,0033)	0,73 (0,94)
Re^{185} 0,05 (0,044) Re^{187} 0,085 (0,075)	0,59	W^{184} 0,15 (4,43) W^{186} 0,14 (4,12)	Os^{184} 0,0002 (0,00034) "screened"	1,07
Ir^{191} 0,316 (0,223) Ir^{193} 0,505 (0,356)	0,63	Os^{190} 0,264 (0,45) Os^{192} 0,41 (0,7)	Pt^{190} 0,0001 (0,00035) Pt^{192} 0,0127 (0,0226)	0,62
Tl^{203} 0,0319 (0,05) Tl^{205} 0,0761 (0,12)	0,42	Hg^{202} 0,0844 (0,098) Hg^{204} 0,0194 (0,0225)	Absent Pb^{204} 0,0063 (0,122)	3,3 (0,68)

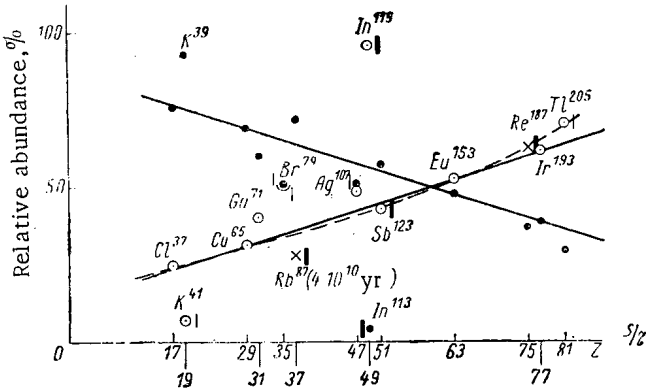

Relation between the relative abundances of odd-even isotopes and the Z value. The abundances of light isotopes are indicated by points, those of heavy isotopes by circles. Radioactive nuclei Rb^{87} and Re^{187} are indicated by crosses. The solid line indicates that the nucleus is "screened" by stable isobars, the dotted line indicates the presence of a long-life isobar with a half-life $>10^4$ years. The lines on the left relate to isobars with $Z-1$; those on the right, to $Z+1$.

rapid synthesis – as a result of statistically averaging the probabilities of formation of these isotopes with respect to a large number of precursors. We must be clear as to which of these synthesis mechanisms could lead to the observed law and why there are appreciable deviations from this law for a number of nuclei.

First, the presence of the law itself and the deviations from it indicate the predominance of neutron synthesis for all these nuclei, including chlorine isotopes. The deviation of K^{39} and Ga^{71} nuclei may be due to the fact that these nuclei have a magic number of neutrons (20 and 40, respectively), and are therefore more resistant to neutron burnup than K^{41} and Ga^{69} nuclei (in this respect, it is more surprising that chlorine nuclei are governed by this law).

The deviation from the law in the case of rubidium isotopes is most naturally explained by decay of the Rb^{87} nucleus, and the age of rubidium then calculated from this deviation. But in the given case we can only speak of the order of the value, because the half-life of Rb^{87} is too great and, therefore, its deviation from the curve too small to obtain the accepted accuracy by this method. Furthermore, two more opposing factors could affect the abundance of this nucleus: the magic character must have led to an increase in its abundance, and the presence of the Sr^{87} stable nucleus, "screening" Rb^{87} on the higher Z-value side, to a decrease in its abundance. As is seen by way of example of Sb^{123} and Re^{187} nuclei, the presence of a stable nucleus on the high Z side is a virtually negligible factor here, but it cannot be left out of consideration in the case of Rb^{87}. These considerations are wholly applicable to the Re^{187} nucleus, for which, moreover, we do not have reliable direct measurements of the half-life at present. If the latter is more than 10^{11} years, the position of the rhenium isotopes on the curves is understandable.

Assuming that the deviation of Rb^{87} from the curve (~25%) is due entirely to its decay, the age of rubidium (at $T_{Rb} = 4 \cdot 10^{10}$ years), is

$$t_{Rb} \simeq 1.7 \cdot 10^{10} \text{ years.}$$

The considerable deviation in the case of the In^{113} nucleus is due to the fact that it is "screened" by the stable Cd^{113} nucleus on the side of the neutron-excess isobars.

The large number of cases of a decrease in the abundance of isotopes which are "screened" on the side of the neutron-excess isobars leads one to think that it is for this reason that the Br^{79} and Ag^{107} do not comply with this general law. Both these nuclei are "screened" by long-life nuclei: the first by the Se^{79} nucleus with a half-life of $7 \cdot 10^4$ years, and the second by the Pd^{107} nucleus with a half-life of $7 \cdot 10^6$ years (furthermore, fission fragments may affect the value of the ratio of the silver isotopic abundances).

If this explanation of the bromine deviation is also valid for other isotopes, we have a means of assessing the duration of the slow neutron synthesis of nuclei.

In fact, the presence of a long-life β-precursor may affect the abundance of the final nucleus in two cases only: when rapid synthesis was repeated during the existence of the precursor, or when the duration of slow synthesis was comparable with the lifetime of this nucleus.

The table gives the abundances of synthesized nuclei and their closest (n, γ)-precursors, from the data of various authors.

A comparison of column two, which gives the ratio of the synthesized nuclei abundances, with column five, which contains the ratios of the sums of the initial nuclei abundances, shows a definite correlation. The marked discrepancies of these values in the case of chlorine, potassium, and thallium may be due both to the differences of the neutron cross sections for the synthesized and initial nuclei, and to the fact that the present values of the absolute abundances of sulfur, argon, and lead are far too low.

In the case of slow synthesis, bromine, antimony, and rhenium isotopes could have been formed for the most part only by a (n, γ)-reaction on isotopes of their direct precursors: selenium, tin, and tungsten. Therefore, for these isotopes there is a possibility of solving the problem of the synthesis type experimentally by measuring the corresponding (n, γ)-cross sections.

If it is found that in these three cases the bulk of the nuclei appeared as a result of slow synthesis, the characteristic slow nuclear synthesis time can be determined from known cross sections, the known half-life of Se^{79} and the value of the deviation of Br^{79} from the above law (see figure). For the moment, it may be expected that the figure would be more than 10^3 years and less than, or at most, 10^5 years. This follows from the fact that the presence of a Co^{63} nucleus (with a lifetime of about 180 years) "screening" the Cu^{63} nucleus, could not have affected the abundances of copper isotopes, whereas the presence of the Se^{79} nucleus, with a lifetime of about 10^5 years, "screening" the Br^{79} nucleus, led to a reduction in the abundance of Br^{79} to half the value which might be expected from the curve.

In [7], bromine, rubidium, silver, antimony (Sb^{123}), europium, rhenium, and iridium isotopes were included in contrast to chlorine, potassium, indium, and thallium isotopes, in the class of nuclei formed as a result of fast neutron synthesis in supernova stars. It is possible that the discrepancies in the case of bromine and silver are due to this fact, but it would then be necessary to explain why the other nuclei, formed as a result of fast and slow synthesis, lie so satisfactorily on the straight line.

Another useful consequence of the regularity observed in the figure is revealed in connection with the determination of the interval between the end of nuclear synthesis and the formation of the solid phase, by the Reynolds method [2]. The equation for calculating this period of time from the excess Xe^{129} observed in a meteorite contains the initial ratio I^{129}/I^{127}. Since no case of deviation of open and nonmagic nuclei from this law is known, it may be expected that by the end of nuclear synthesis this ratio was close to unity.

LITERATURE CITED

1. T. Kohman, Ann. N. Y. Acad. Sci., 62, 505 (1956).
2. L. Reynolds, Phys. Rev. Lett., 4, 8, and 351 (1960).
3. W. Fowler and F. Hoyle, Ann. Phys., 10, 280 (1960).
4. P. Kuroda, Geochim. et cosmochim. acta, 24, 40 (1961).
5. E. Anders, Rev. Mod. Phys., 34, 287 (1962).
6. I. P. Selinov, The Periodic System of Isotopes [in Russian] (Izd. AN SSSR, Moscow, 1962).
7. E. Burbidge et al., Rev. Mod. Phys., 29, 547 (1957).
8. H. Suess and H. Urey, Rev. Mod. Phys., 28, 53 (1956).

CAUSALITY IN PRESENT-DAY FIELD THEORY

D. I. Blokhintsev

Translated from Atomnaya Énergiya, Vol. 14, No. 1,
pp. 105-109, January, 1963
Original article submitted August 30, 1962

Causality, as we usually understand it, is only a small part of the universal relation, but (materialistic addition) a part not of the subjective, but of the objectively real relation. V. I. Lenin, Works, Vol. 38, page 150.

Introduction

In spite of the modest estimate that V. I. Lenin made of causality, this principle is nevertheless of fundamental importance in science as being the simplest form of relation between phenomena.

The principle of causality is of especially great importance in physics, and not only in a general philosophical sense; the most important thing is the mathematical form in which causality is expressed.

In present-day physics, the mathematical form of causality is based on two physical ideas: the homogeneous and isotropic space – time idea of Einstein and Minkowskii, and the idea of transmission of interaction by physical fields (electromagnetic field, meson and neutrino fields, etc.).

In addition it is known that applying these principles to especially small distances and small time intervals leads to physically absurd results: the interaction energy of particles at small distances, and the inherent energy of the particles become infinitely large. This unsatisfactory conclusion arises in both quantum and classical physics, and possibly indicates that the difficulties have a common origin in both cases.*

Causality in Classical Physics

In classical physics, the propagation of a weak (linear) signal from the world point $\mathscr{P}_1(x_1t_1)$ to the world point $\mathscr{P}_2(x_2t_2)$ is determined by the Green's function $\mathfrak{G}$, which is a function of the difference between the coordinates of the points $\mathscr{P}_1$ and $\mathscr{P}_2$: $x = x_1 - x_2$ and $t = t_1 - t_2$.

This expresses the homogeneity of space – time. The requirement of isotropic space – time leads to the condition that the Green's function does not depend simply on the differences $\underline{x}$ and $\underline{t}$, but also on the four-dimensional intervals $s^2 = x^2 - t^2$. Finally, it is possible to introduce a direction of time ε and a direction along the space ray η: $\varepsilon = \frac{t}{|t|} = \pm 1$, and $\eta = 0$ for $s^2 < 0$, and $\eta = \frac{x}{|x|} = \pm 1$ and $\varepsilon = 0$ for $s^2 > 0$. Thus, the Green's function may be written in the form

$$\mathfrak{G} = \mathfrak{G}(s^2, \varepsilon, \eta). \tag{1}$$

This function is invariant under the Lorentz transformation. Now, in addition, the causality requirements are imposed: 1) the signal cannot be propagated at a velocity greater than the velocity of light $\underline{c}$, and, 2) the signal is only propagated from past to future. These requirements lead to further specialization of the function $\mathfrak{G}$:

$$\left.\begin{aligned} &\mathfrak{G} = \mathfrak{G}(s^2, +1, 0) \text{ for } \varepsilon = +1, \eta = 0; \\ &\mathfrak{G} = 0 \qquad\qquad \text{otherwise.} \end{aligned}\right\} \tag{2}$$

The figure shows a region of space – time where the function $\mathfrak{G}$ is different from zero. Note that the Fourier components of $\mathfrak{G}(s^2, +1, 0)$, which we denote as $\mathfrak{G}(\omega, k)$, depends only on the invariant $m^2 = \omega^2 - k^2$ [$\mathfrak{G}(\omega, k) = F(\omega^2 - k^2)$], and is only different from zero when $m^2 > 0$. For $m^2 < 0$ we would obtain the function $\mathfrak{G}(s^2, 0, \pm 1)$, which is different from zero in the space – like region and, accordingly leads to signals propagated at a velocity greater than the velocity of light.

It is shown by experiment that for large $\underline{x}$ and $\underline{t}$ (asymptotically), the wave field always admits of a corpuscular

*Some philosophical problems of causality and field theory are discussed in [1].

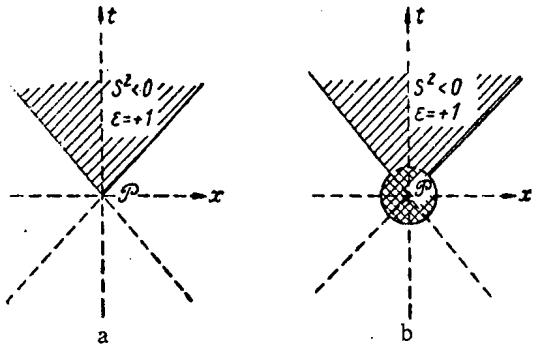

The space–time region where the Green's function is different from zero. In the left-hand figure (a), the cross-hatched area shows the space–time region admissible on the usual theory for the propagation of signals coming from the point $\mathcal{P}$. In the right-hand figure (b) the doubly cross-hatched area shows the possible anomalous causality region (for example, an elliptical type of field equation).

interpretation, and this means that at infinity we have a set of waves with discrete values of the quantity $m^2 = m_1^2, m_2^2, \ldots, m_s^2, \ldots, \geq 0$.*

The Fourier component $F(\omega^2 - k^2)$ has poles at $\omega^2 = k^2 + m_s^2$, and the function $\mathfrak{G}(s^2, +1, 0)$ has a singularity of the form $\delta(s^2)$. In view of the properties of the interval s^2, the singularity is also carried over into the region of small x, t (as long as $s^2 = 0$), and there produces undesirable infinities.

Thus, the physically justified assumptions of isotropic space and time for large x and t are automatically carried over to the range of infinitely small x and t.

Causality in Quantum Physics

However strange it may seem, quantum theory retains the classical conception of causality in all its essential features. In particular, in quantum theory, the propagation of a signal (or an interaction) is also determined by the Green's function $D_C(s^2)$ which is also called the causal function. This function relates the quantum transition in the vicinity of the point $\mathcal{P}_1$ with the quantum transition in the vicinity of the point $\mathcal{P}_2$.**

In contrast with the classical Green's function, this function is not equal to zero even for $s^2 > 0$, but only to the scale $\sim h/mc$ (Compton wavelength of the particle). The "vicinities" must be fairly large in order to be able to detect the fact of the emission of a signal (quantum) with positive energy from the vicinity of the point $\mathcal{P}_1$, and the fact of its being absorbed in the vicinity of the point $\mathcal{P}_2$. Just as in the case of the uncertainty relation for a quantum signal with energy E and momentum p, the dimensions of the vicinities of the points $\mathcal{P}_1$ and $\mathcal{P}_2$ must be, in time, $T \gg h/E$, and in space, $L \gg h/p$.

Further, the vicinities cannot overlap (distance between them $|x| \gg L$, and time interval $|t| \gg T$). As was shown by Firts [3] for point particles, under these conditions the properties of the function $D_C(s^2)$ give a purely classical causal relation between the vicinities of the points $\mathcal{P}_1$ and $\mathcal{P}_2$, i.e., a relation equivalent to the one given by the Green's function $\mathfrak{G}(s^2, +1, 0)$. Under conditions where the above inequalities are not satisfied, the uncertainty relations do not in general permit us to find the nature of the causal relation (what happened later and what earlier). If the causal function $D_C(x)$ is different from zero in the space region, this leads to the existence of space-form factors for the elementary particles F(q), where q is the momentum given to a particle.

In accordance with a form-factor of this sort, the particle must be given a rigid space distribution of charges and currents of the type $\varrho(x) = \int F(q) e^{iqx}\, d^3q$. This rigid distribution allows a signal to propagate from the periphery of the particle to its center at an infinitely large velocity.

However, it was shown in [4] that even in this case the uncertainty relation makes it impossible to "catch" the particle when the signal is being propagated at a velocity greater than the velocity of light. In spite of the difference noted between the causal Green's function $D_C(s^2)$ and the classical Green's function $\mathfrak{G}(s^2, +1, 0)$, the situation with the singularities remains in essence the same in the quantum theory as in the classical theory; the singularities of the propagation functions, which are natural for large x and t, are inexorably carried over into the range of small space and time scales.

Some Possible Generalizations of the Causal Relation

The nature of the singularities in the propagation functions indicate that it is necessary to give up carrying the macroscopic laws of signal (interaction) propagation over into the range of very small space–time scales, and that it

*In quantum field theory, the value of m determines the mass of the particle associated with the field in question.

**The causality principle in its usual form was used by N. N. Bogolyubov for a new representation of present-day field theory [2].

is necessary to try to modify them. What has been said above on the importance of the uncertainty relation enables us to count on the possibility of reconciling the ordinary form of macrocausality with the other forms of microcausality in small space–time regions. Let us now consider some of the possible generalizations of the theory.

Nonlinear Theory. The Green's functions having the singularities described above are associated with the propagation of weak fields obeying linear equations.

As was first pointed out by Born [5], strong fields are able to obey other, nonlinear equations. In this case, the velocity of propagation V of the signal depends on the strength and form of the signal [6-8].

Actually, the characteristics of a nonlinear equation are, generally speaking, different from the straight lines $dx/dt = \pm c$, characteristic of linear theory. Accordingly, the velocity V of a nonlinear signal is a function of the field intensity φ and its derivatives $\partial\varphi/\partial x$, and $\partial\varphi/\partial t$; thus:

$$\frac{dx}{dt} = \pm V\left(\varphi, \frac{\partial\varphi}{\partial x}, \frac{\partial\varphi}{\partial t}\right). \tag{3}$$

It was shown in [5] that in some versions of the nonlinear theory the value of V may be made imaginary, and the hyperbolic equation for the field reduces to an equation of elliptic type. Far from the source and receiver of the signal (far from the particles), the field will, as before, obey a linear equation, and the Green's function will have the usual singularities of the type $\delta(s^2)$. However, in the vicinity of the particles, where the fields are large, the character of the singularities will change. For example, if the equation becomes elliptic, the singularity in the Green's function as $x \to 0$ and $t \to 0$ will have the form $1/R^2$, where $R^2 = x^2 + t^2$.

This possibility of a change in type of field equation near the particles suggests the situation on the wing of an airplane flying at a velocity close to the velocity of sound. There, as we know, when the local stream velocity around the wing exceeds the velocity of sound, the elliptic type of equation changes to one of hyperbolic type.

The figure shows the region in which causality may become anomalous (b). The disturbance of relativistic invariance near $x = 0$ and $t = 0$ is only apparent, and is due to the space–time point (where the field source is located), which is distinguished by the fact that precisely in the vicinity of the point the nonlinear field itself forms the medium for its own propagation.

The possibility of a change in the type of field propagation equation in the vicinity of the particles, and together with it the possibility of changing the form of the causal relation, is very attractive. However, nobody has yet been able to find a quantum analog of this field theory model.

Also, the question is still undiscussed of the changes in definition of the segment of length and time interval which can entail nonlinearity in the propagation of the signal. Einstein's definitions unquestionably assume linearity of the signal.

Change in Causality for Small Space–Time Scales. We have seen that in homogeneous space–time it is impossible to change the causal relation law on a small scale without changing it on a large scale. A possible way of making the change is suggested by the ideas of nonlinearity discussed above. The departure from the usual laws governing signal propagation does not occur everywhere, but only around the sources and receivers of the signal, i.e., near the particles; in other words, where the homogeneity of space is disturbed by the particle located there. This indicates that it is possible for the usual signal propagation laws to be disturbed near the particles [9, 10].

The possibility is realized mathematically by the appearance of new invariants in addition to s^2, ε, and η. Actually, a total energy-momentum vector P(E, **p**) is associated with the particle or system of interacting particles, and this vector commutes with the relative coordinates and with the other internal dynamic variables.* In addition to the invariant $I_1 = s_2$, new invariants appear, such as $I_2 = P^2 = -m^2$ (where m is the rest mass of the whole system), $I_3 = (P, s)$, etc. This makes it possible to form new invariant combinations, for example,

$$R^2 = I_1 + \frac{I_3^2}{I_2}; \tag{4}$$

$$T^2 = \frac{I_3^2}{I_2}, \tag{4'}$$

*This fact has enabled Yu. M. Shirokov to give a correct solution to the problem of the relativistic top [11].

which, in the center-of-mass system, reduce to r^2 and t^2, respectively, and further transform according to (4) and (4') [12].

In view of this, the Green's function associated with the system of particles may be written in the form

$$\mathfrak{G} = \mathfrak{G}(I_1,\ I_2,\ I_3). \tag{5}$$

Having the invariants I_2 and I_3 makes it possible to change the behavior of $\mathfrak{G}$ near r, t = 0.

The figure may be used to illustrate the behavior of the function $\mathfrak{G}$ which, for $R^2 < a^2$, has an elliptic structure, and for $R^2 > a^2$ reduces to the usual Green's function with singularities on the cone $s^2 = 0$.

The causal function $D_C(s^2)$ may be changed in a similar way if it is associated, not with the vacuum, but with the particles located in the vacuum and having the relative coordinate $x = x_1 - x_2$ and the total momentum $p = p_1 + p_2$:

$$D_c = D_c(I_1,\ I_2,\ I_3). \tag{6}$$

A complete scheme of this type has not yet been worked out, and it is still unclear what field theory model it corresponds with. In particular, no investigation has been made to find out whether or not the scattering matrix remains unitary.

Change in the Metrics of the Physical Vacuum. Some other possibilities for changing the form of the causality are related with the idea of changing the geometry of our space–time for small space–time regions.

One of these possibilities consists in fluctuations of the metric tensor $g_{\mu\nu}$ which in principle may be produced by fluctuations of the zero energy of the vacuum. Fluctuations of this type lead to fluctuations in the space–time interval

$$s^2 = \int_{\mathcal{P}_1}^{\mathcal{P}_2} g_{\mu\nu}\, dx_\mu\, dx_\nu. \tag{7}$$

Accordingly, all the functions, such as $\mathfrak{G}(s^2)$ and $D_C(s^2)$ are "blurred" [13, 14]. However, these fluctuations, if we exclude infinities, are real in space–time regions of the order $L_0 = \left(\frac{h\varkappa}{c^3}\right)^{\frac{1}{2}} = 0{,}82 \cdot 10^{-32}$ cm, where $\varkappa$ is the gravitational constant. These scales are too small to play any important role in the world of particles. Introducing another scale for the vacuum fluctuation l_0 would mean introducing a new physical hypothesis, the consequences and the internal consistency of which are still far from being investigated.

Space–Time "Quantization." The old idea of space–time "quantization" [15] has been resurrected several times [16-18]. Current tendencies in the development of this idea rest on the assumption that the metrics of momenta in space is of a non-Euclidian character [19]. In particular, the interval in space of the momenta p_1, p_2, p_3, and p_4 is taken equal to

$$d\sigma^2 = a_{\mu\nu}\, dp_\mu\, dp_\nu. \tag{8}$$

The radius of curvature of this metric space plays the role of a limiting cutoff momentum P_0. The coordinates of ordinary space–time, x_1, x_2, x_3, x_4, canonically conjugated with these momenta, are here the mutually noncommuting operators

$$[x_\mu,\ x_\nu] = ib_{\mu\nu}. \tag{9}$$

The theory is constructed in such a way that it reduces to the ordinary theory for scales $l \gg h/P_0$. It is clear that in this theory the ordinary conception of causality is unsuitable (at least in space–time regions $\sim h/P_0$). Actually, it is impossible to speak of propagation of a signal from the point $\mathcal{P}_1(x_1' x_2' x_3' x_4')$ to the point $\mathcal{P}_2(x_1'' x_2'' x_3'' x_4'')$ if the coordinates of the points are themselves undetermined. In this theory, the process by which a signal is propagated only takes on physical meaning for quite large $|x_\mu|$, where the right-hand side of Eq. (9) may be neglected. For smaller scales, the relation between the phenomena can only be described mathematically by using momentum space. The theory of quantized space–time has not yet received completely consistent development.

Conclusion

The form of causality used in present-day theory follows from basic space–time concepts.

It has been borrowed from macroscopic physics and, in view of the nature of the singularities in the Green's functions, it is carried over automatically to infinitely small scales. This leads to divergencies (infinities) in a number of the more important physical quantities associated with elementary particles.

In this paper we have discussed some of the preliminary theoretical schemes which, while retaining macroscopic causality, produce substantial changes in causality for small space–time scales.

We do not know which of these schemes will bring us closest to the truth – we are still playing blind man's buff with it.

LITERATURE CITED

1. D. I. Blokhintsev, Collection: Philosophical Questions of Modern Physics [in Russian] (Izd. AN SSSR, Moscow, 1952), p. 358.
2. N. N. Bogolyubov and D. V. Shirkov, Introduction to the Theory of Quantum Fields [in Russian] (Gostekhteorizdat, Moscow, 1957), Section 17.
3. M. Firts, Collection: Latest Developments in Quantum Electrodynamics [Russian translation] (IL, Moscow, 1954), p. 238.
4. D. I. Blokhintsev, OIYaI Preprint [in Russian] (Dubna, 1962).
5. M. Born, cited in the book by W. Heitler, Quantum Theory of Radiation [Russian translation] (IL, Moscow,1956).
6. D. I. Blokhintsev, DAN SSSR, 32, 669 (1952).
7. D. I. Blokhintsev, Nuovo Cim., Suppl., No. 4, Ser. 10, 3, 629 (1956).
8. D. I. Blokhintsev and V. Orlov, ZhETF., 25, 513 (1953).
9. D. I. Blokhintsev, Uch. zap. MGU, Ser. Fizika, 3, 77, 201 (1945).
10. D. I. Blokhintsev, ZhÉTF., 16, 480 (1946).
11. Yu. M. Shirokov, ZhÉTF., 22, 539 (1952).
12. D. I. Blokhintsev, V. Barasenkov, and V. Grisin, Nuovo Cim., Ser. 10, 9, 249 (1958).
13. S. Deser, Rev. Mod. Phys., 29, 417 (1957).
14. D. I. Blokhintsev, Nuovo Cim., 18, 193 (1960).
15. Y. Ambarcumyan and D. Ivanenko, Z. Phys., 64, 563 (1930).
16. H. Snyder, Phys. Rev., 71, 38 (1946).
17. Yu. A. Gol'fand, ZhÉTF., 37, 504 (1959); 43, 256 (1962).
18. V. G. Kadyshevskii, ZhÉTF., 41, 1885 (1961). See also OIYaI Preprints P-1017 and P-1018 [in Russian] (Dubna, 1962).
19. M. Born, Proc. Roy. Soc., A165, 291 (1938).

All abbreviations of periodicals in the above bibliography are letter-by-letter transliterations of the abbreviations as given in the original Russian journal. *Some or all of this periodical literature may well be available in English translation.* A complete list of the cover-to-cover English translations appears at the back of this issue.

LOBACHEVSKIAN KINEMATICS AND GEOMETRY

Ya. A. Smorodinskii

Translated from Atomnaya Énergiya, Vol. 14, No. 1,
pp. 110-121, January, 1963
Original article submitted October 1, 1962

Introduction

Although many years have passed since the time when F. Klein discovered, in 1909 [1], that the velocity space of the special theory of relativity is the Lobachevskian space, i.e., the space of constant negative curvature, this geometrical model has been exploited only to an inadequate extent for its potentialities in describing relativistic kinematics.

The correspondence between the law of composition of velocities in relativistic mechanics and the law of composition of vectors in Lobachevsky's geometry, noted by Sommerfeld in his earlier works [2,3], has remained, for all practical purposes, the sole illustration of the geometrical properties of the space of velocities.

The geometry of velocity space underwent a more extended and detailed development in a monograph by Kotel'nikov [4], which is known to a very restricted audience. In recent years, the problem was revived by N. A. Chernikov [5,6], an active proponent of Labachevsky's ideas. In the realm of textbooks and monographs, adequate attention is devoted to Lobachevskian geometry only in the works authored by V. A. Fok [7].

The description of relativistic kinematics based on Lobachevskian geometry demonstrates the straightforward meaning of various formulas which lost their transparency in their usual form. This applies in particular to the kinematics of rotating bodies, and in the case of quantum mechanics to the kinematics of particles possessing spin.

We cite, below, several examples of the application of Lobachevskian geometry to the physics of elementary particles and nuclear reactions. In so doing, we make no demands upon the reader as to a prior acquaintance with this geometry, and we intend to develop all the necessary tools as we proceed in our work.

It is a signal honor for me to dedicate this article to the memory of Igor' Vasil'evich Kurchatov, who harbored a great love for theoretical physics.

1. Vectors in Velocity Space

Let us begin with a slight digression into the realm of ordinary vector algebra. A vector is an assemblage of three quantities which transform in rotations of the system of coordinates such that the coordinates are components of a radius vector $\underline{r}$. Clearly, the problem of how any other quantities involved transform in the process may be solved only on the basis of physical considerations. In Newtonian mechanics, the velocity of a particle is also considered a vector; this is due to the fact that the time interval is a scalar and accordingly the operation of differentiation with respect to time is a scalar operation. This implies that the velocity space $\Omega(v)$ possesses the same geometrical properties as the coordinate space $\Omega(r)$, being a Euclidean space. Moreover, since the mass of a particle is a scalar quantity in Newtonian mechanics, the momentum of a particle transforms in the same manner as the velocity, and the momentum space is consequently likewise a Euclidean space. In Newtonian mechanics, therefore, all three three-dimensional spaces $\Omega(r)$, $\Omega(v)$, and $\Omega(p)$ exhibit the same metric.

The situation is changed in Einsteinian mechanics. In this case, the space of coordinates and the space of momenta possess, as we know, a pseudo-Euclidean metric with the invariants $c^2(\Delta t)^2 - (\Delta l)^2 = (\Delta s)^2$ and $\varepsilon^2 - c^2p^2 = m^2$, and their properties are specified everywhere.

In what follows, we shall be interested in the properties of a third space, the velocity space. The four-dimensional velocity, or the 4-velocity for short, is the derivative of the coordinate of a particle with respect to proper time $\frac{1}{c}\frac{dx_\alpha}{ds}$. This velocity has the components

$$\left.\begin{aligned} u_x &= \frac{\beta_x}{\sqrt{1-\beta^2}}\ ; \\ u_y &= \frac{\beta_y}{\sqrt{1-\beta^2}}\ ; \\ u_z &= \frac{\beta_z}{\sqrt{1-\beta^2}}\ ; \\ u_0 &= \frac{1}{\sqrt{1-\beta^2}}\ , \end{aligned}\right\} \tag{1.1}$$

where β is the ordinary nonrelativistic velocity in units of the velocity of light ($0 < \beta < 1$). The velocity $\underline{u}$, although a 4-vector (it is the momentum-to-mass ratio of the particle), does not entirely correspond to the physical concept of velocity. The term velocity as we generally employ it refers to the quantity β equal to the momentum-to-energy ratio $\beta = p/\varepsilon$ of a particle. This quantity may be also taken as the length of a three-dimensional vector determining the relative velocity of the particle and of the origin of some selected system of coordinates. The geometry of the relative velocities is what constitutes the subject matter of our presentation.

One characteristic feature of the 4-velocity is the fact that its 4-length is equal to unity:

$$u_0^2 - u_x^2 - u_y^2 - u_z^2 = u_0^2 - \mathbf{u}^2 = 1. \tag{1.2}$$

Therefore, the tips of the 4-velocity vector always lie, in pseudo-Euclidean space, on the surface of one of the sheets of a hyperboloid of two sheets (1.2), and to be precise, on that sheet which corresponds to the positive value of the u_0 component. The velocities of all the particles accordingly correspond to points situated on a three-dimensional surface, while their momenta (at different mass values) may fill the entire space. The velocity is, therefore, in essence a three-component quantity represented by a point on the upper sheet of the hyperboloid. The geometry of the velocities may be treated either as a vector geometry in four-dimensional space having a pseudo-Euclidean metric, or as a geometry of points on the surface of the hyperboloid in that space. This is reminiscent of the situation prevailing on the surface of the earth, whose surface properties may be described, of course, as the properties of a surface in three-dimensional space, but which are more convenient described by means of spherical geometry in two dimensions.

In describing velocity space as the surface of a hyperboloid, there is no need to specify the origin of the coordinates, and all the relationships are expressed solely in terms of the relative distances of points on that surface.

If the imaginary coordinate $v_4 = iv_0$ is introduced in place of the real coordinate v_0, then the hyperboloid will become converted to a sphere of imaginary unit radius, and the velocities of the particles will be in correspondence with the points lying on the upper half of this sphere. In this representation, the formulas of spherical trigonometry are useful in computations, with the radius $\underline{a}$ replaced by ia (in what follows, the radius $\underline{a}$, equal to the velocity of light, will be assumed equal to unity).

2. Newtonian Kinematics

We recall briefly, at this point, the principal kinematical relationships in nonrelativistic mechanics. Consider the reaction

$$a + b \rightarrow c + d.$$

The particles $\underline{c}$ and $\underline{d}$ may be either the same particles as the particles $\underline{a}$ and $\underline{b}$ (scattering), or may be different particles (reaction). Once the masses of the particles are known, the velocity of the center of inertia $\underline{u}$ may be found. The velocities of the particles per se will be designated by the same letters a, b, c, and d. The velocities $\underline{c}$ and $\underline{d}$ are governed by the laws of conservation of energy and momentum. The kinematical relationships are usually illustrated by means of circles (cf. [8]). We will find it more convenient to make use of a quadrangle diagram (Fig. 1). In this diagram, the points correspond to the tips of the velocity vectors of particles, being three-dimensional in nonrelativistic mechanics, four-dimensional in relativistic mechanics. The distances separating the points correspond to the relative velocities in nonrelativistic mechanics and to the hyperbolic arc tangents of those velocities in relativistic mechanics. The segment ua is the velocity of the particle $\underline{a}$ relative to the point $\underline{u}$, i.e., the velocity $\underline{a}$ in the center-of-mass system. The segment ab is the velocity $\underline{b}$ in the system in which $\underline{a}$ is at rest, etc.

In considering scattering in any specified frame of reference, we must attribute certain directions to the segments which form the sides and diagonals of the quadrangle. For example, if scattering is considered in the system in which the particle $\underline{a}$ is at rest, then an impinging particle is described by a vector directed from $\underline{a}$ to $\underline{b}$, two

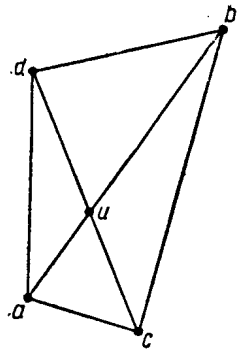

Fig. 1. Quadrangle describing the kinematics of the reaction a + b → c + d.

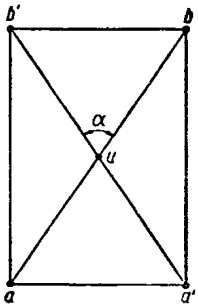

Fig. 2. Elastic collision between identical particles a + b → a' + b'.

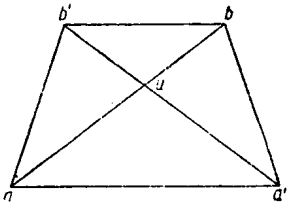

Fig. 3. Elastic collision between different particles.

particles, the reaction products, are described by vectors directed from point a to points c and d, respectively.

Consider two examples:

1. In the case of scattering of two identical particles (Fig. 2), the point u is situated at the same distance from all the vertices and the figure becomes transformed into a rectangle. This means that the angle between velocities a' and b', i.e., between the particles flying apart in this system, where a is at first at rest, is $\pi/2$.

2. If the masses of particles a and b are different, but the scattering is elastic, then the figure will be transformed into a trapezium (Fig. 3), ub = ub', ua = ua'. The velocity of particle b after scattering in the system where a starts off at rest (segment ab') is related to the scattering angle θ (in that system, the angle bab'), by the formula found from the triangle b'ua:

$$\cos\theta = \frac{b_u^2 - a_u^2 - b_a'^2}{2a_u b_a'}.$$

Here, a_u and b_u are the velocities of particles a and b in the u system (independent of scattering angle); b_a' is the velocity of particle b after scattering in the system where a starts off at rest.

Clearly, from these examples, plane trigonometry completely describes the relationships existing between the velocities of the particles in the several systems of coordinates (as well as the relationships between the relative velocities) and the scattering angle. It might be added that if it is required to deal with motion relative to some other system of coordinates, it will not be difficult to derive all the necessary kinematical relationships by drawing in still another point (in the same plane or in the space) and connecting it to the angles of the quadrangle. Note further that at certain specified mass values the quadrangle is determined by two parameters: the length of the diagonal – the relative velocity of the particles, and the angle formed between the diagonals – the scattering angle in the system u.

This described correspondence between kinematics and plane trionometry is a consequence of what we termed the Euclidean character of velocity space.

This description of kinematics turns out to possess a most important property. The accompanying diagrams need not be altered in the conversion to Einsteinian mechanics, the formulas of plane trigonometry need only be replaced by the formulas of hyperbolic geometry (or spherical geometry with imaginary radii).*

3. Lobachevskian Geometry in Velocity Space

Lobachevsky's geometry differs from conventional Euclidean geometry in the suppression of Euclid's axiom on parallel lines. This refers in the first instance to the fact that the sum of the angles of a triangle are no longer equal to π, but are in fact consistently less than π. At the same time, equal angles may exist only in equal triangles: this geometry does not admit of similar triangles.

The simplest and most vivid representation of Lobachevskian geometry is the upper sheet of a hyperboloid in four-dimensional space with a pseudo-Euclidean metric, or the surface of a sphere of radius i.**

In order to establish the correspondence between Lobachevskian geometry and the three-dimensional velocity space, it will be necessary to determine the relationship linking the distances on the surface of the hyperboloid and

*If calculations are performed in momentum space instead of velocity space, then the more involved geometrical relationships associated with the properties of ellipses will arise in relativistic kinematics (cf. [8]).

**Lobachevskian geometry frequently is described in the language of projective geometry, by projecting the points

the relative velocities. Remember that a point on the surface of the hyperboloid describes a four-dimensional velocity; clearly, however, the interval spanning the two points (determined as $ds^2 = du_0^2 - du^2$) has nothing in common with relative velocity. If we define the distances on the surface of the hyperboloid as length of the segment of a geodesic hyperbola joining these points, then this quantity may be expressed in terms of the relative velocity. For this purpose, let us consider two 4-velocity vectors u_1 and u_2, and form their four-dimensional scalar product:

$$u_1 u_2 = u_{10} u_{20} - \mathbf{u}_1 \mathbf{u}_2. \qquad (3.1)$$

Since this product is invariant, it is most simply calculated in the system where one of the particles is at rest, i.e., the system in which one of the velocities, say u_1, possesses only the one component $u_{10} = 1$. In that system, $u_{20} = (1-\beta^2)^{-\frac{1}{2}}$ where β is the relative velocity. Therefore,

$$u_1 u_2 = \frac{1}{\sqrt{1-\beta^2}}. \qquad (3.2)$$

The 4-lengths u_1 and u_2 being equal to unity, the scalar product of two unit vectors in a space with a Euclidean metric would be equal to the cosine of the angle between them. In a space with a pseudo-Euclidean metric, it is natural to make this product equal to the hyperbolic cosine:

$$u_1 u_2 = \operatorname{ch}(u_1 u_2) = \frac{1}{\sqrt{1-\beta^2}} \equiv \gamma_{12}. \qquad (3.3)$$

Designating γ_{12} as the Lorentz factor, we note that it is defined as the relative velocity of the first and second particles. From this definition we see that

$$\operatorname{sh}(u_1 u_2) = \frac{\beta}{\sqrt{1-\beta^2}}; \qquad (3.4)$$

$$\operatorname{th}(u_1 u_2) = \beta. \qquad (3.5)$$

The arguments of the hyperbolic functions are constituted by the hyperbolic angle determined most straightforwardly from the scalar product (3.3). The definition of the arc, coinciding with the symbol for the scalar product, could hardly result in any misunderstanding.*

Equations (3.3) and (3.4) establish the relationship linking the distances between points u_1 and u_2 on the surface of the hyperboloid (or imaginary sphere) with scalar relative velocity. After this, we may draw in the points of the hyperboloid on the plane, but the formulas of hyperbolic geometry are employed in the calculations. In this geometry, the sum of the angles of the triangle are less than π, while the difference between π and the sum of the angles of the triangle is equal to the area of the triangle:

$$S = \pi - A - B - C. \qquad (3.6)$$

One of the consequences of Eq. (3.6) is the fact that similarity of triangles is unknown in hyperbolic geometry. Triangles having equal angles are simply equal to each other. The physical explanation follows immediately from the limiting character of the velocity of light. In Newtonian kinematics, the relationships between the velocities undergo no change when all the velocities vary by the same number of times. In Einsteinian kinematics this is not valid any longer, since the ratio of the velocities of the particle to the velocity of light will vary. This example affords an excellent illustration of the connection between the finiteness of the velocity of light and the non-Euclidean geometry of velocity space.

To achieve still greater clarity, we may draw a triangle having concave sides, preserving the angles between them (Fig. 4); the lengths of the sides will be distorted, of course, in the process.

There are several standard formulas for solving triangles in hyperbolic geometry [9].

---

of a sphere or hyperboloid onto the plane tangent to those figures. This projection varies the angles, but transforms a curvilinear triangle into a straight-line triangle. There are alternative descriptions of the geometry. Details (not required in this treatment) may be found in any text on non-Euclidean geometry.

* If the mass of one of the particles is m, then, in the system in which the other particle is at rest, the energy of the particle will be $m \cosh(u_1 u_2)$, and the momentum will be $p = m \sinh(u_1 u_2)$.

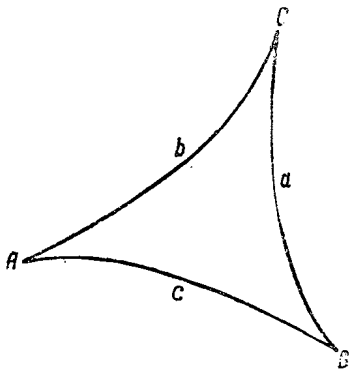

Fig. 4. Schematic diagram of a hyperbolic triangle. Sum of angles not equal to π.

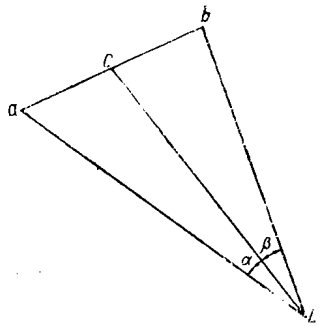

Fig. 5. Decay of particle c → a + b.

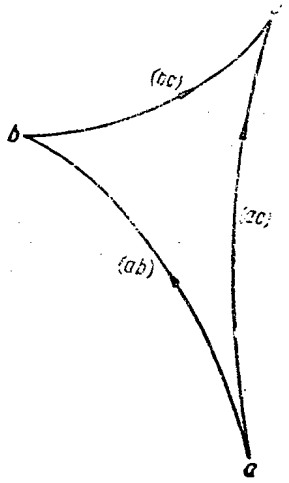

Fig. 6. Composition of velocities in hyperbolic geometry: ab + bc = ac.

The cosine formula is

$$\mathrm{ch}\, a = \mathrm{ch}\, b\, \mathrm{ch}\, c - 2\,\mathrm{sh}\, b\, \mathrm{shc} \cos A. \tag{3.7}$$

As the curvature tends to zero (i.e., as the lengths of the sides tend to zero, since we let the radius of curvature be zero), Eq. (3.7) becomes the cosine theorem for plane trigonometry.

A second cosine formula is

$$\cos A = -\cos B \cos C + \cos B \cos C \,\mathrm{ch}\, a \tag{3.8}$$

and this becomes an identity at A + B + C = π.

The sine formula is

$$\frac{\mathrm{sh}\, a}{\sin A} = \frac{\mathrm{sh}\, b}{\sin B} = \frac{\mathrm{sh}\, c}{\sin C}. \tag{3.9}$$

To this, we may add still another formula for the area of the triangle:

$$\cos \frac{S}{2} = \frac{1 + \mathrm{ch}\, a + \mathrm{ch}\, b + \mathrm{ch}\, c}{4\,\mathrm{ch}^2 \frac{a}{2}\,\mathrm{ch}^2 \frac{b}{2}\,\mathrm{ch}^2 \frac{c}{2}}. \tag{3.10}$$

Now if we employ these formulas and avoid resorting to the corollaries of the theorem on parallel lines (equality of angles lying opposite, theorems based on the area of the triangle, etc.), we may readily derive the kinematic relationships from the drawings relevant to plane geometry.

As an example, consider the collision of identical particles. Let us return to Fig. 2. The distance separating points a and b corresponds to the relative velocities of particles a and b:

$$\left.\begin{aligned} \mathrm{ch}\,(ab) &= \gamma_{ab}; \\ \mathrm{th}\,(ab) &= \beta_{ab}. \end{aligned}\right\} \tag{3.11}$$

The velocity of the center-of-mass system is determined, as before, by the point u, dividing the segment ab in half; this velocity is

$$\beta_{au} = \mathrm{th} \frac{ab}{2} = \sqrt{\frac{\mathrm{ch}\,(ab) - 1}{\mathrm{ch}\,(ab) + 1}}. \tag{3.12}$$

If the coordinates of all the vertices (i.e., the velocities and the angle of scattering in the center-of-mass system) are given, then the post-scattering velocities of the particles, e.g., in the a system, will be determined from the cosine formula:

$$\gamma_{ab'} = \mathrm{ch}^2 (au) + \mathrm{sh}^2 (au) \cos \alpha; \tag{3.13}$$

$$\gamma_{aa'} = \mathrm{ch}^2 (au) - \mathrm{sh}^2 (au) \cos \alpha. \tag{3.14}$$

The angle between the scattered particles (angle a'ab') in the a system is expressed in terms of the hyperbolic defect:

$$\angle (a'ab') = \frac{\pi}{2} - \frac{\delta}{2}, \tag{3.15}$$

where δ is the hyperbolic defect, and the area of the triangle a'ab' (in c^2 units) is defined as in formula (3.10) from the known lengths of the triangle sides. All the kinematical relations are thus defined if the coordinates of the vertices and the intersects of the diagonals of the rectangle are specified (the diagonals of the quadrangle in the general case). Once the lengths of all the sides and the areas of the triangles have been determined, we have obtained the complete solution of the problem. Note that all the relations so derived depend solely on the velocities of the particles, and not on their masses.

If information is required on the kinematical relations in some other coordinate system, then we need only plot

the point describing this system on the velocity plane, and joint this point to the vertices of the basic quadrangle. After that, the problem yields to solution by the same method.

This situation in fact arises when we are describing the decay of a single particle into two particles. In that case, one of the diagonals of the quadrangle degenerates to a point; the decay process is illustrated in Fig. 5, where L is the velocity of the observer's system; c is the velocity of the particle undergoing disintegration; a and b are the velocities of the reaction products (and c is simultaneously the velocity of the center-of-mass system of the decay products). The velocity a in the L system is related to the angle of emission α in that system by the cosine formula:

$$\cos\alpha = \frac{-\operatorname{ch}(ac) + \operatorname{ch}(La)\operatorname{ch}(Lc)}{\operatorname{sh}(La)\operatorname{sh}(Lc)}. \tag{3.16}$$

Moreover, we may express these quantities in terms of the energy and momenta of the particles (as is usually done, in fact), but it will not be quite so evident, in that case, that the relationship depends solely on the velocities and not on the particle masses. Note here that the minimum and maximum velocities are determined if we rotate ab about the point c, such that the point lies on the line Lc.

Of course, the examples selected above are deceptively simple and could be studied with ease by the conventional algebraic method, but nevertheless there is compelling evidence that the geometric approach is much more straightforward.

4. Composition of Velocities

As mentioned in the earlier discussion, the term velocity is applied in the present context to two different quantities: the velocity vector and the relative velocity – the distance between two points in hyperbolic geometry. 4-Velocities add by the ordinary rules of a linear vector space, while the addition of relative velocities obeys a completely different set of rules.*

First of all, we must note that the direction of the velocity is not subject to determination in hyperbolic geometry; since the geodesic is a curve, its direction varies. In particular, then the direction of the velocity of particle b in the a system does not coincide (rather, is not strictly opposed) to the direction of the velocity of particle a in the b system (although the magnitudes of the velocities are equal).

The angle between directions ab and –ba is nothing else than the angle of rotation of an infinitely small vector in a parallel translation along the curve ab. Clearly, it is determined solely by the length of ab. Below, it will be shown that this angle α is found from the formula

$$\sin\alpha = \operatorname{th} x. \tag{4.1}$$

*The relative velocity enters into the determination of the invariant reaction cross section. If the densities of the colliding particles are ρ_1 and ρ_2, then the number of events typical of the reaction, in a volume dN and during an interval dt, is determined generally by the formula

$$\frac{dN}{dt\,dV} = \varrho_1\varrho_2\sigma V. \tag{X}$$

Here, $V^2 = (\boldsymbol{\beta}_2 - \boldsymbol{\beta}_1)^2 - (\boldsymbol{\beta}_1 \times \boldsymbol{\beta}_2)^2$, where $\boldsymbol{\beta}_1$ and $\boldsymbol{\beta}_2$ are the velocity vectors of the particles. The formula may be recast in the form

$$\frac{dN}{dt\,dV} = (j_1^2 j_2^2)^{1/2}\operatorname{sh}\alpha\sigma. \tag{XX}$$

Here, $j_{1,2}^2 = \rho_{1,2}^2 - \mathbf{j}_{1,2}^2$ are the 4-lengths of the current vectors; α is the "angle" between them. Letting ρ_{01} and ρ_{02} denote the densities (number of particles per unit volume) in the intrinsic systems of coordinates, then (XX) may be written as

$$\frac{dN}{dt\,dV} = \varrho_{01}\varrho_{02}\sigma\operatorname{sh}\alpha. \tag{XXX}$$

Accordingly, the relative velocity in the nonrelativistic formula transforms, in the relativistic formula, into sinh α (cf. [10]).

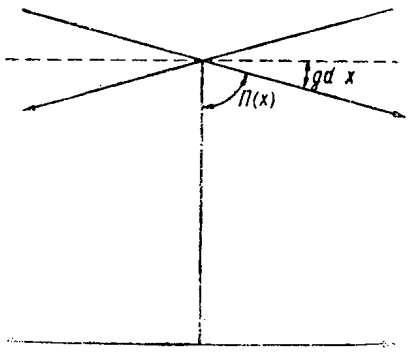

Fig. 7. Parallel lines, left and right, on the Lobachevskian plane. Π(x) is the Lobachevsky angle of parallelism; gd x + Π(x) = π/2.

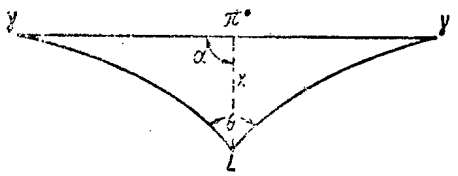

Fig. 8. Decay $\pi^0 \to 2\gamma$.

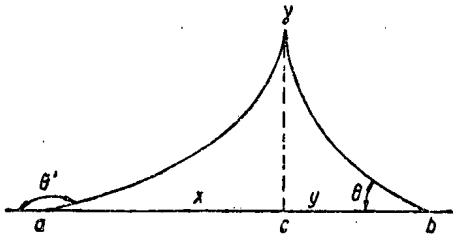

Fig. 9. Aberration. The observer a sees the photon at an angle θ'; the observer b sees it at an angle θ.

The formulas used to solve hyperbolic triangles make it possible to also solve the laws of vector addition. Turn to Fig. 6. The physical significance of this diagram is the following: the b system moves relative to the a system at a velocity determined by the length of the segment ab, i.e., at the velocity tanh(ab). In the b system, the particle c moves at the velocity tanh(bc). Then tanh(ac) is the velocity of particle c relative to system a. The value of ac is found from the cosine formula:

$$\operatorname{ch}(ac) = \operatorname{ch}(ab)\operatorname{ch}(bc) - \operatorname{sh}(ab)\operatorname{sh}(bc)\cos b, \tag{4.2}$$

where b is the angle at that vertex. The angle a is found from the sine theorem:

$$\sin a = \operatorname{sh}(bc)\frac{\sin b}{\operatorname{sh}(ac)}. \tag{4.3}$$

These are the formulas obeying the law of composition of velocities in Einsteinian kinematics.

5. Parallel Lines. Particles of Zero Mass

Now consider a massless particle, e.g., photons and neutrinos. Their velocity, equal to unity, is depicted by a point situated at an infinite distance. The geodesics joining this infinitely removed point to two other points are by definition parallel (as lines intersecting at infinity). The angle between two such geodesics (at an infinitely removed vertex) is again, by definition, zero. In Lobachevskian geometry, this kinematical diagram corresponds to an assertion that a straight line parallel to the given one can be drawn through each point. There exist two such straight lines: one intersects the original straight line on the right (at infinity); the other intersects it on the left (Fig. 7). The angle formed by the parallel straight line with the perpendicular is called the Lobachevsky angle of parallelism, and is designated as Π(x), where x is the distance to the original straight line. At x = 0, clearly, Π(x) = π/2. As the distances x increase, Π(x) tends to zero. The angle of parallelism is related to the distance x by the formula

$$\operatorname{th} x = \cos \Pi(x). \tag{5.1}$$

Instead of the angle of parallelism, we may consider its complement relative to π/2. This quantity is known as the hyperbolic amplitude, or gudermanian:

$$gd\, x = \frac{\pi}{2} - \Pi(x). \tag{5.2}$$

Then formula (5.2) is restated as

$$\operatorname{th} x = \sin(gd\, x). \tag{5.3}$$

Angle α in Eq. (4.1) is precisely gd x. These formulas may be given a kinematical interpretation. The parallel straight lines intersecting at an infinitely remote point correspond to the velocities of the photon (or of the neutrino) relative to two other coordinate systems of any kind. If, for example, a π^0-meson decays into two quanta (Fig. 8), then the kinematical diagram will have two angles equal to zero. Angle θ of the divergence of two such quanta is the angle at the vertex of the hyperbolic triangle, and the two other angles are zero angles. The magnitude of the triangle may be expressed in tanh x, in the velocity of the π^0-meson and angle of flight α in the π^0 system relative to the observer's velocity L. It is readily seen that the angle θ is of minimal size when the angle of flight α is π/2. In that case, θ is clearly the doubled angle of parallelism (tanh x = β):

$$\theta_{\min} = 2\Pi(x) = 2 \arccos \beta, \tag{5.4}$$

where β is the velocity of the pion.

As a first example, consider relativistic aberration: the transformation of the angle between a photon (or neutrino) and the relative velocity of two systems ba (Fig. 9).

The angle of emission of the photon in the system a relative to the velocity ba is designated as θ'. The same angle in the system b is designated as θ. The broken line denotes the perpendicular dropped to ab.

The "straight lines" $a\gamma$, $b\gamma$, and $c\gamma$ are parallel. Consequently,

$$\left.\begin{aligned} -\cos\theta' &= \operatorname{th} x; \\ \cos\theta &= \operatorname{th} y. \end{aligned}\right\} \tag{5.5}$$

By constructing $\tanh(x + y)$, which is equal to β (the velocity a in the system b), we obtain

$$\frac{\cos\theta - \cos\theta'}{1 - \cos\theta\cos\theta'} = \beta. \tag{5.6}$$

Solving Eq. (5.6) for one of the cosines, we derive the ordinary formulas. If the angle θ' is equal to $\pi/2$, the triangle will become a right triangle (one angle θ, the other $\pi/2$). In this triangle, the angle θ will be equal to $\arccos\beta$ (from the properties of the parallel lines). A photon which is flying at an angle $\pi/2$ in system a arrives in system b at an angle almost coincident with the direction of motion (at $\beta \simeq 1$). Consequently, the observer "sees" a luminous object from system a rotated through the angle $\pi/2$. This beautiful phenomenon of rotation of a rapidly moving object was detected by Terrell [11].

It is interesting to note that there exists a triangle in hyperbolic geometry which has all three angles equal to zero and in which, as a consequence, the sides are pairwise parallel. The area of such a triangle is $\pi/2$, since it is equal to the difference between $\pi/2$ and the sum of the angles of the triangle. This kinematical triangle is encountered in the treatment of the decay of a particle into three photons, and corresponding to this event we have three infinitely removed points.

6. Top and Thomas Precession

Now consider the kinematics of a rotating particle. In this case, the advantage conferred by hyperbolic geometry will become even more tangible.

In nonrelativistic mechanics, rotation is described by the three-dimensional angular velocity vector. The transition to Einsteinian mechanics requires a certain caution. We may assume the angular velocity to be a part of an antisymmetric tensor of second rank, as in the case of the magnetic field. Then, in the relativistic case, we have to introduce still another three-dimensional vector similar to the electric field. This approach leads to the combining of angular velocity and velocity of center of mass in a single tensor similar to the tensor uniting the electric and magnetic dipole moments. The physical significance of this combination consists in the fact that an orbital velocity is added to the angular velocity. The tensor so constructed is simply related to the total angular momentum of the particle (the sum of the orbital and spin angular momenta). It is possible, however, to avoid complicating the picture by dragging the orbital motion into the discussion. Consider a top rotating in a uniformly moving system of coordinates. Each point on its surface moves relative to the observer, at rest in the laboratory system of coordinates, along a curve consisting of the sum of the rotational and translational motions. The Lorentz transformation from the top system to the laboratory system relates the pure rotation to the motion on the open curve. When we speak of rotation, we intuitively distinguish translational motion and rotation per se. It is not difficult to give a rigorous kinematic sense to an operation of this kind. For this purpose, we define the angular velocity 4-vector such that, in the intrinsic system of coordinates, it will have only the three spatial components coinciding with the components of the nonrelativistic angular velocity. The covariant expression of this property will be the orthogonality of the angular velocity 4-vector, the linear velocity of the particle

$$\omega u = 0. \tag{6.1}$$

Equation (6.1) serves to define the 4-vector in any other coordinate system. Viz., the angular 4-velocity of a particle moving at a velocity $u = (\gamma, \mathbf{u})$, where $\gamma = (1 - \beta^2)^{-\frac{1}{2}}$, is defined by formulas

$$\left.\begin{aligned} \boldsymbol{\omega}' &= \frac{(\boldsymbol{\omega}\mathbf{u})\,\mathbf{u}}{1+\gamma} + \boldsymbol{\omega}; \\ \omega_0' &= (\boldsymbol{\omega}\boldsymbol{\beta}). \end{aligned}\right\} \tag{6.2}$$

In hyperbolic geometry, formulas (6.2) demonstrate that the angular velocity vector lies in a three-dimensional

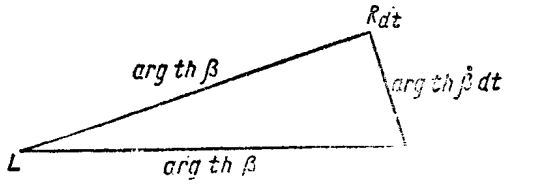

Fig. 10. Thomas precession. Rotation of the axis of the top is equal to the triangle area, in the first approximation, the triangle being formed by velocities of the top at two instants t and t + dt.

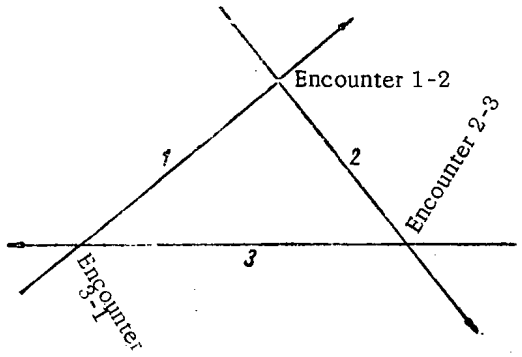

Fig. 11. Diagram of synchronization of coordinate systems and clocks involving three observers.

space orthogonal to the particle's velocity vector, i.e., the angular velocity vector always remains a three-dimensional vector. Consider the components of this vector from the viewpoint of different observers. In order to successfully compare the components, the observers must somehow agree on a method for comparing the systems of coordinates per se. If the observer's system is L, and the system of the particle is R, then the description of the angular velocity in terms of Eqs. (6.2) is its description in system L. We may use a different approach, constructing another system of coordinates, this time corresponding to the R system, within the L system. Then the observer in R will be able to communicate, to the observer in L, the three components of the velocity vector which could be used to construct the vector in the L system. Here we run up against the way in which the problem of comparing vectors situated at different points of space is non-Euclidean geometry is handled. In order to be able to make such a comparison, we must bring the vectors to be compared to a common point. We are then confronted with the problem of how to define such an operation in an invariant manner. To begin with, both observers may define one of the axes in the direction of their relative velocity (whereupon one of the observers will assume the velocity to be positive, the other observer will assume it to be negative).

In order to define the second axis, we must draw the normal to the plane. We choose still another auxiliary system with the velocity this time not parallel to the relative velocity of the L and R systems. We designate this system as U. Then, with the aid of an antisymmetric tensor of rank four, we construct the 4-vector N:

$$N_\alpha = \varepsilon_{\alpha\beta\gamma\delta} L^\beta R^\gamma U^\delta. \tag{6.3}$$

It is readily seen that, in each of the three systems L, R, and U, this vector will be reduced to a conventional three-dimensional vector product. Actually, in these systems one of the indices will be zero, while the other two will range through exclusively spatial values.

Accordingly, two spatial axes each are constructed in the R and L systems. The third axis in each system is constructed as a perpendicular to the other two. The geometrically described construction corresponds to the parallel translation of the vector along the geodesic joining points R and L.* It is clear here that, since the observers are present in different systems, this "synchronization"** of the coordinate systems cannot result in any contradiction whatever. We will encounter a new phenomenon when we execute a parallel translation along a closed circuit. As is generally known from geometry, in a parallel translation along a closed circuit the vector does not return to the initial position, but rather rotates through an angle equal to the area swept out by the circuit. Rotation proceeds in the direction opposite to the motion along the circuit (i.e., the vector fails to regain its initial position). In the case of a triangle, the area is equal to the hyperbolic defect.

The simplest example of this type is what we know as Thomas precession. Consider a top flying at a velocity $\boldsymbol{\beta}$. Let it acquire an acceleration $\dot{\boldsymbol{\beta}}$, and its velocity will become $\boldsymbol{\beta} + \dot{\boldsymbol{\beta}}dt$ in a time dt*** (Fig. 10). In order to ascertain

*We stated that the direction of the relative velocity of R from the viewpoint of L is not completely opposed to the direction of the velocity of L from the viewpoint of R. This "rotation," associated with a pseudo-Euclidean metric, is responsible for reducing the 4-vector to a three-dimen three-component counterpart. The magnitude of this rotation is gd(LR) = (π/2) − Π(LR).

**We use the term "synchronization" by analogy with the operation of synchronizing clocks − an analogy fraught with profound significance, as we shall see later on.

***The triangle drawn here is an isosceles triangle, since $\dot{\boldsymbol{\beta}}dt$ is infinitesimally small.

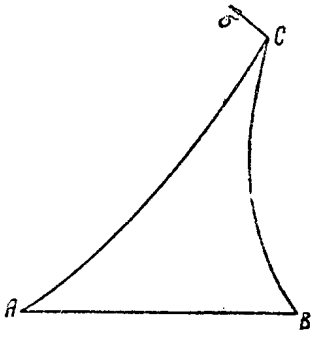

Fig. 12. Direction of spin from the viewpoint of two observers A and B. Angles formed by the spin σ with the relative velocities AC and BC differ from each other by the angle C. This constitutes the rotation of the spin in the conversion from one coordinate system to the other. When C = 0 (case of photon or neutrino), no rotation takes place.

how the direction of the angular velocity varies, we must compare the angular velocity vector converted from the initial system of the top R to the system of the observer L, with the angular velocity vector in the top system R_{dt} likewise converted into the L system.

The difference of interest here is none other than the rotation of the vector in the parallel translation along the perimeter of the triangle equal to the area of the triangle. To compute this perimeter, we find it convenient to ignore Eq. (3.10) and instead use its equivalent

$$\sin S = \frac{1+\operatorname{ch} a+\operatorname{ch} b+\operatorname{ch} c}{8\operatorname{ch}^2\frac{a}{2}\operatorname{ch}^2\frac{b}{2}\operatorname{ch}^2\frac{c}{2}}\,|\varepsilon u_A u_B u_C|. \tag{6.4}$$

In this formula, the last term is the length of the normal to the plane of the triangle with vertices u_A, u_B, and u_C. In the system where, e.g., $\underline{a}$ is at rest, this multiplicative factor is simply equal to the length of the vector product of the spatial parts of 4-velocities $\underline{b}$ and $\underline{c}$. Put $\tanh a = \tanh b = \beta$. Now note that the magnitude of $\dot{\beta}\,dt$ is infinitesimally small and that $\cosh a = \cosh b \equiv \gamma$, $4\cosh^2(a/2) = 1+\gamma$, and put

$$S = \frac{\gamma}{1+\gamma}\,|\beta\times\dot{\beta}|\,dt. \tag{6.5}$$

Consequently, the top processes, in response to an acceleration $\dot{\beta}$, at an angular velocity

$$\Omega = -\frac{\gamma}{1+\gamma}\,|\beta\times\dot{\beta}|. \tag{6.6}$$

In a lower order of magnitude with respect to velocity, the precessional velocity will be

$$\Omega \simeq -\frac{1}{2}\,|\beta\times\dot{\beta}|, \tag{6.7}$$

i.e., equal to the area of the triangle computed from the formula used in Euclidean geometry. This effect is known as Thomas precession, and its derivation is usually quite cumbersome (cf. [12]).

With respect to Thomas precession, we might dwell in somewhat greater detail on the problem of synchronizing the coordinate systems. Suppose that there exist three systems of observers moving uniformly, such that system 1 at first goes through an encounter with system 2, then system 2 later encounters system 3, and finally, system 3 completes the circuit by an encounter with system 1. System 1 must possess dimensions large enough to facilitate the last encounter (clearly, the encounter will take place in some other part of system 1). If, during the first encounter, observers 1 and 2 synchronize their coordinate systems, then, following that, during the encounter with observer 3, observer 2 transmits to observer 3 the direction so obtained, we should find that as the information returns to system 1 at the time of the second encounter participated in by observers 3 and 1, the system will be rotated through the Thomas angle of precession Ω. Consequently, no unique three-dimensional coordinate systems can be selected in moving systems. This effect is similar to the familiar clock paradox illustrated in Fig. 11. If the observers transmit information on the time at the encounters, then the clocks will be running slow at the return to system 1. The amount of time by which they run slow will, of course, be equal to the perimeter of the triangle (in conventional space), and the extent to which the coordinate systems will be lagging behind will be equal to the area of the triangle (in velocity space).*

*The clock paradox is usually considered in discussions involving only two observers. In this case, we have to introduce nonuniform motion on the part of one of these observers (rotation to the backward path). This difficulty is obviated in the three-system case, but we have to speak in terms of the synchronization of clocks relative to the first system, since encounters 1-2 and 3-1 occur at different points in the first system. Moreover, the synchronization of the clocks relative to a coordinate system executing uniform motion presents no difficulty. Both effects: the clocks running slow and the rotation of the coordinate axes, of course also depend on the curvature of the space.

7. Spin

Everything said about the top also refers to the kinematics of spin.* In particular, the law of spin transformation is in agreement with Eq. (1.2), since the transformation is a kinematical operation dependent solely on velocity. This is, however, valid only for free particles. If the particle is in an external field, then the situation changes. The particle present in an external field has no specific momentum and velocity and, therefore, no system of rest can be introduced for it. Consequently, it is not possible to make a straightforward determination of the spin. As a result, admixtures of states with a lower spin assignment appear for a particle in a field, which must be coped with by the introduction of various additional conditions. Only for particles of half-integral spin (and, of course, spinless particles) and for a photon does spin remain a well-defined concept, because of gauge invariance. We shall therefore limit our remarks to free particles.

If spin is drawn as a vector in its own system, then it is clear from Fig. 12 that, from the point of view of two observers A and B, the angle formed by the spin and the velocity differs by the angle at the vertex C, the intrinsic system of the particle. If the particle has mass, then the angle at C is zero. Clearly then, a longitudinally polarized zero-mass particle remains longitudinally polarized in any coordinate system, i.e., the concepts of a longitudinally polarized neutrino and circularly polarized photon are relativistically invariant concepts.

If a particle possessing spin is scattered, which is the analog of acceleration of the particle in the classical problem, then, in addition to the changes in spin direction Φ in nonrelativistic scattering, the spin also undergoes a Thomas rotation Ω, calculated from the area of the triangle with vertices corresponding to the laboratory system and to the rest systems of the particle before and after scattering.** The total rotation ψ of the spin is therefore [16]

$$\psi = \Phi - |\Omega|.$$

The precession of the spin plays an important role in scattering. Rotation of spin in scattering, e.g., of an electron in a Coulomb field, signifies spin-orbit coupling in classical mechanics. The Thomas rotation consequently serves as the reason for the spin-orbital splitting in the hydrogen atom and polarization of the electron in scattering on nuclei – phenomena which are incomprehensible from the classical standpoint, since Coulomb interaction is not explicitly dependent on spin.

Parallel translation of the spin makes possible a clear illustration of the addition of spins in systems of particles. Since a parallel translation makes it possible to bring all the spins to a single point (one coordinate system) and the angles between the translated spins are calculated in a straightforward manner from the formulas of hyperbolic geometry, the problem reduces to the addition of spins in a single coordinate system, i.e., to an ordinary nonrelativistic problem.

Summary

Our purpose in this article has been to direct attention to the almost too obvious fact that a knowledge of the geometry of velocity space is a prerequisite to working effectively with vectors in velocity space. Just as one may proceed in ordinary geometry by the exclusive use of analytical formulas, without ever resorting to the diagrammatical methods of trigonometry, one may also get along in Einsteinian kinematics without the use of drawings and trigonometrical formulas. However, this approach, which was in its time the ideal pursued in Lagrangian mechanics,*** could hardly be the ideal variant in our times. The apparatus of theoretical physics has now becomes so complex that any pictorial representations (and rigorous ones all the more so), are destined to play an increasingly more prominent role in science.

In conclusion, I should like to express my acknowledgements to N. A. Chernikov for his valuable and kind discussions of the problems touched upon in this article.

*Reference is also valid to the other multipole moments of nuclei, which we shall not discuss here (cf. [13]). The relationship between spin and Lobachevskian geometry was taken up earlier by the author [14].

**This effect has been described by Stapp [15].

***Lagrange wrote, in the preface to his Mecanique Analytique, that his "methods...require neither constructions, nor geometrical or mechanical reasoning, resting exclusively on algebraic operation subject to a correct and unified development" [17].

LITERATURE CITED

1. F. Klein, Symposium: New Ideas in Mathematics [in Russian] (St. Petersburg, 1909), No. 5, p. 144.
2. A. Sommerfeld, Phys. Zeit., 10, 286 (1909).
3. A. Sommerfeld, Electrodynamics [Russian translation] (IL, Moscow, 1958), p. 322.
4. N. P. Kotel'nikov, Symposium in Memory of Lobachevsky [in Russian] (Publ. of State Univ., Kazan', 1928).
5. N. A. Chernikov, Nauchn. doklady vyssh. shkoly, 2, 158 (1958).
6. N. A. Chernikov, OIYaI Preprint No. 723 [in Russian] (Dubna, 1961).
7. V. A. Fok, Theory of Space, Time, and Gravitation (2nd Edition) [in Russian] (Phys. Math. Press, Moscow-Leningrad, 1961).
8. L. Landau and E. Lifshits, Field Theory (4th Edition) [in Russian] (Phys. Math. Press, Moscow-Leningrad,1962).
9. A. R. Yampol'skii, Hyperbolic Functions [in Russian] (Phys. Math. Press, Moscow, 1960).
10. N. A. Chernikov, DAN SSSR, 114, 530 (1957).
11. J. Terrell, Phys. Rev., 116, 1041 (1959).
12. C. Moller, Theory of Relativity (Oxford, 1952), p. 53.
13. V. L. Lyuboshits and Ya. A. Smorodinskii, ZhETF., 42, 846 (1962).
14. Ya. A. Smorodinskii, ZhETF., 43, 6, 2217 (1962).
15. H. Stapp, Phys. Rev., 103, 425 (1957).
16. G. Wick, Ann. Phys., 18, 65 (1962).
17. J. Lagrange, Analytical Mechanics (2nd Edition) [Russian translation](State Technical and Theoretical Literature Press, 1950), Vol. 1, p. 3.

All abbreviations of periodicals in the above bibliography are letter-by-letter transliterations of the abbreviations as given in the original Russian journal. *Some or all of this periodical literature may well be available in English translation.* A complete list of the cover-to-cover English translations appears at the back of this issue.

ELECTROKINETIC EFFECTS IN LIQUID MERCURY

A. R. Regel' and S. I. Patyanin

Translated from Atomnaya Énergiya, Vol. 14, No. 1,
pp. 122-127, January, 1963
Original article submitted August 15, 1962

Introduction

Recently, much attention has been paid to the electrical properties of samples of small cross section, principally films. In [1-7] it was shown that when the transverse dimensions of the sample are comparable with the free path length of the current carriers, anomalous values of the conductivity, Hall effect, etc., are observed.

According to the Thomson–Fuchs hypothesis, this is due to the fact that only the ε proportion of the carriers is reflected elastically from the inner surface of the sample, the other, $(1-\varepsilon)$, part of the carriers undergoes inelastic (diffuse) scattering at the boundary. As a result, in a thin boundary layer (thickness $\sim 3\lambda$), the free path length and the concentration of the current carriers will be less than within the sample as a whole.

In [8] it was shown that in liquid conductors with a small cross section (capillaries with liquid metal), electrokinetic effects will be observed at $(1-\varepsilon) \neq 0$. For example, if a current is passed through the capillary, an electroosmotic pressure

$$p_E = 0{,}8\,(1-\varepsilon)\,enV\left(\frac{\lambda}{r_w}\right)^2 \qquad (1)$$

is created. On the other hand, if liquid metal flows through the capillary at a pressure p, a difference in potentials V is set up at the ends of the capillary (transfer potential):

$$V_w = -0{,}1\,(1-\varepsilon)\,\frac{en\lambda^2}{\sigma\eta}\,p, \qquad (2)$$

where e is the electron charge; n and λ are the concentration and free path length of the current carriers, respectively; σ is the conductivity of the liquid metal; r_w is the radius of the working capillary.

The value and direction of the electrokinetic effects are independent of the type of conductivity of the metal.

This paper gives the results of investigations into the electrokinetic effects in mercury at room temperature, and the procedure employed for this work.

Experimental Procedure

The investigation was carried out by two methods: measurement of the electrokinetic mobility α of the mercury level in a type A apparatus (Fig. 1), and measurement of the difference in levels in a type B apparatus while passing a current through the working capillary.

For mercury, Klemm [9] found an electrokinetic mobility $\alpha = (v/E) = 2.5 \cdot 10^{-3}$ cm/V · sec in a diaphragm in the form of a 1.5-mm diameter capillary, filled with ~0.1-mm diameter glass pellets (v is the rate of displacement of mercury under the effect of a potential E).

It should be noted that in this case the values of the electrokinetic effects cannot be calculated exactly, because of the indeterminancy of the geometric form of the conductor cross section. Therefore, we conducted the experiments in cylindrical capillaris [$r_w = (5\text{-}20) \cdot 10^{-3}$ cm], so as to check the correctness of the theory effects, given as an approximation of the theory of free electrons in [8].

Determination of the Value $(1-\varepsilon)$ from the Mobility of the Level. Mercury (twice distilled) was poured from flask 1 in position II into capillary 10 (see Fig. 1), evacuated to $\sim 10^{-3}$ mm Hg, and dried at 150-200°C, in such a way that the level of the mercury was located approximately in the middle of horizontal areas a and b of the measuring capillaries. The position of the levels was recorded by counting microscopes, graduated in $(1.35\text{-}2) \cdot 10^{-4}$ cm/div.

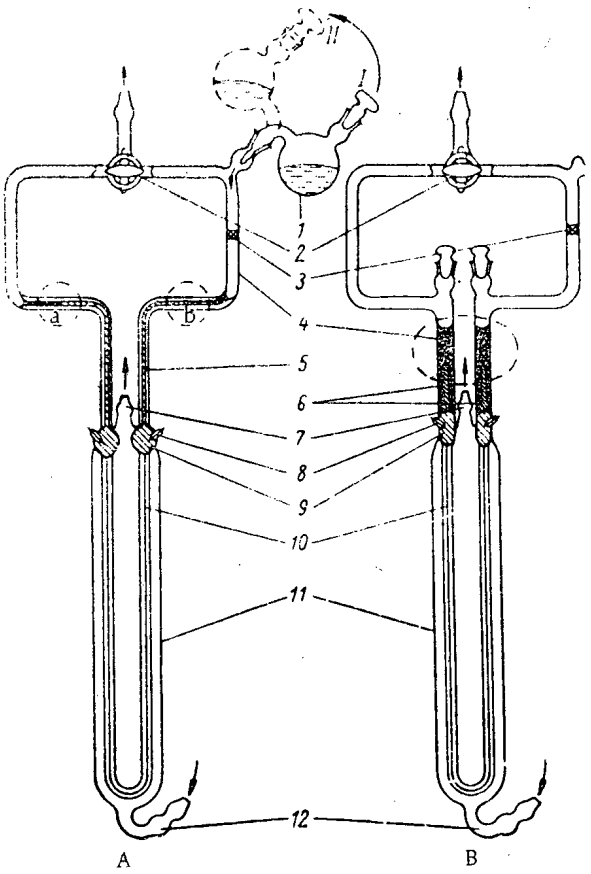

Fig. 1. Diagram of the apparatuses. A) Apparatus for measuring electrokinetic mobility. B) Apparatus for measuring the difference in levels. 1) Flask with liquid metal; 2) vacuum cocks; 3) glass filters; 4) measuring tubes with liquid wetting the surface of the glass and mercury; 5) measuring capillary; 6) floats; 7) and 12) outlet and inlet pipes for the thermostatic-control liquid; 8) current conducting electrodes; 9) electrode-vicinity mercury; 10) working capillary; 11) air jacket.

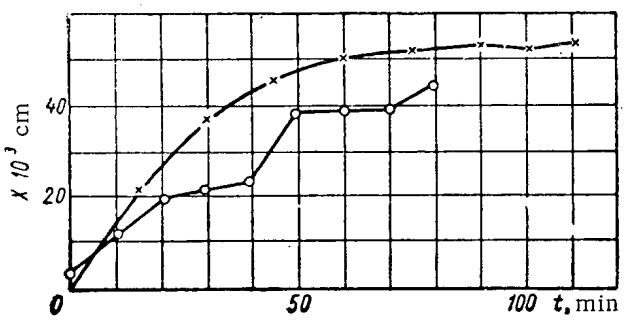

Fig. 2. Velocities of displacement of the levels.

Since apparatus A was very sensitive to temperature changes (displacement of the levels by about 400 div/deg), it was necessary to employ very accurate thermostatic control. The apparatus was therefore located in a Dewar flask and was entirely heat-insulated, except for small sectors in the area of levels a and b. Furthermore, to reduce the Peltier effect we used platinum electrodes (this effect is small at a mercury – platinum contact), located within a considerable volume of mercury, which assisted intense heat dispersion; the temperature of the electrodes was measured by iron-constantan thermocouples to an accuracy of up to $\sim 2 \cdot 10^{-3}$ °C.

The velocity of displacement of the levels at a predetermined V was measured (Fig. 2) after temperature equilibrium of the apparatus had been attained (points X: at 90 min, the current was switched on, at 100 min the direction of the current was changed; length of capillary L = 12 cm; $r_w = 5 \cdot 10^{-3}$ cm; V = 0.18V), or after the change in velocities of the levels in the linear area of thermal expansion with a change in the current direction at 10-20 min intervals (points O: L = 16 cm; $r_w = 88 \cdot 10^{-3}$ cm; V = 0.36V). The velocity of displacement of the levels was about 10^{-5} to 10^{-6} cm/sec. The lesser slope of the broken part of the curve corresponds to a positive potential at the electrode near this level. The curves were obtained in different apparatuses.

The mobility of the level was determined from the equation

$$\alpha_0 = \frac{v_0}{E}\left(\frac{r_m}{r_w}\right)^2 = \frac{L_w}{V}\left(\frac{r_m}{r_w}\right)^2 v_0, \qquad (3)$$

where v_0 is the observed rate of movement; r_m is the radius of the measuring capillary; L_w is the length of the working capillary.

Allowance for friction during movement of mercury in the measuring capillary gives the relation

$$v_0 = \frac{Q}{S_m} = \frac{\pi r_w^4}{8\eta L S_m}\left(p_E - \frac{F}{S_m}\right), \qquad (4)$$

where η is the viscosity of mercury; Q is the volume of mercury; S is the cross section of the capillary; F is the friction force in the measuring capillary, equal to

$$F = 2\pi\eta L_m v_0.$$

Hence, the observed mobility of the level

$$\alpha_0 = \alpha - \frac{1}{4}\frac{L_m}{L_w}\left(\frac{r_w}{r_m}\right)^2 \frac{L_w}{V} v_0. \qquad (5)$$

Taking Eq. (3) into account, we obtain

$$\alpha = \alpha_0\left[1 + \frac{1}{4}\frac{L_m}{L_w}\left(\frac{r_w}{r_m}\right)^4\right]. \qquad (6)$$

The relationships

$$L_0 \simeq L_w; \quad \frac{r_w}{r_m} \simeq 10^{-1},$$

were generally obtained in apparatus A, i.e., the second term within the brackets in Eq. (6) was of the order 10^{-4}, and the correction introduced by this was considerably less than the measurement error.

Therefore, it was assumed that

$$\alpha = \alpha_0. \tag{7}$$

Measurement of the Difference in Levels of the Mercury. Determination of $(1-\varepsilon)$ by the difference in levels of the mercury was carried out in a type-B apparatus (see Fig. 1), which differed from apparatus A only with respect to the upper measuring part. The area above the levels was filled with a solution of mercury in nitric acid or silicone oil, in which glass floats, in contact with the mercury level, were located. The whole system was located in a Dewar flask up to the heads of the floats and a change in room temperature did not affect the position of the levels and, therefore, the floats. Observations were carried out on the position of the heads of the floats.

The sensitivity of the system to temperature variations was reduced considerably as a result of the large cross section of the measuring areas and the possibility of improved thermostatic control; it was about 3-15 div/deg or 10^{-3} to 10^{-2} cm/deg. Movement of the level (rise or fall) as a result of the effect of electroosmotic pressure was very slow because of the low value of the latter, and the volume of mercury necessary to flow over before equilibrium was established ($p_E = h_0 d$), was relatively large; therefore, the flow-over time t_f was considerable (d is the sp. gravity of mercury; h_0 is the initial difference in levels of the mercury).

To reduce the time of a measurement, we employed the following calculation method. If the level in an "elbow" was displaced by a value X in a time $t \ll t_f$, it could be assumed that "flow-over" took place under the effect of an average pressure $p_{av} = (p_E + p_X)/2$. But $p_X = p_E - 2Xd$ and $p_{av} = p_E - Xd$. Hence, the average rate of "flow-over" is

$$v_{av} = v_0 \left(\frac{r_m}{r_w}\right)^2 = \frac{X}{t}\left(\frac{r_m}{r_w}\right)^2 = \frac{r_w^2}{8\eta L_w}(p_E - Xd). \tag{8}$$

Friction within the measuring tube may be neglected because

$$\left(\frac{r_m}{r_w}\right)^2 \simeq 10^2.$$

Expressing the radius of the capillary by its length, conductivity, and the resistance of the mercury in the capillary, we obtain

$$(1-\varepsilon) = \frac{\eta L_w c X}{0{,}1 e n \lambda^2 V t} + \frac{d\rho L_w X}{0{,}8\pi e n \lambda^2 V R}, \tag{9}$$

where ρ is the specific resistance of mercury; R is the resistance of the capillary.

Experimental Results

Determination of the Temperature of the Boundary Layer. The temperature of the mercury in the working capillary was determined as the sum of the temperature T_T of the thermostatic-control liquid flowing around the capillary and the temperature fall ΔT_J at the walls of the working capillary as a result of liberation of Lenz – Joule heat in the working capillary:

$$T = T_T + \Delta T_J.$$

We will assume that the temperature of the contacting surfaces of mercury and the walls of the capillary are both equal to the temperature T of the mercury in the boundary layer (it is this boundary layer temperature which is of interest to us), and that the temperature of the outer surface of the capillary is equal to the temperature T_T of the thermostatic-control liquid.

The heat flow q through a layer of thickness dr in the wall of the capillary will be

$$q = -\Lambda 2\pi r L_w \frac{dT}{dr} = \frac{V}{R} . \tag{10}$$

Hence,

$$\Delta T_J = \frac{V^2 \ln\left(\frac{r_0}{r_w}\right)}{2\pi\Lambda L_w R} .$$

For the temperature of the boundary layer of mercury we obtain

$$T = T_T + \frac{V^2 \ln\left(\frac{r_0}{r_w}\right)}{2\pi\Lambda L_w R} , \tag{11}$$

where r_0 and r_w are the outer and inner radii of the working capillary; Λ is the thermal conductivity of the glass.

Under our experimental conditions the temperature fall at the walls of the capillary was $4 \cdot 10^{-3}$ to 15°C, and in cases where $\Delta T < 3$°C we did not take it into account.

Choice of the Values of n and λ. For calculating the value of $(1 - \varepsilon)$ in Eq. (9), the viscosity of mercury was taken from [10], and the concentration of the carriers was calculated from the Hall constant $R_H = -74.6 \cdot 10^{-5}$ (in emu units) [11]. The value obtained, $n = 8.4 \cdot 10^{22}$ cm^{-3}, agrees very closely with the value of n_α calculated on the assumption that there are two conductivity electrons per atom of mercury.

The value of the mean free path length λ of the conductivity electrons is obtained from the relation

$$\varrho\lambda = 3{,}6 \cdot 10^{-11} \ \Omega \cdot \text{cm}^2, \tag{12}$$

derived by experiment for solid mercury [3, 6] at low temperatures. We employed this relation on the assumption that the specific role of "short-range order" is retained in liquid mercury, and that relation (12) remains effective for the latter. Hence,

$$\lambda = 3{,}7 \cdot 10^{-7} \text{ cm}.$$

Displacements of the Levels of ΔN_1 and ΔN_2. These displacements are resulting displacements, first – by the effect of the current $\Delta N_{E_{1,2}}$ and, second, as a result of the change in temperature of mercury in the apparatus, $\Delta N_{T_{1,2}}$:

$$\Delta N_{1,2} = \pm \Delta N_{E_{1,2}} \pm \Delta N_{T_{1,2}}. \tag{13}$$

Displacements ΔN_{E_1} and ΔN_{E_2} have different signs in the left-hand and right-hand elbows of the apparatus, whereas the $\Delta N_{T_{1,2}}$ signs are the same (the right-hand and left-hand sections of the apparatus are under the same temperature conditions). Therefore, by taking the difference in displacement of the levels in a time t, and taking the sign into account, we eliminated to some extent the effect of temperature on the value X:

$$X = \frac{(\pm \Delta N_{E_1} + \Delta N_{T_2}) - (\pm \Delta N_{E_2} \pm \Delta N_{T_2})}{2} = \pm \frac{\Delta N_{E_1} + \Delta N_{E_2}}{2} . \tag{14}$$

Since the displacement of one of the levels in the U-shaped capillary takes place under the effect of a small electroosmotic force $F_E = p_E S_w$, the force of viscous friction $F_{fr} = 2\pi\eta L_w \dot{X}$ $\left(\dot{X} = \frac{dx}{dt}\right)$, and the force occurring as a result of the difference in levels 2X, equal to $F_\alpha = 2dXS_w$, the equation of movement of the level will have the form

$$\ddot{X} + 2\beta\dot{X} + \omega^2 X = A, \tag{15}$$

where $\beta = \frac{\eta}{\delta r_w^2}$; $\omega^2 = \frac{2g}{L_w}$; $A = \frac{h_0 g}{L_w}$ (δ is the density; $h_0 = 2h$ is the difference in the levels at $p_E = h_0 d$; g is the gravity acceleration).

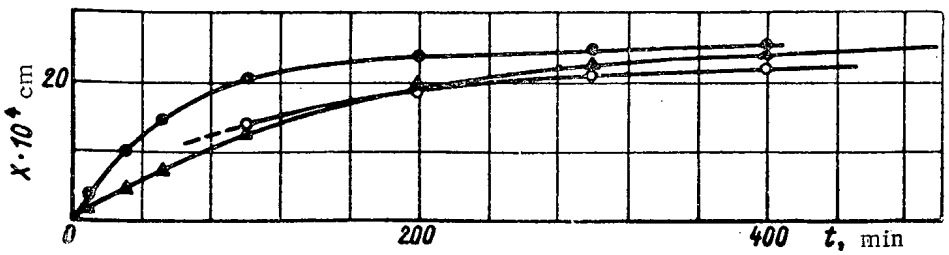

Fig. 3. Displacement of the level in relation to time (apparatus B).

The solution of Eq. (15) gives aperiodic variations of the level

$$X = h\left\{1 - \frac{\alpha_2}{\alpha_2 - \alpha_1} \exp\left[\alpha_1 \left(\frac{r_m}{r_w}\right)^2 t\right]\right\}, \tag{16}$$

where $\alpha_{1,2} = -\beta \pm \sqrt{\beta^2 - \omega^2}$ are the roots of the characteristic equation corresponding to differential equation (15).

The electrokinetic mobility α was measured in apparatuses with capillaries of radius $r_w = (5\text{-}15) \cdot 10^{-3}$ cm at current densities 10^2 to 10^3 A/cm^2. The mean of measurements at T = 20-30°C is

$$\alpha = (2{,}5 \pm 1{,}2) \cdot 10^{-3} \text{ cm}^2/\text{V} \cdot \text{sec},$$

which agrees with Klemm's results [9], obtained in experiments with a diaphragm of glass pellets. It follows theoretically [8] (and taking into account Poiseuille's formula for a viscous liquid) that the electrokinetic mobility

$$\alpha = \frac{v}{E} = \frac{Q}{SE} = \frac{0{,}1\,(1-\varepsilon)\,en\lambda^2}{\eta} \tag{17}$$

is independent of the dimensions and geometric form of the cross section of the sample and is a property of the substance, depending on the values n, λ, η, and $(1 - \varepsilon)$.

By measuring the value $(1 - \varepsilon)$ from the difference in levels, we obtained for mercury

$$(1 - \varepsilon) = (2{,}4 \pm 1{,}4) \cdot 10^{-2}.$$

However, employing the electrokinetic mobility at $n = 8.4 \cdot 10^{22}$ cm^{-3}, $\lambda = 3.7 \cdot 10^{-7}$ cm, and $\eta = 1.54 \cdot 10^{-2}$ poise, we obtain

$$(1 - \varepsilon) = \frac{\alpha\eta}{0{,}1en\lambda^2} \simeq 2{,}1 \cdot 10^{-2}.$$

As may be seen, both methods of measurement give the same results.

Reverse Electrokinetic Effect. An attempt was made to measure the transfer potential. The experiments showed that an electrokinetic effect exists, its value being $V_w/p \simeq 10^{-9}$ V/mm Hg. We detected heating of the mercury flowing through the capillary, causing the appearance of a thermal electric potential at the mercury – platinum contacts, of the same order as V_w. It may be expected that by increasing the sensitivity of the apparatus and increasing the volumes of metal at the electrodes, or by locating the latter further from the ends of the capillary, it will be possible to eliminate the thermal emf effect and measure the transfer potential.

Discussion of the Results

The results of our experiments showed that electrokinetic effects in mercury may be measured readily not only in diaphragms of increased sensitivity [9], but also in capillaries alone.

These results show that at room temperatures the system behaves as if virtually specular reflection from the boundaries of the electrons and holes occurred.

However, it may be assumed that all the electrons (the current carriers, in general) have diffusion scattering at the interface ($\varepsilon = 0$), but in the layer at the wall, of thickness $\sim 3\lambda$, the viscosity of the liquid is increased substantially, which leads to a reduction in the electrokinetic effect. This assumption is very probable if the experimental data and theories in [3-7, 12-15] are taken into account.

Since the electrokinetic effects are determined by processes in the boundary layer only, it may be approximately

assumed that the viscosity η, included in the equation of electrokinetic mobility (17), is the mean value for a boundary layer of thickness $\sim 3\lambda$.

The assumption that the viscosity at the wall is different to that within the liquid as a whole may be considered as a consequence of the theory of liquid viscosity [12]. As was shown by theoretical calculation in [14], the mobility of mercury particles in a monomolecular layer at the wall of a glass capillary is 10^4-fold less than the mobility within the liquid as a whole, and is expressed by the relation

$$\frac{u_b}{u} \simeq \exp \frac{W - W_b}{kT},$$

where W is the surface energy of a microcavity within the liquid, appearing as a result of transfer of a particle from a given equilibrium position to another one; W_b is the same, but in a monomolecular layer at the wall. Determination of the mean mercury viscosity at $\varepsilon = 0$ (at the accepted values of $\underline{n}$ and λ), gives

$$\eta_{av} = \frac{0{,}1en\lambda^2}{\alpha} = 0{,}7 \text{ poise}.$$

Therefore, the mean viscosity of mercury in the immediate vicinity of the mercury – glass boundary in a layer of thickness $\sim 3\lambda$ is nearly twice as high as within the mercury as a whole.

Figure 3 gives a comparison of the curves plotted from Eq. (16) for the viscosity of mercury at 20°C within the mercury as a whole $\eta_1 = 1.5 \cdot 10^{-2}$ poise (●) and $\eta_{av} = 0.7$ poise (▲), with the experimental curves (○). As may be seen from this figure, the points of the experimental curve ($r_w^2 = 4.7 \cdot 10^{-5}$ cm, $L_w = 42$ cm, $h_0 = 48 \cdot 10^{-4}$ cm, V = 8.4V) lie near the curve with mean viscosity.

The temperature and the admixtures must have a marked effect on the properties of the boundary layer (wetting, contact potential, viscosity, etc.). A marked relation may be expected between the electrokinetic effects and the temperature and admixtures.

There is a definite possibility of investigating viscosity anomalies near solid body – liquid boundaries by examinations of the electrokinetic effects.

LITERATURE CITED

1. J. Thomson, Proc. Camb. Phil. Soc., 11, 120 (1901).
2. K. Fuchs, Proc. Camb. Phil. Soc., 34, 100 (1938).
3. R. Dingle, Proc. Roy. Soc., A201, 545 (1950).
4. R. Chambers, Proc. Roy. Soc., A202, 378 (1950).
5. R. Chambers, Nature, 165, 239 (1950).
6. E. Andrew, Proc. Phys. Soc., A62, 77 (1949).
7. A. R. Regel' and V. I. Kaidalov, ZhTF., 28, 407 (1958).
8. G. E. Pikus and V. B. Fiks, FTT., 1, 1062 (1959); V. B. Fiks and G. E. Pikus, FTT, 1, 1147 (1959).
9. A. Klemm, Z. Naturforsch., 13A, 1039 (1958).
10. Liquid Metals Handbook (AEC, Washington, 1950).
11. P. Kendal and N. Cusack, Phil. Mag., 6, 419 (1961).
12. Ya. I. Frenkel', Kinetic Theory of Liquids [in Russian] (Izd. AN SSSR, Moscow-Leningrad, 1955).
13. O. A. Gerashchenko and M. M. Nazarchuk, ZhTF., 27, 12 (1957).
14. D. M. Tolstoi, DAN SSSR, 85, 5, 1089 (1952).
15. B. V. Deryagin, V. V. Karasev, and Z. M. Zorin, The Structure and Physical Properties of a Substance in the Liquid State [in Russian] (Izd. Kievskogo univ. im. T. G. Shevchenko, 1954), p. 114.

BIBLIOGRAPHY OF THE PUBLISHED WORKS OF ACADEMICIAN I. V. KURCHATOV*

Translated from Atomnaya Énergiya, Vol. 14, No. 1,
pp. 128-131, January, 1963

"Experience gained in the use of harmonic analysis for the investigation of the tides of the Black Sea," Dekad. byull. pogody, izd. Gimetsentrom Chernogo i Azovskogo morei, No. 28 (1924).

"The radioactivity of snow," Zh. geofiz. i met., No. 1-2, 17-32 (1925).

"Seishes in the Black Sea and Sea of Azov," Izv. Ts. Gidromet. byuro Tsumora, No. 4, 149-158 (1925).

"The electrolysis of a solid body. Remarks on Rubandt and Schmidt's report," Nauchn. izv. Azerbaidzh. Politekhn. in-ta, No. 2, 39-42 (1926).

"Electrolysis in the presence of an aluminum anode," Izv. Azerbaidzh. Gos. un-ta, otd. est.-med., 4, 121-133 (1926) (with Z. Lobanova).

"The passage of slow electrons through thin metal foil," Tr. Leningr. fiz.-tekh. lab. Symp. of Applied Physics Reports, No. 3, 67-71 (1926) (with K. D. Sinel'nikov). The same article appeared in Phys. Rev., 28, 2, 367-371 (1926).

"The mobility of ions in crystals of common salt," Zh. Russk. fiz.-khim. o-va. ch. fiz., 59, No. 3-4, 421-422 (1927) (with A. K. Val'ter, P. P. Kobeko, and K. D. Sinel'nikov).

"High-voltage polarization in solid dielectrics," Zh. Russk. fiz.-khim. o-va, ch. fiz., 59, 3-4, 327-329 (1927).

"On electrical strength of dielectrics," DAN SSSR, A, 4, 65-68 (1927) (with A. F. Ioffe and K. D. Sinel'nikov).

"Evolution of oxygen at the anode during electrolysis of glass," DAN SSSR, A, 11, 187-192 (1928) (with P. P. Kobeko).

"Ionic and mixed conductivity of solid bodies," Usp. fiz. nauk, 8, 3, 361-393 (1928) (with P. P. Kobeko).

"An investigation of the breakdown mechanism of certain resins," Zh. Russk. fiz.-khim. o-va. ch. fiz., 60, 3, 211-217 (with P. P. Kobeko and K. D. Sinel'nikov).

"Faraday's law in collision ionization," Zh. Russk. fiz.-khim. o-va, ch. fiz. m, 60, 6, 509-518 (1928) (with P. P. Kobeko).

"Breakdown of solid dielectrics," Tr. Leningr. fiz.-tekh. lab., No. 5, 5-19 (1928) (with P. P. Kobeko and K. D. Sinel'nikov).

"Unipolar conductivity of certain salts," Zh. Russk. fiz.-khim. o-va, ch. fiz., 60, 2, 145-149 (1928) (with P. P. Kobeko).

"The validity of Faraday's law for currents due to ionization by collision," DAN SSSR, A, 1, 7-8 (1928) (with P. P. Kobeko).

"The rectifying mechanism of certain salts," Zh. Russk. fiz.-khim. o-va, ch. fiz., 61, 5, 459-475 (1929) (with B. V. Kurchatov).

"The similarity principle in the electrical conductivity of solid dielectrics," Zh. Russk. fiz.-khim. o-va, ch. fiz., 61, 4, 321-332 (1929) (with B. V. Kurchatov).

"Breakdown of rock salt," Zh. Russk. fiz.-khim. o-va, ch. fiz., 61, 4, 379-384 (1929) (with P. P. Kobeko).

"Electric breakdown of gases (Criticism of the ionization theory of breakdown)," Usp. fiz. nauk, 9, 6, 685-699 (1929).

"Some electric anomalies of Rochelle salt crystals," Zh. Russk. fiz.-khim. o-va, ch. fiz., 62, 3, 251-265 (1930) (with P. P. Kobeko). The same article appeared in Z. Physik, 66, 3-4, 192-205 (1930).

"The dielectric properties of Rochelle salt crystals," Zh. Russk. fiz.-khim. o-va, ch. fiz., 62, 3, 251-265 (1930) (with P. P. Kobeko). The same article appeared in Z. Physik, 66, 3-4, 192-205 (1930).

"Dielectric properties of Rochelle salt," Fiz. i proizvodstvo, 1, 6-13 (1930) (with P. P. Kobeko).

Electric Strength of a Substance [in Russian] (Gosizdat RSFSR, Moscow, 1930), 111 pp.

"Investigations of the dielectric constant of Rochelle salt in the presence of brief electric pulses," ZhÉTF., 1, 2-3, 121-128 (1931) (with A. K. Val'ter and K. D. Sinel'nikov).

"Discussion of the Conference on Solid Rectifiers and Photocells (from revised shorthand reports of the sessions on September 23, 1931)," Zh.TF., 1, 7, 725-730 (1931).

*Compiled by I. S. Zhiryakova. Under the editorial direction of Cand. Phys.-matem. Sci., B. V. Kurchatov. Central Scientific-Technical Library of the I. V. Kurchatov, Order of Lenin Institute of Atomic Energy, Academy of Sciences of the USSR.

"An investigation of the dielectric constant of Rochelle salt in different crystallographic directions," ZhÉTF., 1, 4, 164-166 (1931) (with G. Ya. Shchepkin).

"Solid rectifiers," ZhTF., 1, 7, 632-645 (1931).

"Solid or rectifier photocells," Report to the Conference on Solid Rectifiers and Photocells, September 23, 1931. ZhTF, 1, 7, 655-671 (1931) (with K. D. Sinel'nikov).

"The Reboule effect. (The movement of an electron in a material medium in very high electric fields.)," ZhTF., 1, 2-3, 261-265 (1931).

"Rectifier photocells," Usp. fiz. nauk, 12, 4, 365-388 (1932).

"Gaseous discharge. (Report to the First All-Union Conference on Chemical Reactions in an Electric Discharge, Leningrad, 1932)," In the book Problems of Kinetics and Catalysis [in Russian](Leningrad, 1935), pp. 8-25.

"The dielectric constant of solid HCl," ZhÉTF., 2, 4, 245-253 (1932) (with G. Ya. Shchepkin).

"The lower Curie point in ferroelectrics," ZhÉTF., 2, 5-6, 319-328 (1932) (with B. V. Kurchatov). The same article appeared in Phys. Z. Sow., 3, 3, 321-334 (1933).

"Electric properties of Rochelle salt crystals containing NaRb, $C_4H_4O_6 4H_2O$ and NaTl $C_4H_4O_6 4H_2O$," ZhÉTF., 2, 2, 102-107 (1932) (with M. A. Ermeev, P. P. Kobeko, and B. V. Kurchatov).

"The electrolysis and breakdown of rock salt crystals," Phys. Z. Sow., 1, 3, 337-352 (1932) (with K. D. Sinel'nikov, O. N. Trapeznikova, and A. K. Val'ter).

"An investigation of the breakdown of rock salt," Phys. Z. Sow., 1, 3, 353-370 (1932) (with K. D. Sinel'nikov and O. P. Trapeznikova).

"A review of the Conference on Rectifier Photocells and Contact Rectifiers," Phys. Z. Sow., 1, 1, 3-5 (1932).

"An investigation of rectifier photocells, I," Phys. Z. Sow., 1, 1, 23-42 (1932) (with K. D. Sinel'nikov).

"An investigation of rectifier photocells. II," Phys. Z. Sow., 1, 1, 42-60 (1932) (with K. D. Sinel'nikov and M. D. Borisov).

"The mechanism of electric breakdown," Z. Phys., 73, 11-12, 775-777 (1932) (with A. F. Ioffe, P. P. Kobeko, and A. K. Val'ter).

"An investigation of self-regulating carborundum resistances," ZhTF., 3, 8, 1163-1184 (1933) (with N. A. Kovalev, T. Z. Kostina, and L. I. Rusinov).

"The relation between polarization and field strength in ferroelectrics outside the region of spontaneous orientation," ZhÉTF., 3, 3, 181-188 (1933).

"Ionic polarization in solid bodies," ZhÉTF., 3, 2, 153-155 (1933).

"Reports on the physics of gaseous discharge to the Conference at Naurheim, September 20-24, 1932," ZhTF., 3, 5, 787-791 (1933).

"Results of recent investigations on disconnection processes in an ac arc and their use in rectifier design. Review of reports to the Zurich Conference," ZhTF., 3, 4, 664-667 (1933).

"Rochelle salt in the region of spontaneous orientation," ZhÉTF., 3, 6, 537-544 (1933). The same article appeared in Phys. Z. Sow., 5, 200-212 (1935).

Ferroelectrics (in the series Problems of Modern Physics) [in Russian] (Gostekhizdat, Leningrad-Moscow, 1933), 104 pp., illus.

"The effect of temperature on the x-raying of rock salt," Phys. Z. Sow., 3, 3, 262-268 (1933) (with K. D. Sinel'nikov, A. K. Val'ter, and S. Litvinenko).

"Unipolarity of polarization in Rochelle salt crystals," Phys. Z. Sow., 4, 1, 125-130 (1933).

"Fast electrons from neutron-bombarded fluorine," DAN SSSR, 3, 8-9, 572-575 (1934) (with G. Ya. Shchepkin and A. I. Vibe).

"The possibility of nuclear fission by neutrons with emission of three heavy particles," DAN SSSR, 3, 4, 230 to 232 (1934) (with L. V. Mysovskii, N. A. Dobrotin, and I. I. Gurevich).

"Gamma rays during proton bombardment of boron," DAN SSSR, 1, 8, 486-487 (1934) (with G. Ya. Shchepkin et al.).

"Disintegration of Li^6 by protons," ZhÉTF., 4, 6, 548-549 (1934) (with K. D. Sinel'nikov. The same article appeared in Phys. Z. Sow., 5, 6, 919-921 (1934).

"The radioactivity of He^3," ZhÉTF., 4, 6, 545-547 (1934) (with K. D. Sinel'nikov, G. Ya. Shchepkin, and A.K. Vibe). The same article appeared in Phys. Z. Sow., 5, 6, 922-926 (1934).

"The Fermi effect in aluminum. I.," DAN SSSR., 3, 226-229 (1934) (with B. V. Kurchatov, G. Ya. Shchepkin, and A. I. Vibe). Part II, DAN SSSR, 3, 422-424 (1934) (with L. B. Mysovskii, B. V. Kurchatov, G. Ya. Shchepkin, and A. I. Vibe).

"The Fermi effect in aluminum. II," DAN SSSR, 3, 422-424 (1934) (with L. V. Mysovskii, B. V. Kurchatov, G. Ya. Shchepkin, and A. I. Vibe).

"The Fermi effect in phosphorus," DAN SSSR, 3, 221-223 (1934) (with L. V. Mysovskii, A. I. Vibe, and G. Ya. Shchepkin).

"An investigation of artificial radioactivity during neutron bombardment. I," Vestn. rengenologii i radiologii, 15, 6, 431-439 (1935) (with G. D. Latyshev, L. M. Nemenov, and I. P. Selinov).

"Artificial radioactivity during neutron bombardment of gold," ZhÉTF., 5, 6, 467-469 (1935) (with G. D. Latyshev). The same article appeared in Phys. Z. Sow., 7, 5-6, 652-655 (1935).

Physics Course. Molecular Physics. Gases and Radiations [in Russian] (Kharkov-Kiev, Derzh. naukovo-tekhn. vid., 1935), 323 pp. (With N. N. Semenov and Yu. B. Khariton.) The same appeared in Phys. Z. Sow., 7, 3, 262-266 (1935).

"Observations on the Fermi effect in a Wilson chamber," ZhÉTF., 5, 5, 367-370 (1935) (with G. D. Latyshev). The same article appeared in Phys. Z. Sow., 7, 3, 262-266 (1935).

"Scattering of slow neutrons by hydrogen," ZhÉTF., 5, 5, 355-359 (1935) (with M. A. Eremeev and G. Ya. Shchepkin). The same article appeared in Phys. Z. Sow., 7, 3, 267-274 (1935).

"Scattering of slow neutrons by iron and other elements," ZhÉTF., 5, 8, 671-676 (1935) (with B. Z. Budnitskii). The same article appeared in Phys. Z. Sow., 8, 2, 170-178 (1935).

"Nuclear splitting," (in the series Problems of Modern Physics. Under gen. ed. direction of Acad. A. F. Ioffe et al., No. 27) (Moscow-Leningrad Princ. Ed. General-tech. course., 1935), 212 pp. The same appeared in Phys. Z. Sow., 7, No. 4, 474-483 (1935).

"Neutron scattering by water and lead," ZhÉTF., 5, 6, 459-466 (1935) (with M. A. Deizenrot-Mysovskaya, G. D. Latyshev, and L. V. Mysovskii). The same article appeared in Phys. Z. Sow., 7, 5-6, 656-669 (1935).

"Absorption of slow neutrons, I," ZhÉTF., 5, 8, 659-670 (1935) (with L. A. Artsimovich, L. V. Mysovskii, and P. A. Palibin).

Electronic Phenomena (with D. N. Nasledov, N. N. Semenov, and Yu. B. Khariton) [in Russian] (Narkompros RSFSR as a textbook for universities, ONTI, Khimtrest, Leningrad, 1935), 388 pp., illus.

"Neutron energy and the Fermi effect," ZhÉTF., 5, 5, 371-375 (1935) (with L. V. Mysovskii, M. A. Ermeev, and G. Ya. Shchepkin). The same article appeared in Phys. Z. Sow., 7, 3, 257-274 (1935).

"Inversion phenomena in polarization of ferroelectrics," ZhÉTF., 5, 8, 751-755 (1935) (with A. Sharikov). The same article appeared in Phys. Z. Sow., 7, 5-6, 631-639 (1935).

"Capture of slow neutrons by nuclei," Compt. rend., 200, 2159-2162 (1935) (with L. A. Artsimovich, L. V. Mysovskii, and P. A. Palibin).

"The artificial radioactivity of neutron-bombarded ruthenium," Compt. rend., 200, 2162-2163 (1935) (with L. M. Nemenov and I. P. Selinov).

"Disintegration of boron by slow neutrons," Compt. rend., 200, 1199-1201 (1935) (with B. V. Kurchatov and G. D. Latyshev).

"A case of artificial radioactivity caused by neutron bombardment without neutron capture," Compt. rend., 200, 1201-1203 (1935) (with B. V. Kurchatov, L. V. Mysovskii, and L. I. Rusinov). (Ed. note: This report describes the discovery of bromine isomerism.)

"Contact phenomena in carborundum resistances," Phys. Z. Sow., 7, 2, 129-154 (1935) (with T. Z. Kostina and L. I. Rusinov).

"Artificial radioactivity in neutron bombardment," Phys. Z. Sow., 8, 6, 589-594 (1935) (with G. D. Latyshev, L. M. Nemenov, and I. P. Selinov).

"Absorption of neutrons in water, paraffin, and carbon," Phys. Z. Sow., 8, 4, 472-486 (1935) (with L. A. Artsimovich, V. A. Khramov, and G. D. Latyshev). ("Neutron splitting of nuclei," A lecture given in the Academician Zelinskii Univ. of Phys. Chem. and Power, Moscow, 1936, fiz.-khim. fak., No. 7).

"An investigation of artificial radioactivity during neutron bombardment. II," Vestn. rentgenologii, 16, 1, 3-9 (1936) (with G. D. Latyshev, L. M. Nemenov, and I. P. Selinov).

"Continuous spectrum of beta-rays from bromine with a half-life of 36 hours, from observations in a Wilson chamber," Symposium in Honor of the 50th Anniversay of the Scientific Work of Academician V. I. Vernadskii [in Russian] (Izd. AN SSSR, 1936), pp. 547-551 (with L. V. Mysovskii, R. A. Eikhel'berg, and G. D. Latyshev).

"Discussion on I. E. Tamm's report: The problem of the atomic nucleus," Izv. AN SSSR, ser. fiz., No. 1-2, 339-342 (1936).

Neutron Splitting of Nuclei [in Russian] (Tipografiya Mezhdunarodn. agrarn. in-ta, Moscow, 1936), 27 pp.

"On the selective absorption of neutrons," Phys. Z. Sow., 9, 1, 102-105 (1936) (with G. Ya. Shchepkin).

"The absorption of thermal neutrons in silver at low temperatures," Phys. Z. Sow., 10, 1, 103-105 (1936) (with V. P. Fomin, F. G. Khouterman, A. I. Leipunskii, L. V. Shubkinov, and G. Ya. Shchepkin).

The Molecular Field in Dielectrics (Ferroelectrics) [in French] (Hermann, Paris, 1936), 46 pp.

"Reactions of neutrons with nuclei: Report and discussion at the Second All-Union Conference on the Atomic Nucleus, Moscow, September 20-26, 1937," Izv. AN SSSR, ser. fiz., 1-2, 157-171, 205-208 (1938).

"Splitting of boron by slow neutrons," ZhÉTF., 8, 8-9, 885-893 (1938) (with A. V. Morozov, G. Ya. Shchepkin, and P. I. Korotkevich).

"Diffusion investigation of neutrons in a cyclotron," DAN SSSR, nov. ser., 24, 1, 31-32 (1939) (with D. G. Alkhazov, M. G. Meshcheryakov, and V. N. Rukavishnikov).

"Metastable level of the gadolinium nucleus," DAN SSSR, nov. ser., 25, 2, 112-114 (1939) (with D. G. Alkhazov, I. I. Gurevich, and V. N. Rukavishnikov).

"Academician Abram Fedorovich Ioffe (In Honor of His 60th Birthday)," Élektrichestvo, No. 10, 34-36 (1940).

"Metastable level of the gadolinium nucleus," Izv. AN SSSR, ser. fiz., 4, 2, 327-329 (1940).

"Operation of the cyclotron of the Radium Institute, Academy of Sciences, USSR," Izv. AN SSSR, ser. fiz., 4, 2, 372-375 (1940).

"Fission of heavy nuclei," Izv. AN SSSR, ser. fiz., 5, 4-5, 578-587 (1941).

"All-Union Conference on Nuclear Physics, November, 1940," Usp. khimii, No. 3, 350-358 (1941).

"Fission of heavy nuclei," Usp. fiz. nauk, 25, 2, 159-170 (1941).

"Isomerism of atomic nuclei," Jubilee Symposium in Honor of the 30th Anniversary of the October Revolution [in Russian] (Izd. AN SSSR, 1947), Vol. 1, pp. 285-304. (Return of the Governmental Delegation to Moscow from Great Britain. Speech by I. V. Kurchatov, Pravda, 1956, May 1; Izvestiya, May 1)

"Atomic power engineering: present development and future prospects," (Conversation with Academician I. V. Kurchatov), Izvestiya, May 10 (1956).

"Problems of the development of atomic power engineering in the USSR," Atomnaya énergiya, 3, 5-10 (1956). The same article appeared in Élektrichestvo, 7, 1-5 (1956).

Problems of the Development of Atomic Power Engineering in the USSR [in Russian] (Moscow, 1956), 27 pp., illus.

"Problems of the development of atomic power engineering," Pravda, May 20 (1956).

"The possibility of thermonuclear reactions in a gaseous discharge," Atomnaya énergiya, 3, 65-75 (1956).

The Possibility of Thermonuclear Reactions in a Gaseous Discharge (Review of Reports by the Academy of Sciences, USSR) [in Russian] (Moscow, 1956), 35 pp., illus.

"The possibility of thermonuclear reactions in a gaseous discharge," Usp. fiz. nauk., 59, 4, 603-618 (1956).

"The possibility of controlled thermonuclear reactions by means of gaseous discharges," Pravda, May 10 (1956).

"Effective exchange of scientific knowledge (Conversation with Academician I. V. Kurchatov)," Krasnaya Zvezda, May 27 (1956).

Speech by Comrade I. V. Kurchatov at the 20th Session of the Communist Party of the Soviet Union. Pravda, February 20, 1956.

"Nuclear power engineering. Modern science has discovered a boundless source of energy – the thermonuclear reaction," Tekhnika molodezhi, 7, 2-5 (1956).

"Major scientific discoveries of Soviet Physics," Trudy uchenykh fiz. inst. AN SSSR. P. A. Cherenkov, I. E. Tamm, and I. M. Frank. Pravda, October 29, (1958).

"Thermonuclear power engineering – not hydrogen bombs (Conversation with Academician I. V. Kurchatov)," Sovetskii Soyuz., 4, 37-38 (1958).

"For the great objective (Successes of Soviet science)," Pravda, March 16 (1958).

"Controlled thermonuclear reactions (Conversation with Academician I. V. Kurchatov, Director of the Institute of Atomic Energy, Academy of Sciences, USSR)," Pravda, February 6, (1958).

"Some reports of the Institute of Atomic Energy, Academy of Sciences, USSR on controlled thermonuclear reactions," Atomnaya énergiya, 5, 2, 105-110 (1958).

"Thermonuclear energy – the basis of the future," Pravda, February 28 (1958).

Nuclear Radiations in Science and Industry [in Russian] (Moscow, 1958), 53 pp.

Speech at the Joint Session of the Council of the Union and the Council of Nationalities of the Supreme Soviet of the USSR. March 31, 1958, Stenographic report, pp. 365-369 (1958).

Speech by I. V. Kurchatov at the Special 21st Conference of the Communist Party of the Soviet Union," Pravda, February 5 (1959).

"Man will become master of nature (Work in the Institute of Atomic Energy of the Academy of Sciences,USSR; Conversation with the Director of the Institute, Academician I. V. Kurchatov)," Moskovskaya Pravda, November 15 (1959).

Speech at the Joint Session of the Council of the Union and the Council of Nationalities of the Supreme Soviet of the USSR. January 15, 1960. Stenographic report, pp. 141-144 (1960).

"Development of atomic physics in the Ukraine," Pravda, February 7 (1960).

"Some results of investigations on controlled thermonuclear reactions, obtained in the USSR," Usp. fiz. nauk, 73, 4, 605-609 (1961).

Soviet Journals Available in Cover-to-Cover Translation

ABBREVIATION	RUSSIAN TITLE		TITLE OF TRANSLATION	PUBLISHER	TRANSLATION Vol.	Issue	BEGAN Year
AÉ	Atomnaya énergiya		Soviet Journal of Atomic Energy	Consultants Bureau	1	1	1956
Akust. zh.	Akusticheskii zhurnal		Soviet Physics – Acoustics	American Institute of Physics	1	1	1955
Astr(on). zh(urn).	Astronomicheskii zhurnal		Soviet Astronomy – AJ	American Institute of Physics	34	1	1957
Avto(mat). svarka	Avtomaticheskaya svarka		Automatic Welding	Br. Welding Research Assn. (London)	12	1	1959
	Avtomatika i Telemekhanika		Automation and Remote Control	Instrument Society of America	27	1	1956
	Biofizika		Biophysics	National Institutes of Health**	6	1	1961
	Biokhimiya		Biochemistry	Consultants Bureau	21	1	1956
Byull. éksp(erim). biol. (i med.)	Byulleten' éksperimental'noi biologii i meditsiny		Bulletin of Experimental Biology and Medicine	Consultants Bureau	41	1	1959
DAN (SSSR) Dokl(ady) AN SSSR	Doklady Akademii Nauk SSSR (The translation of this journal is published in sections)	Life Sciences	Doklady Biological Sciences Sections (includes: Anatomy, biochemistry, biophysics, cytology, ecology, embryology, endocrinology, evolutionary morphology, genetics, histology, hydrobiology, microbiology, morphology, parasitology, physiology, zoology)	National Science Foundation*	112	1	1957
			Doklady Botanical Sciences Sections (includes: Botany, phytopathology, plant anatomy, plant ecology, plant embryology, plant physiology, plant morphology)	National Science Foundation*	112	1	1957
		Chemical Sciences	Proceedings of the Academy of Sciences of the USSR, Section: Chemical Technology	Consultants Bureau	106	1	1956
			Proceedings of the Academy of Sciences of the USSR, Section: Chemistry	Consultants Bureau	106	1	1956
			Proceedings of the Academy of Sciences of the USSR, Section: Physical Chemistry	Consultants Bureau	112	1	1957
		Earth Sciences	Doklady Earth Sciences Sections (includes: Geochemistry, geology, geophysics, hydrogeology, lithology, mineralogy, oceanology, paleontology, permafrost, petrography)	American Geological Institute	124	1	1959
			Proceedings of the Academy of Sciences of the USSR, Section: Geochemistry	Consultants Bureau	106-123	1-6	1956-1958
			Proceedings of the Academy of Sciences of the USSR, Section: Geology	Consultants Bureau	112-123	1-6	1957-1958
		Mathematics	Soviet Mathematics – Doklady	American Mathematical Society	130	1	1960
		Physics	Soviet Physics – Doklady (includes: Aerodynamics, astronomy, crystallography, cybernetics and control theory, electrical engineering, energetics, fluid mechanics, heat engineering, hydraulics, mathematical physics, mechanics, physics, technical physics, theory of elasticity sections)	American Institute of Physics	106	1	1956
	Elektrosvyaz'		Telecommunications	Am. Inst. of Electrical Engineers		1	1957
Entom(ol). oboz(r).	Entomologicheskoe obozrenie		Entomological Review	National Science Foundation**	37	1	1958
FMM	Fizika metallov i metallovedenie		Physics of Metals and Metallography	Acta Metallurgica	5	1	1957
FTT, Fiz. tv(erd). tela	Fizika tverdogo tela		Soviet Physics – Solid State	American Institute of Physics	1	1	1959
Fiziol. Zh(urn). SSSR	Fiziologicheskii zhurnal imeni I.M. Sechenov		Sechenov Physiological Journal USSR	National Institutes of Health**	47	1	1961
Fiziol(ogiya) rast.	Fiziologiya rastenii		Plant Physiology	National Science Foundation*	4	1	1957
	Geodeziya i aerofotosyemka		Geodesy and Aerophotography	American Geophysical Union			1962
	Geokhimiya		Geochemistry	The Geochemical Society	1	1	1956
Geol. nefti i gaza	Geologiya nefti i gaza		Petroleum Geology	Petroleum Geology	2	1	1958
	Geomagnetizm i aeronomiya		Geomagnetism and Aeronomy	American Geophysical Union	1	1	1961
	Iskusstvennye sputniki zemli		Artificial Earth Satellites	Consultants Bureau	1	1	1958
Izmerit. tekhn(ika)	Izmeritel'naya tekhnika		Measurement Techniques	Instrument Society of America	7	1	1958

Izv. AN SSSR O(td). Kh(im). N(auk)	Izvestiya Akademii Nauk SSSR: Otdelenie khimicheskikh nauk	Bulletin of the Academy of Sciences of the USSR: Division of Chemical Science	Consultants Bureau	16	1	1952
Izv. AN SSSR O(td). T(ekhn). N(auk): Metall). i top.	(see Met. i top)					
Izv. AN SSSR Ser. fiz(ich).	Izvestiya Akademii Nauk SSSR: Seriya fizicheskaya	Bulletin of the Academy of Sciences of the USSR: Physical Series	Columbia Technical Translations	18	3	1954
Izv. AN SSSR Ser. geofiz.	Izvestiya Akademii Nauk SSSR: Seriya geofizicheskaya	Bulletin of the Academy of Sciences of the USSR: Geophysics Series	American Geophysical Union	7	1	1957
Izv. AN SSSR Ser. geol.	Izvestiya Akademii Nauk SSSR: Seriya geologicheskaya	Bulletin of the Academy of Sciences of the USSR: Geologic Series	American Geological Institute	23	1	1958
Iz. Vyssh. Uch. Zav., Tekh. Teks. Prom.	Izvestiya Vysshikh Uchebnykh Zavedenii Tekhnologiya Tekstil'noi Promyshlennosti	Technology of the Textile Industry, USSR	The Textile Institute (Manchester)	4	1	1960
Kauch. i rez.	Kauchuk i rezina	Soviet Rubber Technology	Palmerton Publishing Company, Inc.	18	3	1959
	Kinetika i kataliz	Kinetics and Catalysis	Consultants Bureau	1	1	1960
	Koks i khimiya	Coke and Chemistry, USSR	Coal Tar Research Assn. (Leeds, England)		8	1959
Kolloidn. zh(urn).	Kolloidnyi zhurnal	Colloid Journal	Consultants Bureau	14	1	1952
	Kristallografiya	Soviet Physics – Crystallography	American Institute of Physics	2	1	1957
Metallov. i term.	Metallovedenie i termicheskaya obrabotka metallov	Metals Science and Heat Treatment of Metals	Acta Metallurgica	6	1	1958
	Metallurg	Metallurgist	Acta Metallurgica		1	1957
Met. i top.(gorn.)	Metallurgiya i toplivo (gornoye delo)	Russian Metallurgy and Fuels (mining)	Scientific Information Consultants, Ltd.		1	1960
Mikrobiol.	Mikrobiologiya	Microbiology	National Science Foundation*	26	1	1957
	Ogneupory	Refractories	Acta Metallurgica	25	1	1960
OS, Opt. i spektr.	Optika i spektroskopiya	Optics and Spectroscopy	American Institute of Physics	6	1	1959
Paleontol. Zh(urn)	Paleontologicheskii Zhurnal	Journal of Paleontology	American Geological Institute		1	1962
	Pochvovedenie	Soviet Soil Science	National Science Foundation**	53	1	1958
	Poroshkovaya Metallurgiya	Soviet Powder Metallury and Metal Ceramics	Consultants Bureau	2	1	1962
	Priborostroenie	Instrument Construction	Taylor and Francis, Ltd. (London)	4	1	1959
Pribory i tekhn. éks(perimenta)	Pribory i tekhnika éksperimenta	Instruments and Experimental Techniques	Instrument Society of America	3	1	1958
Prikl. matem. i mekh(an).	Prikladnaya matematika i mekhanika	Applied Mathematics and Mechanics	Am. Society of Mechanical Engineers	22	1	1958
PTE	(see Pribory i tekhn. éks.)					
	Problemy Severa	Problems of the North	National Research Council of Canada		1	1958
	Radiokhimiya	Radiochemistry	Consultants Bureau	4	1	1962
Radiotekh.	Radioteknika	Radio Engineering	Am. Institute of Electrical Engineers	16	1	1961
Radiotekhn. i élektron(ika)	Radiotekhnika i électronika	Radio Engineering and Electronic Physics	Am. Institute of Electrical Engineers	6	1	1961
	Stal'	Stal (in English)	Iron and Steel Institute	19	1	1959
	Stanki i instrument	Machines and Tooling	Production Engineering Research Assoc.	30	1	1959
Stek. i keram.	Steklo i keramika	Glass and Ceramics	Consultants Bureau	13	1	1956
Svaroch. proiz-vo	Svarochnoe proizvodstvo	Welding Production	Br. Welding Research Assn. (London)	5	4	1959
Teor. veroyat. i prim.	Teoriya veroyatnostei i ee primenenie	Theory of Probability and Its Application	Soc. for Industrial and Applied Math.	1	1	1956
Tsvet. metally	Tsvetnye metally	The Soviet Journal of Nonferrous Metals	Primary Sources	33	1	1960
UFN	Uspekhi fizicheskikh nauk	Soviet Physics – Uspekhi (partial translation)	American Institute of Physics	66	1	1958
UKh. Usp. khimi	Uspekhi khimii	Russian Chemical Reviews	Chemical Society (London)	29	1	1960
UMN	Uspekhi matematicheskaya nauk	Russian Mathematical Surveys	Cleaver-Hume Press, Ltd. (London)	15	1	1960
Vest. mashinostroeniya	Vestnik mashinostroeniya	Russian Engineering Journal	Production Engineering Research Assoc.	39	4	1959
Vop. onk(ol).	Voprosy onkologii	Problems of Oncology	National Institutes of Health**	7	1	1961
Zav(odsk). lab(oratoriya)	Zavodskaya laboratoriya	Industrial Laboratory	Instrument Society of America	24	1	1958
ZhAKh, Zh. anal(it). Khim(ii)	Zhurnal analiticheskoi khimii	Journal of Analytical Chemistry	Consultants Bureau	7	1	1952
ZhETF Zh. éksperim. i teor. fiz. ZhFKh	Zhurnal eksperimental'noi i teoreticheskoi fiziki	Soviet Physics – JETP	American Institute of Physics	28	1	1955
Zh. fiz. khimii ZhNKh	Zhurnal fizicheskoi khimii	Russian Journal of Physical Chemistry	Chemical Society (London)	33	7	1959
Zh. neorg(an). khim. ZhOKh	Zhurnal neorganicheskoi khimii	Journal of Inorganic Chemistry	Chemical Society (London)	4	1	1959
Zh. obshch. khim. ZhPKh	Zhurnal obshchei khimii	Journal of General Chemistry USSR	Consultants Bureau	19	1	1949
Zh. prikl. khim. ZhSKh	Zhurnal prikladnoi khimii	Journal of Applied Chemistry USSR	Consultants Bureau	23	1	1950
Zh. strukt(urnoi) khim.	Zhurnal strukturnoi khimii	Journal of Structural Chemistry	Consultants Bureau	1	1	1960
ZhTF	Zhurnal tekhnicheskoi fiziki	Soviet Physics – Technical Physics	American Institute of Physics	26	1	1956
Zh. tekhn. fiz.	Zhurnal vychislitel'noi matematika i matematicheskoi fiziki	U.S.S.R. Computational Mathematics and Mathematical Physics	Pergamon Press, Inc.	1	1	1962
Zh. vyssh. nervn. deyat. (im. Pavlova)	Zhurnal vysshei nervnoi deyatel'nosti (im I. P. Pavlova)	Pavlov Journal of Higher Nervous Activity	National Institutes of Health**	11	1	1961

*Sponsoring organization. Translation published by Consultants Bureau.
**Sponsoring organization. Translation published by Scripta Technica.

SOVIET PROGRESS IN NEUTRON PHYSICS

Edited by P. A. Krupchitskii

A collection of 40 original and review papers by Soviet specialists, publication of which was deemed essential by the editorial board of the *Soviet Journal of Atomic Energy*. The collection includes 18 contributions on moderation, resonance absorption, and neutron diffusion; 12 on the interactions of fast neutrons with nuclei; 6 on fission, fragments, and secondary neutrons; and 4 papers on gamma-radiation in neutron capture. The abundance of new data on neutron physics is of great interest, as is the material on the shielding of nuclear reactors and that on theoretical physics. Included among the authors are such important researchers as *G. I. Marchuk, A. D. Galanin, A. V. Stepanov, V. V. Orlov, V. I. Popov* and *N. S. Lebedeva.*

Contents include:

Measurement of the Energy Dependence of the Cross Section of the Cl (n,γ) Reaction • Gamma-Radiation in Inelastic Interaction between Fast Neutrons and Atomic Nuclei • Spectra of γ-rays which Accompany the Capture of Thermal Neutrons by Mo, Nb, Ho, Tu, and La Nuclei • Inelastic Scattering of Neutrons with Energies from 3.2 to 4.5 Mev on Beryllium • Spatial Distributions of Neutrons in Mixtures of Boron Carbide with Iron and Lead • Fragment Yields in the Fission of U^{235} and U^{238} by Fast Neutrons • Yields of Certain Fragments in Th^{232} Fission by 14.3-Mev Neutrons • Effect of the Resonance Structure of Cross Sections on Neutron Diffusion • Multigroup Method of Calculating the Energy-Space Distribution of Thermal-Neutron Flux, and the Application of the Perturbation Method • Neutron Scattering by Crystals in the Incoherent Approximation • Theory of Thermal Neutron Diffusion with Velocity Distribution Taken into Account

278 pages $40.00

PHOTONEUTRON METHOD OF DETERMINING BERYLLIUM

by Kh. B. Mezhiborskaya

***"of value to all analysts using the photoneutron method"*—Current Engineering Practice**

***"extremely useful...well presented"*—The Analyst**

The radioactivation or photoneutron method for the determination of beryllium in mineral raw materials and hydrometallurgical products has been widely used in the Soviet Union. One of the foremost Soviet scientists in this field, Kh. B. Mezhiborskaya, presents the results of more than eight years of research.

A highly efficient technique for determining beryllium, the photoneutron method is usually employed by analysts having little knowledge of nuclear physics methods. This report presents a detailed discussion of the fundamentals of the method, apparatus for determining and prospecting for beryllium, recording methods, analysis procedures, effects of interference, standards, etc.

In addition, PHOTONEUTRON METHOD OF DETERMINING BERYLLIUM deals with the safety problems which occur during the practical use of this nuclear analysis method. Complete instructions on safety precautions are given, including shielding materials, dosimetric checking, space and equipment requirements.

This technical report will be of value to all analysts using the photoneutron method, as well as to those medical researchers concerned with radiation hazards and their prevention.

A Consultants Bureau Special Report 16,000 words $12.50

CONSULTANTS BUREAU
227 W. 17 ST., NEW YORK 11, N. Y.

Declassified and Approved For Release 2013/09/25 : CIA-RDP10-02196R000600100001-7

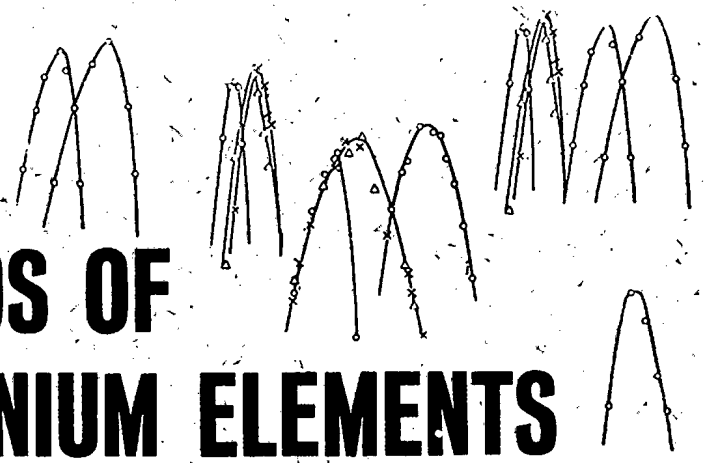

COMPLEX COMPOUNDS OF TRANSURANIUM ELEMENTS

by A. D. Gel'man, A. I. Moskvin, L. M. Zaitsev and M. P. Mefod'eva
Institute of Physical Chemistry, Academy of Sciences, USSR

Complex compounds play an extremely important part in the identification and isolation of transuranium elements. The valence states and chemical properties of many of the elements synthesized have been studied extensively with their help, even before these elements were obtained in weighable amounts. These compounds are of particular interest because they extend the possibilities of investigating unstable derivatives of transuranium elements, making it possible to determine the position of the latter in the periodic system more accurately.

Although complex compounds of transuranium elements are being studied thoroughly in many countries and extensive experimental data has been collected, this volume is the first to deal with all aspects of material thus far obtained. This book will be of interest not only to radiochemists and specialists in complex compounds, but also to a wide group of chemists concerned with this important field of investigation which is extending the boundaries of the periodic system and providing new applications of the coordination theory.

CONTENTS include:

220 pages *Translated from Russian* **$12.50**

CONSULTANTS BUREAU 227 West 17th Street, New York 11, N. Y.